CEDA
Central Dredging Association

EUROPORT 2009
connecting the maritime world

DREDGING DAYS 2009

WELCOME

Welcome from Anders Jensen, CEDA President

Welcome from Ronald Paul, Maasvlakte 2 Managing Director

Introduction by Professor Cees van Rhee, Chairman of CEDA Dredging Days 2009 Papers Committee

Welcome from Anders Jensen, CEDA President

CEDA Dredging Days was last dedicated to dredging tools and technology in 2003 – only six years ago, but we've seen many technological innovations since. With them have come new experiences and exciting new opportunities, not least those driven by climate change-induced demands for beach nourishment and flood protection dredging, the appearance of new customers along with increasing dredging requirements in new regions and the need for sustainable dredging solutions.

We're also facing new challenges, among them financial market turbulence, rising energy costs, looming legislation governing emissions, plant shortages and the never-ending tightening of national and international environmental regulations.

And all are helping shape both today's industry and that of the near future – which is why CEDA Dredging Days 2009 is so important in demonstrating how the dredging industry responds to these new trends. Scientists and practitioners representing equipment manufacturers, consultancies, dredging companies and academia will present their achievements and – in particular – their visions for the future.

So, on behalf of the CEDA board and the Technical Papers Committee, I look forward to welcoming delegates, exhibitors and partners to this exciting event in the knowledge that, like me, you will take full advantage of the opportunities to learn from each other – and to enjoy Rotterdam's hospitality.

Welcome from Ronald Paul, Maasvlakte 2 Managing Director

The Netherlands is becoming a little larger thanks to the Port of Rotterdam, whose Maasvlakte 2 expansion is being reclaimed from the North Sea.

It's a vital expansion as the port's more or less reached the limits of its capacity and no longer has sufficient room for large new container terminals and chemical clusters. But with Maasvlakte 2 we're creating this much-needed space – and with a draught of 20m, it will be the only port in Europe able to welcome the world's largest container ships 24 hours a day.

After an international call for tenders, the PUMA consortium (Project Uitbreiding Maasvlakte, comprising Koninklijke Boskalis Westminster and Van Oord) was contracted to build the first sites – due for delivery to customers in 2013 when the first ship is also planned to dock. Maasvlakte 2 is being built in phases and it's the rate at which Rotterdam Port Authority acquires customers that will determine the speed of its construction.

The first phase, however, will cover 700ha and require 240M m^3 of dredged sand. Following delivery, PUMA will be responsible for maintaining the seawalls for a further five years as an integral part of the contract.

Maasvlakte 2's construction began with the creation of a small, banana-shaped island about 3km offshore built by trailing suction hopper dredgers (TSHDs) that gathered sand at an average distance of 10km off the coast. As I write, four to nine TSHDs are operating continuously, resulting in more new islands that can be seen above water, even during high tide – the beginning of the project's seawalls. It's a major milestone and I can proudly state that the project is well on schedule, with construction work on the first container terminal's quay planned to start in 2010. Truly, Port of Rotterdam Authority is dredging for the future!

It could not be more appropriate to organize a conference entitled Dredging Tools for the Future in Rotterdam. I am therefore delighted that once again CEDA Dredging Days 2009 takes place in our city. Several subjects in the technical programme are directly relevant both for the ongoing extension work at the port and for its future infrastructure. I wish all attendees a very successful conference and an enjoyable stay.

Introduction by Professor Cees van Rhee, Chairman of CEDA Dredging Days 2009 Papers Committee

A dredging project cannot be designed, executed and monitored without the appropriate 'tools' – which are becoming more and more important given the dredging industry's future challenges, such as rising energy costs, climate change, increasing demands for dredging services in new regions, the appearance of new customers, plant shortages and the need for sustainable dredging solutions.

And knowledge is very much a 'tool,' as marine director of the International Chamber of Shipping UK, Peter Hinchliffe, will advise in his keynote address that will update delegates about coming regulatory challenges for the shipping industry – and the consequences for dredging vessel and equipment design and operation. The tools presented during this conference will be diverse, ranging from equipment specially designed for extreme conditions – such as hard sediments in sensitive areas and devices for very deep water – as well as tools for modeling and monitoring of dredging projects. All will be highlighted by distinguished speakers.

Dredging research and technology are also vital tools and in the Academic Session, university students and other young professionals are given the opportunity to present their achievements and latest developments.

New this year is the CEO Forum: renowned international experts representing various facets of the dredging and marine construction fields will share their views on the latest issues and trends and discuss them with delegates. Panel members are:

- Govert Hamers, chairman of IHC Merwede
- Peter Lundhus, managing director of Femern Baelt
- Koos van Oord, president of the IADC, and
- Dimitrios Theologitis, head of the Maritime Transport & Ports Policy, Maritime Security Unit of the European Commission.

In all, CEDA Dredging Days 2009 can be viewed as a tool that's sure to add value to your professional life – and it's a chance to meet and network with your fellow dredging enthusiasts.

Content

Thursday 5 November

SESSION 1: DREDGING TOOLS AND INCREASINGLY STRICTER ENVIRONMENTAL REGULATIONS

SESSION 2: DREDGING TOOLS AND EXTREME CONDITIONS

Friday 6 November

SESSION 4: Academic Session

Water jets surrounded by an air film – experimental research
Vinke F. and Talmon A.M. – Delft University of Technology
Nobel A. – Royal Boskalis Westminster
The Netherlands

The use of flocculants to enclose silt particles in pore volume of dredged soil
Mol J.N. and van Hemmen AJM – Royal Boskalis Westminster
Talmon A.M. – Delft University of Technology
The Netherlands

Hindered erosion of granular sediments
Bisschop F. – ARCADIS/Delft University of Technology
Visser P.J. and van Rhee C. – Delft University of Technology
The Netherlands

Material behaviour and constitutive modelling of organic soils
Mathijssen FAJM – Royal Boskalis Westminster / Delft University of Technology
Boylan N. – University of Western Australia, Australia
Long M. – University College Dublin, Ireland
Leroueil S. – Laval University Québec, Canada
Molenkamp F. – Delft University of Technology, The Netherlands

SESSION 5: Dredging Tools and Energy Scarcity / Operational Efficiency

Wear-resistant dredge cutter teeth – a look at the development of the tooth and its impact on the economical and environmental aspects of the dredger, logistics and foundry
Wijma K. – VOSTA LMG, The Netherlands

Future dredging tools made from ‘new’ materials
Bugdayci H.H., Smeets F. and van Opstal T.A. – IHC Parts & services, The Netherlands

Estimating the immeasurable: soil properties
Braaksma J., Osnabrugge J. and de Keizer C. – IHC Systems, The Netherlands

SESSION 6: DREDGING TOOLS AND DYNAMICS OF NATURE

Working with nature
Brooke J. – for PIANC Environmental Commission, UK

Safe disposal of dredged material in a sensitive environment – operational planning of dredging activities based on innovative plume predictions
Aarninkhof S. – Royal Boskalis Westminster
Luijendijk A. – Deltares
The Netherlands

A special unit for water injection dredging
de Vries G. – Vuyk Engineering Rotterdam, The Netherlands
Beyen J. – DEME, Belgium

Measuring the effects of dredging in relation to the dynamics of nature
Koomans R.L. and Limburg J. – Medusa Explorations, The Netherlands

A field survey of a dredging plume during gravel dredging
Breugem W.A., Bollen M. and Sas M. – IMDC, Belgium
Vandenbroeck J. – SDI, DEME Group, France

ORGANIZERS

CEDA Dredging Days 2009 conference and exhibition is organised by the Central Dredging Association (CEDA) in association with Ahoy Rotterdam. CEDA Dredging Days 2009 are being held in conjunction with Europort 2009.

The Central Dredging Association (CEDA) is an independent, international, professional association. It is an easy-to-access leading platform for the exchange of knowledge and an authoritative reference point for impartial technical information. Working with nature, CEDA contributes to sustainable development. CEDA members are corporations, professionals and stakeholders involved in any kind of activity related to dredging and marine construction.

CEDA operates in Europe, Africa and the Middle East. Under the umbrella of the World Organisation of Dredging Associations (WODA), CEDA is part of the global network of professionals which includes the Western Dredging Association (WEDA) for the Americas and the Eastern Dredging Association (EADA) for Asia, Australia and the Pacific.
For more information visit: www.dredging.org.

COMMITTEES

International Technical Paper Committee

Chairman:

C. van Rhee	(Delft University of Technology, The Netherlands)

Members:

E. van der Blom	(IHC Merwede, The Netherlands)
A. Csiti	(CEDA, The Netherlands)
P. Hakstege	(Rijkswaterstaat, Centre for Public Works, The Netherlands)
J. van't Hoff	(Jan van't Hoff Consultancy, The Netherlands)
A. Jensen	(Femern Baelt, Denmark)
B. Malherbe	(Jan De Nul, Belgium)
M. Maloney	(Antony Bates Consultancy, UK)
S. Vandycke	(Dredging International, Belgium)

COORDINATING COMMITTEE

A. Jensen	(CEDA, President)
A. Csiti	(CEDA, General Manager)
R. Siliakus	(Exhibition Manager Ahoy Rotterdam)

DREDGING DAYS 2009

DISCLAIMER

The papers in this publication reflect the opinions of the authors and do not necessarily reflect the opinions of the CEDA Board, or members of the Central Dredging Association.

The organisers of Dredging Days 2009 bear no responsibility for any statements made and or opinions that may be included in this publication. The papers have been reproduced from the authors' original PDF files. The possibility that this publication may contain some errors cannot be excluded and those who make use of it do so entirely at their own risk. On behalf of CEDA and of all who have contributed in any way to this publication CEDA disclaims all responsibility for damages, whether direct, incidental or consequential, arising from the application or from any other use information contained in this publication.

When citing papers from the proceedings the following references should be used:
Authors: 2009; Title of paper; CEDA Dredging Days 2009, Rotterdam, the Netherlands;
ISBN 978-90-809883-3-0

Central Dredging Association

DREDGING DAYS 2009

SPONSORS

The Organizers wish to thank the following organizations for their support.

Gold Sponsor:

Wärtsilä Nederland

Silver Sponsors:

Allard Europe NV

Cable Arm Inc.

Damen Dredging Equipment BV

IHC Holland Merwede BV

Projectorganisatie Maasvlakte 2

PUMA

Seatools BV

Vuyk Engineering Rotterdam BV

Vereniging van Waterbouwers

Central Dredging Association

DREDGING DAYS 2009

Exhibitors

Company	*Country*	*Stand number*
Aqua Vision BV	Netherlands	6
Bandeirantes Dragagem e Construcao Ltda.	Brazil	5
CEDA	Netherlands	9
DEME	Belgium	2 + 3
GEO.XYZ	Belgium	13
IHC Merwede BV	Netherlands	10
Inchcape Shipping Services	Dubai, UAE	14
Projectorganisatie Maasvlakte 2	Netherlands	16
PUMA Projectorganisatie Uitbreiding Maasvlakte	Netherlands	15
QPS Quality Positioning Services BV	Netherlands	1
SEATOOLS BV	Netherlands	4
Vosta LMG	Netherlands	11 + 12
Wärtsilä Netherlands B.V.	Netherlands	7

The Corporate Members of CEDA

Members who make a major contribution to our activities for which we thank them

ACADEMIC BODIES AND EDUCATIONAL INSTITUTES

Delft University of Technology
The Netherlands
Tel.: +31(0)15 278 6882 - Fax: +31(0)15 278 1836
Email: info@3me.tudelft.nl
Web: www.3me.tudelft.nl
CEDA Contact Point: Prof. Dr. ir C. van Rhee

Hanzehogeschool, Hogeschool van Groningen
The Netherlands
Tel.: +31(0)50 5954 646 - Fax: +31(0)50 595 49 99
Email: w.t.van.rossum@pl.hanze.nl
Web: www.hanze.nl
CEDA Contact Point: Ir. M.P. Parlevliet

Scheepvaart en Transport College
The Netherlands
Tel.: +31(0)10 44 86 000
Email: baggerinfo@stc-r.nl
Web: www.stc-r.nl
CEDA Contact Point: Mr. E.N.G. Wentink

Skilltrade B.V.
The Netherlands
Tel.: +31(0)7156 113 65 - Fax: +31(0)71 5611503
Web: www.skilltrade.nl
CEDA Contact Point: Mr. M.J. Stam

ASSOCIATIONS

CEDA
The Netherlands
Tel.: +31152682575 - Fax: +31152682576
Email: ceda@dredging.org
Web: www.dredging.org
CEDA Contact Point: Ms. A. Csiti

Hafentechnische Gesellschaft E.V.
Germany
Tel.: +49 40 42847 2178
Email: service@htg-online.de
Web: www.htg-online.de
CEDA Contact Point: Dipl.-Ing. G. Kaschel

IRO
The Netherlands
Tel.: +31(0)79 341 19 81 - Fax: +31(0)79 341 97 64
Email: info@iro.nl
Web: www.iro.nl
CEDA Contact Point: Ir. H. P. de Boer

Vereniging van Waterbouwers
The Netherlands
Tel.: +31(0)182 567 367 - Fax: +31(0)182 567 373
Email: info@waterbouwers.nl
Web: www.waterbouwers.nl
CEDA Contact Point: Mr. F. Heinis

CONSULTANCIES AND RESEARCH INSTITUTES

Advantis Consulting
Morocco

Anthony Bates Partnership Dredging and Costal Consultants
UK
Tel.: +44 (0)1934 732 380 - Fax: +44(0)1934 733 439
Email: mail@anthonybates.co.uk
Web: www.anthonybates.co.uk
CEDA Contact Point: Mr A. Bates

Aqua Vision
The Netherlands
Tel.: +31(0)30 245 98 72 - Fax: +31(0)30 245 94 99
Email: info@aquavision.nl
Web: www.aquavision.nl
CEDA Contact Point: Ms. M. de Vries

Arcadis U.S. Inc.
USA
Tel.: +1(0)206 325 5254 - Fax: +1(0)206 325 8218
Web: www.Arcadis-us.com
CEDA Contact Point: Ms. S. P.A. Spadaro

Centre d'Etudes Techniques Maritimes Et Fluviales (CETMEF)
France
Tel.: +33(0) 344 92 60 00 - Fax: +33(0)3 44 92 06 75
Email: cetmef@équipement.gouv.fr
Web: www.cetmef.equipement.gouv.fr
CEDA Contact Point: Mr. O. Piet

COWI A/S
Denmark
Tel.: +45(0)459 722 11 - Fax: +45(0)459 722 12
Email: cowi@cowi.dk
Web: www.cowi.com
CEDA Contact Point: Mr. T. Dahlgren

Deep B.V.
The Netherlands
Tel.: +31(0)20 634 36 76 - Fax: +31(0)20 634 46 86
Email: info@deepbv.nl
Web: www.deepbv.nl
CEDA Contact Point: Mr. G.J. Hein

Deltares
The Netherlands
Tel.: +31(0)15 285 85 85 - Fax: +31(0)015 285 85 82
Email: info@deltares.nl
Web: www.deltares.nl
CEDA Contact Point: Ir. J.G.S. Pennekamp

DEMAS Dredging Consultants B.V.
The Netherlands
Tel.: +31(0)182 546 798 - Fax: +31(0)182 546 802
Email: demasnl@demas.nl
Web: www.demas.nl
CEDA Contact Point: Mr. K. Ooms

DHI Water & Environment
Denmark
Tel.: +45 45 16 92 00 - Fax: +45 45 16 92 92
Email: dhi@dhi.dk
Web: www.dhi.dk
CEDA Contact Point: Ms. Jennifer Oakley

DHV B.V.
The Netherlands
Tel.: +31(0)33 468 3325 - Fax: +31(0)33 468 2801
Email: pwcd@dhv.com
Web: www.dhv.com
CEDA Contact Point: Mr. D. Rijks

Dredging Consultancy Van 't Hoff & Partners B.V.
The Netherlands
Tel.: +31(0)30 69 20 294 - Fax: +31(0)30 69 20 362
Email: info@hoff-consultancy.com
Web: www.hoff-consultancy.com
CEDA Contact Point: Mr. J. van 't Hoff

Dredging Research Ltd.
U K
Tel.: +44 (0) 1491 835381 - Fax: +44 (0) 1491 832233
Email: drl@hrwallingford.com
Web: www.drl.com
CEDA Contact Point: Mr. N. Bray

Ecorem N.V.
Belgium
Tel.: +32(0)3 87 10 900 - Fax: +32(0)3 87 10 901
Email: info@ecorem.be
Web: www.ecorem.be
CEDA Contact Point: Mr. W. Mondt

Foby Engineering Company Ltd.
Nigeria
Tel.: +234 84 239 478 - Fax: +234 84 239 479
Email: FobyUSA@aol.com
CEDA Contact Point: Mr. R. Ere

G-Tec S.A.
Belgium
Tel.: +32(0)43 878 500 - Fax: +32(0)438 78509
Email: info@gtec.be
Web: www.gtec.be
CEDA Contact Point: Mr. F. Renardy

Gems International N.V.
Belgium
Tel.: +32 50 55 95 95 - Fax: +32.50 55 95 57
Email: info@gems-group.com
Web: www.gems-group.com
CEDA Contact Point: Mr. J. Deschuyter

GLM van der Schrieck B.V.
Netherlands
Tel.: 023-5244525 - Fax: 023-5443201
Email: glm@vanderschrieck.nl
CEDA Contact Point: Ir. G.L.M. van der Schrieck

Halcrow Group Ltd.
U K
Tel.: +44(0)1793 812 479
Email: halcrow@halcrow.com
Web: www.halcrow.com
CEDA Contact Point: Mr. B. Hamer

HR Wallingford Group Ltd.
U K
Tel.: +44 (0) 1491 835381 - Fax: +44 (0) 1491 832233
Email: info@hrwallingford.co.uk
Web: www.hrwallingford.co.uk
CEDA Contact Point: Mr. M. Costaras

Svasek Hydraulics
The Netherlands
Tel.: +31(0)10 467 13 61 - Fax: +31(0)10 467 45 59
Email: info@svasek.com
Web: www.svasek.com
CEDA Contact Point: Ir. A.J. Bliek

Members who make a major contribution to our activities for which we thank them

International Marine & Dredging Consultants nv (IMDC)
Belgium
Tel.: +32(0)3 270 92 95 - Fax: +32(0)3 235 67 11
Email: info@imdc.be
Web: www.imdc.be
CEDA Contact Point: Mr. J. Smits

JFA Consultants Pty Ltd.
Australia
Tel.: +61(0)892 427 522 - Fax: +61(0)892 427 298
Email: jfa@jfaconsultants.com.au
Web: www.jfaconsultants.com.au
CEDA Contact Point: Ms. L. Whitson

Knowles Ltd.
U K
Tel.: +44(0)8707530616 - Fax: +44(0)8707481700
Email: info@jrknowles.com
Web: www.jrknowles.com
CEDA Contact Point: Mr. T. Clarke

LICengineering A/S
Denmark
Tel.: +45-39 62 16 42 - Fax: +45-39 62 54 80
Email: rsl@liceng.dk
Web: www.liceng.dk
CEDA Contact Point: Mr. R. S. Lorenz

Marine Structure Consultants B.V.
The Netherlands
Tel.: +31(0)10 2320 800 - Fax: +31(0)10 2320 801
Email: MSC@MSCoffshore.nl
Web: www.MSCoffshore.nl
CEDA Contact Point: Mr. C.J. Mommaas

MDCE bvba
Belgium
Tel.: +32(0)50 35 03 77 - Fax: +32(0)50 68 00 88
Email: info@mdce.be
Web: www.mdce.be
CEDA Contact Point: Mr. M. Druyts

MWH N.V.
Belgium
Tel.: +32(0)15 27 69 58 - Fax: +32(0)15 27 76 74
Web: mwhglobal.com
CEDA Contact Point: Mr. J. Vandekeybus

NC2
Morocco
Tel.: +21(2)22 232 792 - Fax: +21(2)22 232 792
CEDA Contact Point: Mr. Y. El Houssain

QCubes Marine
The Netherlands
Tel.: +31 (0)10 458 7505
Web: www.qcubesmarine.com
CEDA Contact Point: Mr. B.C. Maljers

Royal Haskoning
U K
Tel.: +44(0)1392 447 999 - Fax: +44(0)7887 781 276
Web: www.royalhaskoning.com
CEDA Contact Point: Mr. S. Challinor

Seaworks.be bvba
Belgium
Tel.: +32 3 206 86 70 - Fax: +32 3 206 86 79
Email: info@seaworks.be
Web: www.seaworks.be
CEDA Contact Point: Mr R. Van Santvoort

Stema Survey Services B.V.
The Netherlands
Tel.: +31(0)345 580 395 - Fax: +31(0)345 570 649
Email: stema@stema-survey.com
Web: www.stema-survey.com
CEDA Contact Point: Mr. J.W.L. Mars

DESIGNERS, BUILDERS AND SUPPLIERS OF ANCILLARY EQUIPMENT

Allard-Europe
Belgium
Tel.: +32 14 42 11 11 - Fax: +32 14 42 52 00
Email: jd@allard-europe.com
Web: www.allard-europe.com
CEDA Contact Point: Mr. P. Burdack

Bakker Sliedrecht Electro Industrie B.V.
The Netherlands
Tel.: +31(0)184 43 66 66 - Fax: +31(0)184 43 66 77
Email: info@bakker-sl.nl
Web: www.bakkersliedrecht.com
CEDA Contact Point: Mr. A. Boer

Bosch Rexroth B.V.
The Netherlands
Tel.: +31 (0) 411 651 764 - Fax: +31 (0) 411 651 453
Email: paulette.teulings@boschrexroth.nl
Web: www.boschrexroth.nl
CEDA Contact Point: Mr. P. Goossens

Future Pipe Industries B.V.
The Netherlands
Tel.: +31(0)523 280500 - Fax: +31(0)523 280700
Email: g.faber@futurepipe.nl
Web: www.futurepipe.com
CEDA Contact Point: Mr. G. Faber

Holland Marine Technologies B.V.
The Netherlands
Tel.: +31 (0)348 416075 - Fax: +31 348 410019
Email: info@HollandMT.com
Web: www.HollandMT.com
CEDA Contact Point: Mr. J.W. de Wit

IHC Hytop B.V.
The Netherlands
Tel.: +31(0)184 43 19 33 - Fax: +31(0)184 43 16 16
Email: info@hytop.com
Web: www.hytop.com
CEDA Contact Point: Ing. T.H.M Henquet

Konutherm
The Netherlands
Tel.: +31(0)3412 642 83 - Fax: +31(0)341 264 893
Email: info@konutherm.nl
Web: www.konutherm.nl
CEDA Contact Point: M. de Jonge

Matecs Holding B.V.
The Netherlands
Tel.: +31(0)165 581840 - Fax: +31(0)165 5818 49
Email: timro@timro.nl
Web: www.timro.nl
CEDA Contact Point: Mr. W. Tims

Quality Positioning Services B.V.
The Netherlands
Tel.: +31(0)30 694 1200/222 - Fax: +31(0)30 692 3663
Email: sales@qps.nl
Web: www.qps.nl
CEDA Contact Point: Mr. J. Koper

Reson B.V.
The Netherlands
Tel.: +31(0)10 245 1500 - Fax: +31(0)10 245 1555
Email: info@reson.nl
Web: www.reson.nl
CEDA Contact Point: Mr. N. van Woerkom

Seatec Underwater Systems B.V.
The Netherlands
Tel.: +31(0)111 45 61 00 - Fax: +31(0)111 45 61 11
Email: info@seatec.nl
Web: www.seatec.nl
CEDA Contact Point: Mr. J.H. de Bie

Seatools B.V.
The Netherlands
Tel.: +31(0)186 680 000 - Fax: +31(0)186 680 001
Email: info@seatools.nl
Web: www.seatools.nl
CEDA Contact Point: Mr. J.C.L. Frumau

Siemens Nederland N.V. Bruinhof Marine
The Netherlands
Tel.: +31(0)10 497 0801 - Fax: +31(0)10 483 4995
Email: info@bruinhof.nl
Web: www.bruinhof.nl
CEDA Contact Point: Mr. J. Baas

Soremar
Morocco
Tel.: +21(2)22 248 236/+21(2)22 248 252 - Fax: +21(2)22 405 050
Email: gnaou@soremar.co.ma
CEDA Contact Point: Mr. G. Nourredine

Van Heck B.V.
The Netherlands
Tel.: +31(0)561 43 17 39 - Fax: +31(0)561 43 17 66
Email: vanheck@tip.nl
Web: www.vanheckpumps.nl
CEDA Contact Point: Mr J.G.M. Van Heck

VandeGrijp Pipes & Parts
The Netherlands
Tel.: +31(0)78 644 64 64 - Fax: +31(0)78 644 64 65
Email: info@vandegrijp.com
Web: www.vandegrijp.com
CEDA Contact Point: Mr. J.R. Kraaijeveld van Hemert

Wärtsilä Nederland B.V.
The Netherlands
Tel.: +31(0)10 427 7100 - Fax: +31(0)10 -427 7170
Web: www.wartsila.com
CEDA Contact Point: Mr. D. Heidelberg

The Corporate Members of CEDA

Members who make a major contribution to our activities for which we thank them

DESIGNERS, BUILDERS AND SUPPLIERS OF DREDGING VESSELS

AJB Dredgeco Ltd.
Ireland
Tel.: +353(0)28 327 04 - Fax: +353(0)28 31 145
Email: ajbdredgeco@eircom.net
Web: www.ajbdredgeco.com
CEDA Contact Point: Mr. A. Birth

AVV Design LCC UA
Ukraine
Tel.: +380 44 583 02 60 - Fax: +380 44 501 53 80
Email: info@avv.com.ua
Web: www.avvdesign.com
CEDA Contact Point: Mr. Oleksii Chernysh

Boogaard Sliedrecht C.V.
The Netherlands
Tel.: +31(0)184 41 51 44 - Fax: +31(0)184 41 14 02
Email: mail@boogaardbrokers.com
Web: www.boogaardbrokers.com
CEDA Contact Point: Mr. G. B. van Leeuwen

Chantiers et Ateliers du Maroc
Morocco
Tel.: +21(2)22 319 030 - Fax: +21(2)22 317 019
Email: info@cam-industries.com
CEDA Contact Point: Mr. E. Chafiq

Commercial Centre, Transport, Les JSC
Russia
Tel.: +7 (812) 784 97 52 - Fax: +7 (812) 784 82 21 7 812
Email: cctl@cctl.ru
Web: www.cctl.ru
CEDA Contact Point: Mrs. Y.A. Abrosimova

Damen Dredging Equipment B.V.
The Netherlands
Tel.: +31(0)33 247 40 40 - Fax: +31(0)33 247 40 60
Email: info@damendredging.com
Web: www.damendredging.com
CEDA Contact Point: D. Tenwolde

Damen Shipyards
The Netherlands
Tel.: +31(0)183 63 99 11 - Fax: +31(0)183 63 21 89
Email: europe@damen.nl
Web: www.damen.nl
CEDA Contact Point: Mr. J.M.J. Neven

IHC Merwede B.V.
The Netherlands
Tel.: +31(0)184 41 15 55 - Fax: +31(0)184 41 18 84
Email: info@ihcmerwede.com
Web: www.ihcmerwede.com
CEDA Contact Point: Ms. R. van Krimpen-Baudesson

Machinefabriek De Hollandsche Yssel B.V.
The Netherlands
Tel.: +31(0)348 56 14 41 - Fax: +31(0)348 56 33 24
Email: info@hollandscheijssel.nl
Web: www.hollandscheijssel.nl
CEDA Contact Point: Ir. R. Vollenbrock

Seadrec Ltd.
U K
Tel.: +44(0)141 887 41 31 - Fax: +44(0)141 887 64 67
Email: seadrec@aol.com
CEDA Contact Point: Mr. B. A. McKinney

VOSTA LMG B.V.
The Netherlands
Tel.: +31(0)20 493 66 66 - Fax: +31(0)20 493 66 70
Email: info@vostalmg.com
Web: www.vostalmg.com
CEDA Contact Point: Mr. R. Dietze

Vuyk Engineering Rotterdam B.V.
The Netherlands
Tel.: +31(0)10 450 25 00 - Fax: +31(0)10 458 72 45
Email: vuyk@vuykrotterdam.com
Web: www.vuykrotterdam.com
CEDA Contact Point: Mr. G. de Vries

DREDGING AND MARINE CONTRACTORS

Archirodon Group N.V.
The Netherlands
Tel.: +31(0)78 613 62 33 - Fax: +31(0)78 613 62 55
Email: info@archirodon.net
Web: www.archirodon.net
CEDA Contact Point: Mr. A. Thedoropoulos

Atlantic Dredging Corporation
Morocco
Tel.: +212 22 947 639 - Fax: +212 22 947 601
CEDA Contact Point: Mr. A. Benali

Baeck & Jansen N.V.
Belgium
Tel.: +32(0)14 31 78 41 - Fax: +32(0)14 31 78 46
Email: bj@baeck.be
Web: www.baeck.be
CEDA Contact Point: Mr. A. Baeck

Baggerwerken Decloedt & Zoon N.V.
Belgium
Tel.: +32(0)59 24 21 40 - Fax: +32(0)59 24 21 80
Email: infodecloedt@deme.be
Web: www.decloedt.be
CEDA Contact Point: Mr. B. Verboomen

De Hoop Terneuzen B.V.
The Netherlands
Tel.: +31(0)115 68 09 11 - Fax: +31(0)115 61 10 66
Web: www.dehoop-terneuzen.nl
CEDA Contact Point: Mr. B.C. van der Peijl

Drapor S.A.
Morocco
Tel.: +212(0)22 54 03 01 - Fax: +21(0)22 23 47 54
Email: gharbi@drapor.com
Web: www.drapor.com
CEDA Contact Point: Mr. M. Bachiri

Dredging and Contracting Rotterdam B.V.
The Netherlands
Tel.: +31(0) 164 266 144 - Fax: +31(0)164 260 454
Email: info@dcrnl.com
Web: www.jandenul.com
CEDA Contact Point: Mr. G. Groot Nibbelink

Dredging Co., Ltd.
Russia
Tel.: +7 911 847 66 76 - Fax: +7 812 440 36 61
Email: igor98@inbox.ru
Web: www.dredging.ru
CEDA Contact Point: Mr. I. Kryukov

Dredging International N.V.
Belgium
Tel.: +32(0)3 250 52 11 - Fax: +32(0)3 250 56 50
Email: dredging@dredging.com
Web: www.dredging.com
CEDA Contact Point: Mr. A. Bernard

Duik Combinatie Nederland B.V.
The Netherlands
Tel.: +31(0)164 21 43 43 - Fax: +31(0)164 25 69 79
Email: info@dcnbv.nl
Web: www.dcndiving.com
CEDA Contact Point: Mr. R. Vriens

Dutch Dredging B.V.
The Netherlands
Tel.: +31(0)184 41 19 99 - Fax: +31(0)184 41 19 98
Email: info@dutchdredging.nl
Web: www.dutchdredging.nl
CEDA Contact Point: Ir. C.J. van de Graaf

E.A. Temile & Sons, Development Company Nigeria Ltd
Nigeria
Tel.: +234 8033 886 231
Email: enquiries@temile.com
Web: www.temile.com
CEDA Contact Point: Mr. G. E. Temile

EDT Marine Construction
Cyprus
Tel.: +35 725 899 000 - Fax: +35 725 899 005
Email: miki@edtmc.com
Web: www.edtmc.com
CEDA Contact Point: Ms. G. M. M. P. Miki Peleg

Emirates Dredging Co. LLC
United Arab Emirates
Tel.: +97 (0)2 634 2700 - Fax: +97(0)2 6334525
Email: edc@anholdings.com
CEDA Contact Point: Mr. A. N. N. A. Al Masaabi

EMODRAGA Mozambican Dredging Company
Mozambique
Tel.: +258 23 327 038 - Fax: +258 23 323 841
Email: emodraga@teledata.mz
Web: www.emodraga.co.mz
CEDA Contact Point: Mr. T. A. C. Adamo

Ghent Dredging N.V.
Belgium
Tel.: +32(0)9 222 6157 - Fax: +32(0)9 222 6106
Email: info@ghentdredging.be
Web: www.ghentdredging.be
CEDA Contact Point: Mr. W. De Schipper

Grab Specialist B.V.
The Netherlands
Tel.: +31(0)356 255 155 - Fax: +31(0)356 255 140
Email: info@tgs-grabs.nl
Web: www.tgs-grabs.nl
CEDA Contact Point: Mr. E. Bleyenberg

Members who make a major contribution to our activities for which we thank them

Jan De Nul N.V.
Belgium
Tel.: +32(0)53 73 15 11 - Fax: +32(0)53 78 17 60
Email: info@jandenul.com
Web: www.jandenul.com
CEDA Contact Point: Mr. J. De Nul

Josef Moebius Bau-Aktiengesellschaft
Germany
Tel.: +49(0)40 800 90 30 - Fax: +49(0)40 800 48 10
Email: kontakt@moebiusbau.de
Web: www.moebiusbau.de
CEDA Contact Point: Mr. W. Moebius

JSC “Mezhregiontruboprovodstroy”
Russia
Tel.: +7(0)95 779 6066 - Fax: +7(0)95 719 4478
Email: pavlov03y@yandex.ru
Web:
CEDA Contact Point: Mr. S. Pavlov

Land and Water Group
U K
Tel.: +44(0)1483 202733 - Fax: +44(0)1483 202 510
Email: enquiries@land-water.co.uk
Web: www.land-water.co.uk
CEDA Contact Point: Mr. A. Gascoyne

Luckamos Limited
Nigeria
Tel.: +234 8060776 914 - Fax: +234 80617 0776914
Email: luckamos@yahoo.com
CEDA Contact Point: Mr. L. Amos

National Marine Dredging Co.
United Arab Emirates
Tel.: +971(0)2 5516 000 - Fax: +971(0)2 5516 500
Email: nmdc@emirates.net.ae
Web: www.nmdc.ae
CEDA Contact Point: Mr. Ahmed Hamad Nasser Al-Mazroui

National Port Authority of South Africa
South Africa (W)
Tel.: +27(0)31 361 8575 - Fax: +27(0)31 361 8395
Email: dredging@npa.co.za
Web: www.npa.co.za
CEDA Contact Point: Mr. P. Mannar

Royal Boskalis Westminster N.V.
The Netherlands
Tel.: +31(0)78 696 9822 - Fax: +31 78 69 69 020
Email: royal@boskalis.nl
Web: www.boskalis.com
CEDA Contact Point: Mr R T Schuttevaer

Shoreline Chemicals & Oil Services
Nigeria
Tel.: +23(4) 84 23 94 29 /48 51 71 - Fax: +23(4)84 84 23 07 33
Email: shoreline@shorelineng
Web: www.shorelineng.com
CEDA Contact Point: Mrs. L. Amos Oluwole

Terramare Oy
Finland
Tel.: +358(0)9 613 621 - Fax: +358(0)9 613 62700
Email: terramare@terramare.fi
Web: www.terramare.fi
CEDA Contact Point: Mr. J. Sederholm

UK Dredging (ABP)
U K
Tel.: +44(0)29 2086 5200 - Fax: +44(0)29 2083 5216
Email: ukd@abports.co.uk
Web: www.abports.co.uk
CEDA Contact Point: Mr. P. Mitchell

Van den Herik / Sliedrecht B.V.
The Netherlands
Tel.: +31(0)184 41 28 81 - Fax: +31(0)184 41 98 21
Email: Sliedrecht@Herik.nl
Web: www.Herik.nl
CEDA Contact Point: Mr. A. Struijk

Van der Kamp International B.V.
The Netherlands
Tel.: +31(0)38 421 75 47 - Fax: +31(0)38 421 59 75
Web: www.vanderkampbv.nl
CEDA Contact Point: Mr. H. Veerman

Van Oord Dredging and Marine Contractors B.V.
The Netherlands
Tel.: +31(0)10 447 84 84 - Fax:
Email: info@vanoord.com
Web: www.vanoord.com
CEDA Contact Point: Ir. S. Burgmans

Wasa Dredging Ltd.
Finland
Tel.: +358 6 3444 112 - Fax: +358 6 3444 110
Web: www.wasadredging.fi
CEDA Contact Point: Mr. K. Backlund

Wilol Nigeria Ltd.
Nigeria
Tel.: +44(0)205 317 10 10 - Fax: +44(0)205 317 10 10
CEDA Contact Point: Mr. E. Williams

GOVERNMENT ORGANISATIONS AND PUBLIC WORKS

British Waterways
U K
Tel.: +44(0)113 284 52 00 - Fax: +44(0)113 281 68 86
Email: enquiries.hq@britishwaterways.co.uk
Web: www.britishwaterways.co.uk
CEDA Contact Point: Mr. N. Smith

Centre for Environment, Fisheries and Aquaculture Science (CEFAS)
U K
Tel.: +44 (0)1502 527703 - Fax: +44(0)1502 513865
Email: infoservices@cefas.co.uk
Web: www.cefas.co.uk
CEDA Contact Point: Dr. A. Birchenough

Danish Coast Authority
Denmark
Tel.: +45-99 63 63 63 - Fax: +45-99 63 63 99
Email: kdi@kyst.dk
Web: www.kyst.dk
CEDA Contact Point: Ms. S. Ingvardsen

Femern Baelt A/S
Denmark
Tel.: +45 33 41 63 00 - Fax: +45 33 41 63 01
Email: info@sbf.dk
Web: www.fehmarnlink.com
CEDA Contact Point: Mr A. Jensen

German Federal Ministry of Transport, Building and Urban Affairs
Germany
Tel.: +49(0)228 300 4245 - Fax: +49(0)228 300 3428
Web: www.bmvbs.de
CEDA Contact Point: Mr. H. Koethe

GIE Dragages-Ports
France
Tel.: +33(0)2 32 7645 50 - Fax: +33(0)2 32 7645 52
Email: dir.dp@dragages-ports.fr
CEDA Contact Point: Mr. M. David

Instituto Portuario e dos Transportes Maritimos
Portugal
Tel.: +351(0)21 391 4579 - Fax: +315 (0)21 91 4762
Email: imarpor@mail.telepac.pt
Web: www.imarpor.pt
CEDA Contact Point: Ms. E. Dias

Marine Laboratory Aberdeen
U K
Tel.: +44(0)1224 876 544 - Fax: +44(0)1224 295 524
Web: www.marlab.ac.uk
CEDA Contact Point: Mr. J. McKie

Marsa Maroc
Morocco
Tel.: +21(2)22 232 23 24 - Fax: +21(2)22 257 481
Email: secdg@odep.org.ma
CEDA Contact Point: Mr. M. Abdeljalil

Ministry of the Flemish Community
Belgium
Tel.: +32(0)3 222 08 69 - Fax: +32(0)3 222 08 51
Web: www.lin.vlaanderen.be/awz/
CEDA Contact Point: Mrs. I. De Jonghe

Ministry of the Flemish Community, Coastal Waterways Division
Belgium
Tel.: +32(0)59 554 207 - Fax: +32 59 554 207(0)
Web: www.awz-kust.be
CEDA Contact Point: Ir. B. De Putter

Ministry of Water Resources
Iraq
Tel.: +96 47 901 388 592 - Fax: +96 455 610 60
Web: www.iraq-mowr.org
CEDA Contact Point: Mr. S.H. Shakir

Rijkswaterstaat Dir. Noordzee
The Netherlands
Tel.: +31(0)70 336 66 08 - Fax: +31(0)70 390 06 91
Email: secretariaat-bvmd@rws.nl
Web: www.noordzee.org
CEDA Contact Point: Ir. J. Visser

Seprob
Morocco
Tel.: +21(2)22 2003 89 - Fax: +21(2) 22 2001 22
Email: sebrob@techno.net.ma
CEDA Contact Point: Mr. M. Mohamed

The Corporate Members of CEDA

Members who make a major contribution to our activities for which we thank them

MEDIA

Clarkson Research Services Ltd.
U K
Tel.: +44(0)15 31 63 4561 - Fax: +44(0)1531634 239
Email: opl@oilpubs.com
CEDA Contact Point: Ms. J. Vatson

Lloyd's Register Fairplay
U K
Tel.: +44(0)1 737 379 000 - Fax: +44(0)1 737 379001
Web: www.lrfairplay.com
CEDA Contact Point: Mr. T. Slinn

Marine and Coastal Construction Service (MACCS)
U K
Tel.: +44 20 7060 3000 - Fax: +44 20 7060 3099
Web: www.maccs.co.uk
CEDA Contact Point: Mrs D Heijer

PORT, MARITIME AND NAVIGATIONAL AUTHORITIES

Administration Des Ports
Guinee

Gemeentelijk Havenbedrijf Antwerpen
Belgium
Tel.: +32(0)3 205 23 44 - Fax: +32(0)3 205 23 35
Web: www.portofantwerp.be
CEDA Contact Point: Ir. E. De Broe

Hamburg Port Authority
Germany
Tel.: +49 (0)40 428 47 2791 - Fax: +49(0)40 428 47 2794
Web: www.hamburg-port-authority.de
CEDA Contact Point: Mr. A. Netzband

Port Autonome De Conakry
Guinee

Port Autonome de Dakar
Senegal
Tel.: +22(1)849 45 45 - Fax: +22(1)823 36 06
Web: www.portdakar.sn
CEDA Contact Point: Mr. A. Kane

Port Autonome de Lome
Togo
Tel.: +228 227 47 42 - Fax: +228 227 26 27
CEDA Contact Point: Mr B. Awa

Port Autonome de Nouakchout
Mauritania
Tel.: +22(2)525 17 94 - Fax: +22(2)525 16 15
CEDA Contact Point: Mr. O.D.M. Mahmoud

Port Autonome de Nouhadibou
Mauritania
CEDA Contact Point: Mr. Waddou

Port of London Authority
U K
Tel.: + 44(0)1474 562241 - Fax: +44(0)1474 562314.
Web: www.portoflondon.co.uk
CEDA Contact Point: Ms. K. Harris

Port of Rotterdam N.V.
The Netherlands
Tel.: +31(0)10 252 10 10 - Fax: +31(0)10 252 49 65
Email: info@portofrotterdam
Web: www.port.rotterdam.com
CEDA Contact Point: Ir. T. Vellinga

Satram
Gabon
Tel.: + 241 55 37 40 - Fax: +241 56 28 63
CEDA Contact Point: Mr. G. Raymond

SERVICES (E.G. INSURERS, LAW FIRMS, FINANCIAL AGENCIES, TOWAGE COMPANIES)

Acta Marine Waterweg
The Netherlands
Tel.: +31(0)223 615 666 - Fax: +31(0)223 614 360
Email: info@actamarine.com
Web: www.actamarine.com
CEDA Contact Point: Mr. J. Peute

Aon Hudig
The Netherlands
Tel.: +31(0)104487660 - Fax: +31(0)104769691
Web: www.aon.com
CEDA Contact Point: Mr. J. Kuyper

Atlas Services Group B.V.
The Netherlands
Tel.: +31(0)24 110 43 - Fax: +31(0)24 110 77
Email: info@atlasgroep.nl
Web: www.atlasgroep.nl
CEDA Contact Point: Mr. D. Streefkerk

Damen Shiprepair Rotterdam B.V.
The Netherlands
Tel.: +31(0)10 204 12 22 - Fax: +31(0)10 473 25 77
Email: dsr@damenshiprepair.com
Web: www.damenshiprepair.com
CEDA Contact Point: Mr. J. van Leuven

Dockwise Shipping B.V.
The Netherlands
Tel.: +31(0)76 548 41 00 - Fax: +31(0)76 548 42 99
Email: headoffice@dockwise.com
Web: www.dockwise.com
CEDA Contact Point: Mr. R. Schoenmaker

Inchcape Shipping Services
Dubai, U.A.E.
Tel.: +971 4 374 3737 - Fax: +971 4 374 3707
Email: offshorelogistics@iss-shipping.com
Web: www.iss-shipping.com
CEDA Contact Point: Mr. D. Whysall

Independent Risk Solutions B.V.
The Netherlands
Tel.: +31(0)10 440 0555 - Fax: +31(0)10 440 0556
Web: www.irs-risksolutions.nl
CEDA Contact Point: Mr. H. Liem

IPS Group
The Netherlands
Tel.: +31(0)104479494 - Fax: +31(0)102357878
Email: info@ipspersonnel.com
Web: www.ipspersonnel.com
CEDA Contact Point: Mr. L. Th. Oostendorp

Lloyd's Register EMEA
The Netherlands
Tel.: +31(0)10 414 50 88 - Fax: +31(0)10 411 51 05
Email: LROS@lloyds-register.nl
Web: www.lloyds-register.nl
CEDA Contact Point: Ir. T. F. van der Werff

Rabobank Nederland Corporate Clients
The Netherlands
Tel.: +31(0)30 216 47 69 - Fax: +31(0)30 216 19 75
Web: www.rabobank.com
CEDA Contact Point: Mr T. Wouterse

RGR Shipping & Forwarding
The Netherlands
Tel.: +31(0)180 692 600 - Fax: +31(0)180 692 611
Web: www.rgr.nl
CEDA Contact Point: Mr. R. van den Berg

SAIO Safety Training (Offshore Division)
The Netherlands
Tel.: +31 (0)10 204 22 55 - Fax: +31(0)10 204 22 44
Email: info@saio.nl
Web: www.saio.nl
CEDA Contact Point: Mr. H. Heyster

STC B.V. Location MSR
The Netherlands
Tel.: +31(0)10 486 66 54 - Fax: +31(0)10 484 60 71
Email: info@stc-r.nl
Web: www.msr-r.nl
CEDA Contact Point: Mrs. M. Behrend

Transport & Offshore Services
The Netherlands
Tel.: +31(0)10 436 6293 - Fax: +31(0)10 436 6286
Email: info@tos.nl
Web: www.tos.nl
CEDA Contact Point: Mr. R. van der Kolk

Univers Beton
Morocco

OTHER

Nationaal Baggermuseum
The Netherlands
Tel.: +31(0)184 414166 - Fax: +31(0)18410 2894
Email: info@baggermuseum.nl
Web: www.baggermuseum.nl
CEDA Contact Point: Mr. Drs J. Wijn

Sigeprag
Gabon

DREDGING ROCK WITH A HOPPER DREDGER: THE ROAD TO THE RIPPER DRAGHEAD

R.F.J. Neelissen[1], A. Tanis[2], V.C. van Gool[3]

Abstract: After an extensive selection process in 2004 Boskalis Australia Pty Ltd was selected by the Port of Melbourne Corporation to execute the Melbourne Channel Deepening Project. The aim of the project was to make the Port of Melbourne accessible for 14 meter draught vessels at all tidal conditions. One of the most challenging parts of the project was the deepening of the Entrance to Port Phillip Bay, which is located in an environment characterized by a rock bottom, strong tidal currents, a persistent and long swell, regular shipping traffic and a National Marine Park abundant in deep reef fauna nearby. The metocean conditions prohibited the deployment of a cutter suction dredger and the use of drilling and blasting. The latter method was also not preferred because of social and environmental reasons. Seeing the metocean constraints, a trailing suction hopper dredger remained as the preferred equipment for the project. However, the layered, cemented limestone was too strong to be dredged with conventional dragheads. This paper describes the development of a ripper draghead, capable of dredging rock.

Several parts of the dredging process were object of research. Literature and former tests were analyzed to derive the forces required for cutting the rock. A model was made to predict the cutting capabilities of ripper dragheads. Several types of pickpoints and cutting geometries were investigated during cutting tests with a test-cart equipped with measuring and logging instruments in a quarry. The ripper draghead was engineered and constructed after having determined the optimal teeth configuration with respect to forces and dimensions of the cut rock. In addition, vessel motion and vessel maneuvering studies were undertaken to investigate the operational limits of the dredger. The vessel crew was trained on a dredging vessel simulator whereby the actual currents and the predicted cutting forces were used as inputs.

A full scale trial dredging campaign was undertaken with a trailing suction hopper dredger, the Queen of the Netherlands, in 2005. The trial demonstrated that the rock at the Entrance could be dredged with the ripper draghead. Extensive video monitoring showed that the dredging process had to be optimized with respect to the loose material left behind after dredging. Additional laboratory tests with a scale model of the ripper draghead were performed at the Delft Hydraulics Laboratory. The tests focused on the optimization of the suction process by investigating the effectiveness of the draghead's water jets and the influence of different draghead geometries. Based on the laboratory results, the existing ripper dragheads were modified and the work method was amended.

The entire Entrance was successfully dredged from April to September 2008. The realized productions accorded with the estimated productions and video surveys proved that the quantity of loose material left behind was well within expectations.

Keywords: ripper draghead, rock, exposed working area, morphology

[1] Development Engineer, Baggermaatschappij Boskalis bv, Rosmolenweg 20, P.O. Box 43, 3350 AA, Papendrecht, The Netherlands, +31 (0)78 6969657, r.f.j.neelissen@boskalis.nl

[2] Technical Engineer, Baggermaatschappij Boskalis bv, Rosmolenweg 20, P.O. Box 43, 3350 AA, Papendrecht, The Netherlands, +31 (0)78 6969327, a.tanis@boskalis.nl

[3] Production and Planning Engineer, Boskalis Australia, 31 South Wharf, 583-611 Lorimer Street, Fisherman's Bend, VIC 3207, Australia, +61 (0) 399221736, vincent.vangool@portofmelbourne.com

1. INTRODUCTION

The size of trailing suction hopper dredgers (TSHD) has been significantly enlarged over the last decennia. Starting with the first jumbo dredger Pearl River, built in 1994, the hopper volumes have increased from 17.000m^3 up to 35.500m^3 nowadays, such as the Queen of the Netherlands. Currently, TSHD's are being built with a hopper volume of approximately 46,000 m^3. Obviously, the total installed power, the propulsion power, the dimensions of the suction tubes, and the size and weight of the dragheads have also increased. Due to these developments harder soils and even rock, which are normally dredged with a cutter suction dredger (CSD), can now also be dredged with a TSHD.

But why deploying TSHD's in harder materials if CSD's are already capable of dredging rock?
A significant difference between the TSHD and the CSD is the workability. Large CSD's can not work in wave heights exceeding 1m, but TSHD's are capable of dredging in waves up to 3m. For a CSD, strong currents prevent the use of a floating discharge line, whereas the maneuvering of a TSHD will be slightly affected only. In addition, jumbo trailing suction hopper dredgers can dredge significantly deeper than CSD's and they are much more flexible in relation to shipping traffic. In general the costs for mobilization of a CSD are higher than for a TSHD.
For the Melbourne Channel Deepening project, workability and shipping traffic were the drivers to explore the dredging of rock with a TSHD further.

For deepening the Entrance to Port Phillip Bay to -17.3 meter, a thickness of approximately 3 meter of rock had to be dredged at Nepean Bank and Rip Bank. The Entrance is a channel of 235m wide with regular shipping traffic. Severe metocean conditions (strong currents and high swell) excluded dredging by a CSD. In addition to metocean constraints, also environmental and social constraints prohibited the use of drilling and blasting of the rock. However, vessel motion and vessel maneuvering studies showed that the workability for a jumbo trailing suction hopper dredger was good.

The Port of Melbourne Corporation conducted a soil investigation with a jack-up platform in the Entrance in 2003. This investigation took 8 weeks to complete and comprised 10 boreholes (see figure 1), showing that the seabed is underlain by a layered sequence of “dune calcarenites”; siliceous calcarenite, calcareous sandstone and sand belonging to the Bridgewater Formation. Strength tests and seismic investigation indicate that for this type of rock a CSD would normally be deployed.

As a TSHD was the preferred dredger to be used, the focus was on the development of a draghead, capable of dredging the rock in the Entrance.

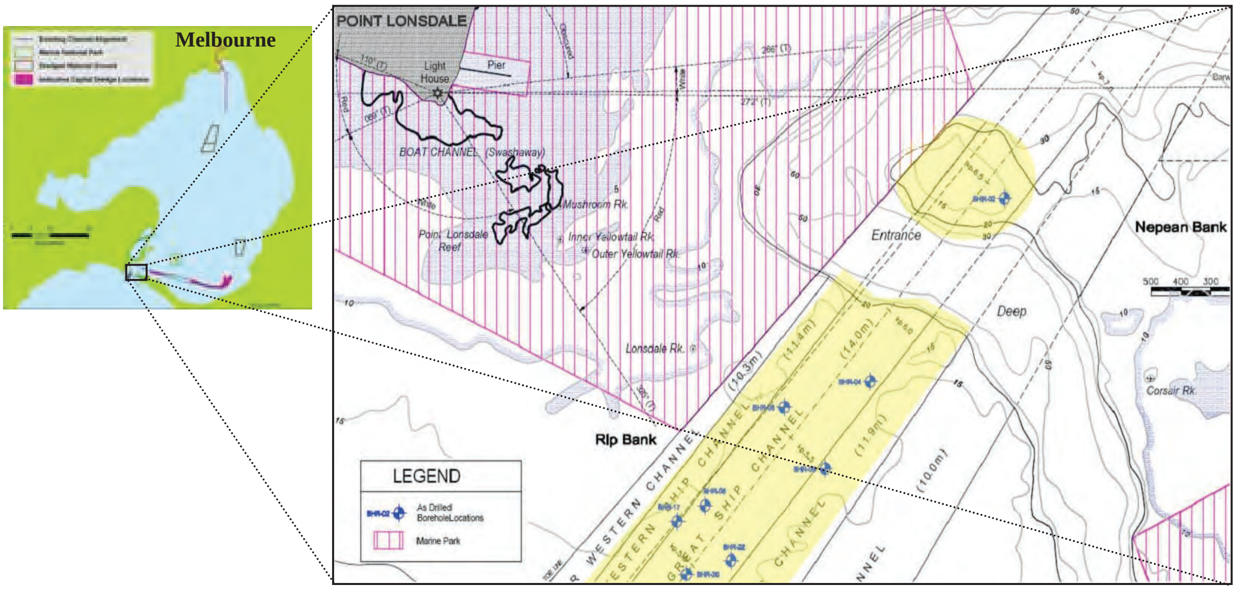

Figure 1: Overview of Port Phillip Bay (left) and the Entrance, showing the Nepean Bank (upper area), the Rip Bank, the area to be dredged (yellow) and the locations of boreholes (right).

This project was incorporated in the R&D program of Boskalis and a project group was formed by the R&D Department, Technical Department and Dredging Department to integrate knowledge regarding the cutting process, production levels, soil characteristics and construction details.

The development process started with a desktop study. This study comprised an inventory of rock cutting theories, analysis of laboratory cutting tests and collecting knowledge on ripping by bulldozers in various rock types.

The desktop study led to relations between properties of the rock and the force levels required for cutting the rock. A model was set up for the cutting of rock with a TSHD equipped with a ripper draghead. This model predicts the maximum strength of rock that can be dredged, depending on characteristics like propulsion power, trailing speed, draghead weight and draghead layout. The cutting production, depending on the strength of the rock, is also predicted. Figure 3 shows a generic result of the model for a particular TSHD equipped with a ripper draghead with different numbers of teeth:

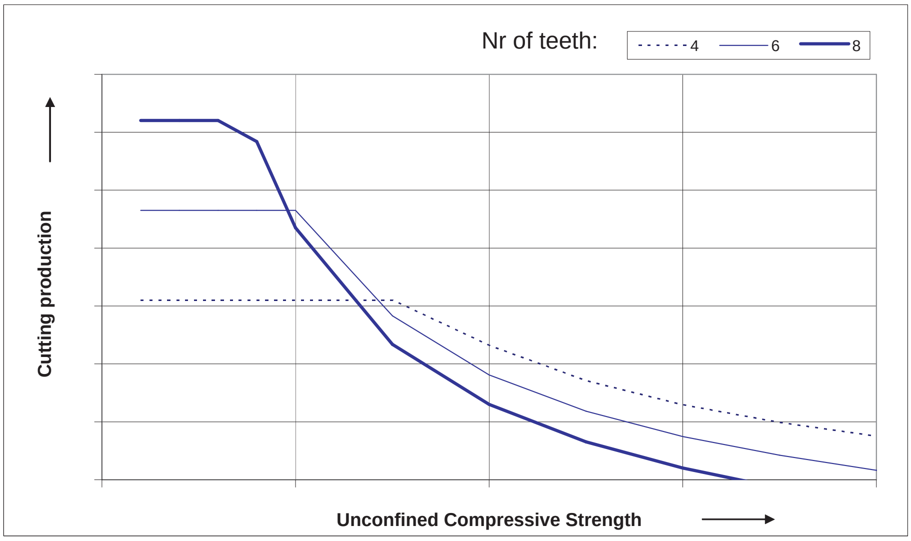

Figure 3: Example of calculated cutting production depending on rock strength

The figure indicates that the teeth won't penetrate if the rock strength exceeds a certain limit. As a consequence, the production will be zero unless the number of teeth is reduced.

2. CUTTING TRIALS IN THE QUARRY

For the optimization of the design of the draghead an experimental test program in an Australian quarry was proposed. The general set up comprised a bulldozer pulling a test cart equipped with ripper teeth or pickpoints. The aim of the tests was to gain insight in the cutting forces, penetration forces and the size of the cut rock. The size of the cut rock is important because large rock lumps might block the drag head or even worse, block the dredging pump.
Several quarries in the vicinity of Melbourne were visited, and the geological setting and mechanical properties of the present rock were investigated. The quarry for the test program was selected based on the good similarity with the rock properties in the Entrance. Seismic velocities measured in the quarry were approximately the same as those measured in the Entrance. The conclusion from the study was that the rock in the quarry was representative of the rock in the Entrance, with respect to strength, layering and cementation.

A test cart with ripping teeth was built, to be pulled by a bulldozer, see figure 4:

Figure 4: Bulldozer pulling the test cart with ripper teeth

At the quarry two sites were selected for testing. The first site consisted of weakly cemented sands with densely cemented rock concretions and extensive rock ridges, representing the areas at the Entrance where caprock is present. The second pit consisted of layered aeolianite rock that compared well with the rock encountered in the boreholes at the Entrance. During each test the cutting forces and penetration forces on the ripper teeth were derived from load pins. After removal of the cut rock in the track, the groove patterns were mapped. From these measurements the cutting production and the specific energy of the rock could be derived. The dimensions of the cut rock were measured after each test. Samples of the cut rock were collected for strength analysis.
The cart was constructed in such a way that the number of teeth, the type of teeth and the space in between the teeth could be varied. In addition, the cutting depth and cutting angle of each tooth could also be varied.

Although the cutting process above and under water show many similarities, there are some differences: cutting in dry rock is a drained process, while cutting under water in saturated rock might be an undrained process. To quantify the differences between the cutting process above and under water, a separate study was conducted by Delft Hydraulics. The results of this desktop study were used to translate the measured forces, breakout patterns and production levels in the quarry to the underwater situation.

Fifty tests were conducted to achieve an optimal layout of the cutting geometry with acceptable force levels and production levels. The size of the cut rock was sufficiently small to pass the suction mouth of the draghead and the pump, minimizing the risk of blocking, see figure 5. Based on the quarry tests the basic design criteria for the ripper draghead were established, like the weight of the draghead and number and type of the pickpoints. Also the optimal cutting depth and the spacing between the pickpoints were derived from the quarry tests.

Figure 5: Results of 3 tests, showing significant difference in dimensions of the cut rock

3. DESIGN OF THE RIPPER DRAGHEAD

The data of the cutting tests in the quarry and the results of the desk studies on the cutting and the breaking of rock were used as inputs for the design phase of the ripper draghead.

First issue was to define the design criteria and the risks. The forces which could be expected during normal operation were known from the quarry tests. However, besides these normal cutting forces, the expected harsh operational conditions will cause external forces affecting the construction. The ripper draghead or suction pipe may hit the edge of the Rip Bank and additional vertical forces will be generated when the draghead lands on the rock bottom while the ship is rolling in 3 meter waves. The draghead may be subject to sideward movements when the motions of the ship and the suction pipe are influenced by the long waves and strong currents in the Entrance. All teeth may simultaneously hit a hard rock edge and cause extreme force levels.
The greatest risk is damage to the suction pipe and to the connection of the suction pipe with the ship’s hull. Several measures were designed to protect the construction against these peak loads and to avoid damage of the construction.
To determine the force levels for the design of these safety measures vessel motions, vessel maneuverability and the structural integrity of the suction pipe and the vessel were analyzed into great detail. An extensive study was started to find out which limit should be observed to minimize the risk of incurred delays due to damage.

Based on the results of the quarry tests and risk analysis the design criteria could be translated into the design of the ripper draghead and the protection of the pipe construction. The draghead consists of a helmet and a visor.. The helmet is the base construction, including the suction mouth, which has to collect the ripped rock. The function of the visor is to cut the rock with its teeth. A safety break pin construction was designed in the connection of the visor with the helmet. This construction was based on a pre-stressed pin, which should break before the construction is overstressed. If an overload occurs due to too high forces on the teeth, the pin will break and the visor can swing away to the back and the teeth will loose contact with the rock. The sensitivity for fatigue is a weak point of a normal break pin construction, and because of that, the lifetime of the pin material is affected. If this would cause to break instead of an overload, it would result in an unnecessary delay of the ship.

The lower part of the suction pipe is exposed to bending by its own weight and the forces generated by the ripper draghead. Besides that, a typical risk at the Melbourne project concerns the collisions of the pipe with the sharp edges of protruding rock ridges and with the edge of the canyon, a geological erosion feature in the Entrance. This will cause buckling and bending of the pipe, followed by breaking. To guarantee the integrity a protection unit was constructed and installed at the lower side of the suction pipe. Impact by collisions is damped in this way. During the project this has proven to be effective.

For picking up the rock, a minimum speed of the water flow is required. Proper matching of the dredge pump capacity and the suction inlet of the helmet is very important to avoid blockage and spillage behind the draghead. The photos and films which were made of the quarry tests were very helpful to examine how the rock was cut by the teeth and what would be the best design in which the water flow would pick up as much rock as possible.

Another point of attention was the wear of the draghead. The dragging of the heavy draghead on the rock bottom and the hydraulic transport of the stones with high suction speed causes enormous wear of the construction. To combat the wear, wear resistant material was added on several critical locations in the design.

The design of the draghead was optimized by means of FEM calculations. All expected load cases were considered in these calculations.

During the final design phase a selection procedure for a manufacturer of the dragheads was started. Criteria for the selection were: Quality of steelwork and welding, references of similar jobs, organization of the orders, capacity, price and delivery time. After the selection three ripper dragheads were built in Australia according to high quality standards. The construction was observed and checked by a superintendent every day.

4. FULL SCALE TRIAL AT THE ENTRANCE

To determine the environmental effects of dredging in general and to see whether the TSHD was able to dredge the rock at the Entrance of Port Phillip Bay, a full scale dredging trial was conducted in 2005,. Part of the Entrance to Port Phillip Bay was designated as trial area. In August, the TSHD Queen of the Netherlands dredged for two weeks to demonstrate that the ripper draghead technology (figure 6) was capable of dredging the rock in the Entrance.

Figure 6: The ripper draghead at the suction pipe of the Queen of the Netherlands

An extensive follow-up program of the trial was set up. Amongst other attention points it comprised the measurement of production, vessel motions and stresses and loads in the suction tubes. Also the properties of the dredged material were analyzed in detail. A wave buoy located nearby was used for real time monitoring the wave height and direction. Also two ADCP profilers were installed on the bottom near the trial area to obtain current and wave spectrum information. Every day the survey vessel performed a survey at the trial area to gain insight in the progress and in the development of the bottom roughness.
The forces in the suction tubes were measured by load pins in the hinges. No stress limits were exceeded, the theoretical models were confirmed and the integrity of the suction pipe and hull connection could be guaranteed. The cutting forces were roughly comparable with the forces measured during the tests at the quarry. Minor damage to the draghead was encountered, probably caused by collisions with seabed ridges. To reduce the bottom roughness, the dredging method initially aimed at high spots in order to flatten the sea bottom. The survey after the trial showed a significantly smoother sea bottom than before starting the operations, see figure 7:

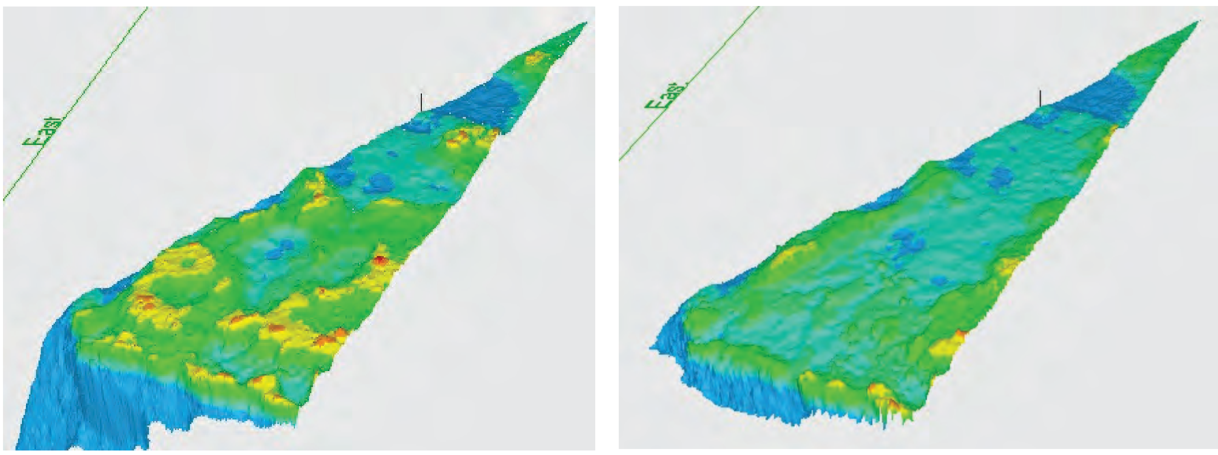

Figure 7: The insurvey (left) and outsurvey (right) of the trial area

During the two week trial in the Entrance about 30.000m^3 was dredged, which was well in agreement with the production levels estimated from the quarry tests. At hard spots the production was lower, sometimes significantly, but the trial showed that all rock could be dredged.

Rock samples were collected from the draghead and from the hopper. Geotechnical analysis by the University of Melbourne showed that UCS values generally varied between 1 - 30 MPa. The strength of two very dense samples was respectively 71 and 112 MPa.

During the trial the work method was evaluated and optimized. At the time the crew got used to the complex currents, the sailing patterns were adjusted. The setting of the swell compensator, determining the effective weight of the draghead, was optimized and two pickpoint types were tested. Eventually an optimal balance was derived between effective draghead weight, forces in the pipe and production.

Several photo and video inspections were made by divers and a comparison was made between the actual dredging test and the ripping tests in the quarry. Both situations are shown in figure 8.

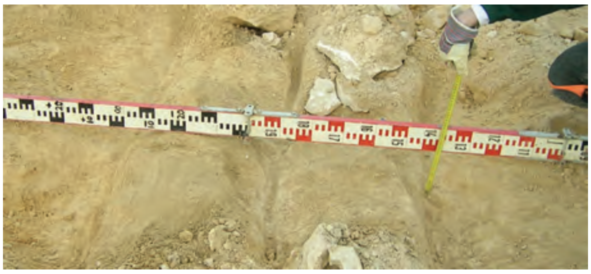

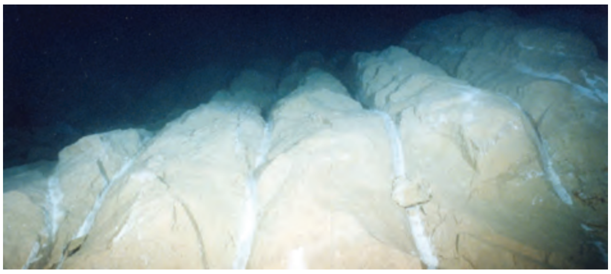

Figure 8: Groove patterns, measured in the quarry (left) and photographed by divers at the trial area (right)

However, the inspections also showed that the amount of stones remaining on the seabed after dredging should be reduced. These stones were not stable under the present currents and waves and could potentially be relocated to other areas, which was not acceptable.

5. LABORATORY RESEARCH

The full scale trial showed that the cutting process of the ripper draghead was well in line with the expectations, but additional research was necessary to improve the suction characteristics of the draghead, aiming at minimization of the amount of stones left behind on the sea bottom. Experiments with a scale model draghead appeared the best way to visualize and analyze the suction process. Because of their experience and their suitable laboratory facilities Delft Hydraulics was engaged for the test program. A scale model of the ripper draghead was constructed and the sea bottom was simulated by preparing a layer of cemented gravel in the dredging flume. A test comprised a passage of the draghead through the prepared bed over several metres. The passage was monitored through a glass wall. Underwater video cameras were used for registration and sensors were installed for measuring operational parameters.

The test program was focused on the variation of relevant parameters like suction flow, jet flow, geometry of the drag head and suction mouth. Operational parameters were scaled in accordance with Froude's law. Because a flat sea bottom does not represent reality, also the influence of the topography of the sea bottom was investigated.
The material left behind after passage of the draghead was measured by a laser survey system (see figure 9) and checked by simple weight measurements of the loose material. The test program was arranged into resemblance tests, insight tests and optimization tests.

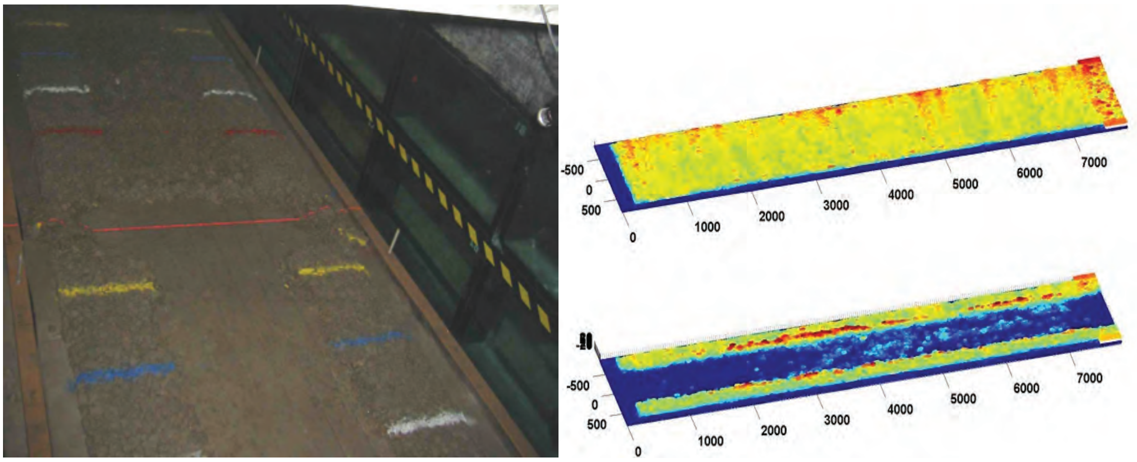

Figure 9: Measuring bottom topography with laser (left) and result of laser measurement before and after the passage of the draghead (right).

The resemblance tests, in which the model draghead and operational parameters were equal to the draghead used at the full scale trials in Melbourne, showed that not all cut material was removed. Then the influence of the jet flow, suction flow, geometry of the draghead and suction mouth was investigated and adjusted during insight tests. The final lay-out of the draghead was established in the optimization tests. Compared with the original lay out, a significant improvement in suction characteristics was achieved, as can be seen in the next pictures:

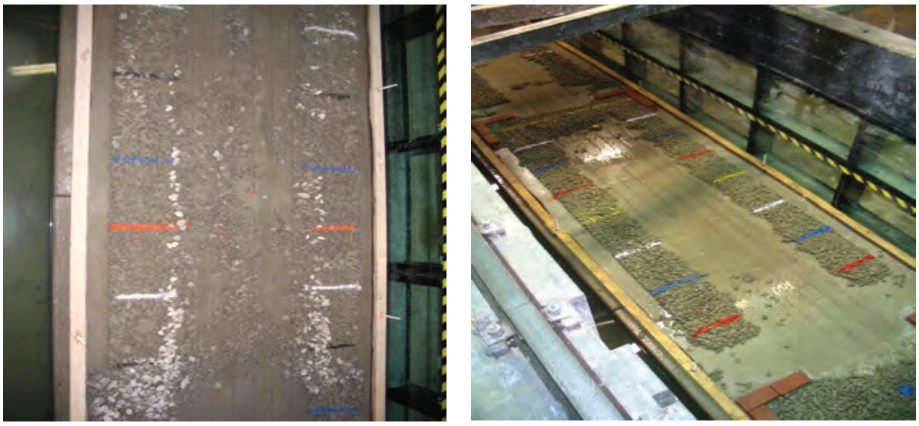

Figure 10: Test with the original draghead layout showing spill in the track (left) and results of the optimal draghead with a very clean bottom (right)

In accordance with the results of the laboratory tests the ripper dragheads in Australia were modified and tested further on the Salalah project in Oman where approximately 1.000.000 m^3 was dredged. The dredging of the Entrance of the Melbourne Channel Deepening project could start with fully developed and well tested ripper dragheads in the beginning of April 2008.

6. MELBOURNE PROJECT

A total of 140.000 m^3 of rock had to be dredged at the Nepean Bank and 135.000m^3 at the Rip Bank. The borehole data suggests that a Holocene aged layer of gravelly sand and blocks of cemented carbonate overlies in patches a Bridgewater Formation siliceous calcarenite, calcareous sandstone and sand (figure 11 and 12). Petrological analysis (Holdgate & Wallace, 2004) indicates that in some cases, additional cementation has taken place near the seabed surface, probably adding to the strength near the seabed surface. This additional cementation is of marine origin (i.e. calcite precipitated directly from sea water). Marine cements are also present in the gravel fragments overlying the Bridgewater Formation. This contrary to the older calcite cement of the rock, which is of fresh water origin (cement precipitated from meteoric water when the dune deposits were above sealevel).

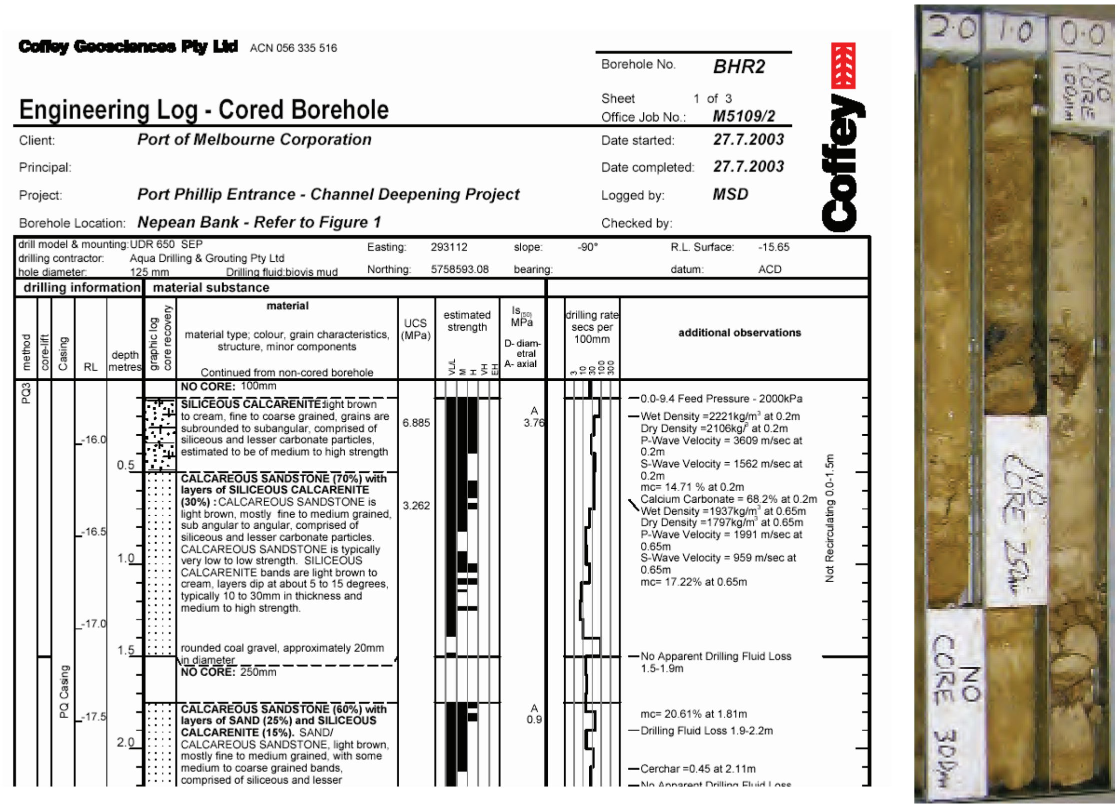

Figure 11: The only available borehole on Nepean Bank, with indication of a hard top layer

Figure 12: Typical Bridgewater formation found on shore and assumed to be similar to the formation in the dredge area

Based on the available soil information, it was estimated that a small amount of the total volume could not be dredged directly by the ripper dragheads. As contingency, a dedicated hydraulic hammer system was designed which could be positioned using a dynamically positioned vessel and swell compensated arm, to pre-treat this harder rock.

With 80% of the time waves having a significant height (H_s) larger than 1.0 meter (see figure 13) and currents up to 3.5 m/s, and approximately every hour a vessel passing by, conditions were more suitable for a jumbo trailer suction hopper dredger, than any other type of dredge.

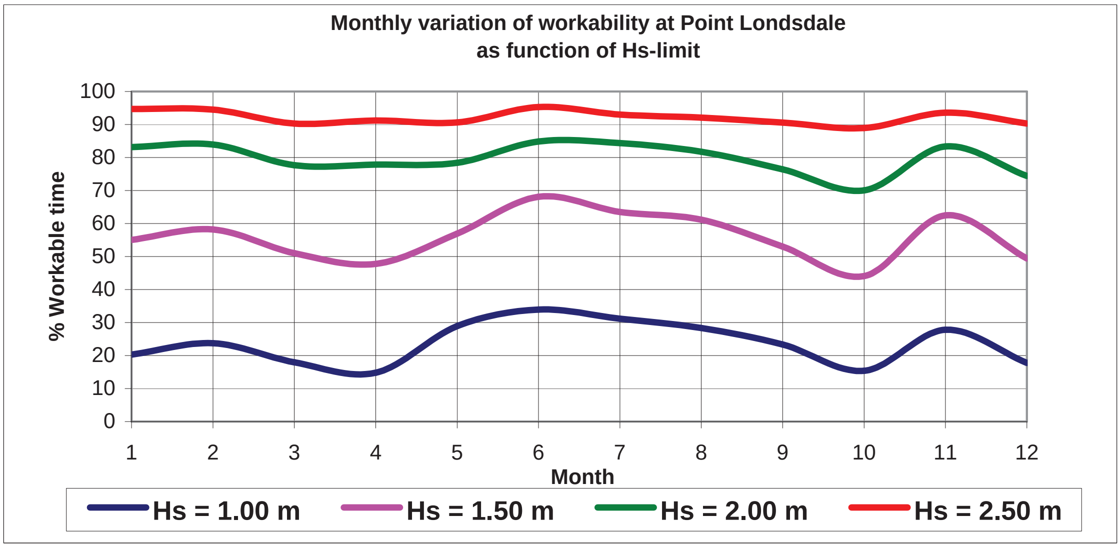

Figure 13: Workability graph

To protect the Port Phillip Heads Marine National Park close to Nepean Bank, a ridge of at least 5 m wide along the north-west edge of the Nepean Bank had to be left in place, until the remaining area was dredged to the required design depth. Strict environmentally enforced control was set to prevent loose material to fall into the adjacent deep, locally known as the canyon. In addition, dredging of the canyon edges (North edge of the Rip Bank and all edges of the Nepean Bank), was conducted from the canyon towards the plateau. When dredging towards the canyon, the dragheads were lifted so that no rock was removed within 5m of the edge.

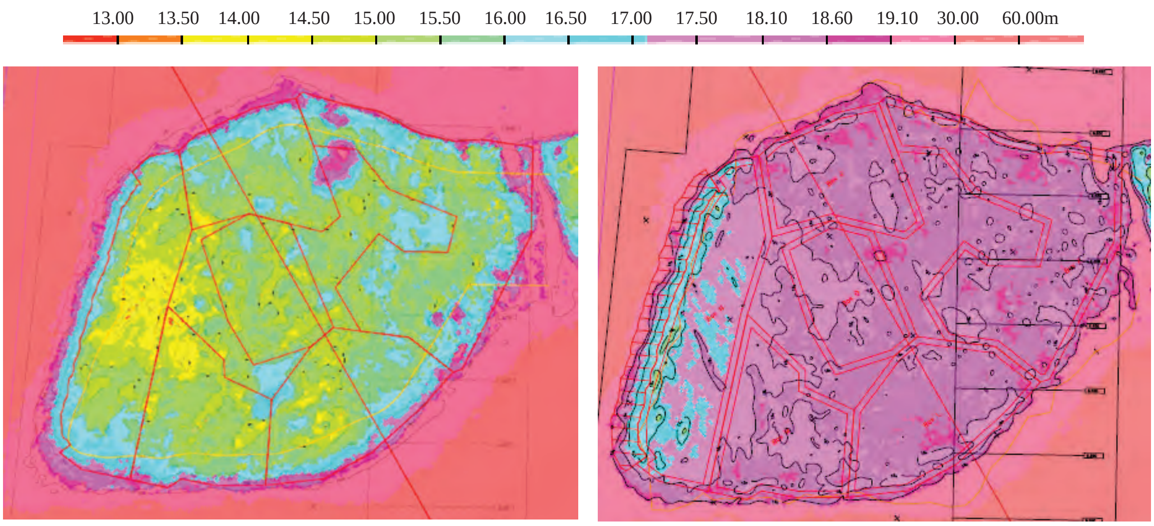

Figure 14: The NW Ridge of the Nepean Bank was left in place until the remaining area was dredged to design. Left: insurvey, Right: survey before start of removal of the NW Ridge

Regular clean up of the dredged area was required to avoid accumulation of loose material on the seabottom. Special teeth were fitted on the ripper dragheads and the swell compensator pressure was set on a high level to avoid that new material was cut during clean up. A dedicated software application was used to register the area covered during the clean up operation.
During the dredging works, dragheads were inspected on a regular basis. During these inspections, rock samples were collected. All samples were selected on having only fresh cut sides, so it can be assumed they were ripped from the bed by the dragheads and not already present as loose stones beforehand. Only larger rock lumps with

a certain minimum strength got stuck in the draghead. In the hopper the very weakly cemented part of the volume was found as sand or as coin sized fragments.

Figure 15: Typical samples of rock that are removed from the draghead.

With all available soil information, together with production figures and survey progress, it could be confirmed that the initial estimated amount of hard rock (UCS=15–30 MPa for a few percent of the total volume), was approximately correct. It was possible to remove all material with the ripper dragheads. Mobilization of the contingency equipment such as the under water hammer system was not necessary.
The mechanical, operational and monitoring measures were taken to manage and control damage to the pipes and the dragheads, were effective. The mechanical measures included a fender attached to the lower suction pipe, a breaking bolt between helmet and visor as described before. In addition, special care was taken for the "streamlining" of the dragheads.
At the start of the works, dredging focused on the shallowest parts first. This reduced the bottom roughness and thus the risk of rock ridges impacting the dredge pipe. Figure 16 shows a distribution of the measured sea bottom depth before and after the dredging.

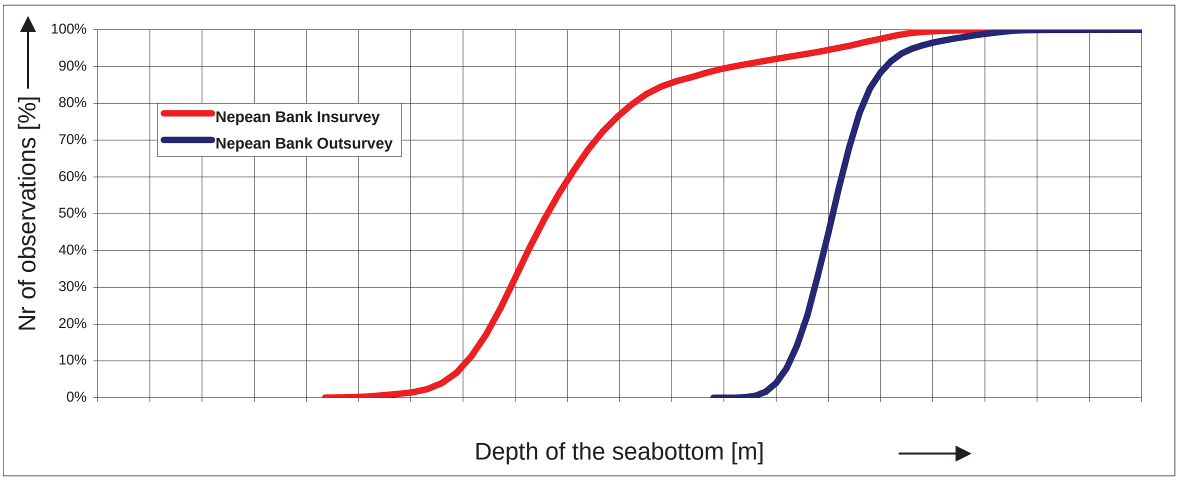

Figure 16: Bottom roughness was reduced.

Software was developed to help the operator to lift the pipe in time. In addition to the standard instrumentation load pins were installed in the cardan between upper and lower suction pipe to monitor the level and fluctuations of forces in the suction pipes.

A semi-quantitative approach was chosen to investigate and classify the rock spill. Towed video surveys were conducted 4 weeks after technical completion. A total of 35 km of video transects were sailed resulting in 33 hours of video footage. Then, from the video footage, 1280 pictures were captured and selected, wich evenly covered both the Nepean and Rip Bank dredged areas. All pictures were independently reviewed by 5 persons and visually divided into 5 classes, based on a percentage of the area covered by loose material (4 classes are shown in figure 17).

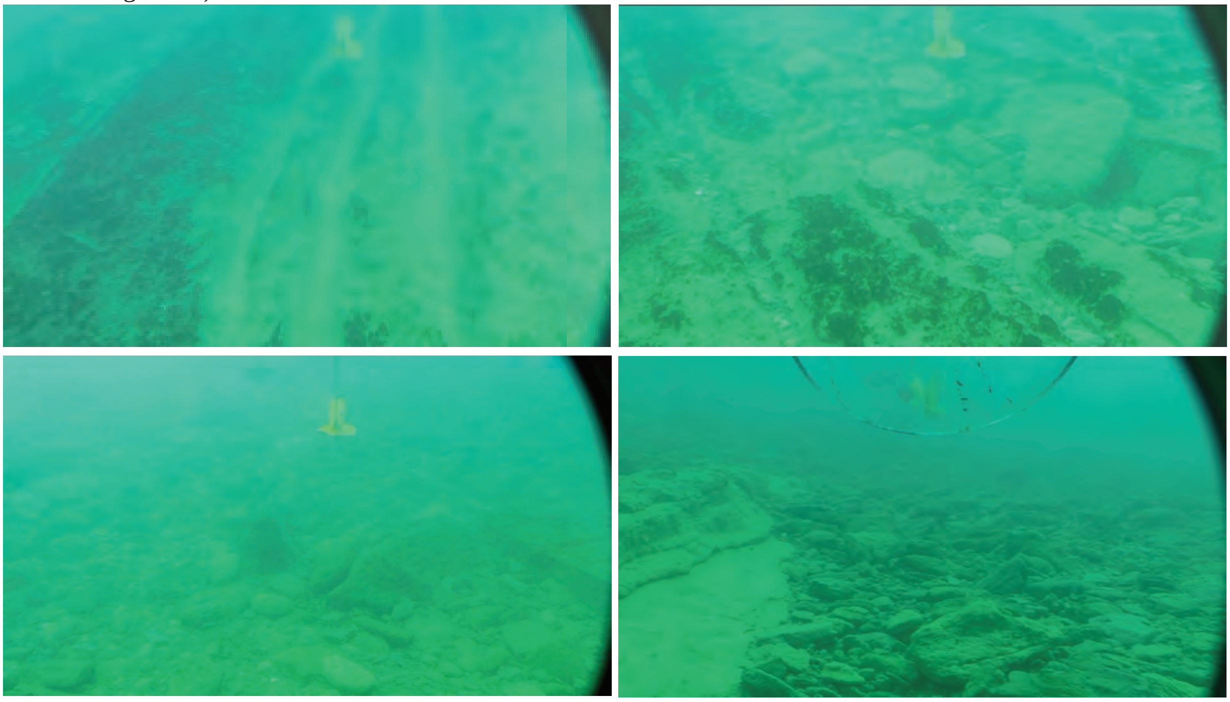

Figure 17: Examples of pictures with resp. 0-5%, 5-20%, 20-50% and 50-90% of the area covered with loose material

Based on this classification procedure it could be derived that about 12% of Nepean Bank and about 20% of Rip Bank was covered with rock spill. This was well within the predictions of the Supplementary Environmental Effects Statement (SEES).

7. CONCLUSIONS

This article describes the successful development of a ripper draghead, capable of dredging rock with a Trailing Suction Hopper Dredger. The cutting forces were determined by cutting tests in a quarry and the suction characteristics were optimized by scale model tests in the laboratory. This research resulted in the construction of a ripper draghead that has proven to be very effective at the Channel Deepening Project in Melbourne. The ripper draghead was sufficiently strong to withstand all occurring forces and the protection measures of the suction pipe were appropriate. The dredging of the Entrance of Port Phillip Bay was executed well within time. Due to the optimized draghead design and the well prepared work method the amount of spill was minimal.

8. ACKNOWLEDGEMENTS

The dredging of the Entrance has been successfully executed thanks to thorough and well executed research and preparation. The work has benefited from the continuous interest and support of our Alliance partner, the Port of Melbourne. Besides the authors the following persons have made significant contributions to the project at their specific field of knowledge: G.J. Grundlehner who supervised the workability studies, R.J.M. van Maastrigt who conducted the production calculations, W.F. Rosenbrand as manager of the R&D department of Boskalis, F. Uelman as the engineering manager of the Channel Deepening Project, P.N.W. Verhoef who did the engineering geological investigation and last but not least the crew of the Queen of the Netherlands.

9. REFERENCES

Holdgate, G.R. & M.W. Wallace (2004): Geological review of the Rip drilling, Southern Port Phillip. Report University of Melbourne (Report for Port of Melbourne Channel Deepening Alliance).

Verhoef (1997): Wear of Rock Cutting Tools. Implications for the investigation of rock dredging projects. Balkema, Rotterdam

MATERIAL BEHAVIOUR AND CONSTITUTIVE MODELLING OF ORGANIC SOILS

François Mathijssen[1] *Corporate member, CEDA;* Noel Boylan[2], Frans Molenkamp[3], Serge Leroueil[4], and Michael Long[5]

Abstract: This paper presents a historical overview of the developments in the understanding of the material behaviour of organic soil. The main areas of uncertainty and implications on the resulting design of embankment construction and reclamations are presented.
Due to the complex and heterogeneous nature of organic soils, the uncertainty of the correlations between in-situ, laboratory measurements and field observations is larger when compared to clay and sand. The reliability of geotechnical designs on organic soils could be improved when advanced coupled constitutive models, including fibre reinforcing effects, are used to back-analyse data, resulting from advanced in-situ and laboratory tests, thus reducing the risks involved.

Keywords: organic soils, material behaviour, constitutive modelling, fibres, anisotropy

[1] Senior project engineer/ PhD candidate, Royal Boskalis Westminster nv / Delft University of Technology Citg, P.O. Box 43, Papendrecht, 3350 AA, The Netherlands, T: +31 786969693, F: +31 786969869, F.A.J.M.Mathijssen@boskalis.nl, www.boskalis.nl
[2] Research Associate, Centre for Offshore Foundation Systems, The University of Western Australia, 35 Stirling Highway, Crawley, WA 6009, Australia, T: +61 864882473, F: +61 864881026, boylan@civil.uwa.edu.au, www.uwa.edu.au
[3] Professor Emeritus soil mechanics, Delft University of Technology Citg, P.O. Box 5048, Delft, 2600 GA, The Netherlands, T: +31 152785280, F: +31 152783328, Frans.Molenkamp@citg.tudelft.nl, www.tudelft.nl
[4] Professor soil mechanics, Laval University, Faculté des sciences et de genie, Pavillon Adrien-Pouliot, Québec (Québec), Canada, T: +1 4186562601, F: +1 4186562928, serge.Leroueil@gci.ulaval.ca, www.ulaval.ca
[5] Senior Lecturer, University College Dublin, School of Architecture, Landscape and Civil Engineering, Newstead Building, Belfield, Dublin 4, Ireland, T: +35 317167333, F: +35 317167399, mike.long@ucd.ie, www.ucd.ie

1 INTRODUCTION

A substantial level of development in Western Europe takes place in areas with very soft silty clay and organic soil deposits. Especially for projects where risk and lifecycle management are controlling parameters, strict design requirements are often formulated. This urges for a better understanding of the material behaviour resulting in more reliable geotechnical designs and a reduction of the risks involved.

In engineering practice at present, specific material models for organic soils are lacking and a rather empirical approach is used, while some theoretical academic concepts are postulated which require thorough validation using experimental evidence. After an introduction to the specific nature of organic soils and its classification, the resulting uncertainty observed during in-situ testing, laboratory testing on samples with varying degree of disturbance and field measurements are discussed in the following sections.

2 CLASSIFICATION

2.1 General

Over the years many different systems of identification and classification of peat have been developed, which are not individually presented in this paper. The main purpose of this section is to outline the predominant difference between organic soils and in particular peat with other natural soils, like sand, silt and clayey soils. Organic soils are formed during the decomposition of dead organic substances like remnants of plants and animals as indicated in Figure 2-1. The formation is stimulated at high temperatures, suitable humidity and access to oxygen from the air. The variety of stems, leaves, biological matter and biochemical circumstances are main causes for the natural heterogeneity of these soils. Furthermore, the definition of the morphological stage, i.e. fen, transition or bog, is according to Hobbs (1986, 1987) of significant added value.

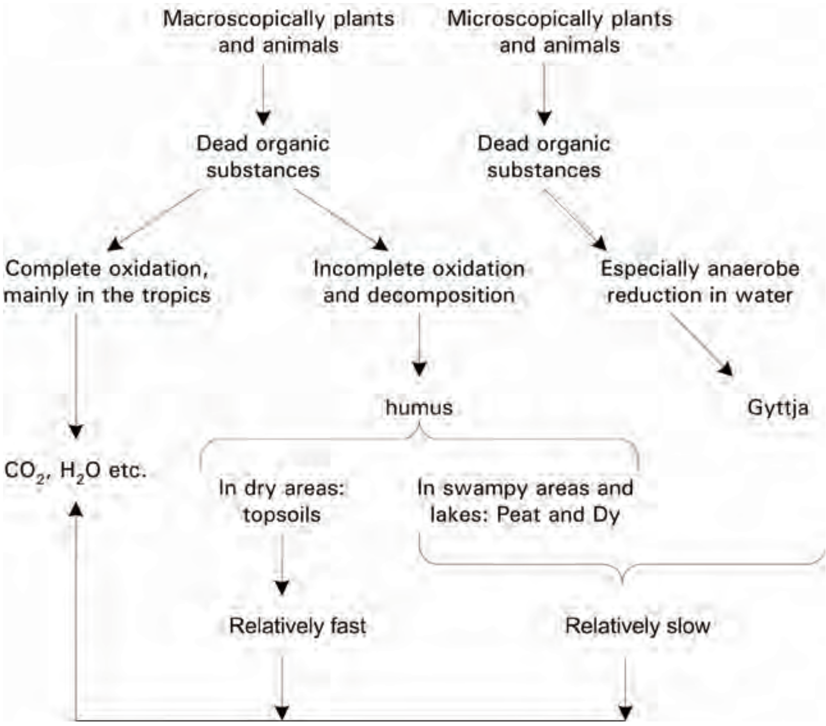

Figure 2-1 Schematic presentation of decomposition of organic matter (Fig. 1.1 - Hartlén & Wolski, 1996).

First the fabric and structure of peat is examined rather than indirect determination of their effects by change of geotechnical properties.

2.2 Peat fabric and structure

Peat fabric and structure of Escuminac Sphagnum and Sedge peats are investigated by Landva & Pheeney (1980), using various index tests and standard and scanning electron microscope examinations. The banded (aelotropic) nature of peat is in accordance with Taylor's definition (1948) resulting from deposition or load application rather than stratification. The layers appear to have a high tensile strength but can easily be pealed off.

The main constituents of peat are important information for engineering purposes given the resulting difference in behaviour. The most appropriate classification to date is the modified Von Post classification proposed by Landva & Pheeney (1980), which consists out of the following aspects:

1. Genera (such as: B = Bryales (moss) ; C = Carex (sedge); Eq = Equisetum (horse tail); Er = Eriophorum (cotton grass); H = Hypnum (moss); W = Lignidi (wood); N = Nanolignidi (shrubs); Ph = Phragmites; Sch = Scheuchzeria (aquatic herbs); S = Sphagnum (moss)).
2. Designation. Natural peat consists of a mixture of two or more genera, which are designated in descending order of content.
3. Humification (H) according to von Post & Granlund (1926) classification presented in Table 2-1.
4. Water content (B)
5. Fine fibres (F)
6. Coarse Fibres (R)
7. Wood (W) and Shrub (N) remnants

The above classification is performed based on visual observation of the material resulting from sampling ranging between undisturbed block sampling and tube sampling. An example of the use of the modified Von Post classification is presented in Figure 2-2. This profile of a raised bog consists out of Sphagnum peat with Sphagnum-Carex and Carex-Sphagnum in the lower section. The rather constant mineral content and highly variable water content indicate that correlations with conventional engineering properties are rather difficult. The classification may be influenced by sampling-induced disturbance (see section 4.1). The classification is rather subjective and may yield different interpretations, even for experienced users.

Table 2-1 Degree of humification according to Von Post & Granlund (1926)

Degree of humification	Decomposition	Plant structure	Content of amorphous material	Material extruded on squeezing (passing between fingers)	Nature of residue
H_1	None	Easily identified	None	Clear, colourless water	
H_2	Insignificant	Easily identified	None	Yellowish water	
H_3	Very slight	Still identifiable	Slight	Brown, muddy water; no peat	Not pasty
H_4	Slight	Not easily identified	Some	Dark brown, muddy water; no peat	Somewhat pasty
H_5	Moderate	Recognizable, but vague	Considerable	Muddy water and some peat	Strongly pasty
H_6	Moderately strong	Indistinct (more distinct after squeezing)	Considerable	About one third of peat squeezed out; water dark brown	
H_7	Strong	Faintly recognizable	High	About one half of peat squeezed out; any water very dark brown	
H_8	Very strong	Very indistinct	High	About two thirds of peat squeezed out; also some pasty water	Plant tissue capable of resisting decomposition (roots, fibres)
H_9	Nearly complete	Almost not recognizable		Nearly all the peat squeezed out as a fairly uniform paste	
H_{10}	Complete	Not discernible		All the peat passes between the fingers; no free water visible	

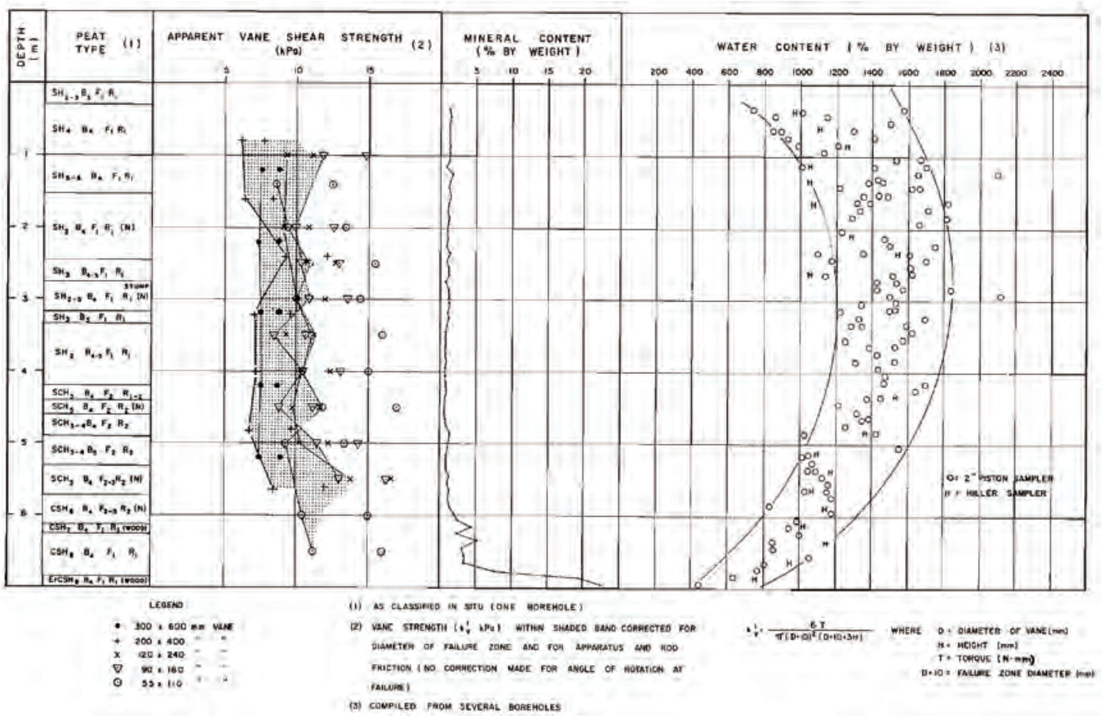

Figure 2-2 Modified Von Post classification with field vane values, mineral and water content for typical boring log from Escuminac, New Brunswick peat (Fig. 1 – Landva & Pheeney, 1980).

Landva & Pheeney (1980) state that standard and Scanning Electron Microscope (SEM) investigations, as presented in Figure 2-4, can be used to quantify the amount and nature of leaves, stems and fibres of organic soils and peat at different stages of humification. Landva & Pheeney (1980) determined for the Escuminac peat case, presented in Figure 2-3, that about one third of the total water content is free (inter) water and two third is bonded (intra) water. Although the mere existence of free and bonded water is not disputed, the feasibility to distinct one from the other during measurements is questioned by the authors given the biochemical processes that play a role when oven drying for determining the dry weight and their effects on the cell structure and ignition loss, as indicated by Skempton & Petley (1970). Other methods of drying, like using zero humidity at any constant temperature, may yield a temperature dependent dry weight and water content. Furthermore, both the level of saturation and temperature will affect the rate of in-situ decomposition and corresponding deformation through the corresponding more favourable biochemical process.

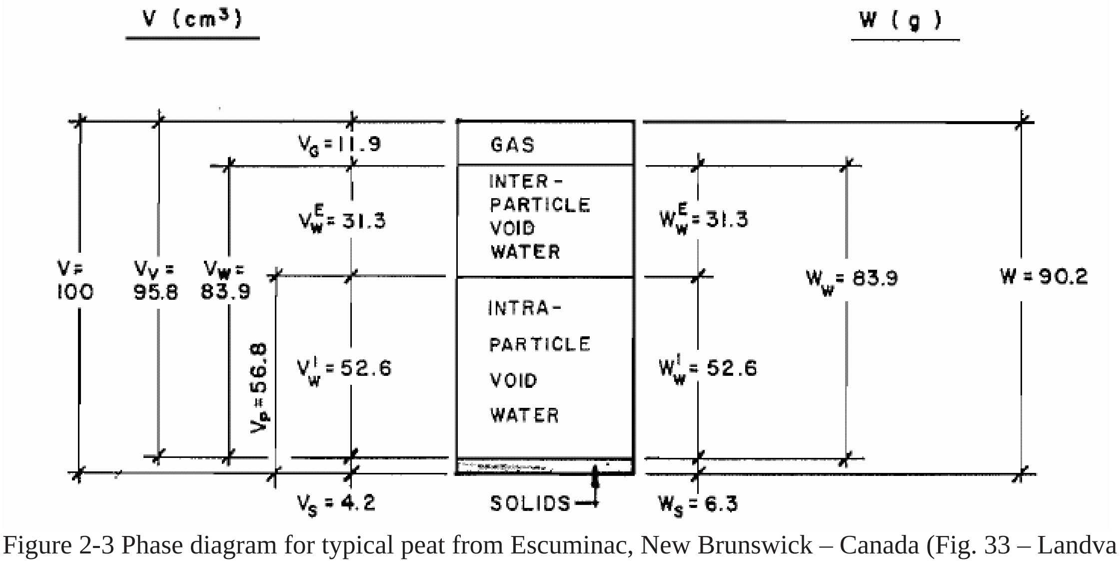

Figure 2-3 Phase diagram for typical peat from Escuminac, New Brunswick – Canada (Fig. 33 – Landva & Pheeney, 1980).

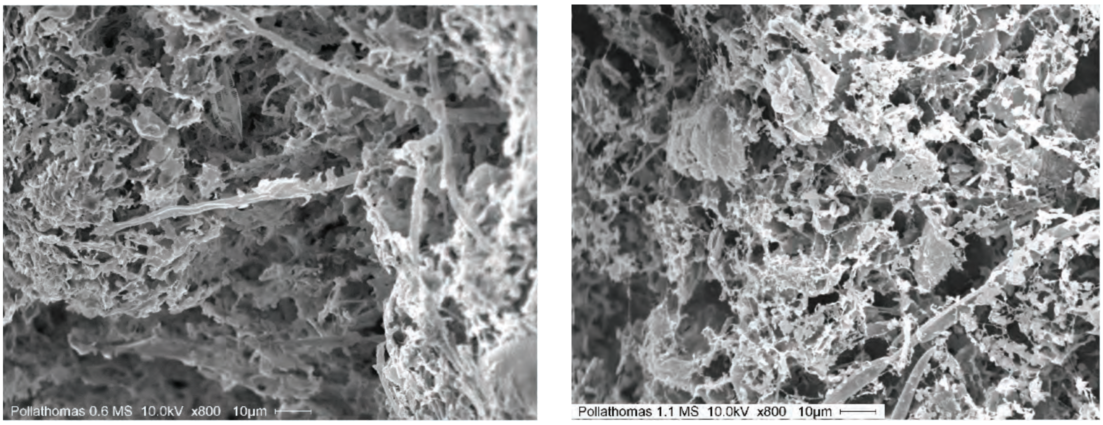

Figure 2-4 Scanning Electron Microscope image of: a) Slight to moderate (H4-H5) decomposed Loughrea peat. b) Strong to very strong (H7-H8) decomposed Loughrea peat (Fig. 1 – Boylan & Long, 2006b).

The porosity of the cell tissue of the leaves and stems increases in natural circumstances with higher degree of decomposition, also affecting the compressibility and amount of free water. Therefore, both the composition and state of the organic material influence the mechanical behaviour. Proper identification of organic soils should include a description of the morphological stage (Hobbs, 1986, 1987), main constituents, degree of decomposition and water content as well as conventional index properties. The incorporation of biochemical knowledge and processes in the mechanical modelling is in the opinion of the authors an essential step forward in the understanding of the material behaviour of organic soils and its rate of change.

3 IN-SITU TESTING

According to Wroth (1984), in-situ testing in geotechnical engineering serves the following purposes: soil profiling; measurement of a specific property of the ground; control of construction and finally monitoring of performance and back-analysis.
The undrained shear strength, s_u is the soil parameter most often derived from in-situ measurements in soft soils and is defined as the maximum mobilised shear strength assuming ideal undrained conditions. In the following sections, the derivation of the undrained shear strength using field vane testing, static and continuous cone penetration testing and measurements using full flow penetrometers are subject of discussion.

3.1 Field vane testing

The field vane test, developed by Cadling & Odenstad (1950), consists of a cruciform blade with a fixed length which is inserted in the ground and rotated while measuring the resistance or torque. At a certain degree of rotation a maximum resistance value is measured. This maximum resistance divided by the circumference of the blade is often denoted as undrained shear strength. From field and laboratory tests on clay and sand Cadling & Odenstad (1950) concluded that the surface of rupture produced when a vane is rotated closely coincides with the circular cylinder circumscribed round the vane. In-situ vane tests at shallow depth in clay using a two-bladed vane showed an oval shaped failure surface, which was possibly caused by an uneven pressure field.
Helenelund (1967) carried out tests using 2-, 3, 4 and 6 bladed vanes in fibrous peat, which resulted in unusual stress-strain curves with two or more peak values. Helenelund (1967) concluded that vane rotation does not necessarily cause shear failure along the periphery of the vane, but causes an outward bending and rupture behaviour for fibrous peat. The strength of fibrous peat depends therefore not only on internal friction between the fibres but also largely on the number, length and strength of fibres and root threats.
Landva (1980) performed subsurface in-situ vane deformation measurements in Sphagnum Escuminac peat where the deformation field was observed through a Plexiglas pane of which typical results are presented in Figure 3-1. At failure a void is present behind the blades and a distinct influence is noticeable outside the theoretical failure circle of the vane diameter. Failure of the peat appeared to occur under essentially drained conditions, while furthermore the peat in front of the blade is compressed in a tangential manner.
Based on the investigation performed by Helenelund (1967) and Landva (1980) it may be concluded that no distinct failure surface is formed in fibrous peat and the strength measured may be representative of partially drained or drained conditions. It should however be possible to obtain more reliable strength values from vane tests in non-fibrous peat, but the application and interpretation, with emphasis on drainage conditions, should be done with care.

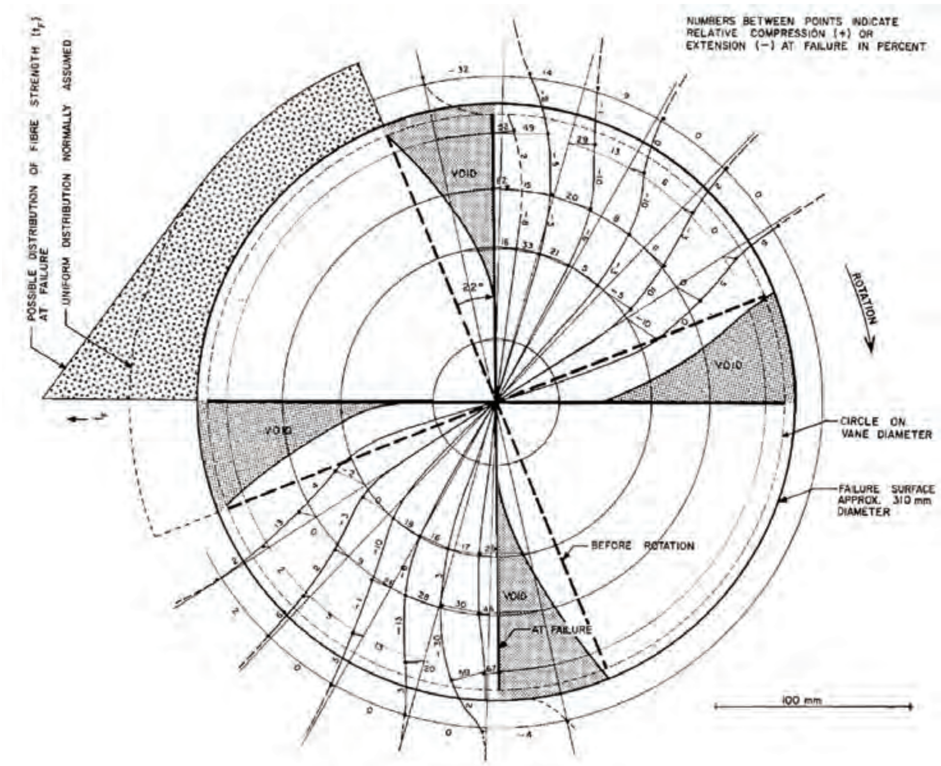

Figure 3-1 In-situ measured vane shear deformation in Spaghnum peat – Escuminac N.B. (Fig. 8 – Landva, 1980).

3.2 Cone penetration testing/ piezocone testing

The principle of the present cone penetration test originates from a penetration rod, consisting of a thin steel rod which was pushed in the ground to verify the bearing capacity of the deeper layers. According to Sanglerat (1972), the first static cone was developed by Barentsen in 1932 using a 36 mm gas pipe with 19mm inner diameter where a 15mm steel rod could freely move up and down with a 10 cm^2 cone with a 60° apex angle. The static cone with the inner rod was first manually pushed down over 150mm eliminating the skin friction followed by the outer casing, while the resulting penetration resistance was read on a manometer.
Keverling Buisman (1940) reported 23m deep cone penetration test-results performed in 1939 using a 10 tons hand-operated penetrometer, encountering 10m of organic soils. Major improvements since then are the friction sleeve (Begemann) and the use of strain gauges enabling registration of transmitted electrical signals enabling continuous readings and easy recording.
In 1974 both Janbu & Senneset and Schmertmann (Sanglerat, 1972) showed the importance of pore water pressure measurement during penetration. The measurement of this additional parameter increases the reliability of parameter determination and soil classification. The saturation of the piezocone is however extremely important while the response of the pressure sensor is depending on the position of the filter on the cone (Lunne et al., 1997a). The most common position is directly behind the cone defined as u_2. In eq. (3-1) the correlation of the piezocone measurements with the undrained shear strength is presented, where q_c = cone resistance; a = net area ratio of cone; u_2 = pore water pressure measurement directly behind the cone, σ_{v0} = total overburden stress and N_{kt} = cone factor depending on soil stiffness and in-situ stress ratio as described in Lunne et al. (1997a). There are also correlations presented in that book between the corrected cone resistance and the undrained shear strength with pore pressure measurement using a cone factor N_{ke}. Both empirical cone factors (N_{ke}, N_{kt}) are determined by (local) correlations with in-situ vane and/ or laboratory testing results. The reliability of the correlation is clearly directly influenced by the quality of the measurement of the idealised undrained shear strength.

$$s_u \approx \frac{q_c + (1-a)u_2 - \sigma_{v0}}{N_{kt}} \tag{3-1}$$

In engineering practice, especially in the Netherlands cone penetration testing results are frequently used for soil classification and a first estimate design tool. For a part of the railroad project Betuweroute 1-2 from Sliedrecht to Gorinchem, the applicability of CPT-based soil classification rules (i.e. Begemann, CUR, Robertson & Campanella, Robertson) as described by Lunne et al. (1997a) were verified using data from adjacent boreholes

(Mollé, 2005). The success rate of the correct determination of the soil description of a soil layer (average decision rule) and correct determination of the main soil constituent were analysed. The results are presented in Table 3-1, showing a very low success rate for the average decision rule and somewhat higher success rate for the average main constituent. The implications for engineering practice are that a larger uncertainty band should be taken into account when providing an estimate solely based on cone penetration data.

Table 3-1 Average success rates for both original and extended CPT classification rules (Table 9.14 – Mollé, 2005).

	Average decision rules-based success rates (%)	Average main constituent-based success rate (%)
Peat	26-33	24-37
Organic clay	45-59	64-70
Inorganic clay	27-58	46-67

Standardisation of the test procedure and formulation of application classes in the European Standard ENISO 22476-1 (2007) is a way to reduce the uncertainty resulting from CPT testing. One example is presented in Figure 3-2 where the effect of temperature calibration prior to in-situ testing on a peat site near Vinkeveen in the Netherlands is tested. Equilibrating the cone in a bucket of water at ground temperature (Figure 3-2a) results in a stabilisation at an ambient temperature and prevents the occurrence of negative cone and sleeve resistances (Figure 3-2b). Due to the large magnitude of the temperature gradient, the zero position of the strain gauges can shift suddenly when the cone is penetrated in the ground resulting in erroneous negative resistances.

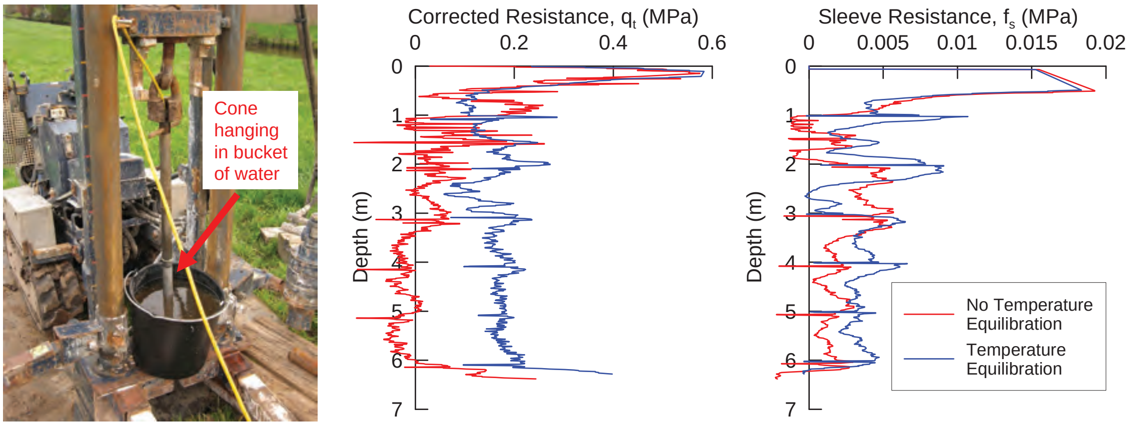

Figure 3-2 Temperature calibration during in-situ testing. a) Cone equilibration to ground temperature. b) Comparison of cone and sleeve resistance results from piezocone testing on Vinkeveen peat – Netherlands. (Fig. 5 & 6, Boylan et al. 2008).

Another way to improve the reliability is to enlarge the tip of the cone. Viergever (1985) performed an extensive soil investigation on fresh reclaimed land in the polder of Flevoland, the Netherlands using CPT's with 36.0, 79.8 and 112.8mm cone diameters. In Figure 3-3 the soil description and cone resistance results from 28 soundings with the large 112.8mm tip are presented. The sensitivity increases due to the large cone area and more important, the larger cone results in an increased homogenisation of the soil and a reduction of the fibre reinforcing effect, resulting in a reduced (30-45%) normalised cone resistance compared to the normal cone area of 10cm^2.

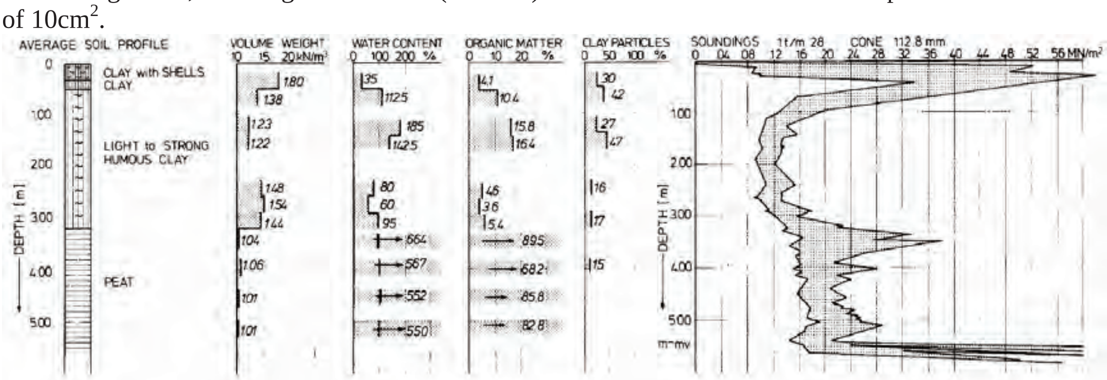

Figure 3-3 Soil description and cone resistance resulting from 28 soundings with the large tip (Fig. 5 – Viergever, 1985).

A larger cone size is mobilising strength and generating excess pore water pressures over a larger area, while the dissipation distance is increased resulting in reduced drainage conditions. The performance of variable rate testing is helpful in the interpretation of the drainage conditions and determination if assuming undrained conditions is appropriate.
Theoretically, when assuming ideal undrained conditions, a higher strain rate would result in higher undrained shear strength. Both Helenelund (1967) and Landva (1980) showed that this wasn't the case for vane tests on fibrous peat, but this could be a result of the distinct failure mechanism and partial drainage discussed in the previous section. In Figure 3-4 the strain rate dependency in Vinkeveen peat was tested using a 10 cm^2 cone during penetration and extraction at Slow (0.2 cm/s), Normal (2cm/s) and Fast (8cm/s) rates. The fast CPTU tests resulted in the lowest average resistance, indicating that undrained conditions are closer approached at this penetration rate.
Various inter- and counteracting factors are expected to play a role during the penetration like for instance heterogeneity, fibre content and - length, partial drainage conditions and dilatancy resulting in different soil responses at different rates. The application of full-flow penetrometers with a larger cone area and improved flow shape for testing in organic soils as discussed in the next section seems a logic step.

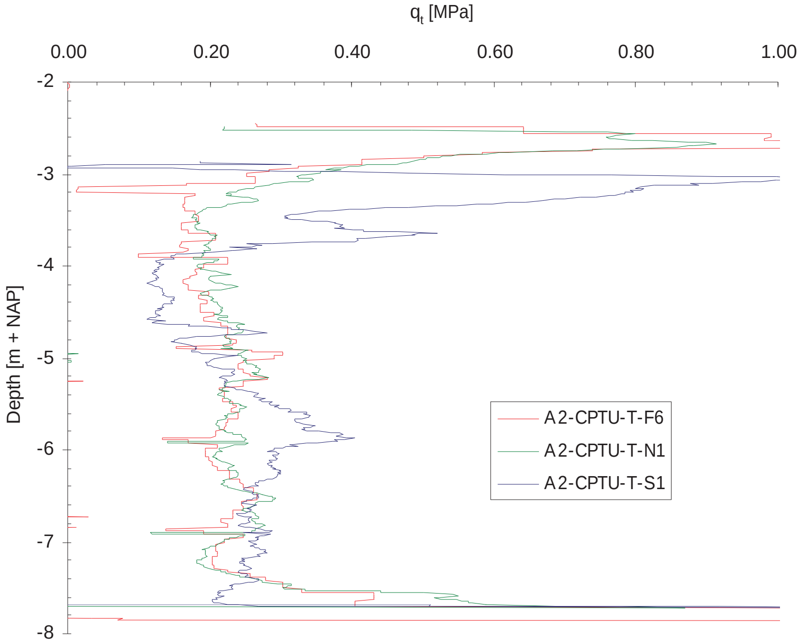

Figure 3-4 Strain rate dependency of cone penetration resistance using a 10cm^2 piezocone in peat near Vinkeveen, the Netherlands (Slow = 0.2cm/s; Normal = 2.0 cm/s; Fast = 8cm/s).

3.3 Full flow penetrometers

The use of full flow penetrometers, such as the ball cone and t-bar presented in Figure 3-5a, have several advantages over the standard CPTU cone (Randolph, 2004).

- The measured resistance requires minimal correction to obtain the corrected cone resistance.
- Improved accuracy is obtained in soft soils due to the larger projected area of 100cm^2 compared to the 10cm^2 of the cone. This results in improved resolution and reduced sensitivity to any load cell drift.
- Plasticity solutions based on simplified assumptions of soil behaviour exist which relate the net resistance to the shear strength of the soil.

Boylan & Long (2006a) performed in-situ tests with all three penetrometers at the same site at Loughrea in Ireland and the results are presented in Figure 3-5b) showing a significant reduction in scatter using the full flow penetrometers indicating a homogenisation of local effects.
The implications of the larger projection areas of the t-bar and ball cone are that the measured cone resistance is lower compared to the conventional cone due to the full flow mechanism of the soil around the penetrometers and different bearing factors ($N_{T\text{-}bar}$ and N_{Ball}) should be used to calculate the mobilized undrained shear strength. Boylan & Long (2006a) derived cone factors for Limerick and Loughrea peat correlating the penetration resistance to the mobilised shear strength from in-situ vane tests and Isotropically Consolidated Undrained triaxial Compression tests (CIUC). The average value of the t-bar approximates the theoretical value of 10.5 according to Randolph & Houlsby (1984), while the value for the Ball cone is much lower than the range of ~11-15 reported by Randolph et al. (2000). Partial drainage effects are believed to play a significant role, which can be analysed by variable rate testing.

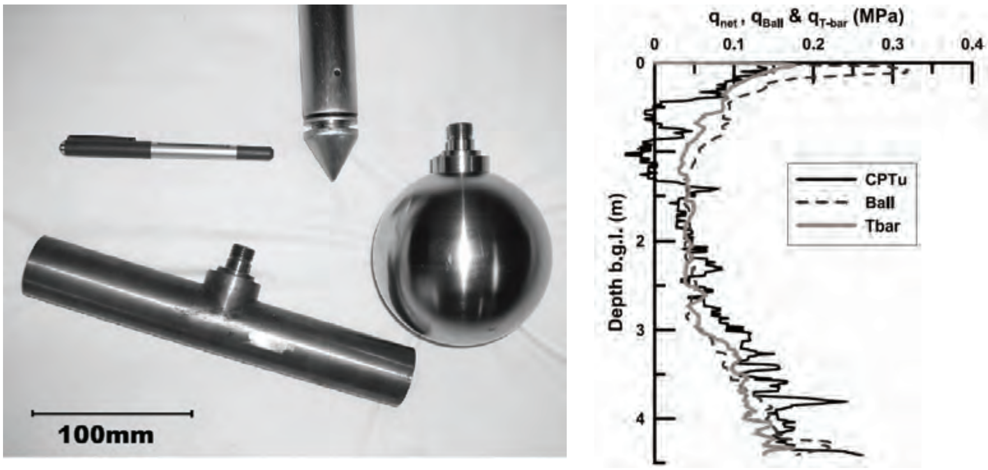

Figure 3-5 a) T-bar and ball cone which can be fitted on the location of a conventional CPTU cone tip (Fig. 2 – Boylan & Long, 2006a); b) Comparison of different cone response results of Limerick peat plotted vs. below ground level (Fig. 1 & 8a – Boylan & Long, 2006a).

The characterization of organic soils using full flow penetrometers in soils with varying degree of humification has been investigated by Boylan & Long (2006b). In Figure 2-4 Scanning Electron Microscope (SEM) of slight to moderate (H4-H5) and strong to very strong (H7-H8) decomposed Loughrea peat are presented. A corresponding depth profile of the Von Post humification, fibrosity and pore pressure parameters for the piezocone and a ball penetrometer with a pore pressure filter are presented in Figure 3-6. The ball penetrometer shows a stronger correlation between humification and fibrosity on one side and the B_{ball} on the other side compared to the pore pressure parameter of the piezocone (B_q).

It can be concluded that in spite of various shortcomings, in especially organic soils, the use of in-situ testing techniques are vital for profiling, characterizing and correlating parameters for engineering purposes. Both the large heterogeneity in formation and content of organic material and the importance to include biochemical processes in the observations makes realistic modelling of the occurring effects even harder.
In the authors opinion the performance of a distinct range of in-situ testing techniques including variable rate testing which are back-analysed in numerical calculation codes, incorporating constitutive models based on advanced laboratory test including fibre reinforcing effects, will improve the understanding and result in more reliable parameter-determination.

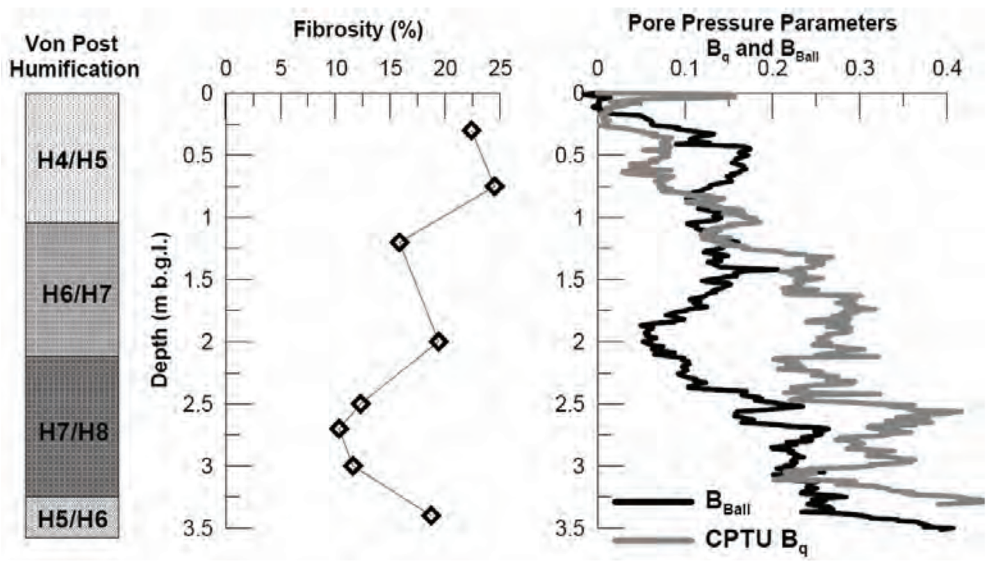

Figure 3-6 Comparison of Von Post classification, fibrosity and pore pressure parameters at Loughrea – Ireland (Fig. 6 – Boylan & Long, 2006a).

4 LABORATORY TESTING

4.1 Sampling induced disturbance

Early studies by Hanrahan (1954) on undisturbed and remoulded samples of peat clearly showed the presence of structure, thus indicating that peat could be susceptible to destructuration and sample disturbance. The undisturbed samples reported by Adams (1965) are resulting from sub-sampled bulk samples.
Helenelund et al. (1972) investigated the influence of sample disturbance on the strength and compressibility properties obtained from fibrous, slightly decomposed Sphagnum peat samples taken with different types of thin walled tubes with various cutting edges and block samples. From the results of unconfined compression and oedometer tests, it was concluded that sampling with conventional thin walled tubes and cutting edges results in peak strengths up to 2.5 times that of block samples and low coefficients of compressibility (see Figure 4-1). The differences identified between conventional tube sampling and block samples was attributed to pre-compression of the peat during the sampling process and was found to be largely overcome by using zig-zag shaped cutting teeth with a small degree of cyclic rotation during penetration.

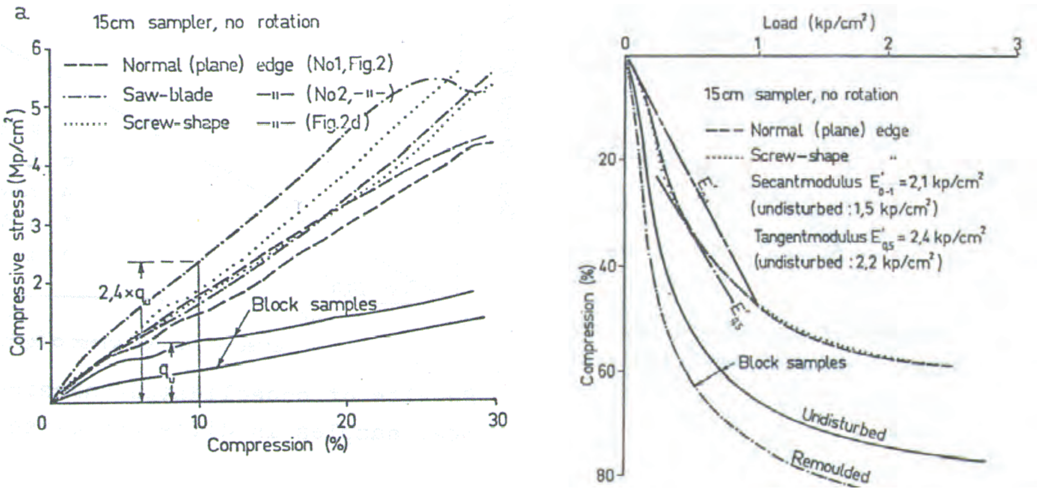

Figure 4-1 Influence of sampling induced disturbance in organics soils. a) Increased compressive strength due to sample disturbance (Fig. 5 – Helenelund et al., 1972); b) Decreased compression due to sample disturbance (Fig. 6 – Helenelund et al., 1972).

Landva et al. (1983) describe the application of a sharp edge 100mm diameter piston sampler and a 250mm square block sampler fabricated to obtain undisturbed samples of fibrous peat. The 100mm piston sampler has a Plexiglas tube to hold the sample, which is protected by bronze tubing during sampling. Undisturbed samples are reported to be obtained through the combined action of suction and sharp cutting edges, for Escuminac peat as well as for soft organic soils and harbour muds. The subsequent samples were assessed to be of good quality from visual comparison of the peat horizons of the sample and the cut face of the sampling location. However, for Carex peat in a blanket bog at St. Shotts, Newfoundland (Landva, 2007) hardly any material was sampled with the 100mm diameter piston sampler at a sampling attempt of 1m deep in a 2m thick peat stratum, indicating that this sampler is not suited for sampling this specific type of peat.
For an elaborate soil investigation campaign on organics soil in the Netherlands, field sampling was conducted at two test sites, near Bodegraven and Vinkeveen (Mathijssen et al., 2008). Sampling was conducted using Ackermann, ELE 100mm piston, hollow auger, Begemann and Sherbrooke block samplers. The range of samplers has been chosen in such a way that Dutch, Irish and UK engineering practices are represented while the high quality block samples were used for reference.
The Sherbrooke block sampler (see Figure 4-2a), developed and described by Lefebvre et al. (1979) and the performance in Dutch peats in Mathijssen et al. (2008), is a specially designed open cage carving tool. A retrieved block sample is placed on a bottom plate, packed in cling foil, aluminum foil, again cling foil and completely waxed with 90% paraffin and 10% bee wax by weight. In Figure 4-2b a fully conserved Sherbrooke block sample is presented before placement in a water bath at 5°C.
In Figure 4-3 (Boylan, 2008) it can be observed that the strength and scatter resulting from UK piston samples is larger than that resulting from adjacent Sherbrooke block samples from the same depth.

Figure 4-2 Sherbrooke block sampling of peat at Motorway A2, Vinkeveen – the Netherlands. a) Retrieved block sample with expert drill team (Fig. 4 – Mathijssen et al., 2008); b) Conservation block sample with bee wax before placement in water bath at 5°C.

4.2 Shear strength and measurement of fibre reinforcement

General

The large heterogeneity in organic soils and especially peat contribute to the uncertainty in definition of strength parameters for these types of soils. While adopting the definitions for cohesion and friction according to Taylor (1948) and Schofield & Wroth (1968), principal questions are whether or not organic soils respond in an essential cohesive or frictional nature. Furthermore, the effect of the fibre tensile strength on the behaviour or organic soils needs to be considered.

Hanrahan (1954) describes triaxial tests on preconsolidated peat, which were allowed to expand resulting in stress relaxation before shearing to failure, resulting in a strength reduction by 20-40%. The largest strength reduction was observed in the more heavily consolidated specimens. The resulting low Mohr strength envelope with apparent friction angle of 5° resulted in the conclusion that the behaviour of these tests was predominant of cohesive nature.

Hanrahan et al. (1967) performed triaxial tests on a macerated (remoulded) peat with humification H4 on the Von Post (1926) scale. After removal of the coarse fibres and preparation of the specimens close to the liquid limit by compaction in a Proctor mould, the samples were extracted using 1 ½ and 4 ½ `` thin walled tubes. The results of normally consolidated triaxial tests on samples with both diameters are reported to agree closely to the same critical state line (Schofield & Wroth, 1969) and behave in a frictional manner. Effective friction angles in the range of 35-50º are reported by Helenelund et al. (1972), where the lower values correspond to higher water contents. However, no convergence to one line in p', q space after failure was observed for peat samples with an overconsolidation ratio larger than 8.

The generation of excess pore water pressures in anisotropic consolidated undrained triaxial compression tests (CAUC) is typically larger than the effective radial stress, σ'_3 resulting in the occurrence of water between membrane and sample. This line in stress space is called the tension cut off line and is presented in Figure 4-3b, where a large scatter is observed for the two UK piston samples and one line for the Sherbrooke block samples. The stress state corresponding to the observed shear stresses is not fully undrained, which complicated the analysis of the strength parameters. Furthermore, partially saturation conditions and the compressibility of organic matter might influence the definition of effective stress (Jennings & Burland, 1961; Lade & de Boer, 1997).

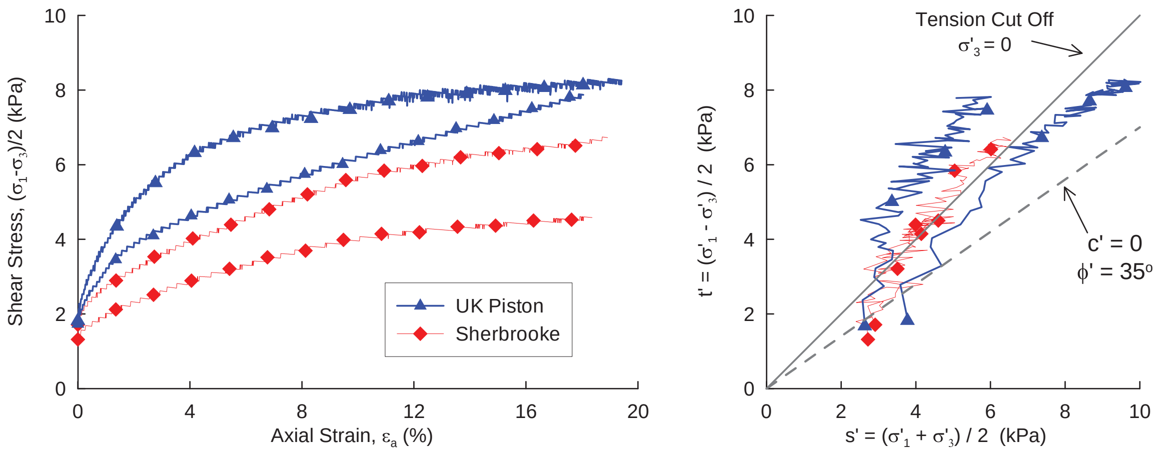

Figure 4-3 Anisotropic consolidated undrained triaxial compression tests on Vinkeveen peat (2-2.5m b.g.l.) for UK piston and Sherbrooke block sample (D=70mm).

The soil response due to an imposed strain rate effect is also directly related to the presence of idealized drained or undrained soil conditions. Hanrahan (1954) indicated an approximate 5% higher triaxial compressive strength for a tenfold increase in shear rate (0.01 and 0.001 inch/s), but reported no measurable effect for application of strain rate testing with the miniature labvane (Hanrahan, 1967). Other tests like the Direct Simple Shear test without (un-) saturation control, reported by Farrell et al. (1999) result again in other values for the mobilised shear strength.

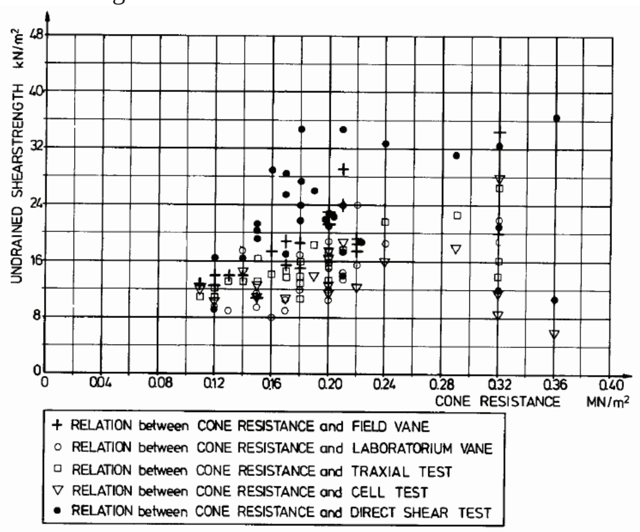

Figure 4-4 Test results between undrained shear strength and cone resistance for Flevopolder, the Netherlands (Fig. 7 – Viergever, 1985).

The use of more advanced constitutive models with fibre reinforcement like Molenkamp et al. (1996) which predict the shear strength, depending on the stress state and load direction is expected to improve the reliability. It is strongly advised to use advanced models to back-analyse in-situ tests instead of direct correlation with limit values of individual tests as indicated in Figure 4-4. This huge scatter is attributed by the authors to sample disturbance, different drainage -, boundary conditions and outdated/ inferior tests like the laboratory vane and the cell test (popular Dutch test until early nineties).

Measurement of fibre reinforcement

Fibrous peat can be modelled using a simple composite model assuming isotropic properties for the bulk material and horizontal fibre reinforcing in the bedding plane (Molenkamp et al., 1996). Landva & La Rochelle (1983) used this idealised assumption and derived the required parameters testing comparable soil samples in both ring shear and triaxial tests. Due to the natural geometrical variability of the soil, combination of results of such laboratory tests requires at least a statistically significant number of tests.

Cola & Cortellazzo (2005) found for Adria and Correzzola peat a bilinear relationship for the fibre reinforcement starting in the origin presented in Figure 4-5, assuming a Mohr Coulomb failure surface, where Landva & La Rochelle (1983) modelled the reinforcement as cohesion offset. The differences in test results can be attributed to specific type of organic soils, but just as well on testing details and degree of sample disturbance.

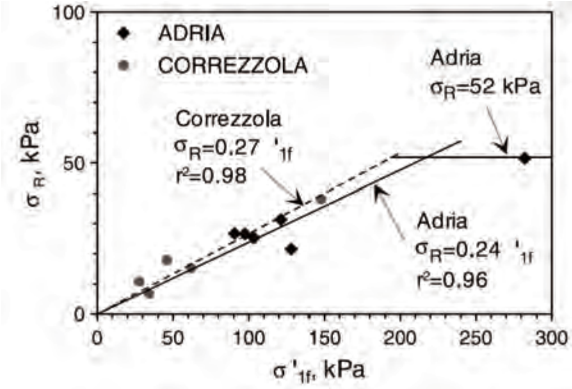

Figure 4-5 Fiber contribution σ_r vs. vertical effective stress σ'_{1f} for Correzzola and Adia peat (Fig. 8 – Cola & Cortelazzo (2005).

The validation that the fibre reinforcing effects are negligible in the horizontal bedding requires an apparatus which can measure the strength anisotropy on one sample. Molenkamp (1998, 2000 & 2001) proposed for this purpose the axial shear apparatus in which an extended triaxial device with rough ends is capable of controlling the shear strain by the horizontal movement of the bottom plane. When a sample with inclined bedding plane is loaded axially, lateral shear deformations are made possible by placing the sample on a roller bearing. To maintain a uniform stress and deformation even during the shearing of the sample the bottom platen is loaded by a horizontal load F_h of such magnitude that the major principal stress in the sample is kept coaxial. The subsequent reinforcing effects of the fibres can be derived in a relatively simple way as indicated in Figure 4-6a).

In close cooperation with GDS instruments Ltd (UK) an unsaturated dynamic Direct Simple Shear/ Axial Shear device, following the principle of Molenkamp (1998, 2000 & 2001), has been developed (see Figure 4-6b). This multifunctional device is capable of mounting samples ranging in diameter from 50-100mm and has the following functions (static & dynamic; saturated and unsaturated):

- Axial shear testing of organic soils and peat in particular measuring the fibre reinforcing effects.
- Direct simple shear testing with (un-)saturation control while measuring bending moments.
- Triaxial and CRS oedometric testing while measuring bending moments.

The control of the tests is done by direct computer control using the measurements of a Stroud (1971) load-cell developed by Cambridge Insitu. Minimisation techniques with all calibration measurements are used to derive the optimum matrix constants for the computer control.

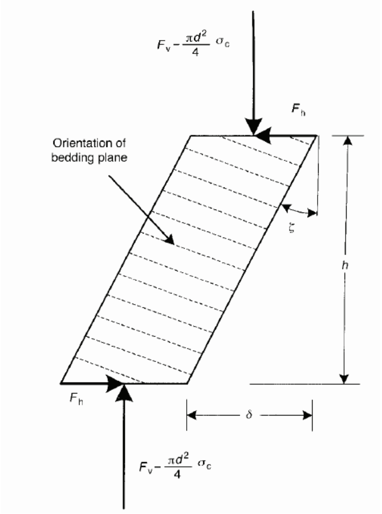

Figure 4-6 a) Global equilibrium of a uniformly shearing sample of an anisotropic soil with an inclined bedding plane and lateral load control of the bottom platen (Fig. 3 – Molenkamp, 1998); b) Calibration DSS/ AS device.

4.3 Consolidation and compressibility

One-dimensional consolidation

Von Terzaghi & Fröhlich (1936) indicate that the consolidation coefficient c (=k/a) is different for loading and unloading but assume them to be equal. Furthermore an unique linear relationship between the void ratio e and vertical effective stress σ'_v is assumed that is independent of loading history and process, although von Terzaghi (1923) earlier showed graphically a highly non-linear relationship between pressure and void ratio. This idealized linear relationship between void ratio and logarithm of permeability was also found by Berry & Postkitt (1972) from constant head permeability tests on two types of peat, presented in Figure 4-7. The less reliable consolidation coefficient c_v, which is an indirect dissipation parameter depending on for instance density, stress and loading gradient is still quite often used in engineering practice.

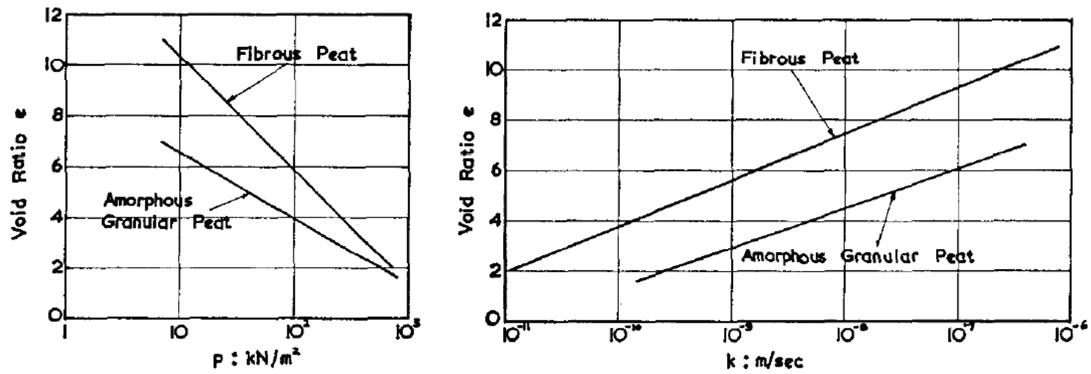

Figure 4-7 Compressibility and permeability of amorphous and fibrous peat (Fig. 2c &d - Berry & Postkitt, 1972).

The definitions for primary and secondary compression for one-dimensional loading were first introduced by Von Terzaghi (1923) and Keverling Buisman (1936) respectively. The oedometer tests on clay and peat samples, presented by Keverling Buisman (1940), typically reached the hydrodynamic period after ~ 6 hours and 6 minutes respectively. However, the secular compression α_s, presented in eq. (4-1), is defined after 1 day due to plotting limitations when using a semi-logarithmic scale where z(t) = settlement at time t; α_p = primary compression; α_s = secular compression (= secondary compression); and t = time after start of loading. This implies that by definition a varying amount of secondary compression is incorporated in the direct or primary compression.

$$z(t) = \alpha_p + \alpha_s \log t \tag{4-1}$$

According to Barden (1969) the following concepts of mechanisms responsible for secondary consolidation were identified in the late sixties:

- Terzaghi-Taylor concept of consolidation considering secondary effects to be due to retarded approach of inter-particle contacts through layers of adsorbed water of ever-increasing structural viscosity.
- Tan's concept of a card-house structure and the jumping of bonds.
- Considering the existence of two levels of structure, with primary consolidation the result of drainage of a system of macro-pores and secondary consolidation the subsequent drainage of a system of micro-pores into the macro-pores (de Josselin de Jong, 1968).

Ladd et al. (1977) describe two hypothesis A and B. In hypothesis A, secondary compression starts after the end of primary compression, while in hypothesis B secondary compression or viscous effects is an inseparable part of soil behaviour.

Keverling Buisman (1940) already performed laboratory measurements and long duration field measurements at the Motorway A12 presented in Figure 4-8, resulting in the conclusion that primary and secondary compression of multiple thin and one thick layer coincides, which is the principle feature of what later was called hypothesis B. Berry & Poskitt (1972) confirmed the validity of hypothesis B for amorphous granular peat and for fibrous peat and as outlined by Leroueil (2006), numerous other authors came to the same conclusion. Until date this widely accepted opinion is disputed by authors like Mesri et al. (1997).

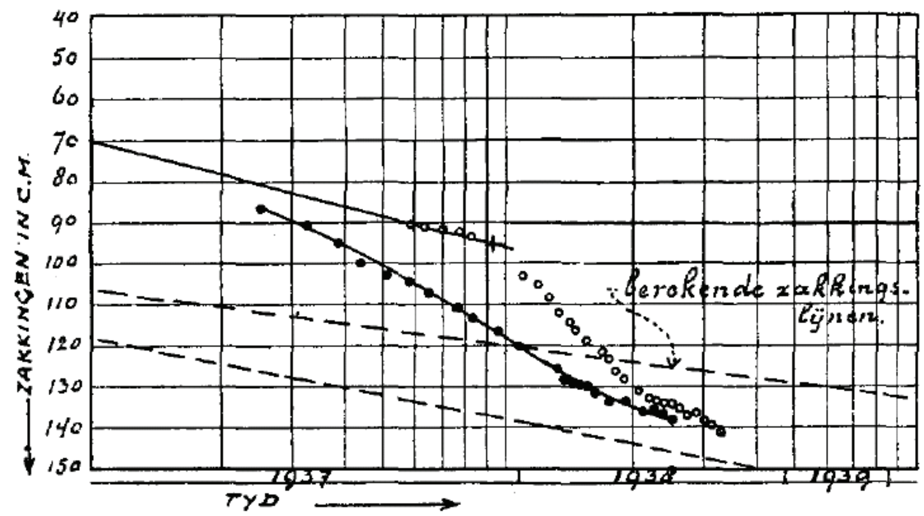

Figure 4-8 Long duration field measurements Motorway No. 12, km 31.3 on foundation with 3m peat overlying 2m clay (Fig. 78 – Keverling Buisman, 1940).

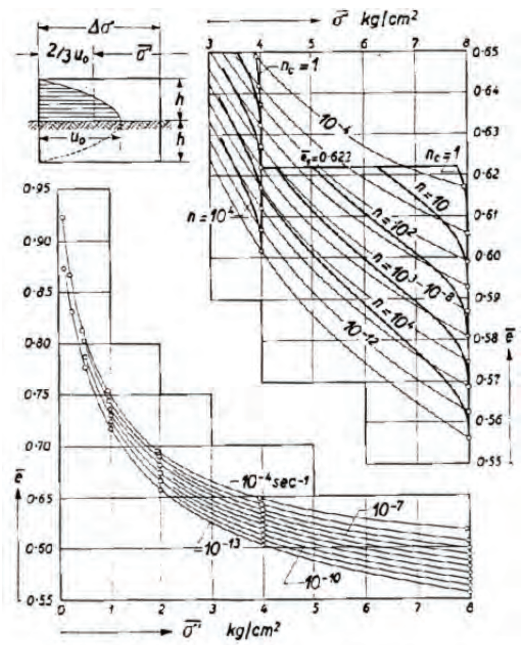

Figure 4-9 Isotaches and compression curves for a suddenly applied load increment and various layer thicknesses (Fig. 3 - Šuklje, 1957).

Keverling Buisman (1940) furthermore reports a larger primary compression compared to the secular compression when rapid load increments are applied. The compression parameters are therefore not constant but vary for each sample (void ratio), load and load increment condition. In line with these observations, Taylor (1948) clearly states that there is not a fixed intergranular pressure for a given void ratio, but that there is a dependence on the speed of compression. For a given void ratio and different speeds of compression various parallel lines can be constructed in the log p′ versus e curve, where $C_c = \Delta e/\Delta \log p'$ is the primary compression index. This concept is further elaborated by Šuklje (1957) and Garlanger (1972) who defined isotaches as graphs relating intergranular pressures σ′ to void ratios e for certain constant void ratio speeds δe/δt, presented in Figure 4-9. Den Haan (1994) and Den Haan & Kruze (2007) present a strong correlation between specific volume (= 1+e) and compression factor b (= Cc/ (1+e)ln(10)), where Hobbs (1986) shows varying relationships, between Cc and water content, for peats of varying origins, morphological stages and degree of decomposition.
Mesri & Godlewski (1977) indicated that the compression ratio α (= $C_{\alpha e}$/ C_c) is constant for a given soil, where a range of viscous parameters for geotechnical materials is presented in Table 4-1. Tavenas et al. (1978) showed that this is only valid on the 1 day limit state surface. Using this relationship, it is easily demonstrated (Leroueil, 2006) that the relationship presented in eq. (4-2) is valid in which in the fourth term the dimensionless relationship $\Delta \log \dot{\varepsilon}_v = -\Delta \log t^m$ according to Tavenas et al. (1978) is used, while taking for convenience for power

m the approximate value $m=1$. In this context the definition of incremental dimensionless quantity $\Delta \log x = \log(x+\Delta x) - \log x$ is noted as valid for any scalar quantity x and its increment Δx. The third column in Table 4-1 presents the vertical effective stress change, normalized with respect to the preconsolidation pressure associated with strain rate. Noting that the first Taylor approximation of $\Delta \log x$ around $x=1$ reads $\Delta \log x = \log(1+\Delta x/x) \approx \Delta x/x$, consequently $\Delta \log \sigma'_p \approx \Delta\sigma'_p/\sigma'_p$. Despite the difference in magnitudes between the second and third columns, from eq. (4-2) it follows that the strain rate dependency per log cycle at any strain or void ratio is constant for a given soil and varies between 0.01 for granular soils to 0.175 for peat and muskeg.

$$\alpha = \frac{C_{\alpha e}}{C_c} = \frac{\Delta \log \sigma'_p}{\Delta \log t} = -\frac{\Delta \log \sigma'_p}{\Delta \log \dot{\varepsilon}_v} \tag{4-2}$$

Table 4-1 Viscous parameters for geotechnical materials (after Table 1 – Leroueil, 2006).

Material	$C_{\alpha e}/C_c$ equal to $\alpha = \Delta \log \sigma'_p / \Delta \log \dot{\varepsilon}$	$\frac{\Delta\sigma'}{\sigma'} \Big/ \Delta \log \dot{\varepsilon}$
Granular soils including rockfill	0.02 ± 0.01	0.023 – 0.072
Shale and mudstone	0.03 ± 0.01	0.047 – 0.096
Inorganic clays and silts	0.04 ± 0.01	0.072 – 0.122
Organic clays and silts	0.05 ± 0.01	0.096 – 0.148
Peat and muskeg	0.06 ± 0.01	0.122 – 0.175

Note: types of material and $C_{\alpha e}/C_c$ values are from Mesri et al. (1995)

Temperature effects and strain rate

Hanrahan (1954) and Hanson et al. (2000) clearly state that the viscosity of the peat during the secondary phase was affected by changes in temperature, which necessitated performing long duration compression tests at constant temperature. Boudali (1995) investigated the effects of temperature on the isotache surface of Berthierville clay from Québec using both oedometer and triaxial testing. The resulting influence of strain rate and temperature on the limit state surface is presented in Figure 4-10.

The original one-dimensional drained compression expression of Bjerrum (1967) can also describe temperature effects when extended with the relation according to Moritz (1995), as presented in eq. (4-3).

$$e_v = e_{v0} - C_c \left(\log\left(\frac{\sigma'_{v;T_0}}{\sigma'_{vc;T_0}} \right) - \alpha_T \log\left(\frac{T_0}{T} \right) \right) - C_{\alpha e} \log\left(\frac{t}{t_{ref}} \right) \tag{4-3}$$

where e_v = current void ratio; e_{v0} = initial void ratio; $\sigma'_{v;T0}$ = current vertical effective stress at temperature T_0; $\sigma'_{vc;T0}$ = preconsolidation stress at temperature T_0; α_T = temperature ratio (~0.15); T_0 = current temperature; T = reference temperature of 20ºC; t = time from start of loading; t_{ref} = reference time.

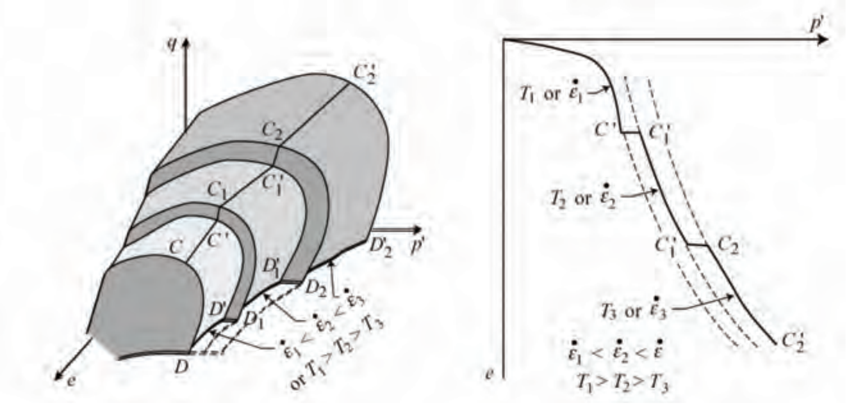

Figure 4-10 Influence of strain rate and temperature on the limit state surface of soils (Fig. 34 – Leroueil, 2006).

5 DISCUSSION AND CONCLUDING REMARKS

The complexity of material behaviour of organic soils is illustrated in the previous sections using historical evidence and recent research results from in-situ and laboratory testing. In this last concluding section the results are summarised and the coherency is illustrated with some case histories.

For soil classification and in-situ testing the following can be concluded:

- Classification of organic soils is due to its heterogeneous nature in content, state and deposition rather subjective. It is recommended to determine the Von Post classification including degree of decomposition, water content, fibrosity and conventional index properties. Biochemical analysis of the various stages of a certain type of organic soil will improve the understanding and stimulate the formulation of more reliable models.
- The performance of a distinct range of in-situ testing techniques including variable rate testing which are back-analysed in numerical calculation codes, incorporating constitutive models including fibre reinforcing effects, will improve the understanding and result in more reliable parameter-determination.
- Full flow penetrometers with pore pressure elements improve the accuracy and interpretation of results due to their larger bearing area and full flow mechanism.

In-situ tests need to be correlated with advanced laboratory tests, where both sampling induced disturbance and test details play an important role. Experience from Helenelund et al. (1972) and this research indicates that sampling induced disturbance reduces compressibility and increases strength, which is the adverse as found for clays (Lunne et al., 1997b). In engineering practice in general a preference is noticeable to correlate in-situ tests to the mobilised undrained shear strength from laboratory tests, thus striving to exclude difficult stress-path effects, assuming a constant soil parameter. The mobilised undrained shear strength is however a device dependent "signature" at a certain stress state after following a certain stress path with all the characteristics of a (partially) undrained analysis using effective strength parameters. Both parameter sets can be directly correlated with an appropriate constitutive model using stress-path analysis.
The specific nature of organic soils with the low mineral content, large contents of bonded and free water and decomposing organic material and fibres complicated the formulation of a constitutive model incorporating all effects. Existing theoretical models like Molenkamp et al. (1996) need to be validated using the newly developed Direct Simple Shear/ Axial Shear apparatus, in combination with advanced laboratory tests using oedometer (IL & CRS), triaxial, direct simple shear and ringshear testing, which is part of this research.
In Figure 5-1 the deformation of an embankment at Escuminac, Canada (Landva & La Rochelle, 1983) at various times after construction is presented. The formation of a compression band under the centre of the embankment and heave and rupture behaviour at the toe is visible. The distinction between deformation and failure is quite difficult and even highly schematised modelling of this particular behaviour is only possible with advanced numerical models including fibre reinforcing effects. The same is true for back-analysis of in-situ and laboratory tests.

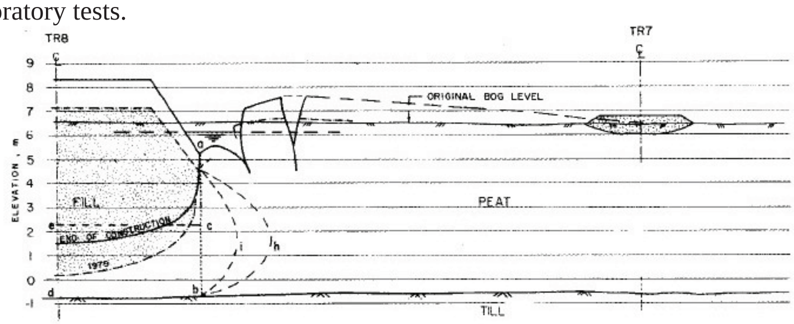

Figure 5-1 Cross section test fill at Escuminac after construction and 4 years after construction (Fig. 19 – Landva & La Rochelle, 1983).

Settlement models of organic soils still have their uncertainties, despite significant developments and experience records. In Figure 5-2 settlement plate data and back-analysis using an isotache model is presented on a Motorway location on Vinkeveen peat. The fit is quite good for a staged construction, but model uncertainties are still present for the initial compression and the effects of preloading. Yoshikuni performed relaxation tests indicating that the strain rate at which the preloading is stopped affects the remaining excess pore pressure which needs to be dissipated (Leroueil, 2006). Furthermore, the effect of strain rate on the formation of microstructure is still unsure and requires additional research.

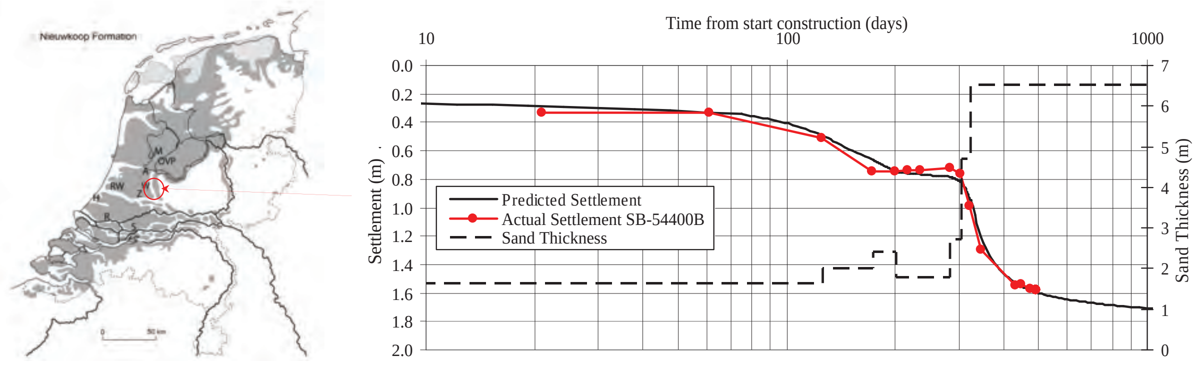

Figure 5-2 Settlement plate data and back-calculated model predictions for staged construction with vertical drains at 1.0m spacing at Motorway A2: Vinkeveen – the Netherlands (Fig. 11 – Dykstra et al. 2008).

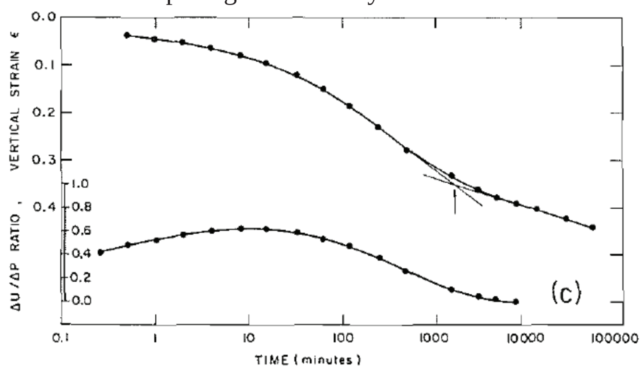

Figure 5-3 Vertical strain and pore pressure response versus time on Sherbrooke block samples of Rubert River, Québec peat (Fig. 11c – Lefebvre et al., 1984).

The settlement due to the staged construction reduces the void ratio and thus the permeability (see Figure 4-7). In Figure 5-3 the vertical strain and pore pressure response of an oedometer tests on a Sherbrooke block sample is presented (Lefebvre et al., 1984). The excess pore water pressure after completion of the primary consolidation period is clearly visible, which can be accurately modelled using coupled models. Lefebvre et al. (1984) report field values of secondary compression which are twice the laboratory values, despite the use of block samples. This might be attributed to biomechanical -, lateral deformation and other effects.

It can be concluded that, due to the complex and heterogeneous nature of organic soils, the uncertainty of the correlations between in-situ, laboratory measurements and field observations is larger when compared to clay and sand. The reliability of geotechnical designs on organic soils could be improved when advanced coupled constitutive models, including fibre reinforcing effects, are used to back-analyse data, resulting from advanced in-situ and laboratory tests, thus reducing the risks involved.

6 ACKNOWLEDGEMENTS

The authors are grateful for the support from Royal Boskalis Westminster/ Hydronamic, Delft University of Technology CiTG and University College Dublin in this research.

For the sampling campaign, special thanks are due to the Norwegian Geotechnical Institute (NGI), Public Works of Rotterdam (GWR), Fugro, Deltares and the contractor combinations: Consortium N11 & A2, Holendrecht – Maarssen.

7 REFERENCES

Adams, J. I. (1965). The engineering behaviour of a Canadian Muskeg. Proc. 6th ICSMFE, Montreal, Canada, Vol. 1, pp. 3-7.

Barden, L. (1969). Time dependent deformation of normally consolidated clays and peats. J. Soil Mech. & Found. Div., Vol. 95, No. SM1, pp. 1-31.

Berry, P. L., & Poskitt, T.J. (1972). The consolidation of peat. Géotechnique, Vol. 22, No. 1, pp. 27-52.

Bjerrum, L. (1967). 7th Rankine Lecture: Engineering geology of Norwegian normally-consolidated marine clays as related to settlements of building. Géotechnique, Vol. 17, No. 2, pp. 81-118.
Boylan, N. (2008) The shear strength of peat. PhD Thesis. University College Dublin.
Boylan, N., & Long, M. (2006a). Characterisation of peat using full flow penetrometers. 4th Int. Conf. on Soft Soil Engineering. Vancouver, Canada, pp. 403-414.
Boylan, N., & Long, M. (2006b). Determination of the decomposition of peat from fibrosity measurements and in-situ penetration tests. 3rd National Symposium on Bridge and Infrastructure Research in Ireland, Plenary session of Geotechnics, Materials and Transport. Dublin, pp. 251-259.
Boylan, N., Mathijssen, F.A.J.M., Long, M. & Molenkamp, F. (2008). Accuracy of Piezocone testing in organic soils. 11th Baltic Sea Geotechnical Conference. Geotechnics in maritime engineering, Gdansk, Poland, pp. 9.
Cadling, L., & Odenstad, S. (1950). The vane borer. An apparatus for determination the shear strength of clay soils directly in the ground. Stockholm, Royal Swedish geotechnical institute proceedings No. 2.
Cola, S., & Cortellazzo, G. (2005). The shear strength behaviour of two peaty soils. Geotechnical and Geological Engineering, Vol. 23, No. 6, pp. 679-695.
Dykstra, C. J., Mathijssen, F.A.J.M., & Molenkamp, F. (2008). Settlement predictions of embankments on organic soils in engineering practice. Geotechnics of Soft Soils – Focus on Ground Improvement – Karstunen & Leoni (eds.). Strathclyde University, Glasgow, Scotland, pp. 13-21.
ENISO 22476-1 (2007). Geotechnical investigation and testing - Field testing - Part 1: Electrical cone and piezocone penetration tests. ISO / CEN, Geneva.
Farrell, E. R., S. K. Jonker, et al. (1999). Use of direct simple shear test for the design of a motorway on peat. Proc. 12th European Conference on Soil Mechanics and Geotechnical Engineering, Amsterdam.
Garlanger, J. E. (1972). The consolidation of soils exhibiting creep under constant effective stress. Géotechnique, Vol. 22, No. 1, pp. 71-78.
den Haan, E. J. (1994). Vertical compression of soils. Civil Engineering, section Geotechnics. Delft, Delft University of Technology. Ph.D. thesis, pp. 96.
den Haan, E. J., & Kruze, G.A.M. (2007). Characterisation and engineering properties of Dutch peats. Characterisation and Engineering properties of natural soils. Tan, Phoon, Hight & Leroueil (eds), Taylor & Francis Group, London, pp. 2101-2133.
Hanrahan, E. T. (1954). An investigation of physical properties of peat. Géotechnique, Vol. 4, No. 3, pp. 108-121.
Hanrahan, E. T., Dunne, J.M., & Sodha, V.G. (1967). Shear strength of peat. Proc. Geotech. Conf. Oslo, Vol. 1, pp. 193-198.
Hanson, J. L., Edil, T.B, & Fox, P.J. (2000). Stress-Temperature Effects on Peat Compression. Soft Ground Technology, Noordwijkerhout, The Netherlands, pp. 331-345.
Hartlén, J., & Wolski, W. (1996). Embankments on organic soils. Amsterdam, Elsevier.
Helenelund, K. V. (1967). Vane tests and tension tests on fibrous peats. Proc. Geotech. Conf. on shear strength properties of natural soils and rocks. Oslo, Vol. 1, pp. 199-203.
Helenelund, K. V., Lindqvist, L-O., & Sundman, C. (1972). Influence of sampling disturbance on the engineering properties of peat samples. 4th International Peat Congress. Otaniemi, Finland, Vol. 2, pp. 229-240.
Hobbs, N. B. (1986). Mire morphology and the properties and behaviour of some British and foreign peats. Quarterly Journal of Engineering Geology and Hydrogeology, Vol. 19, pp. 7-80.
Hobbs, N. B. (1987). TECHNICAL NOTE: A note on the classification of peat. Géotechnique, Vol. 37, No. 3, pp. 405-40.
Jennings, J.E.B., & Burland, J.B. (1962). Limitations to the use of effective stresses in partly saturated soils. Géotechnique, Vol. 12, No. 2, pp. 125-144.
Josselin de Jong, G. de (1968). Consolidation models consisting of an assembly of viscous elements on a cavity channel network. Géotechnique, Vol. 18, No. 2, pp. 195-228.
Keverling Buisman, A. S. (1936). Results of long duration settlement tests. 1st ICSMFE. Cambridge Mass., No. F-7, pp. 103-106.
Keverling Buisman, A. S. (1940). Grondmechanica (in Dutch). Uitgeverij Waltman, Delft.
Ladd, C. C., Foott, R., Ishihara, K., Schlosser, F., & Poulos, H.G. (1977). Stress-Deformation and strength characteristics. 9th ICSMFE, Tokyo, Japan, Vol. 2, pp. 421-494.
Lade, P. V., & de Boer, R. (1997). The concept of effective stress for soil, concrete and rock. Géotechnique, Vol. 47, No. 1, pp. 61-78.
Landva, A. O. (1980). Vane testing in peat. Can. Geotech. J., Vol. 17, No. 1, pp. 1-19.
Landva, A. O., & La Rochelle, P. (1983). Compressibility and shear strength characteristics of Radforth Peats. Testing of Peats and Organic Soils, ASTM STP 820. P. M. Jarrett, pp. 157-191.
Landva, A. O., & Pheeney, P.E. (1980). Peat fabric and structure. Can. Geotech. J., Vol. 17, No. 3, pp. 416-435.

Landva, A. O., Pheeney, P.E., & Mersereau, D.E. (1983). Undisturbed sampling of peat. Testing of Peats and Organic Soils, ASTM STP 820. P. M. Jarrett, pp. 141-156.
Lefebvre, G., & Poulin, C. (1979). A new method of sampling in sensitive clay. Can. Geotech. J., Vol. 16, No. 1, pp. 226-233.
Lefebvre, G., Langlois, P., Lupien, C. & Lavallée, J.-G. (1984). Laboratory testing and in situ behaviour of peat as embankment foundation. Can. Geotech. J., Vol. 21, No. 2, pp. 322-337.
Leroueil, S. (2006). Prof. Šuklje's Memorial Lecture: The isotache approach. Where are we 50 years after its development by Professor Šuklje? XIII Danube-European Geotechnical Engineering Conference. Ljubljana, Slovenia, pp. 34.
Long, M. (2005). Review of peat strength, peat characterization and constitutive modelling of peat with reference to landslides. Studia Geotechnica et Mechanica, Vol. 27, No. 3-4, pp. 67-90.
Lunne, T., Robertson, P.K., & Powell, J.J.M. (1997a). Cone Penetration Testing in Geotechnical Practice. Blackie Academic and Professional, London.
Lunne, T., Berre, T., & Strandvik, S. (1997b). Sample disturbance in soft low plasticity Norwegian clay. Proc. Sym. On Recent Developments in Soil and Pavement Mechanics. Rio de Janeiro, Balkema, pp. 81-92.
Mathijssen, F. A. J. M., Boylan, N., Long, M. & Molenkamp, F. (2008). Sample disturbance of organic soils. Geotechnical and Geophysical Site Characterization - Huang & Mayne (eds). ISC'3. Taipei, Taiwan, Taylor & Francis Group, pp. 1481-1488.
Mesri, G. & Godlewski, R.M. (1977). Time and stress com-pressibility interrelationship. J. Geotech. Eng. Div., Vol. 103, No. GT5, pp. 417-430.
Mesri, G., Stark, T., Ajlouni, M.A, & Chen, C.S. (1997). Secondary compression of peat with or without surcharging. J. Geotech. GeoEnv. Eng, Vol. 123, No. 5, pp. 411-421.
Molenkamp, F. (1998). TECHNICAL NOTE: Principal of axial shear apparatus. Géotechnique, Vol. 48, No. 3, pp. 427-431.
Molenkamp, F. (2000). DISCUSSION: Principle of axial shear test. Géotechnique, Vol. 50, No. 3, pp. 307-310.
Molenkamp, F. (2001). Evaluation of axial shear test using plane strain simulations. Géotechnique, Vol. 51, No. 1, pp. 37-49.
Molenkamp, F. (2006). Effective stress formulation of unsaturated soil mechanics. Modern Trends in Geomechanics, W. Wu and H. S. Yu (eds.), Springer –Verlag, pp. 61-75.
Molenkamp, F., Lane, P.A., & Heshmati, A. (1996). A new model and test procedure for peaty soils. Proc. of Fourth Conference of Association of Computational Methods in Engineering (ACME). Glasgow, pp. 133-136.
Mollé, J. (2005). The accuracy of the interpretation of CPT-based soil classification methods for soft soils. Section for Engineering Geology. Delft, Delft University of Technology. M.Sc. Thesis, pp. 233.
von Post, L., & Granlund, E. (1926). Peat resources in southern Sweden. Sveriges geologiska undersökning, Yearbook 335(19.2 Series C), pp. 1 – 127.
Randolph, M. F. (2004). Characterisation of soft sediments for offshore applications. Proc. of 2nd Int. Conf. on Geotechnical and Geophysical Site Characterization, ISC'2. Porto, Millpress, Vol. 1, pp. 209-232.
Randolph, M. F., & Houlsby, G.T. (1984). The limiting pressure on a circular pile loaded laterally in cohesive soil. Géotechnique, Vol. 34, No. 4, pp. 613-623.
Randolph, M.F., Martin, C.M. & Hu, Y. (2000). Limiting resistance of a spherical penetrometer in cohesive material. Géotechnique, Vol. 50, No. 5, pp. 573-582.
Roscoe, K. H., Schofield, A.N., & Thurairajah, A. (1963). Yielding of clays in states wetter than critical. Géotechnique, Vol. 13, No. 3, pp. 211-240.
Sanglerat, G. (1972). The penetrometer and soil exploration. Interpretation of penetration diagrams - theory and practice. Amsterdam, Elsevier.
Schofield, A. N., & Wroth, C.P. (1968). Critical State Soil Mechanics. London (England), McGraw-Hill.
Skempton, A. W., & Petley, D. J. (1970). Ignition loss and other properties of peats and clays from Avonmouth, King's Lynn and Cranberry Moss. Géotechnique, Vol. 20, No. 4, pp. 343-356.
Šuklje, L. (1957). The analysis of the consolidation process by the isotache method. 4th ICSMFE, London, Vol. 1, pp. 200-206.
Tavenas, F., Leroueil, S., La Rochelle, P. & Roy, M. (1978). Creep behaviour of an undisturbed lightly overconsolidated clay. Can. Geotech. J., Vol. 15, No. 3, pp. 402-423.
Taylor, D. W. (1948). Fundamentals of soil mechanics. London (England), John Wiley & Sons.
von Terzaghi, K. (1923). Die Beziehungen zwischen Elastizität und Innendruk. Sitzungsberichte der mathem. & naturw. Klasse 132(Band, 3. und 4. Heft), pp. 105-124.
von Terzaghi, K. & Fröhlich, O.K. (1936). Theorie der Setzung von Tonschichten. Eine Einführung in die analytische Ton-mechanik, Franz Deuticke, Leipzig und Wien.
Viergever, M.A. (1985). Cone penetration with enlarged tip in cohesive soils. 11th ICSMFE, San-Francisco, pp. 947-950.
Wroth, C. P. (1984). The interpretation of in situ soil tests. Géotechnique, Vol. 34, No. 4, pp. 449-489.

MEASURING EFFECTS OF DREDGING IN RELATION TO THE DYNAMICS OF NATURE

R.L. Koomans[1], J. Limburg[2]

Abstract: The discharge of fines during dredging and the impact of these fines on seafloor habitats is an important aspect in environmental impact assessments. Our vision is that the effects of dredging on the environment, should be related to the impact of the dynamics of nature itself.

The potential effects from sediment plumes on the seafloor sediments can only be understood when the total release of *fine* sediments from the overflow can be related to the natural variation in concentrations of fines in seafloor sediments. Today, the buffering capacity of the seafloor for fine sediments has been estimated, but has hardly been measured. The natural variation of fines and thereby the buffering capacity of the seafloor can be monitored and natural dynamics due to resuspension and large-scale sediment transport patterns can be quantified. The sediments released from the overflow of a hopper dredger are composed of sand and fine silts. Since the sands will behave completely different to the fines, information on the total volume of *fine* material from the overflow is an important parameter. The release of fine material from a hopper overflow during dredging can be measured . With this quantification of sediment release, and the information of the buffering capacity of the seafloor sediments, the net effect of the release of fines during dredging can be related to the dynamics of nature.

Keywords: Sediment composition, monitoring, sediment density, sediment plume

[1]Medusa Explorations BV, Verlengde Bremenweg 4, 9723 JV, Groningen, The Netherlands. tel: 0031(0)50 5770280, koomans@medusa-online.com, www.Medusa-online.com. [2]limburg@medusa-online.com

1 INTRODUCTION

The discharge of fines during dredging and the impact of these fines on seafloor habitats is an important aspect in environmental impact assessments. The scientific community lacks information on resuspension of fines (e.g. buffering of fine material in the upper sediment layer during summer), the release of fines from the overflow during dredging and the net effect of this release on the sediment bed. As a result, various projects have suffered from delay due to unanswered questions on the environmental effects of dredging.

Our vision is that the effects of dredging on the environment, should be related to the impact of the dynamics of nature itself. One can imagine how fine sediments are entrapped in the active layer of the seafloor sediments. During storms, these sediments are released from the bed are brought into suspension in the water column. However due to the small quantities involved, this release in the water column is difficult to measure. For example the complete resuspension of silt from a sediment layer with a silt content of 1% in the top 30 cm of the active bed, will result in a suspended silt concentration of about 300 ppm in a water column of 9m. This low concentration is about an order of magnitude lower than the lower limit of detection of commonly used concentration meters. Measuring variations of silt content in the concentrated form (which is in the seabed) gives higher accuracy, provided that the spatial resolution of the mapping is accurate enough. Detailed monitoring of sediment composition of the seafloor can help to determine the natural variability of silt content in seafloor sediments.

Understanding the effects of dredging on seafloor sediments not only requires understanding of the natural behavior of fine material, but requires detailed information on the losses of fines during dredging operations. One important loss of sediment during dredging is the release of material from the overflow of a hopper dredger. Projects investigating these effects (Aarninkhof, 2008) mainly focus on the total release of material from the overflow and do not distinguish between coarse and fine sediments. For a better understanding of the impact of fines on the seafloor sediments, not only the total release from the overflow should be monitored, also the composition of the released material should be measured. This paper focuses on two aspects:

1) We will show how natural variability of fine material in seafloor sediments can be monitored
2) We will show how the composition of sediments released from the overflow can be monitored during dredging

2 MAPPING SEDIMENT COMPOSITION

Traditionally, silt content in the sediment bed is determined by taking sediment samples by (box)coring or taking grab samples. These measurements give accurate information on one spot, but spatial variation in the silt content e.g. due to the presence of small-scale morphological features as ripple structures can result in data that is not representative for large areas. Spatial variation can be mapped by taking large amounts of sediment samples, which is often too expensive.

Different hydrographic methods exist to map the variation in the composition of the sediments on the seafloor. Analysis of the acoustic signals multi-beam and single-beam echosounders or side-scan sonar, gives high-resolution images of the composition sediments. This information helps to zone the seafloor in a classes with one type of acoustic reflection that can be related to a certain type of sediment. It is though not possible to determine absolute concentrations of silt and sand or absolute values of grain sizes of the sediment bed (du Four et al, 2005). We propose a method that directly measures some chemical constituents of the seafloor sediments, that can directly be related to sediment composition. This relation is established by a calibration in the laboratory.

This system (called Medusa) is towed over the seafloor behind a vessel. Each second, the system measures concentrations of the natural occurring radionuclides of the seafloor. These radionuclides (^{40}K, ^{232}Th and ^{238}U) are present in rocks and sediments since the origin of the earth and can be measured with a gamma spectrometer. The system is completely passive and measures the background radiation that is emitted by soil and sediments. Various research projects have shown how silt, sand and heavy minerals contain different concentrations and ratios of radionuclides (de Meijer, 1998). This method is also commonly used to measure median grain size in the field (Nederbracht and Koomans, 2005). The specific concentrations of these radionuclides for each sediment fraction (also called fingerprint) allows the measurements of the radionuclides in the sediment to be translated into maps of sediment composition.

The advantage of the proposed system over traditional sediment sampling, is that the detailed maps of sediment composition determine the spatial variation at a small scale. Moreover, it is a cost effective method for monitoring purposes.

In a project for Rotterdam harbor, the transport of fine material, relocated to in several gravel pits, was monitored with the medusa system and with a multibeam. Therefore, two surveys have been conducted: one survey prior to disposal and one survey after two years of disposal. An area of 10x9 km^2 was monitored. The entire survey was carried out in four days and comprises about 120 .000 datapoints.

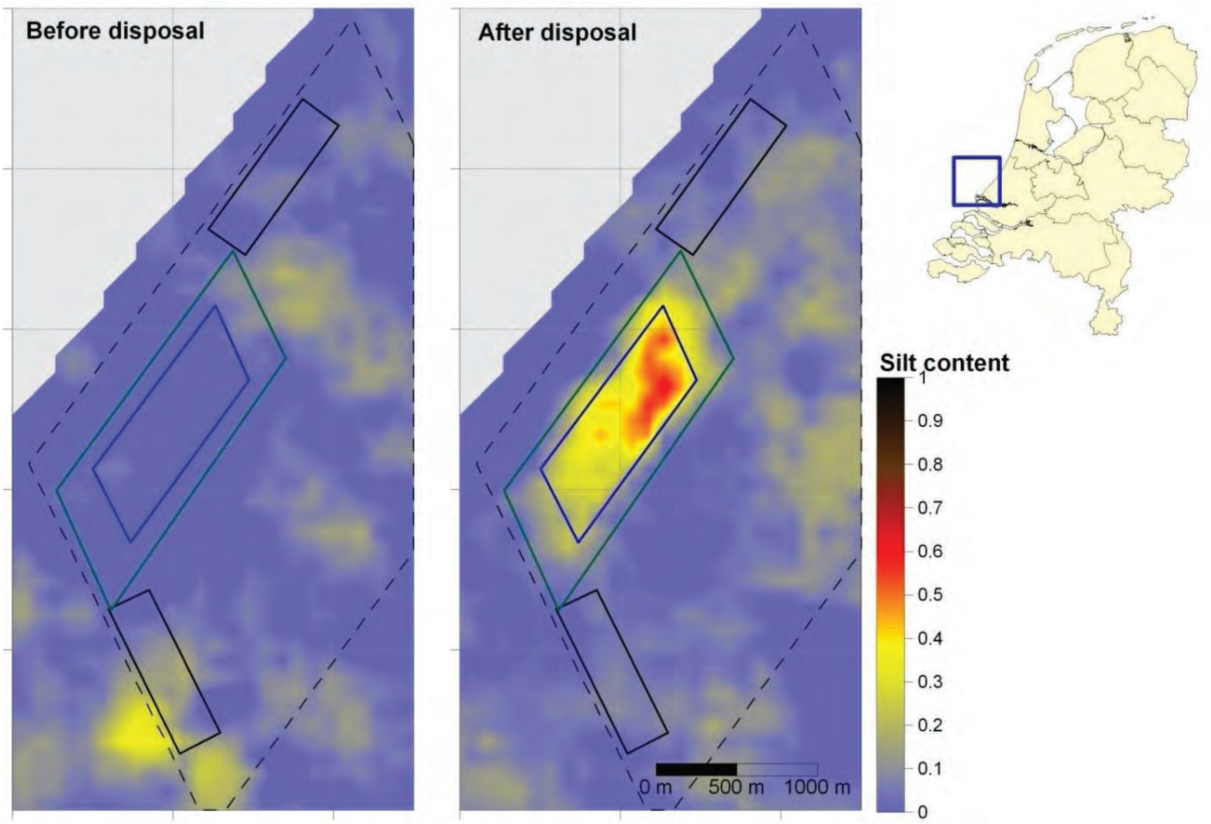

Figure 1: Comparison of silt fraction (ranging from 0 to 1) of totale sediment of the seafloor, before and after disposal.

Figure 1 shows the distribution of fine sediments in the area around the former gravel pits (blue rectangle). At t_0 the disposal site does not contain any sludge. The concentrates of sludge in the other parts of the area originate from a former disposal site (Venema and de Meijer, 2001). At t_1 the disposal of the harbour silts can clearly be noticed by the increased silt concentration in the former gravel pit. The dispersal from the gravel pit is small; the sludge extends only 250 m around the sides of the pit.

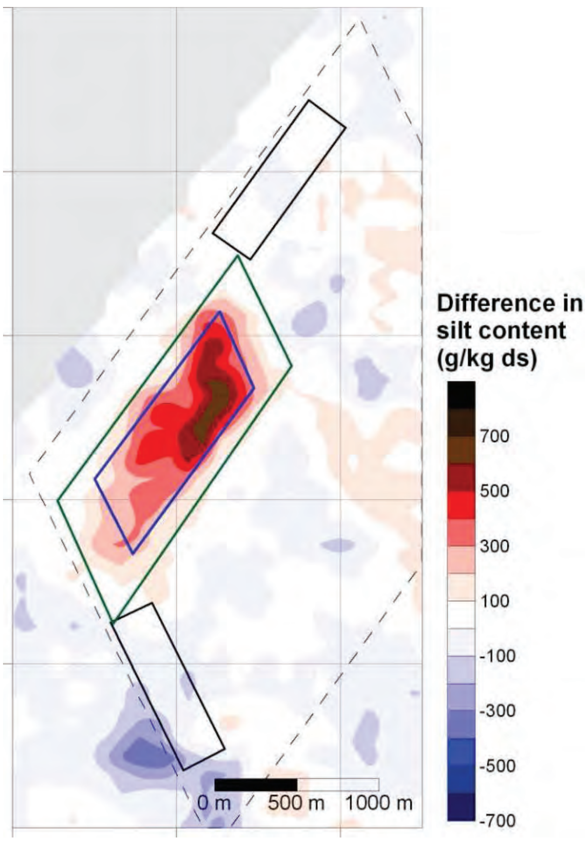

Figure 2: Map of the difference in silt content of the sediment before and after disposal.

The transport of the sludge from the dumping site is quantified with a map showing the difference between the two measurements (figure 2). With this information, a mass balance is constructed that has been used to validate the results of model calculations. The quantitative information on the transport of sediment can help to refine models for an improved assessment of the effectiveness of a spoil depot.

3 MEASURING THE COMPOSITION OF SEDIMENTS RELEASED FROM THE OVERFLOW

The dredging industry is often criticized for having an adverse environmental impact, particularly through generation of sediment plumes during project implementation. Various studies are started to estimate plume generation during dredging (see e.g. Aarninkhof, 2008) with particular emphasis on the sediments released from the overflow during dredging. One of the major difficulties in these studies is the measurement of the total volume of sediment released from the overflow and in particular to differentiate between the loss of fines and the loss of coarse sands during dredging. In these studies, information on the composition of the material released is determined by a number of sediment samples. Apart from the fact that this is a very elaborate procedure, the measurements give only point information from one part of the overflow system.

We have developed a metering system for real-time measurements of the sediment concentration and sediment composition (sand/clay ratio) in the overflow of a hopper dredger. This system has been demonstrated in pilot experiments during dredging operations. The system is based on identical principles as described above (the Medusa system) and uses the fact that the absolute concentration of fine sediments within the overflow system depends on the total concentration of sediments in the water passing the overflow (the sediment/water ratio) and the concentration of fines within the sediment mixture (the clay/sand ratio).

The Medusa system passively measures concentrations of natural occurring radionuclides. When the system is placed in a clay/sand/water mixture, the concentrations of the radionuclides will depend on the amount of water in the medium measured (the signal will be diluted, de Groot et al, 2009) and the signal will depend on the silt/sand ratio in the medium (van Wijngaarden et al, 2002). After a proper calibration of the ‘fingerprint’ of the sediments dredged, the measured signal can be translated in a silt/sand ratio and in a sediment/water ratio. The system can be operated continuously and can be used to make a mass balance of the total amount of fine sediments, and coarse sediments released from the overflow. Measurements in an overflow (figure 3) show the variation in total density during a dredging cycle and show the contribution of mud (silt) to the released material.

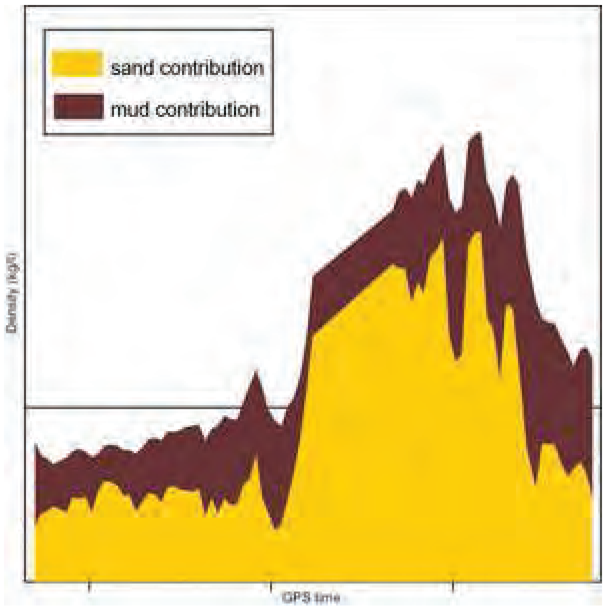

Figure 3: example of density measurements and concentrations of mud and sand from an overflow release.

4 EFFECTS OF DREDGING IN RELATION TO THE DYNAMICS OF NATURE

The potential effects from sediment plumes on the seafloor sediments can only be understood when the total release of *fine* sediments from the overflow can be related to the natural variation in concentrations of fines in seafloor sediments. Today, the buffering capacity of the seafloor for fine sediments has been estimated, but has hardly been measured.

We have shown that successive mappings of seafloor sediment composition can be used to monitor the transport of fines from a disposal site. The natural variation of fines and thereby the buffering capacity of the seafloor can be monitored in a similar way: long term monitoring of the silt content of the seafloor can help to quantify natural dynamics due to resuspension and large-scale sediment transport patterns.

The sediments released from the overflow of a hopper dredger are composed of sand and fine silts. Since the sands will behave completely different to the fines, information on the total volume of *fine* material from the overflow is an important parameter. We have shown that the release of fine material from a hopper overflow during dredging can be measured . With this quantification of sediment release, and the information of the buffering capacity of the seafloor sediments, the net effect of the release of fines during dredging can be related to the dynamics of nature.

5 REFERENCES

Aarninkhof, S. (2008). "The Day After We Stop Dredging: A World Without Sediment Plumes?" Terra et Aqua(110): 15-25

Du Four, I., Deleu, S., Darras, I., Roche, M., Koomans, R., & Van Lancker, V. (2005). Comparison between different seabed classification techniques and validation with sediment samples on two shallow-water dumping sites (Belgian continental shelf). Shallow Survey 2005 4th International conference on high resolution surveys in shallow water, Plymouth, Devon, UK.

de Groot, A.V., E.R. van der Graaf, R.J. de Meijer and M. Maucec (2009). "Sensitivity of in-situ [gamma]-ray spectra to soil density and water content." Nuclear Instruments and Methods in Physics Research Section A: Accelerators, Spectrometers, Detectors and Associated Equipment 600(2): 519-523.

de Meijer, R. J. (1998). "Heavy minerals: from 'Edelstein' to Einstein." Journal of Geochemical Exploration 62(1-3): 81-103

Nederbracht, G. and R. L. Koomans (2005). Nourishment of the slope of a tidal channel: from experiment to practice. Coastal Dynamics, Barcelona, Spain, ASCE.

van Wijngaarden, M., L. B. Venema, R. J. de Meijer, J. J. G. Zwolsman, B. van Os and J. M. J. Gieske (2002). "Radiometric sand-mud characterisation in the Rhine-Meuse estuary Part A. Fingerprinting." Geomorphology 43: 87-101

Venema, L. B. and R. J. de Meijer (2001). "Natural radionuclides as tracers of the dispersal of dredge spoil dumped at sea." Journal of Environmental Radioactivity 55(3): 221-239.

SAFE DISPOSAL OF DREDGED MATERIAL IN A SENSITIVE ENVIRONMENT

Operational planning of dredging activities based on innovative plume predictions

S.G.J. Aarninkhof[1] and A.P. Luijendijk[2]

Abstract: Ras Laffan Port Expansion Program foresees in a major extension of Ras Laffan Port (Qatar) to accommodate ongoing growth of the country's LNG production. Marine works related to dredging, reclamation and construction of breakwaters were inherently associated with the release and accumulation of fine material within the new port area. This fine material had to be removed. As it was not suitable for filling purposes, it had to be disposed in an offshore disposal area.

To demonstrate that such disposal operations could be carried out without violating strict environmental criteria around the disposal areas, a state-of-the-art 3D plume model was used to simulate a variety of disposal scenarios. The results provided valuable insight in the dynamics of sediment plumes over a spring-neap cycle. To enable operational use on-board, a novel interpretation method was developed to transform the model predictions into so-called 'Safe Disposal Maps'. These maps showed green areas where disposal operations could safely be carried out as a function of the tide conditions at hand.

This paper adopts the Ras Laffan case to demonstrate the capability of present-day numerical models to provide realistic simulations of sediment plumes and – at least equally important – the applicability of such complex techniques in dredging practice through innovative interpretation of model results. In the context of increasing environmental awareness on dredging projects worldwide, the availability of such tools is of crucial importance to enable reliable impact assessments and environmentally-safe planning of dredging operations.

Key words: Environment, disposal operations, turbidity, plume prediction

[1] Senior engineer, Royal Boskalis Westminster nv, Hydronamic, P.O. Box 43, 3350 AA Papendrecht, The Netherlands, T: +31 78 6969415, F: +31 78 6969555, E-mail: s.g.aarninkhof@boskalis.nl, www.boskalis.nl

[2] Senior adviser, Deltares, Hydraulic Engineering, P.O. Box 185, 2600 MH Delft, The Netherlands, T: +31 15 2858709, F: +31 15 2858712, E-Mail: arjen.luijendijk@deltares.nl, www.deltares.nl

1 INTRODUCTION

Qatar’s North Field is the focus of attention of some of the world’s largest oil conglomerates. Studies have shown that the certified reserves currently stand at more than 900 trillion cubic feet of natural gas. Large-scale investments in LNG infrastructure enable ongoing growth of the country’s annual LNG production, which is expected to reach 77 million tones per annum by 2010. Ras Laffan is expected to become the major GTL terminal, the single largest complex and most comprehensive gas processing city in the world and one of the biggest producers of ethylene and derivatives. In this context, QP has decided to extensively expand Ras Laffan Port and Ras Laffan Industrial City. The new port will accommodate around 225 million tons of products per year, more than double its present capacity.

a *b*

Fig. 1: Site overview of Ras Laffan Port (Qatar), located in the Arabian Gulf

The first stage of the works commenced in 2005 and covered the large civil marine work related to the engineering, procurement, installation and construction for dredging, reclamation and breakwaters. The approximate quantities involved were:

- 20 million m^3 of hard rock dredging with cutter suction dredgers
- 27 million m^3 of sand reclamation from offshore borrow areas
- 16 million tons of rock from Qatar for breakwater construction
- 7 million tons of rock from overseas for breakwater construction

These large-scale dredging and reclamation activities were inherently associated with the release of fine excess material (due to cutter spill and overflow losses during barge loading), resulting in the accumulation of fine material in the new port area. This material had to be removed. As it was not suitable for filling purposes, it had to be disposed in an offshore disposal area. Numerical models were used to demonstrate that dredging and disposal operations could safely be carried out without violating environmental requirements.

This paper adopts the Ras Laffan case to demonstrate the capability of present-day numerical models to provide realistic simulations of sediment plumes and – at least equally important – the applicability of such complex techniques in dredging practice through innovative interpretation of model results.

2 SAFE DISPOSAL OF DREDGED MATERIAL IN A SENSITIVE ENVIRONMENT

To guarantee safe disposal of excess material at sea, careful selection of a disposal site is of paramount importance. The Environmental Impact Assessment for the Ras Laffan Port Expansion project had demonstrated that the nearshore coastal zone (with water depths less than 20 m) and the waters to the southeast of Ras Laffan are the most sensitive locations from the perspective of biological productivity, fisheries and ecological habitats. Offshore disposal at water depths above 20 m is thus preferred.

The sand mining area JV4 is located at 12 miles northwest of Ras Laffan Port, at water depths of 19 to 25 m (Fig. 2a). Due to the extraction of approximately 6 million m^3 of material for the present port expansion, it offers sufficient space to accommodate the anticipated 3 million m^3 of excess material from Ras Laffan Port. Hence no reduction of water depth would occur. An extended environmental study, carried out prior to the start of the sand mining operations, revealed that the sea bed in the JV4 area was mostly covered with soft material and that benthic communities were not particularly rich. This observation applied to the full sand mining area. The authors are not aware of previous use of JV4 for earlier sand mining operations, however, if so, it is very unlikely that these earlier operations covered the full area of JV4. Consequently, it could be concluded that local ecological sensitivity for the JV4 area was low by nature. To avoid further disturbance in other, pristine areas, it was decided to select JV4 as the primary disposal location.

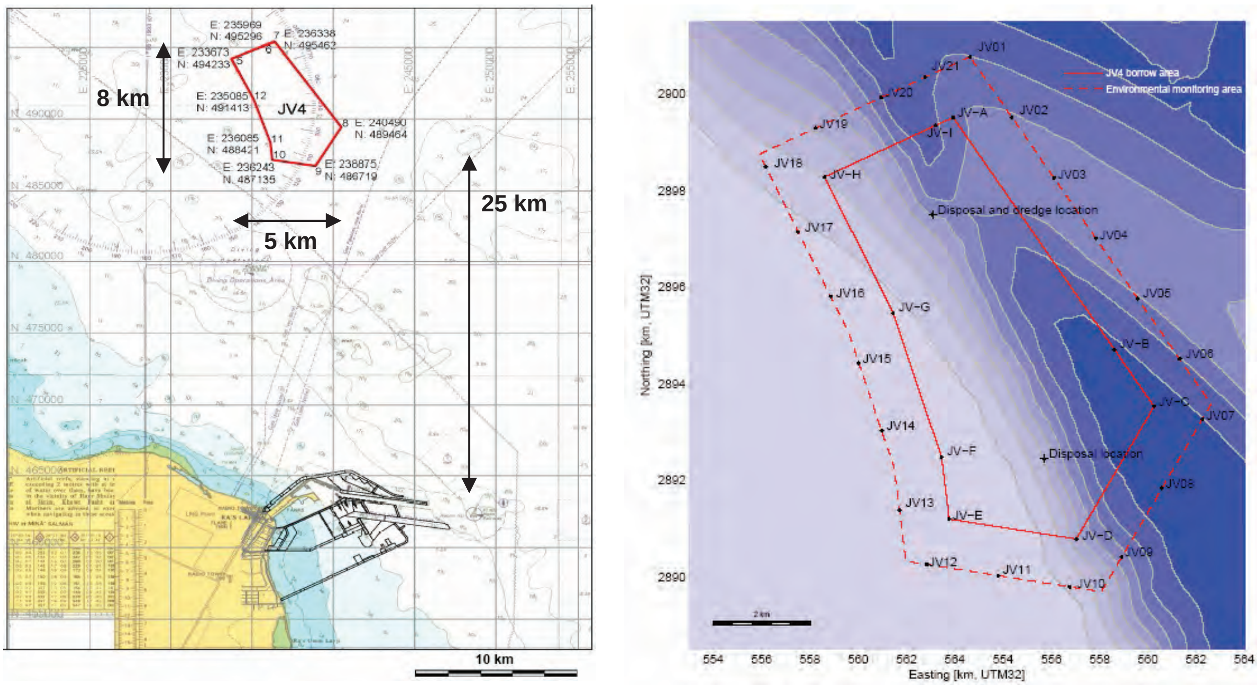

a *b*

Fig. 2: Location of JV4 sand mining area with respect to Ras Laffan Port (a) and environmental boundary surrounding JV4 (b). Area JV4 was identified as the most suitable disposal site.

The sand mining activities in JV4 were subject to environmental requirements to minimize possible environmental impacts to surrounding waters. These requirements stated that during dredging, the concentration of suspended solids was not allowed to exceed a depth-averaged limit level of 30 mg/l on an environmental boundary surrounding JV4 (Fig. 2b). To verify whether these requirements were met, the suspended solids concentration (hereafter referred to as SSC) was measured on a daily basis, at 21 locations along the environmental boundary. SSC measurements were carried out by lowering and subsequent raising a calibrated YSI turbidity sensor through the water column. This yields a vertical concentration profile, which was averaged over depth. Owing to the relatively large distance to the dredging operations, vertical concentration profiles were found to be virtually depth-uniform. It was proposed to apply the same environmental requirements to the execution of the disposal activities as were used earlier during the sand mining operations.

To obtain permission for the start of the disposal works, authorities demanded to demonstrate that the disposal operations could be carried out without exceeding SSC limit levels at the environmental boundary, under all possible current and weather conditions. A state-of-the-art numerical model was used to do so.

3 MODEL PREDICTION OF PLUME DISPERSION

3.1 Approach

The work method for the removal of unsuitable fine material from Ras Laffan Port foresees the use of Trailing Suction Hopper Dredgers (TSHD). After sailing to JV4, this fine material is disposed by opening the bottom doors of the TSHD. This yields a fluid-like jet of fine material that rapidly descends to the sea bed (e.g. Van Rijn, 2005). The bulk behavior of this water-sediment mixture is important, rather than the settling velocity of the individual particles (Winterwerp, 2002). After impact upon the bed, the sediment load will radially flow away from the point of impact over the bed as a density current in the lower 15 to 20% of the water column. This phase is characterized by rapid dissipation of energy and settlement of material. The process of jet release, descend and collapse is generally referred to as the dynamic plume (e.g. Spearman et al., 2007).

While the fine material jet descends through the water column, part of the material gets eroded from the outside of the bulk load (slurry jet) and suspended in the surrounding water (entrainment). After impact on the sea bed, resuspension of fine material occurs from the near-bed density current, caused by turbulence-induced upward mixing at the upper surface of the mud layer. Both mechanisms yield entrained sediments that act as the source term for the so-called passive plume. The passive plume is capable of transporting low-density material away from the direct disposal site owing to advection with tidal currents and diffusion processes.

The near-bed density current propagates, depending on initial density and momentum of the sediment-water mixture, over a distance of typically 100 to 500 m. Given the size (several kilometers) and bed slope (typically 1:1000) of JV4, no sediment will be lost from the disposal area due to migration of the near-bed density current. As a result, the model study focused on the assessment of suspended sediment losses.

Appropriate representation of these processes asked for the use of two coupled models. The first, Jet3D (Koster, 1988, Morelissen, 2007) determined near-field entrainment rates over the vertical during descent of the dynamic plume from the TSHD. Jet3D is a semi-empirical model which calculates the dispersion and entrainment effects of jets based on an experimental database. The second model, Delft3D (e.g. Lesser et al., 2004), assessed the resuspension from the density current and far-field dispersion of disposed sediments. The coupling of the two models is shown in Fig. 3. The calculated entrainment rates from Jet3D together with the durations of disposals served as input for a three-dimensional flow and sediment dispersion model.

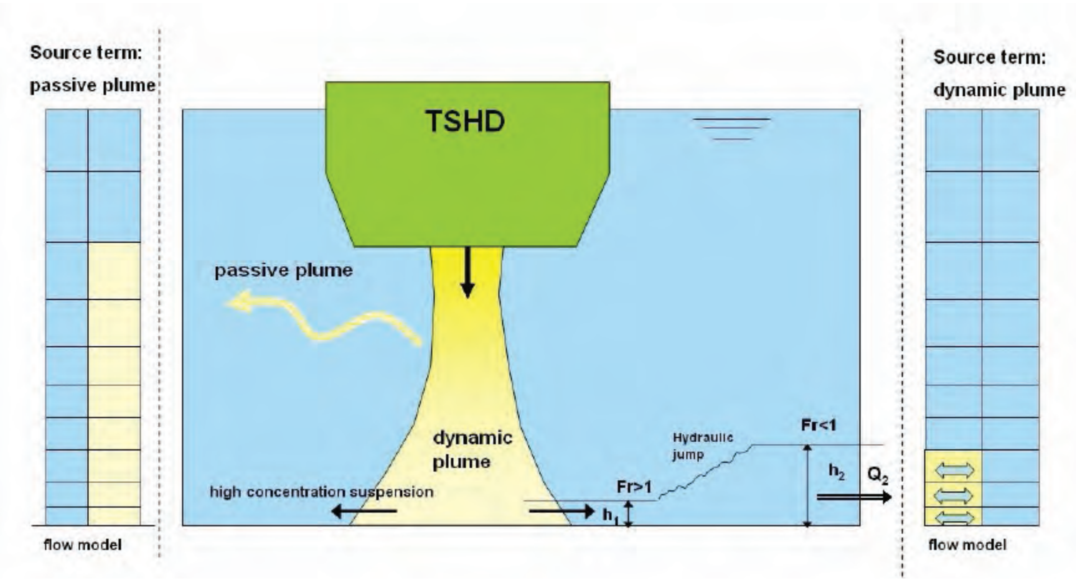

Fig. 3: Coupling of Jet3D and Delft3D models for simulation of Ras Laffan disposal cycles. Jet3D describes the release, descend and collapse of the dynamic plume, which yields the input SSC for the Delft3D model. The latter describes the dispersion of the passive plume due to advection with tidal currents and diffusion processes.

3.2 Model schematization

For the purpose of this study, the computational grid of an existing hydrodynamic model for the Ras Laffan region was refined in and around the JV4 area. The resolution of the new JV4 model varied from 375x155 m offshore to 35x35 m inside the JV4 area. The hydrodynamic model simulates tide-driven flows only; no wind or wave effects are taken into account. The model is set up in three-dimensional mode with 10 vertical layers with increasing resolution towards the bed. This allows for appropriate representation of the near-bed density currents. Model validation against current magnitude and direction data sampled near Ras Laffan Port revealed good performance of the tidal model, with differences in measured and computed current magnitude typically well below 10%. During storm conditions, differences tend to increase, as a result of differences in wind set-up on both sides of Ras Laffan Port. However, as this phenomenon does not play a role at deeper water where JV4 is located, it is concluded that the tidal model is suitable for providing the flow conditions to assess plume dispersion during disposal activities at JV4.

Each disposal event was characterized by a means of a fines release of 8400 kg/s during 300 seconds. Jet3D simulations revealed that approximately 10% of this was entrained during vertical descend through the water column. The remaining 90% of the material forms a density current (after impact on the sea bed and a hydraulic jump at some distance from the disposal, cf. Fig. 3). Both source terms serve as input for the Delft3D plume dispersion model. The sediment involved is schematized by means of three fractions with a D_{50} of 5, 18 and 43 µm, respectively. The model accounts for the effect of hindered settling, while a minimum settlement velocity of 0.10 mm/s is adopted to account for the process of flocculation. The model also computes the settling of the sediments at the bed when the bed shear stresses become small.

The disposals have been applied at two different locations in the JV4 area in order to take into account the variation of the bed slope, water depth and tidal currents. The disposal locations have remained the same throughout the simulations. Due to the frequent disposals, a dredging-induced sediment plume will be produced around these disposal locations. This plume is able to enlarge during some tidal phases and in some cases due to the cumulative build up of sediment concentrations in time. SSC maps are regularly mapped as output during the simulation.

3.3 Model results: SSC maps

The results shown here represent a scenario with two dredgers, each with a cycle time of 6 hours. Each cycle starts with a disposal event (5 minutes), followed by sailing to the mining location within JV4 (20 minutes), dredging (95 minutes – 20 of which with no overflow) and activities outside JV4 (sailing to port, pumping ashore, clean-up dredging and sailing back to JV4, total 240 minutes). The scenario thus combines the disposal of fine sediments in the SE part of JV4 with subsequent sand mining in the NW part of JV4.This allows for a realistic representation of dredging processes in the area as well as to examine possible accumulation of suspended sediment concentrations originating from multiple dredging activities at the same time.

The model simulations for this scenario result in the prediction of SSC maps throughout a 14-day spring-neap cycle. Results are presented by means of depth-averaged suspended sediment concentrations above natural background level. An example SSC map is shown in Fig. 4. Suspended sediment concentrations in the plume typically range between 0 and 50 mg/l, with higher values above 50 mg/l only found in the direct neighborhood of the dredging equipment. The black line denotes the instantaneous location of the (depth-averaged) 30 mg/l concentration contour, while the red line marks the location of the cumulative 30 mg/l exceedence contour. The exceedence contour marks the outer limit of the area where computed suspended sediment concentrations have (at least once) exceeded the 30 mg/l environmental limit level – for the fixed disposal location considered in the simulations. In addition, the SSC maps provide background information on the current tide conditions (water level, flow magnitude & direction) as well as the status of the dredging works (disposal, sailing or dredging).

Animations of such SSC maps over time clearly show the dynamics of Ras Laffan sediment plumes, characterized by large variations in plume direction and extent. In addition, they show the accumulation of suspended sediments in the water column due to cumulative dredging and disposal events. Plume excursion typically increases during spring tide. Perhaps somewhat surprisingly, maximum plume excursions are not found for disposals during periods of maximum tidal velocities, but for disposals carried out 1-3 hours before reaching peak flow velocity. Subsequent flow acceleration causes a maximum excursion of the sediment plume, whereas for disposal at peak velocity, subsequent flow deceleration reduces plume excursion, hence mitigates dredging impacts. This observation reveals the added value of using a non steady-state hydrodynamic model that accurately resolves the dynamics of the tidal motion.

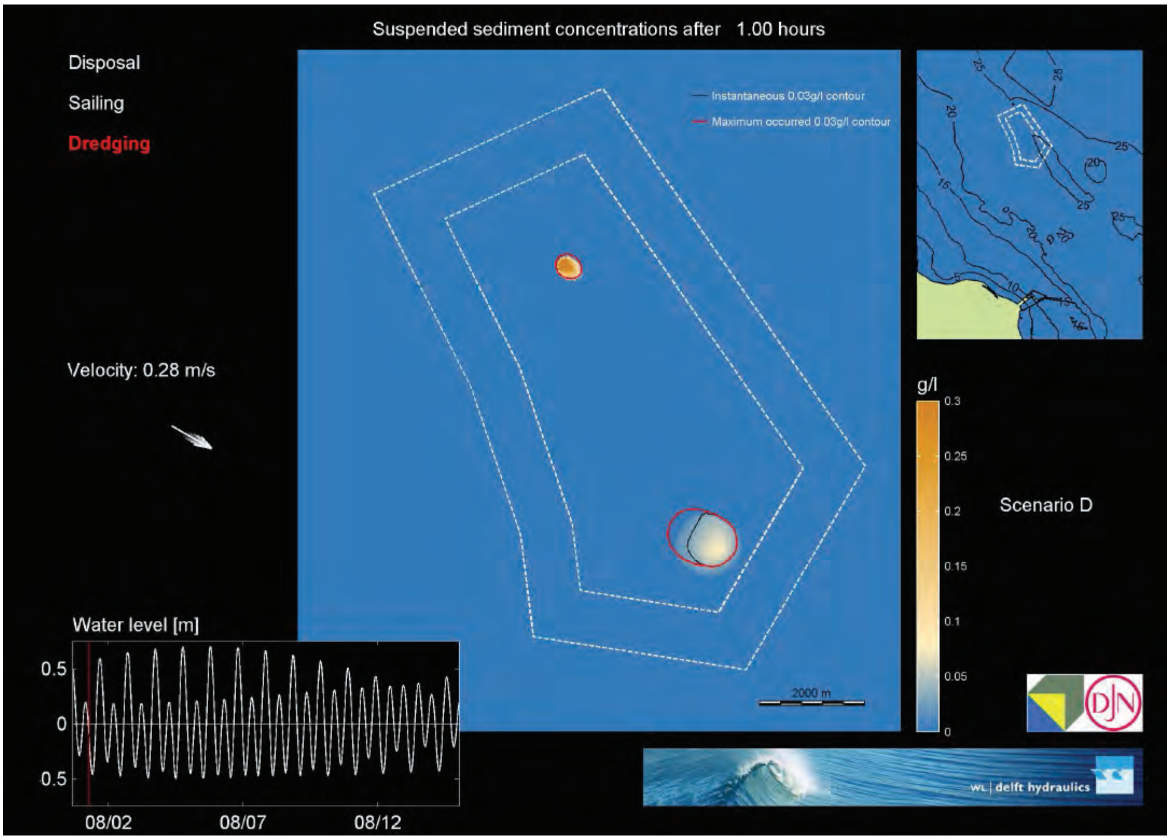

Fig. 4: Model-predicted SSC map for combined dredging (NW part) and disposal (SE part) activities at Ras Laffan JV4. The black line denotes the instantaneous location of the 30 mg/l contour, the red line marks the exceedence line of the 30 mg/l SSC level. The latter is needed for the generation of the Safe Disposal Maps.

The results presented in Fig. 4 can be considered as conservative, particularly because of the chosen schematization of fines (smallest fraction 5 µm with settlement velocity 0.10 mm/s) and the way Jet3D results for a single jet have been interpreted for use with a TSHD with 44 bottom doors, hence 44 different jets. Theoretically Jet3D describes the dynamics of an individual jet fully enclosed by fresh water; however, in reality, each of the 44 jets underneath the TSHD will interact with neighboring plumes during descend under the vessel. Consequently, real-world sediment entrainment rates to the surrounding water are likely to be smaller than predicted by the models, hence calculated suspended sediment concentrations in the plume can be considered as conservative.

4 OPERATIONAL PLANNING OF DREDGING ACTIVITIES AT RAS LAFFAN

4.1 Safe Disposal Maps

The time series of SSC maps throughout a spring-neap cycle provides the starting point for the generation of so-called Safe Disposal Maps. These maps mark the area where sediment can safely be disposed (i.e. without violating the environmental requirements), as a function of the tidal conditions at the time of disposal. Safe Disposal Maps are generated for 10 different tidal stages, each characterized by the flow velocity and direction at the time of disposal. The selected tidal stages are summarized in Fig. 5.

Tidal flow Ras Laffan	Class	Dir.	Velocity	Characterization
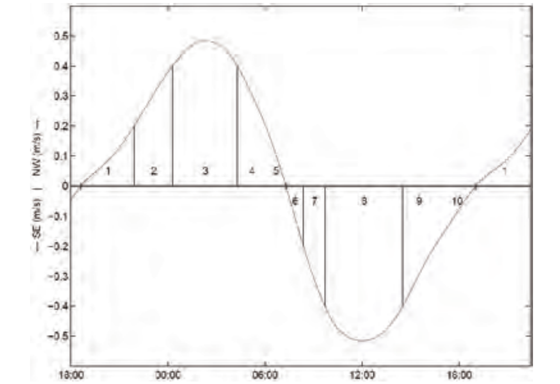	1	NW	0 – 0.2 m/s	Increasing velocity
	2	NW	0.2 – 0.4 m/s	Increasing velocity
	3	NW	> 0.4 m/s	-
	4	NW	0.2 – 0.4 m/s	Decreasing velocity
	5	NW	0 – 0.2 m/s	Decreasing velocity
	6	SE	0 – 0.2 m/s	Increasing velocity
	7	SE	0.2 – 0.4 m/s	Increasing velocity
	8	SE	> 0.4 m/s	-
	9	SE	0.2 – 0.4 m/s	Decreasing velocity
	10	SE	0 – 0.2 m/s	Decreasing velocity

Fig. 5: Definition of tidal stages for generation of Safe Disposal Maps

To generate the Safe Disposal Maps, all disposal events throughout a 14-day spring-neap cycle plus their associated sediment plumes were categorized according to the tidal classes specified in Fig. 5. For each class, the location of the 30 mg/l exceedence contour was determined based on the evolution of the set of sediments plumes in that class. By moving the exceedence contour within the JV4 area along the environmental boundary, areas of *unsafe* disposal are being blanked. Consequently, the remaining area can be marked *safe* disposal zone, or suitable area. In this way, Safe Disposal Maps were generated for all 10 tidal classes specified above.

The outcome of this novel post-processing on model results is presented in Figs 6a/b for the situation of combined dredging/disposal with two TSHDs. The figures show the 30 mg/l exceedence contour (red line) for each of the 10 tidal classes at hand. The results confirm that maximum plume excursions are found for disposals during flow acceleration and, to a less extend, during peak tidal velocities. For disposal during flow deceleration, plume excursions are minimal and SSC typically drop well below 30 mg/l within 1 km from the disposal location. These observations apply to both ebb and flood tides, though absolute plume excursions are larger during flood. As the ebb tidal velocities (towards NW) are only slightly dominant compared to the occurring flood velocities (towards SE), the latter observation indicates that cumulative effects of ongoing dredging and disposal operations plays an important role here.

The green-shaded areas in Figs 6a/b denote the regions where disposal operations can safely be carried out for that particular tidal class. A minimal area of the safe disposal zone is found for situations of flow acceleration, although the available safe area for those conditions (increasing flow velocities between 0.2–0.4 m/s towards NW) still measures about 5 km^2. As expected, safe disposal areas tend to increase with decreasing excursion of the 30 mg/l exceedence line. Ultimately, for situations of flow deceleration, virtually the entire JV4 region can be used for disposal activities without violating the environmental limits.

From the Safe Disposal Maps it is concluded that disposal operations can safely be carried out during each phase in the tidal cycle. However, depending on the tidal phase at the time of disposal, restrictions may exist in the chosen disposal location within JV4. The latter particularly applies to periods of tidal flow acceleration which are associated with maximum dispersion of the dredging-induced sediment plumes.

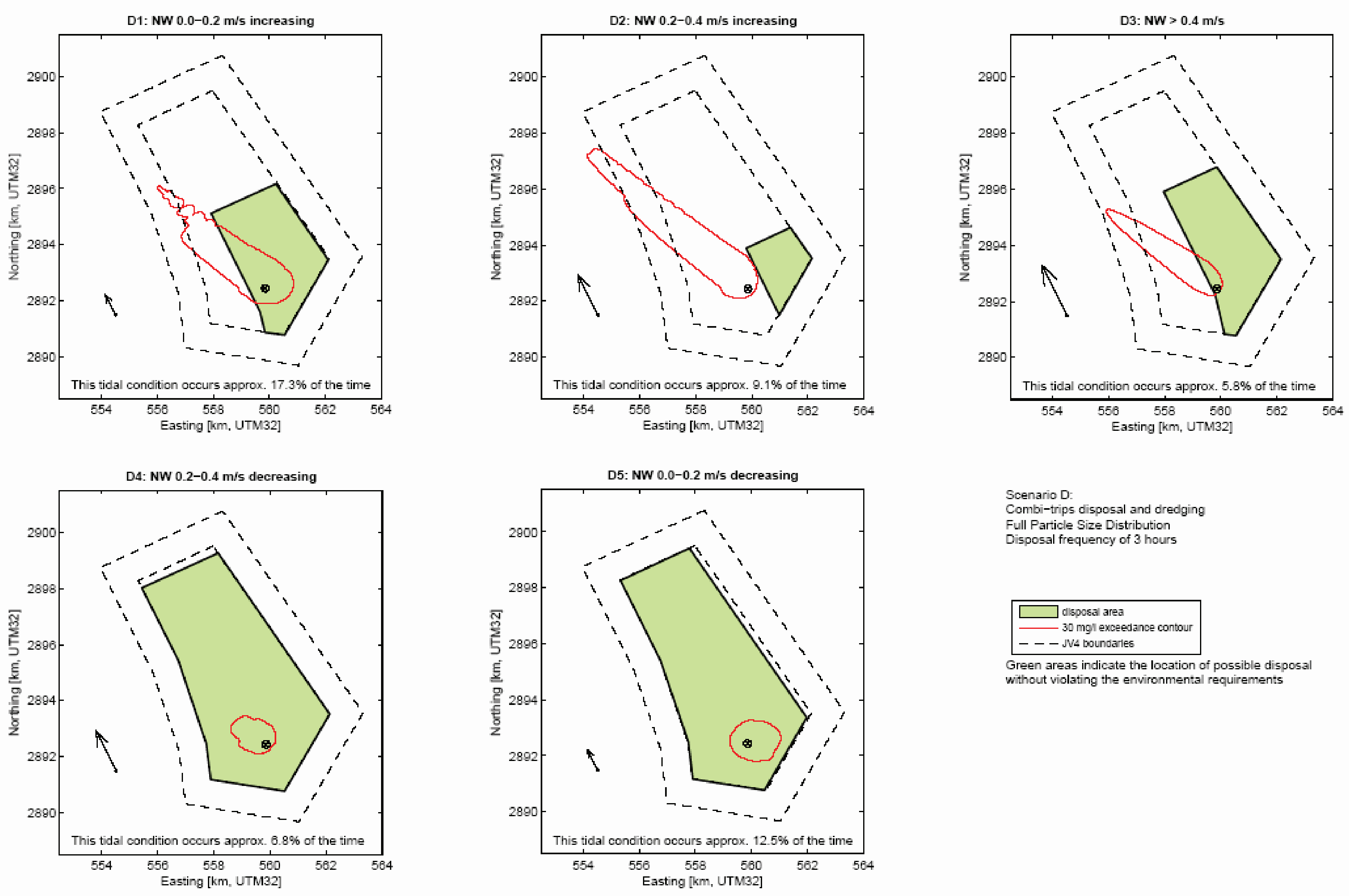

Fig. 6a: Safe Disposal Maps Ras Laffan JV4 for five tidal stages during flood

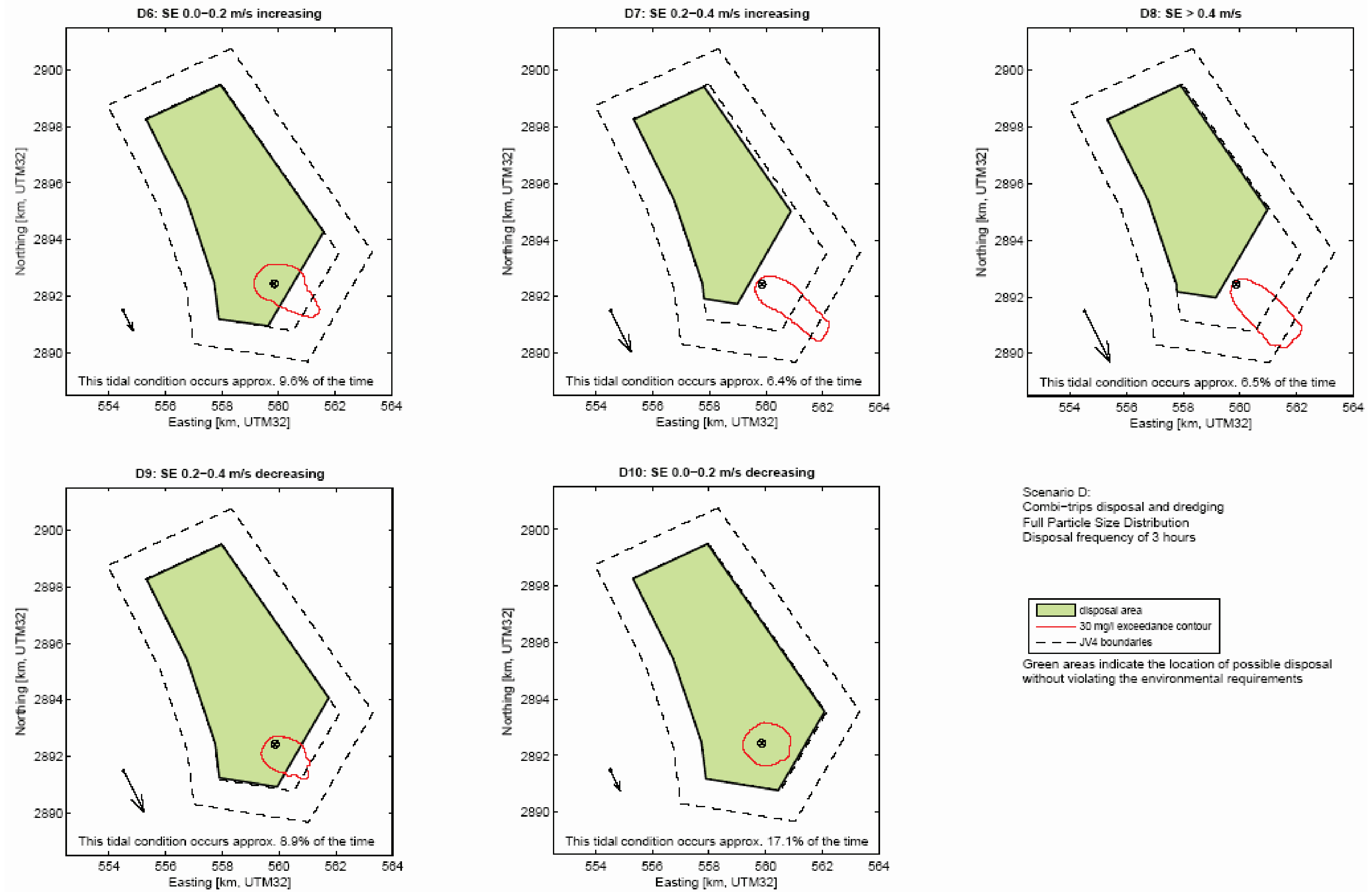

Fig. 6b: Safe Disposal Maps Ras Laffan JV4 for five tidal stages during ebb

4.2 Operational use of Safe Disposal Maps

The Safe Disposal Maps can be used in practice for the determination of suitable disposal locations on a trip-by-trip basis. Steering parameters are the expected tidal conditions (flow magnitude, acceleration or deceleration & direction) at the time of disposal. These parameters can reliably be predicted with the help of a validated numerical model.

For the Ras Laffan Port Expansion project, time series of tidal flows at JV4 were predicted at 20 minute intervals, for the entire period that dredging and disposal operations were carried out. The predicted tidal conditions allow for the identification of the appropriate tidal class and associated Safe Disposal Map for each time step. Results are summarized by means of planning tables for safe disposal operations (Fig. 7), which were provided to site.

Date	Time	Current magnitude	Dir	Ref	Map
02-July-2008	05:00:00	0.20 m/s	NW	Map D5	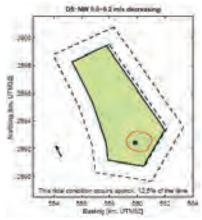
02-July-2008	05:20:00	0.14 m/s	NW	Map D5	
02-July-2008	05:40:00	0.08 m/s	NW	Map D5	
02-July-2008	06:00:00	0.04 m/s	NW	Map D5	
02-July-2008	06:20:00	0.06 m/s	SE	Map D6	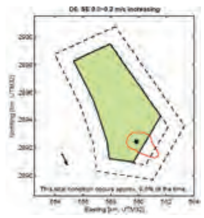
02-July-2008	06:40:00	0.12 m/s	SE	Map D6	
02-July-2008	07:00:00	0.18 m/s	SE	Map D6	
02-July-2008	07:20:00	0.24 m/s	SE	Map D7	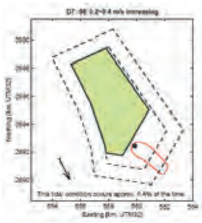
02-July-2008	07:40:00	0.29 m/s	SE	Map D7	
02-July-2008	08:00:00	0.34 m/s	SE	Map D7	
02-July-2008	08:20:00	0.38 m/s	SE	Map D7	
02-July-2008	08:40:00	0.41 m/s	SE	Map D8	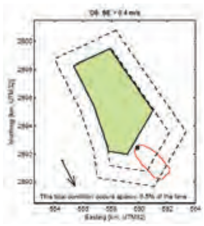
02-July-2008	09:00:00	0.43 m/s	SE	Map D8	
02-July-2008	09:20:00	0.45 m/s	SE	Map D8	
02-July-2008	09:40:00	0.46 m/s	SE	Map D8	
02-July-2008	10:00:00	0.46 m/s	SE	Map D8	

Fig. 7: Planning table for safe disposal operations.

The planning tables and underlying Safe Disposal Maps were successfully used while carrying out dredging and disposal activities for the Ras Laffan Port Expansion project. During execution of the works, turbidity levels along the environmental boundary surrounding JV4 were measured on a daily basis. No environmental limit exceedence was measured throughout the period of dredging and disposal operations, thus confirming good performance of the disposal strategy based on Safe Disposal Maps.

5 CONCLUSIONS

Application of two coupled models to simulate dynamic plume behavior and subsequent passive plume dispersion during dredging and disposal operations at Ras Laffan (Qatar) has demonstrated the capability of present-day numerical models to provide realistic simulations of dredging-induced sediment plumes over a spring-neap cycle. Perhaps somewhat surprisingly, maximum plume excursions are not found for disposals during periods of maximum tidal velocities, but for disposals carried out 1-3 hours before reaching peak flow velocity, during flow acceleration. In addition, cumulative effects caused by ongoing dredging and disposal operations in the area were found to be important.

Novel interpretation of model-predicted patterns of suspended sediment concentration over a spring-neap cycle has resulted in so-called Safe Disposal Maps. These maps were generated for 10 different phases of the tidal cycle and mark the area where disposal operations can safely be carried out. The maps revealed that disposal operations can safely be carried out during each phase of the tidal cycle, although restrictions may apply to the choice of the disposal location depending on the tidal conditions at the time of disposal. This is particularly the case during periods of tidal flow acceleration, which are associated with maximum dispersion of the dredging-induced sediment plumes.

To facilitate operational use of the Safe Disposal Maps, planning tables were generated based on calculations with a validated hydrodynamic model. The planning tables and underlying Safe Disposal Maps were successfully used while carrying out dredging and disposal activities for the Ras Laffan Port Expansion project. No environmental limit exceedence was measured throughout the period of dredging and disposal operations, thus confirming good performance of the disposal strategy based on Safe Disposal Maps.

This paper has thus demonstrated the applicability of complex numerical models in dredging practice through novel interpretation of model results. In the context of increasing environmental awareness on dredging projects worldwide, the availability of such tools is of crucial importance to enable reliable impact assessments and environmentally-safe planning of dredging operations.

Acknowledgements

The work presented in this paper was carried out as part of Ras Laffan Port Expansion project and funded by the Ras Laffan Joint Venture consisting of Jan de Nul Dredging Ltd. and Boskalis Westminster Middle East Ltd. The collaboration with Mr. Tom de Wachter, environmental manager on the project, is gratefully acknowledged.

References

Koster, A.W.J. 1988. Straal3D – ronde straal in stromend medium (3-dimensionaal), Manual for JET3D.

Lesser, G.R., Roelvink, J.A., Van Kester, J.A.T.M. and Stelling, G.S. (2004).Development and validation of a three-dimensional morphological mode. Coastal Engineering, Volume 51 (8-9), pp. 883-915

Morelissen, R. (2007). Modelling and assessment of dredge plumes in ambient conditions: Coupling Jet3D to Delft3D-FLOW. Deltares report H4959

Spearman, J., Bray, R.N., Land, J., Burt, T.N., Mead, C.T. and Scott, D. (2007). Plume dispersion modeling using dynamic representation of trailer dredger source terms. Estuarine and Coastal Fine Sediments Dynamics (editors J.P.-Y. Maa, L.P. Sanford and D.H. Schoellhamer), pp. 417-448.

Van Rijn, L.C. (2005). Principles of Sedimentation and Erosion Engineering in Rivers, Estuaries and Coastal Seas. Aqua Publications, Amsterdam (The Netherlands).

Winterwerp, J.C. (2002).Near-field behaviour of dredging spill in shallow water. Journal of Waterway, Port , Coastal and Ocean Engineering, 128(2), 96-98

A FIELD SURVEY OF A DREDGING PLUME DURING GRAVEL DREDGING

W.A. Breugem[1], M. Bollen[1], M. Sas[1], and J. Vandenbroeck[2]

Abstract: Overflow during dredging with a Trailing Suction Hopper Dredger (TSHD) inevitably leads to the development of a dredging plume, which might impact the coastal ecosystem as well as the dredging operations themselves. A better insight into the behavior of such plumes allows proactive management of dredging operations so as to limit these impacts. Hence, accurate measurements of such plumes are, though quite rare, more than wanted.

In this philosophy, DEME and IMDC have set up a survey in which a dredging plume is observed near a specialized gravel dredger from the DEME group. In order to measure this plume, a separate survey vessel was equipped with a series of sophisticated tools: an ADCP (Acoustic Doppler Current Profiler) to measure the suspended sediment concentrations and the flow velocity, an OBS3A (Optical Backscatter) turbidity meter to measure the sediment concentrations 1.5 m below the free surface, and the newly developed SiltProfiler to measure high-resolution vertical sediment concentration profiles. Simultaneously, samples in the overflow of the TSHD were taken using an airlift pump.

All measurements are reported and the influence on the development of the dredging plume of different parameters like grain size and dredging direction (with regard to the prevailing current) is examined.

Keywords: dredging plume, field survey, gravel dredging, SiltProfiler

[1] International Marine and Dredging Consultants (IMDC). Coveliersstraat 15, B-2600 Berchem (Antwerpen) Belgium
[2] Société de Dragage International (SDI – DEME group). Parc du Pont Royal, 251 Avenue du Bois, Bâtiment I, 59130 Lambersart, France

1 INTRODUCTION

Overflow during dredging with a Trailing Suction Hopper Dredger (TSHD) inevitably leads to the development of a dredging plume, which might impact the coastal ecosystem as well as the dredging operations themselves. A better insight into the behavior of such plumes allows proactive management of dredging operations so as to limit these impacts. Hence, accurate measurements of such plumes are, though quite rare, more than wanted.

It was the objective of this measurement campaign to obtain field measurement data of the sediment concentrations in a dredging plume as well as of the sediment concentrations and particle characteristics that are discharged from a Trailing Hopper Suction Dredger into the environment for different ambient conditions in a tidal flow at open sea while dredging gravel. These data can provide more insight into the behavior of a dredging plume during the dredging process and into its decay after finishing the process. Furthermore, it provides insight into the influence of various parameters on the development of the plume such as the dredging direction and bed grain size. In order to fulfill these goals, IMDC and DEME set up a measurement campaign in which a plume that originated from the THSD during and after the dredging process was surveyed while simultaneously sampling the discharged materials inside the overflow of a TSHD.

In the following, first the measurements are described, starting with a description of the used instruments to survey the plume and to determine the discharge from the overflow, followed by a description of the measurement protocol and the ambient conditions during the measurements. Then the results of the discharge measurement are described with respect to the grain size and sediment concentrations in the overflow of the THSD. This is followed by a description of the results of the measurement of the dredging plume from a separate survey vessel during the dredging process, with special attention to the length and width of the plume. Finally, a description of the behavior of the plume after the measurement process is presented with a particular focus on the time that was needed for the plume into decay to the background concentration after the dredging was finished.

2 METHODS

2.1. Instruments

Inside the overflow of the THSD, an airlift pump was installed in order to take samples of the mixture that was released from the hopper. An airlift pump (Chisholm, 1982) was chosen, because it provides a failsafe construction, which does not contain any moving parts inside the overflow, and thus is very robust for the rather violent conditions that occur here. It has already succesfully been used earlier for similar measurements by Aarninkhof (2008). The airlift pump was made of a steel tube with a length of 5 m and a diameter of 5 cm and a second pipe for the compressed air, which entered the main pipe at a height of 0.5 m above the airlift pump's inflow. In designing the airlift, the criteria with respect to the minimum and maximum depth of the airlift's inflow to obtain well mixed conditions as cited in Aarninkhof (2008) were used. The airlift was tested during a separate dredging campaign and appeared to give representative samples of the material in the overflow.
Samples were taken every 15 minutes on the first day of the survey and every 10 minutes on the other days. From these samples, the sediment concentrations were determined using drying and weighting of the samples. The laser diffraction method was used to determine the distribution and statistical moments of the particle diameters in the samples. This method was applied twice, once on the samples as they were taken, and another time on samples that were treated with ultrasound to prevent any flocculation.

Figure 1 The SiltProfiler, which was used to measure high resolution sediment concentration profiles.

The survey vessel was equipped with an ADCP (Acoustic Doppler velocity meter), which was used to measure flow velocities and sediment concentrations continuously. These concentrations were determined from the acoustic backscatter intensities (Hay 1991, Thorne and Campbell 1992) using the Sediview (DRL 2003) software, which provides a semi-automatic calibration procedure in order to relate the acoustic intensities to the sediment concentrations. The concentrations for the calibration were obtained from samples that were taken regularly during the measurement campaign. Additionally, continuous measurements of sediment concentrations were taken with a D&A OBS 3A, at 1.5 m below the free surface. This instrument consists of an infrared optical backscatter sensor, in combination with a temperature, conductivity and pressure sensor. At various instances in time, the IMDC developed SiltProfiler was used to obtain quick[1] and high-resolution profiles of the sediment concentrations as function of depth. The SiltProfiler consists of a pressure, temperature and conductivity sensor in combination with three different turbidity sensors on one single instrument, which is lowered in free-fall to the bottom (Figure 1). After reaching the bed, the SiltProfiler is winched up and the measurement data are downloaded from the instrument. In this way, a vertical profile of the sediment concentrations and salinity can be obtained with a high spatial resolution. The three turbidity sensors are one backscatter and two forward scatter optical turbidity meters, which each have a different optimal measurement range. This enables us to measure suspended sediments in the range of 0 – 50,000 mg/l. However, the concentrations in the present survey were low, such that only the backscatter sensor needed to be used. Calibration of the optical sensors occurred using data from samples that were taken from the survey vessel.

2.2. Overview of the measurements and measurement protocol

Measurements were performed on three consecutive days in August 2008 during fair weather conditions. Each day, dredging was performed in a different zone at two different transects. From now on, these will be referred to as transect A1 and A3 for the first day, B1 and B3 for the second day and C2 and C3 for the third. Generally, the duration of dredging was between one and two hours. The dredging was performed at open sea at typical water depths between 40 m and 50 m. Typical flow velocities and flow regimes, the stage of the tide, as well as the velocity of the TSHD are given in Table 1. Dredging during these measurements was normally performed

[1] The cycle time of dropping the SiltProfiler, retrieving the instrument and transferring the data to the survey vessel in 25 m of water is typically something like 90 s.

against the mean flow direction, with the exception of the second transect on the first day (A3), where the sailing direction of the TSHD was the same as the flow direction.
The dredged material consisted of gravel and sand. Samples of the bed material taken with a Hamon grab showed that the D_{50} was 12.5 mm in zone A, 4 mm in zone B, and 10 mm in zone C. From these samples, the amount of fines (D_{50} < 63 μm) was also determined. This was 0.6 % for zone A, 1.7% for zone B, and 1.1 % for zone C.

Table 1 Overview of the different measurements and the flow conditions during these measurements. Note that transect A3 was obtained while dredging in the same direction as the mean flow, while all other transects were obtained while dredging against the mean flow.

Transect	Duration [h :mm]	Average flow velocity [m/s]	Average velocity of THSD [m/s]	State of the tide	Flow regime
A1	1:31	1.18	0.58	rising – high water	Constant
A3	1:45	0.85	0.73	falling water	Accelerating
B1	1:19	0.89	0.50	rising water	Constant
B3	0:50	0.51	0.57	high water – falling	Accelerating
C2	1:30	0.83	0.48	falling water	Constant
C3	1:00	0.45	0.48	falling water - low water	Decelerating

Four different protocols were used by the survey vessel for navigating in the neighborhood of the TSHD and thus sampling the dredging plume (Figure 2).

- The protocol “perpendicular” (Figure 2a) was used to measure the width of the plume. In this protocol, the survey vessel sails transects that are perpendicular to the transect of the TSHD starting outside the plume and continuing to transverse the plume until it has left it at the other side, while measuring the sediment concentrations using the ADCP and the OBS.
- The protocol “stationary” (Figure 2b) was used (although quite seldom) to investigate the temporal behavior of the plume. In this protocol, the survey vessel remained at a fixed location, while measuring the sediment concentrations with an ADCP, an OBS and the SiltProfiler, until the dredging plume appeared to have disappeared at this location.
- The most frequently used protocol was “parallel” (Figure 2c), in which the survey vessel was sailing at a transect parallel to the transect of the TSHD. This could be either in the same direction as the TSHD (thus catching up with the TSHD) at a fixed distance from the TSHD or in an opposite direction. These data are especially useful for determining the length of the plume as a function of time.
- The protocol “Lagrangian” (Figure 2d) is a specific case of the protocol “parallel” and it is especially useful for performing measurements after the dredging process has ended. In this protocol, the survey vessel is floating with the mean flow while measuring the concentrations. After the dredging process, the plume is expected according to the theory to be drifting away with the mean flow, while decaying and settling out (IMDC, 2008). Thus this protocol provides a clear view of the time it takes for the plume to disappear. It obtained its name from the Lagrangian frame of reference, where the observer moves with the flow.

In order to obtain data on the background conditions, a separate through-tide measurement was performed on June 20th, 2008, in which the flow conditions were measured using an ADCP and the sediment concentrations were measured using the SiltProfiler. These data showed that the average background concentrations during this measurement were always below the detection limit of 5.0 mg/l.

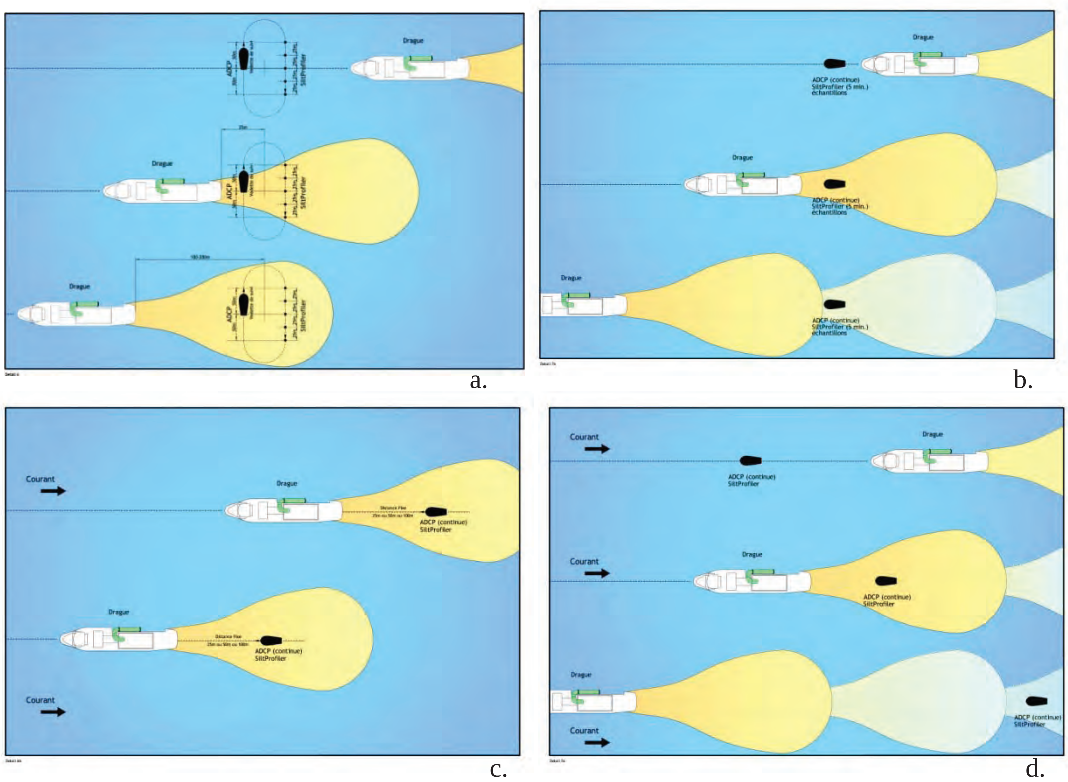

Figure 2 Overview of the measurement protocols. a. perpendicular; b. stationary ; c. parallel ; d. Lagrangian.

3 RESULTS OF THSD OVERFLOW MEASUREMENTS

Using the airlift pump that was installed inside the overflow, samples were taken every 15 minutes on day one, and every 10 minutes on the other days. These samples were analyzed for their sediment concentration and particle size distributions (Table 2). In general, it was found that the particle concentration depended on two factors: the particle size distribution in the bed of the dredging zone and the time. With respect to the particle size, it appeared that the concentrations in the overflow increased if the amount of fine material in the bed was higher (Figure 3). From this, we can infer that the concentrations inside the overflow depend on the amount of fine material that is available. Unfortunately, the number of data points (three) is not sufficient to provide information on the nature of this relation (whether it is linear or not). With respect to the amount of time, it appears that the concentrations increase with increasing time, as the concentrations in the second transect on a day are higher than on the first transect. Note that it is possible that fluctuations on a shorter time scale might occur in the overflow concentrations, but these cannot be resolved with the measurement frequency used here. The reason for this increase in time might be the decreasing depth of the fluid layer in the hopper or the finite timescale that is needed for the average concentration in the hopper to adapt to the concentration of the incoming material.

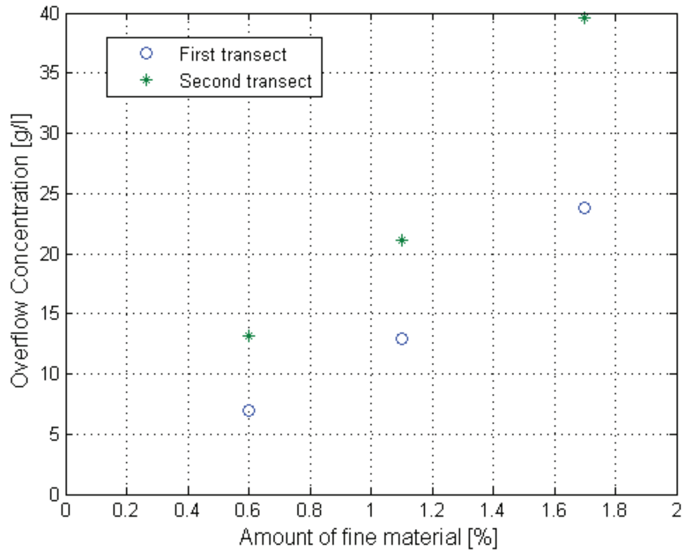

Figure 3 Relation between the overflow concentration and the amount of fine particles in the bed material.

It appeared that the particle sizes did not show significant changes during the course of the measurements (Table 2). Not only were they very similar between two transects on one day, but they also differed very little between the different transects. The particle sizes measured here are very small. Indeed a calculation using Stokes' law yields a typical settling velocity for eight-µm-particles of 0.06 mm/s. This is very small indeed, and has as strong consequence on the behavior of the plume.

Winterwerp (2002) described two kinds of regimes for dredging plumes, viz. 'active' and 'passive'. In the active regime, the increased density of the plume has an important influence on its dynamics (as the driving force for the plume's vertical motion), whereas in the passive regime the higher density of the plume (compared to the ambient fluid) is not important for the behavior of the plume. Winterwerp (2002) provides a graph to predict the occurrence of these two regimes based on the Richardson number and the ratio of the mean flow velocity to the velocity of the jet from the overflow. The Richardson number is defined as:

$$Ri = \frac{\varepsilon g D}{{W_0}^2}$$

Here, ε is the excess density (ρ_m/ρ_f -1) with ρ_m the mixture density and ρ_f the fluid density, g the acceleration due to gravity, D the diameter of the overflow, and W_0, the vertical discharging velocity from the overflow.
Applying this method to our data, we find that all measurements were taken in the passive regime, with Richardson numbers always lower than 0.03 (and normally around 0.01) and typical ratios for the flow to overflow velocity of 0.4 to 0.6. Hence it is expected that density driven flows will not have a strong influence on the behavior of the plumes.

Table 2 Overflow concentrations (average and standard deviation) and particle sizes (after applying ultrasound) from the different dredging transects.

Zone	**Concentration [g/l]**		**D_{10} [µm]**		**D_{50} [µm]**		**D_{90} [µm]**	
	Avg.	**St. dev.**	**Avg.**	**St. dev.**	**Avg.**	**St. dev.**	**Avg.**	**St. dev.**
A1	7.0	3.0	2.1	0.1	7.8	0.6	36.0	10.2
A3	13.1	5.4	1.8	0.2	7.7	0.3	45.9	13.1
B1	23.8	12.0	1.8	0.2	7.5	0.6	68.4	101.5
B3	39.6	11.7	1.6	0.2	7.3	0.6	43.4	13.5
C2	12.9	5.4	1.8	0.2	7.6	0.4	39.4	5.5
C3	21.1	13.5	1.7	0.1	7.6	0.3	41.3	7.4

4 RESULTS OF PLUME MEASUREMENT DURING DREDGING

A typical example of the occurring sediment concentrations as measured by ADCP during the dredging process is given in Figure 4. This measurement was done using the parallel protocol, and in the present occasion, the survey vessel was catching up with the TSHD. This example shows that the highest concentrations are found close to TSHD (i.e. to the right of the plot), and these high concentrations are found close to the free surface. At larger distances from the TSHD, the concentrations decrease, and the plume spreads out over the depth, covering the complete water column. The higher concentrations near the bed close to the TSHD might be an artifact of the backscatter method for measuring sediment concentrations. However, it might also be related to the plume generated by the suction head (Nichols, 1990), or to the dispersion of the sediment concentrations by the mean shear in the tidal flow. Furthermore, this figure shows that the sediment concentrations are quite patchy and that strong gradients exist in the sediment concentrations. These strong inhomogeneities are also clear in Figure 5. This example was measured using the stationary protocol (approximately 20 minutes after the start of the dredging process). In this figure, both the distances to the TSHD and the time are shown. In this measurement protocol, the distance to the THSD increases gradually as it proceeds on its transect. Thus, one measures at different locations of the plume, because in this regime the plume is attached to the TSHD and thus the plume passes the measurement vessel gradually. However at the same time, the plume is increasing in length (see Figure 7), which means that in this stationary protocol, there will also be an influence of the temporal development of the plume. In this example, large patches of sediment can be seen at the middle of the water column and near the bed, separated by areas without large sediment concentrations. The area without sediment near the start of the measurement transect is related to the survey vessel entering the plume. Note that in both these examples, the measurement was far enough from the TSHD, such that the influence of air bubbles on the measurement was quite limited. This is important, because the ADCP is much more sensitive to air bubbles than the other two measurement instruments that were used.

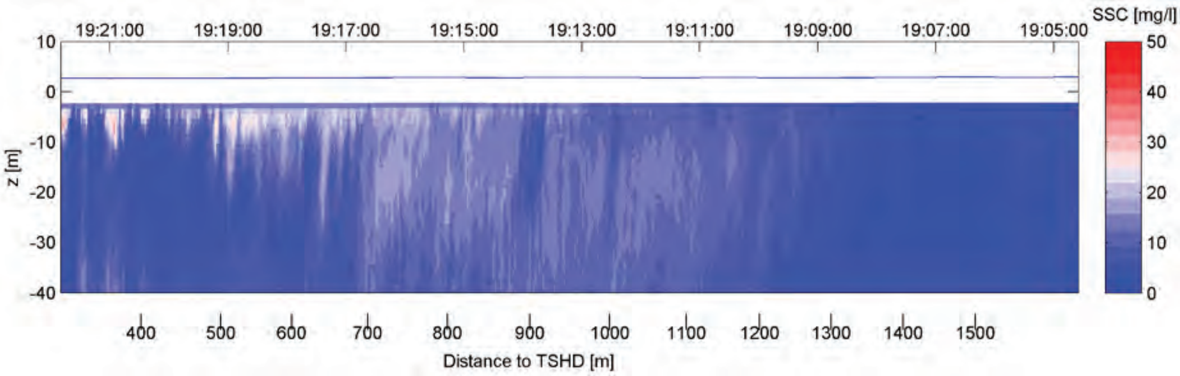

Figure 4 A typical example of the suspended sediment concentrations measured with the ADCP using the parallel Protocol for transect C2 (one hour after the start of the dredging). Note that this image has been mirrored, in order to have increasing distances to the TSHD from left to right.

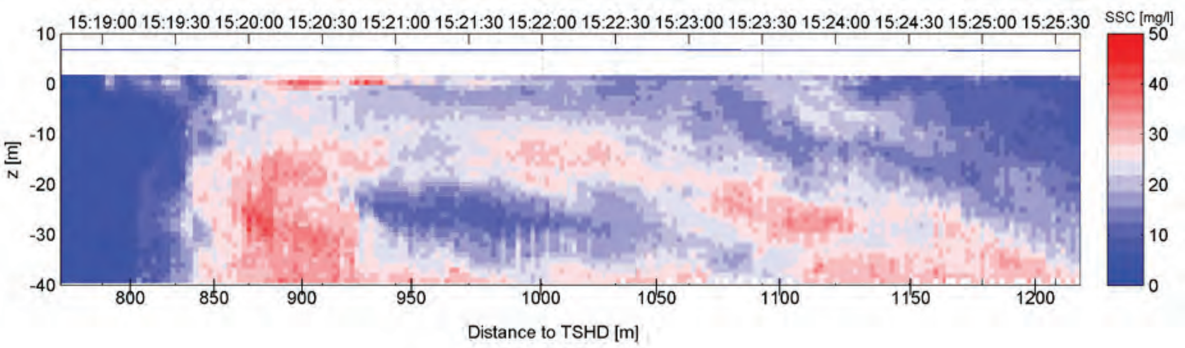

Figure 5 A less typical example of the suspended sediment concentrations measured with the ADCP using the Stationary Protocol for transect B3 (twenty minutes after start dredging).

A clearer picture of the distribution of sediment over the depth is obtained from the SiltProfiler measurements. An example, obtained using the stationary measurement protocol is shown in Figure 6. In this example, from transect A3 (in which dredging occurred in the direction of the flow) the measurement started approximately 10 minutes after the start of the dredging process. This figure shows a similar pattern as Figure 4 with the highest concentration high up in the water column, which decreased with increasing distances from the TSHD and slightly increased near bed concentrations.

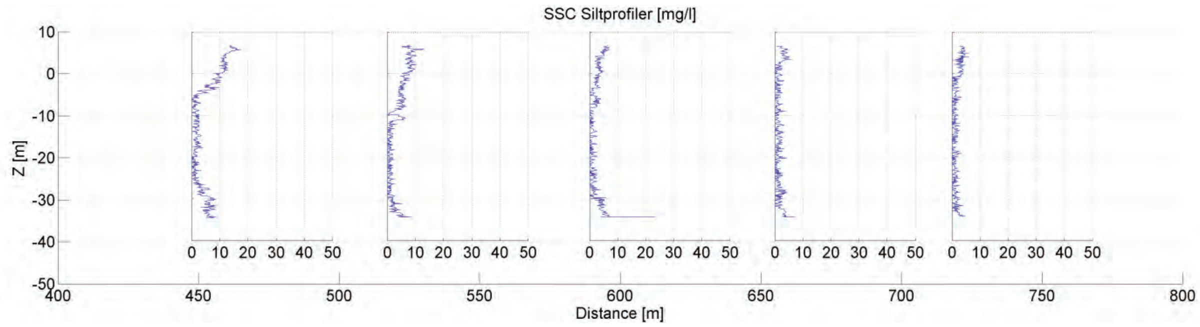

Figure 6 Suspended sediment concentration profiles measured using SiltProfiler from transect A3 (ten minutes after the start of the dredging process).

The previous data suggests that the main physical process for the dispersion of the plume is turbulent diffusion, and that settling due to gravity is not important, which corresponds to the very small settling velocities that were calculated from the measured particles size in the samples of the overflow. In case gravity would have been important, a profile more like a Rouse profile (with the highest sediment concentrations near the bed and a more or less exponential decrease of the concentration upward from the bed) would have been encountered in the far field. The previous examples also agree with the fact that according to the classification of Winterwerp (2002), the present plumes are in the passive regime, which means that density driven downward convection of the plume is not an important process. It might be that the entrained air in the overflow, which is present in the plume in the form of air bubbles, does have some influence in bringing and keeping the plume close to the free surface. However, the present data does not provide information on the importance of the air bubbles.
Typically, the sediment concentrations during this survey were quite low (always under 200 mg/l, with most transects even below 100 mg/l). There was a clear relation between the amount of material that was released from the overflow and the concentrations in the plume, as the concentrations in the plume were always higher during the second transect than during the first transect, as were the concentrations in the overflow. However, this is not the only influence, as the concentrations in the plumes from the two transect C were higher than from transect B. It might be an influence of the mean tidal flow, which was lower for the two cases at location C (thus giving lower turbulent mixing, hence a slower dispersion which leads to higher concentrations).

We proceed by determining the dimensions of the plume during the dredging process from the data obtained during the different measurements. Typically, the length and width of the plume were obtained by determining at which distance from the TSHD the concentrations had decreased to the background concentrations. The background concentration was defined as a concentration of 5 mg/l, as this was the minimum concentration that could be determined in the laboratory from the samples that were used as calibration. It was found during the through tide measurement of the undisturbed conditions that the concentrations indeed never exceeded the value of 5 mg/l during a complete tidal cycle. This limit of 5 mg/l is to some extent arbitrary. However, the obtained results did not appear to be qualitatively sensitive to the exact choice of the definition of the background concentration. Note that by applying this procedure, it is implicitly assumed that the plume length is constant during a transect of the survey vessel (which typically lasted around five minutes). Because this assumption was not completely fulfilled, there is some bias in the results.

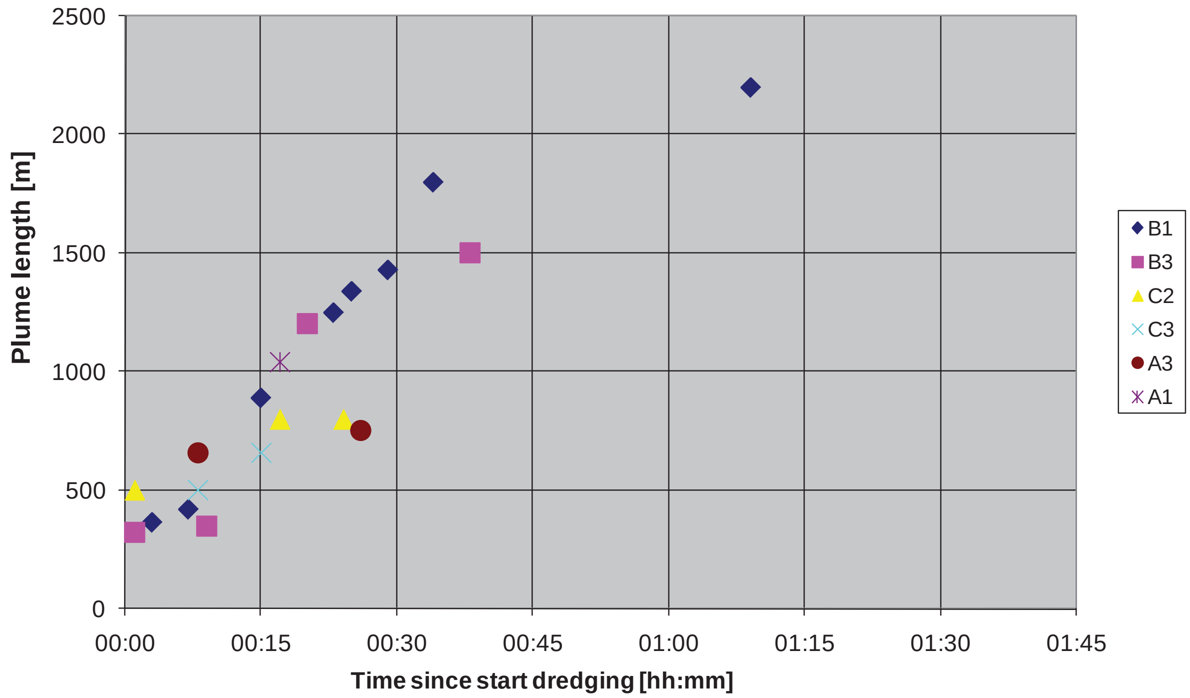

Figure 7 Length of the plume (for all measured transects) as function of time since start dredging.

The length of the plume as function of time (since the start of the dredging) is presented in Figure 7 for all six different cases. It is quite difficult to compare the different cases, because many cases contain relatively few data. Especially at longer times after the start of the dredging process, few data is available. It seems there might be some differences in the results of transect A3 (TSHD transect in the flow direction) and C2 (lowest velocities) compared to the other transects, but not enough data exist to reach a definitive conclusion on the influence of the flow velocity (relative to the velocity of the TSHD) on the length of the plume. It would have been according to expectation to find a significantly shorter plume in case of dredging in the flow direction, because the relative velocity between the TSHD and the flow is much smaller, which prevents the advection of the discharged sediment away from the TSHD. Thus in this situation, the sediment remains close to the dredging vessel and the plume is shorter.

Table 3 Width of the dredging plume

Transect	Time since start dredging [hh :mm]	Distance to the THSD [m]	Width of the plume[m]
A3 (dredging in the flow direction)	00:37	300	270
A3	00:40	500	225
A3	00:43	550	280
A3	00:47	500	225
B3 (dredging opposite to the flow)	00:16	650	85
B3	00:31	1500	140

In the same way, the width of the plume was determined from the data obtained using the perpendicular protocol. Unfortunately, the amount of data was too limited to do a detailed comparison. The limited amount of data was due to the relatively large time that was needed to perform the measurements using the perpendicular protocol. The results are shown in Table 3. It seems from these data that the plume is wider when dredging occurs in the flow direction. This agrees with the expectation of a smaller plume due to lower relative velocity when dredging in the flow direction, because more sediment remains close by and thus more sediment can then be diffused laterally (by the turbulence from the mean flow), which leads to a wider plume. However, the comparison between the two cases in Table 3 is quite awkward, because the measurements were not performed at the same distance from the TSHD (this might be an indication that indeed the plume was shorter when dredging in the flow direction) and not at the same time since the start of the dredging. Especially the latter might have some influence, as one can expect that the plume widens in time. Nevertheless, the amount of widening will be quite small compared to the lengthening of the plume, because the former is driven by turbulent diffusion, while the latter is driven by the mean (relative) velocity.

5 RESULTS OF PLUME MEASUREMENT AFTER DREDGING

When the dredging stopped, the behavior of the plume changed. This is described in the present paragraph. The main difference is that because the source of sediment had stopped (which had been moving with the velocity of the TSHD), the plume is not attached to the dredging vessel anymore. Thus the velocity of the plume changes from the velocity of the TSHD to the mean flow velocity. Also, because the influx of sediment into the plume has stopped, the plume decreases in size and the concentration inside the plume decreases.

The measurements after the dredging were performed using the Lagrangian measurement protocol. Thus the measurements were performed while the survey vessel was floating away inside the plume with the mean flow velocity. A typical example of the development of the concentration in the plume with time after the dredging is shown in Figure 8. In this figure, the depth averages of the concentrations measured using the SiltProfiler and the ADCP are shown together with the concentration measured near the free surface with an OBS. These depth averages were calculated for four different parts of the water column: the complete water column, from the middle of the water column to the free surface (denoted as: highest 50 %), from a quarter to three quarters of the depth (medium 50%), and from the bottom to the middle of the water column (lowest 50%). In this figure, it is clear that the sediment concentrations are highest shortly after the dredging stops and decrease more or less exponentially in time until the background concentration is reached. The SiltProfiler and OBS data also confirm that concentrations are highest in the top of the water column (especially close to the free surface as the OBS data shows) and lowest near the bed over the complete decay period. The ADCP on the other hand, shows larger concentrations in the lower 50% than in the upper 50% from roughly 500 s to 1000 s after the end of the dredging process. A closer inspection of the data demonstrated that the data (in both ADCP and SiltProfiler) showed two concentration peaks, one near the bed and one near the free surface. However, the near bed peak extended much higher (more than half of the water column) in the ADCP data than in the SiltProfiler. A reason for this difference in the results might be the difference in the sensitivity of these two measurement instruments to the particle size of the suspended sediments, maybe in combination with the occurrence of flocculation. Typically, the OBS is more sensitive to smaller particles, whereas the ADCP is more sensitive to larger particles (Creed et al., 2001).

The typical accuracy of an optical backscatter sensor, such as used in the SiltProfiler and OBS is 1 mg/l for the present concentration range. Merkelbach and Ridderinkhof (2005) report that the concentrations they measured using an ADCP were typically within 10 mg/l from those measured using OBS sensors, thus the error in ADCP measurements is an order of magnitude larger than those from an OBS sensor. Also, SSC measurements using ADCP are more sensitive to calibration than measurements using OBS. For these reasons, the measurements made using OBS and SiltProfiler are considered more accurate than the ADCP measurements.

There is a large dip in the data at around 600 s after the end of dredging with a duration of two to three minutes. This dip is most pronounced in the OBS data, but it can also be seen in ADCP data. The reason for this dip is presumably that the measurement vessel had temporarily drifted out of the plume, and thus the increase in the concentrations occured because the ship moved back into the plume.

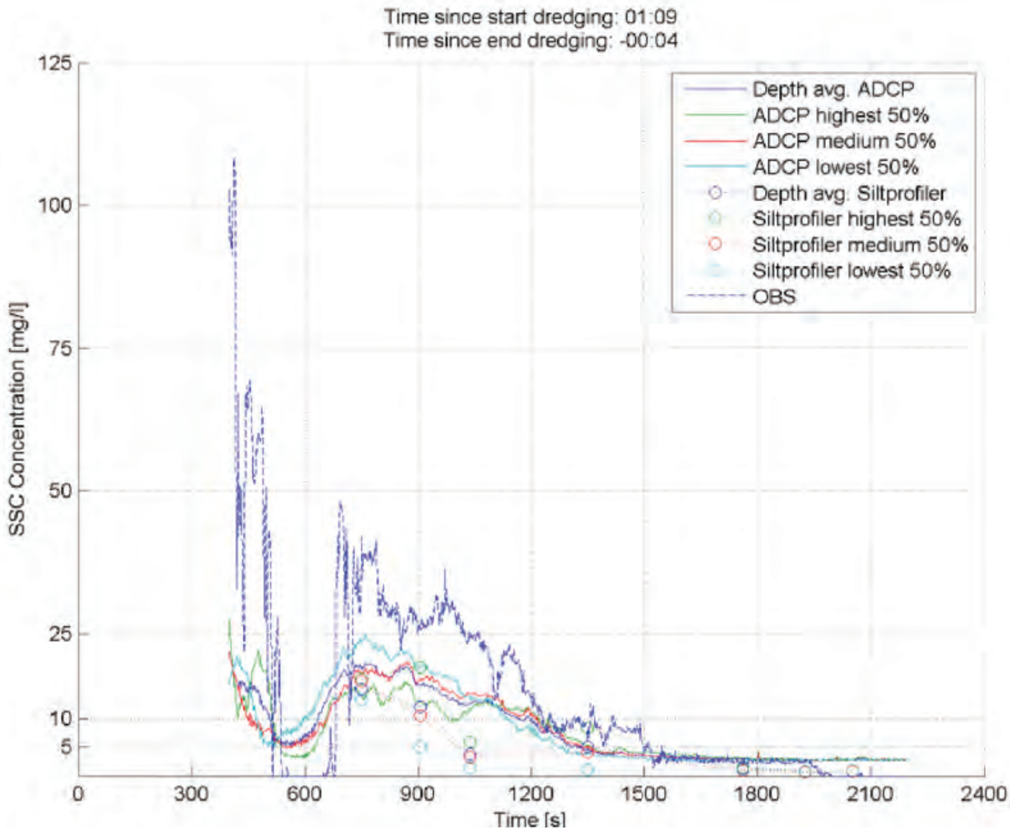

Figure 8 Development of the sediment concentration as function of time after the end of the dredging for transect B1 (Lagrangian measurement).

From these Lagrangian measurements of the sediment concentrations after the dredging had finished, the life time of the plume was determined, by determining the time it took to reach the background concentration (once again defined as a concentration of 5 mg/l). The life times for different measurements are shown in Table 4. This figure clearly shows that the life time of the plume is much larger when dredging was performed in the flow direction (up to double as long). The difference in the life time is much smaller between those cases, where dredging occurred opposite to the mean flow.

Table 4 Lifetime of the plume

Transect	Start time of the measurement since start dredging [h:mm]	Plume life time[s]
A3 (in flow direction)	1:38	2600
B1 (opposite to the flow)	1:09	1500
B3 (opposite to the flow)	0:52	1200
C2 (opposite to the flow)	1:28	1650

It is not possible to determine only from these measurements, where the sediment remains when the concentration decreases. The reason is that these measurements, which were made using the Lagrangian protocol, are basically point measurements. Thus they do not provide spatial information on the length and width of the plume as function of time in this phase of the plume's life. However, given the nature of the turbulent diffusion process, it seems plausible that the length and width of the plume increase as the concentration decreases with increasing time. A strong increase in the depth of the plume was not found in this measurement (not shown). This is plausible, because it is known that the horizontal turbulent diffusion coefficient is much larger than the vertical one (thus horizontal mixing is much stronger than vertical mixing). No measurements were made close to the bed to determine, whether the material deposited or not. However, the flow velocities at this location exceed the threshold of motion for the particles sizes encountered in the samples (section 3), and hence they will probably not deposit on the bed.

6 SUMMARY AND CONCLUSIONS

In this paper, a field measurement campaign was presented, which was set up in order to study the dredging plume from gravel dredging at open sea using a trailing suction hopper dredger (TSHD). In this survey, the amount and characteristics of the discharged material were measured by tacking samples in the overflow of a TSHD using an airlift pump, and the plume was measured using a separate survey vessel equipped with an ADCP, an OBS and a SiltProfiler in order to measure flow velocities and sediment concentrations.

It was found that the released sediment particles in the overflow had very small diameters. Because of this, gravitational settling was not important for the dynamics of the plume, but instead the plume dynamics are governed by the inflow of sediment from the overflow (maybe in combination with the material brought into suspension by the drag head), advection by the mean flow, and turbulent diffusion. The amount of material that was released appeared to be strongly related to the amount of fine material that was present in the bed material at the dredging location. It also depended on the time since the start of the dredging, with the sediment concentrations in the overflow increasing with time. Nevertheless, the concentrations were never high enough to cause the occurrence of a convective settling regime (Winterwerp 2002), where a downward movement of the plume from the overflow is caused by the higher density of the plume compared to the one from the ambient fluid.

In the measurement of the plume, the interpretation of the measurements was divided between two regimes: “during dredging” and “after dredging”. In the first regime, new sediment is added to the plume continuously, which makes that the plume grows and that the plume appears to be attached to the TSHD, and thus the propagation speed of the plume is equal to the sailing velocity of the TSHD. In the second regime, no new sediment is added to the plume, and hence it drifts away from the TSHD with the mean flow velocity while the concentrations decrease.

In the measured plume results “during dredging”, the strong influence of the turbulent diffusion was well visible. The normal behavior of the plume was that the largest concentrations occurred near the free surface close to the TSHD. The concentrations close to the free surface decreased with increasing distance from the TSHD and spread over a larger part of the water column, until at a given distance, the concentration had decreased to the background value over the complete water column. In quite some instances, there is also a much smaller second concentration peak close to the bed. Furthermore, the plume shows a quite patchy pattern and some strong inhomogeneities are visible in the instantaneous results.

It appeared that there was a large influence of the dredging direction (opposite to or along with the flow) on the development of the plume. When the dredging transects were sailed along the flow, the plume was wider, and it might have been shorter as well. This dependency was even clearer after dredging. Then, the decay of the plume toward background concentration appeared to take much more time when dredging occured in the flow direction, than when dredging occured opposite to the flow direction.

7 REFERENCES

Aarninkhof S. (2008), A world without sediment plumes, Dredging and Port Construction pp 41 – 44

Chisholm (1982), Prediction of the performance of airlift pump, Int. J. Heat and Fluid Flow, 3 (3) pp 149-125

Creed E.L., Pence A.M., and Rankin K.L., (2001), inter-Comparison of the turbidity and sediment concentration measurements from an ADP, an OBS-3, and a LISST, Oceans ’01, 3, pp 1750-1755

DRL (2003), Sediview Procedure manual, Surrey UK

Hay A.E. (1991), Sound Scattering from a Particle-laden Turbulent Jet., J. Acoustic. Soc. Am 90 pp 2055

IMDC (2008), Suivi des dragages expérimentaux – Rapport des mesures, I/RA/18049/08.099/MBO

Merkelbach L.M., and Ridderinkhof H., (2006), Estimating suspended sediment concentration using backscatterance from an acoustic Doppler profiling current meter at a site with strong tidal currents, Ocean Dynamics, 56 (3) pp. 153-168

Nichols M., Diaz, R.J., Schaffner L.C. (1990), Effects of hopper dredging and sediment dispersion, Chesapeake Bay, Environ Geol. Water Sci. 15 (1) pp. 31-43

Thorne P.D. and Campbell S.C. (1992), Backscattering by a Suspension of Spheres. J. Acoustic. Soc. Am. 20 (3) pp 283

Winterwerp, J.C. (2002), Near field behaviour of dredging spill in shallow water, J. of Waterway, Port, Coastal and Ocean Engineering, 128(2) pp 96-98

WEAR RESISTANT DREDGE CUTTER TEETH
A LOOK AT THE DEVELOPMENT OF THE TOOTH AND ITS IMPACT ON THE ECONOMICAL AND ENVIRONMENTAL ASPECTS OF THE DREDGER LOGISTICS AND FOUNDRY

Klaas Wijma[1]

Abstract: VOSTA LMG has developed teeth with wear resistant inserts, so called DURACORE ® teeth.
These teeth have big advantages compared with teeth that are made of conventional impact and wear resistant steels. The wear life is several times better which increases the efficiency of the dredger significantly. Apart from this obvious economical advantage is that the total amount of energy and raw materials needed for producing the teeth has been decimated. Transport costs and energy needed to ship the teeth to the dredger has been decimated as well. This paper describes the development of the teeth and the economical and environmental benefits:

Keywords: Wear resistant teeth, Efficiency, Environment

[1] Klaas Wijma, VOSTA LMG, Klaprozenweg 75e, 1033 NN Amsterdam, +31-20 493 6666, +31-20 493 6670, e-mail: wijmak@vostalmg.com

1 INTRODUCTION

When excavating in rocky materials with cutter suction dredgers, the amount of wear and tear on the teeth and adapters used on the rotating cutter head increases rapidly, resulting in often unexpected high cost for these parts and high down time. Since the first big large project in hard rock like in Jubal (Saudi Arabia) in the seventies there has been a request from the dredging world to reduce the wear and tear and make the cutting systems more reliable. Continuous developments in the cutting systems like the development of second generation and the latest state of the art third generation cutting systems like VOSTA T-systems (1) have solved the problems for the wear and tear on the adapters / lockings/cutter heads and have reduced the down time significantly.

But the development for wear resistant tooth was a less successful story although is one of the holy grails in (cutting) dredging, because of the enormous potential cost saving and as it will push the workability of the cutter dredger in hard and abrasive soils to a higher level.
Many attempts have been done including the use of conical and radial bits as used on dry mechanical excavators, applying hard facing on teeth and development of dredge teeth with hard metal parts braced to the tips. None of these solutions have become successful.

As part of the ambitious development program to improve the overall performance of dredge cutter heads (called the D2000 project) a project was started to improve the wear life of the teeth significantly. This was together with Combi Wear Parts whom are producing the above mentioned teeth and adapters. This project resulted in the patented wear resistant and self sharpening Duracore ®tooth. Although the target for this project was not the environment itself the effect of the new teeth on it is significant

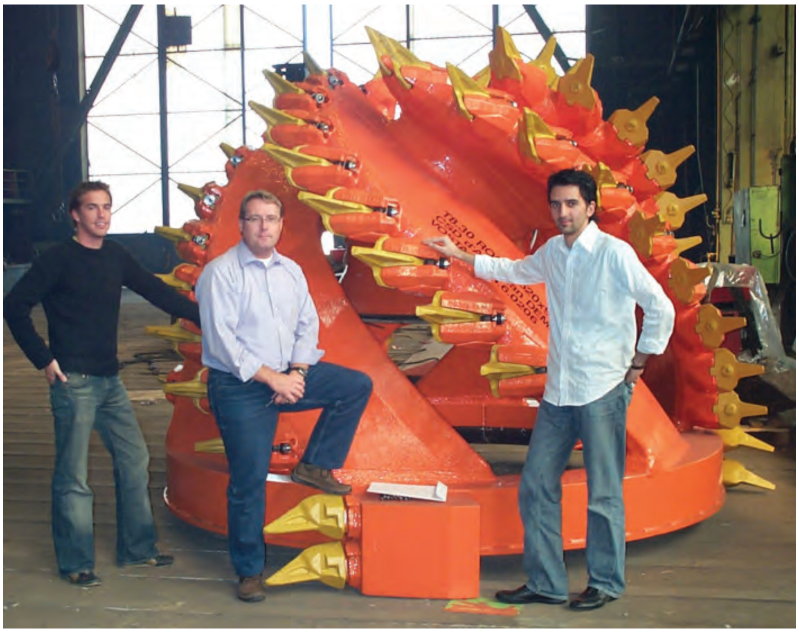

Fig. 1: Rock cutter head for 6000 kW cutter power.

Fig. 2: CSD d'Artagnan with 6000 kW cutter power

2 DESIGN CRITERIA

The following criteria were set:

- Suitable for rock excavation with dredgers
- Preferably fitting on the existing adapters
- Wear life > 2 x better
- Limited effect on the excavating performance
- Suitable for serial production by CWP in the shell mould foundry
- Cutting angles preferably the same
- Suitable for large range of UCS (rock strength) and abrasivity values

Based on these criteria the following options were reviewed and those that were interesting were further investigated.

- Tooth shape
- Conical bits
- Material
- Operating parameters
- Hard facing
- Cladding of teeth
- Alternative steels
- Wear resistant inserts

Each item is briefly described below.

Tooth shape
Length , cross section and angles are optimized already and only small improvements might be possible (less then 20%) and only after a lot of trial and effort. The largest problem is the strength of the teeth. The existing materials do not allow longer or thinner teeth at the same forces. The breakage rate will just become to high.

Conical bits
As stated in the beginning, several tests have been done in the past with conical bits on conventional dredge cutter heads (see picture), without success.

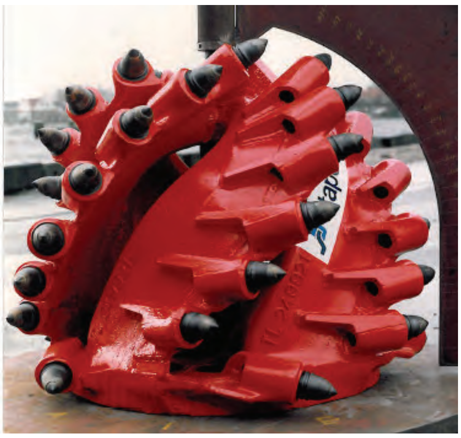

Fig. 3: Dredge cutter head with conical bits

There is a combination of reasons for their lack of success being:

1. Life time of teeth / bit length
The useful length of the hard metal rod in a conical bit is typical a few cm. The useful length of dredge teeth is typically 80-180 mm and although they are made of normal wear resistant steel (HB 500) they will have approx the same wear life due to the much longer wear length.

2. Large variation in swing speed
The conical bits are designed for very small cutting depth (typically) 10-30 mm , dredge teeth are designed for medium to very large cutting depths (typically 50-180 mm).

3. Strength
Dredge teeth / adapter are designed to withstand extreme high loads caused by the large cutting depths. The largest teeth can withstand cutting forces (FC) or normal forces (FN) between 1500 kN and 2000 kN when new. When the teeth are worn this increases even further. Loads for the heaviest conical bits are approx 150 KN

The combination of the above results in fast wear of the tooth (low ratio bits /m3) and adapter (tooth holder) and much higher torque and penetration forces for a dredge cutter head when equipped with conical bits when used at normal swing speeds. Also there will be a lot of breakages.
The same applies for the radial bits.

Fig. 4:Conical bits with hard metal insert used on road headers

Material
Conventional dredging teeth are made of wear resistant steel with great resistance against impact loads. Typical hardness is around 500Hb and tensile strength around 1600 N/mm2.
Several alternative materials were compared with pin on disc tests (see picture) and in the field. This did not bring a significant improvement.

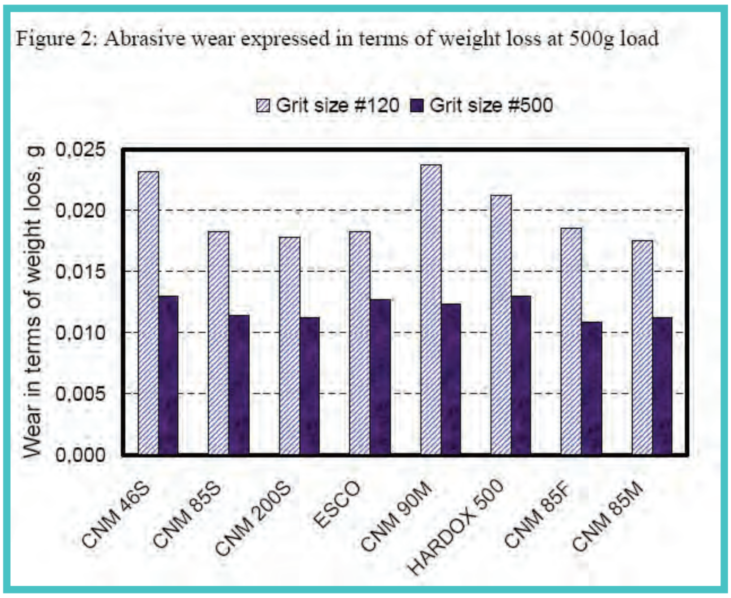

Fig. 5: Results of one of the pin on disk tests

Operating parameters
The excavating performance is governed by cutter power, side winch forces and spud holding force.
As it is the focus of the dredge operator to get maximum production by trimming the above to the maximum, there is little room for improvement

Hard facing teeth
If applied to the wear surface it will quickly wear away and expose the material beneath. That makes no sense. Hard facing can be applied to the rake surface of the tooth where in softer soils it can create a sharp rim on the edge of the tooth that will have a positive effect on the normal forces. Due to the fact that it only works in softer materials, is very expensive to be applied and that the type has to be determined by trials on site it is an impractical solution.


Fig. 6: Teeth with hard facing on the rake surface

Cladding of teeth
Like solding of hard metal to the rake surface of the tooth. The function is more or less similar as hard facing. There have not been successful applications in rock with dredging. It might however be used in softer materials.

Wear resistant inserts
It was investigated to put in the center of the tooth tip an insert being either hard metal, white iron, hardened steel or ceramic
In theory the steel around the insert would wash away quickly until the insert would be protruding enough to take most of load but still would be supported by the steel. As the insert is much more wear resistant compared with steel the wear rate m3/mm wear length should reduce drastically. The other effect being that the wear area of this insert is much smaller then of a normal steel teeth which typically develops quickly a flat surface (blunting) that increases along the wear length. As the wear area is an indication for the penetrating capability this new teeth should give better penetration.

This last option was the most promising.

Fig. 7: Tooth design used for shrinking in inserts.

The questions were:

How far must the insert protrude before the steel stops wearing?
If the steel would continue to wear the insert would be exposed to much and just break off. This could only be checked with full scale field testing.

What would be the wear rate of the insert compared to normal steel?
This depends mainly on the hardness of the soils x the abrasivity of the grains. There was plenty of research done in the past to judge ratio's steel vs. other materials.
In rock the loads can be so high that the more brittle insert will not wear away by grinding but because small pieces of the insert breaks out.

What kind of material to be used?
Because of the above the insert should be tough and because of the continues flexing of the teeth is should be elastic enough to follow the movement of the tooth tip in order to avoid breakages.

From this it was expected ceramics was not a suitable material as its elasticity is practically zero.
One of the tests with a tooth with ceramic insert in which the flexing of the tooth was simulated showed that the ceramic rods was broken in many pieces which proofs the above statement.

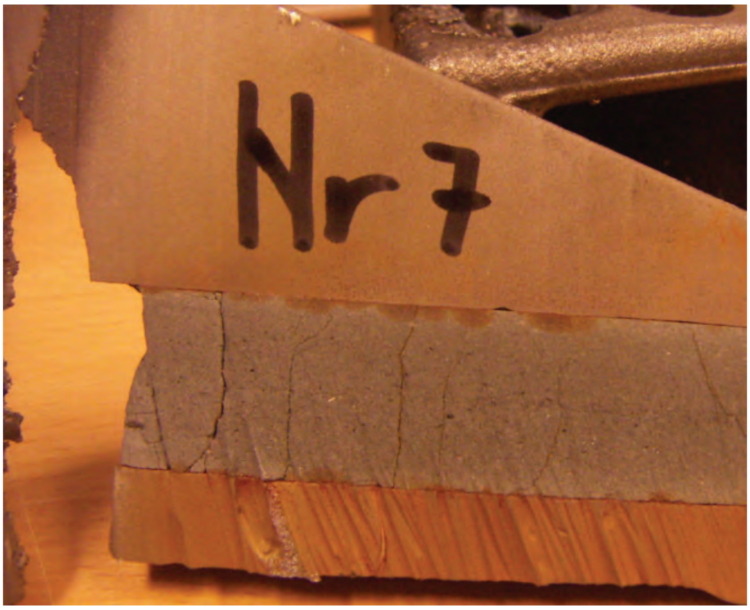

Fig. 8: Cracked ceramic insert after flexing tests

Alternative for the ceramic is hard metal. This material is successfully used in the conical bits for road header / trenchers and looked the most promising. Compared with ceramic it is more elastic.
Other hard materials like hardened steel and white iron were also considered and tested.

How to get the inserts in the casting?
It was generally considered that fixing a hard metal rod in the tooth pattern and fill it up with melted steel would be the most logical choice. However this had never been done before successfully for parts that were subject to high (impact loads).

3 THREE PARTY DEVELOPMENT

When it became obvious that the hard metal was possibly the best option., discussions were started with SANDVIK for a possible co-operation in this development.
SANDVIK is one of the largest companies in the world specialized in hard metals, with as home country Sweden. They agreed to join this development.

The activities / responsibilities were divided as follows:

SANDVIK :	hard metals, grades sizes production method
CWP	Production process , lab tests
VOSTA	Load spectrum / interface tool-rock / field tests

After a lot of trial and error a production method was achieved which secures the rod in the center and gives a good bonding between hard metal and the steel.
That it was not easy to achieve this might be clear by the fact the production method has been applied for as a patent.
The use of the Duracore tooth on rotary cutter heads was also applied for as a patent.

A name for the technology was registered under: Duracore ® which is a combination of Durability and Core.

4 FIELD TESTS

Four closely monitored tests were done in the middle east Area.

A. Al Khor , Qatar with CSD with 900 kW installed cutter power with T4 size
B. Al Khor , Qatar with CSD with 900 kW installed cutter power with T4 size
C. Ras Laffan, Qatar with CSD with 6000 kW cutter power with T8 size
D. Qatalum , Qatar with CSD with 3600 kW cutter power with T6 size

Soil hardness varying from 5-50 Mpa and ratio pp /m3 between 10 and 200 m3/pp for conventional teeth.

Test A and B

Several grades of hard metal inserts were tested, but also white iron, hard metal and ceramics.

The ratio's of wear compared with normal steel teeth were between 1,0-1,5 for the ceramics caused by the constant breaking out of ceramic particles. No sharpening effect could be seen.

The ratio's of wear for the white iron and hard steel were between 1,5-2,0
Little self sharpening effect could be seen. To be able to keep the mechanical properties the rods of this material were shrink fitted into the teeth.

The ratio's of the hard metals selected by Sandvik specialists were between 4- 10 and with a remarkable self sharpening effect. (picture).
Closely monitoring of the production showed that the teeth remained sharp until the rods were finished.

Fig. 9: Used Duracore teeth with different stages of the self sharpening.

Fig. 10: Side view of the self sharpening effect.

Test C

Only the hard metal inserts were tested in with ratio 3-4.
The operator confirmed that when the teeth were worn in and got their distinctive shape the penetration was identical or even lower compared with conventional teeth.

Fig. 11: New T8.C3 Duracore teeth on the cutter head, ready to be tested

Test D

Due to varying soil conditions it was more difficult to get hard ratio numbers but they were also higher then 3. Several tooth broke due to the rod being eccentric. Showing that good alignment is very important.

Fig. 12: Teeth ready for measuring.
Note the flat surfaces of the normal steel teeth on the left and right row.

5 POST TEST

The test results were used to make a final design of the teeth that would become commercially available. Up to the date of this paper , many teeth have been used with similar results as during the test around the world. Confirming the performance of the Duracore tooth. Many more field and lab tests are needed to optimize the rod size and shape, ratio steel to hard metal, grade of hard metal etc.

6 EFFECT ON ECONOMY OF THE DREDGER

One of the effects of the self sharpening is that the excavating production is high all the time until the rod is worn out. With normal teeth the production is high at the start but when the teeth are getting blunt the production often decreases. The teeth can then either be worn out completely but with decreasing production, or the teeth are changed at a point that the operator considers as most cost efficient (at the optimum balance between the cost for reduced production and the cost for new teeth).

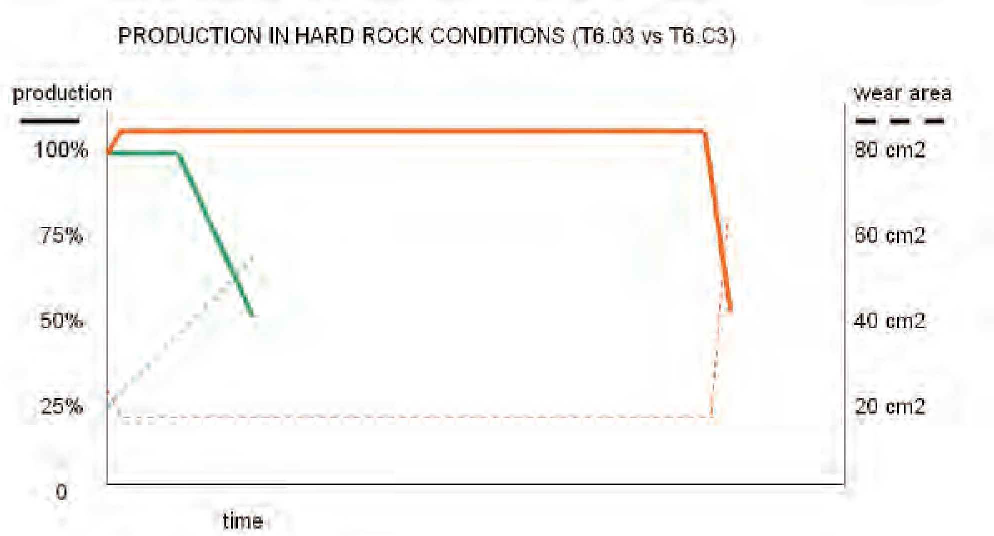

Fig. 13: Graph showing the difference in excavating behavior between steel teeth (green) and Duracore teeth (orange).

Below follows some examples to show the large difference in production when teeth last longer and stay sharp.

Example 1with conventional teeth
Production rate 1000 m3/hr decreasing linear to 800 m3/ hr and tooth change every two hours for 20 minutes.
Production rate effective is 772m3/hr

Example 2 with Duracore tooth that last twice as long
Production rate constant at 1000 m3/hr and tooth change every 4 hours for 20 minutes.
Production rate is 923 m3/hr= +16%

Example 3 with Duracore tooth that last four times longer
Production rate constant at 1000 m3/hr and tooth change every 8 hours for 20 minutes.
Production rate is 960 m3/hr= +20%

Running cost for a large cutter dredger can be around € 400.000 per week and with a 20% higher productivity the cost saving are big.

Due to the more complex production of the tooth and the high price of the hard metals used, the cost for the teeth are much higher. This is typically around a factor of 2.5-4 x ordinary teeth with the existing production methods.

This is in practically all cases well compensated by the much longer wear life and higher production.
Only in case the life time of conventional teeth is already quite long (> one day) , the production does not decrease when the teeth get blunt and the ratio in wear is less then the ratio in cost the teeth are not economical.

Transport
Dredging teeth are shipped all round the world and many times dredge teeth are following a ship even when they are not used for several years. It is estimated that in this last case the transport cost for the teeth when they are finally used can be as high as 50% of the value of the teeth.

When using the Duracore tooth at least two third of the transport can be saved. Also less storage area is used.

7 EFFECT ON ENVIRONMENT

Duracore has very positive environmental effects on the following:

- Production of the teeth
- Transportation
- Starting and stopping pipe line systems and idling of engines

To produce steel teeth a lot of energy and materials are needed. The amount of energy needed for producing Duracore teeth that can excavate the same amount of m3 I only a fraction compared with conventional steel teeth.

Transporting of goods around the world and handling cost s a lot of energy . For the Duracore teeth only a fraction of the transports are needed.

For each time that the dredger needs to change teeth the dredge pipe line has to be flushed before the ladder can be raised above the water. Depending on the pipe line length (which can several km long) this consumes a lot energy. Before excavating can be started the total water mass in the pipe line has to be accelerated from 0 to around 6 m/min. which also consumes a lot of energy.
The amount of times starting and stopping with the Duracore teeth is a lower as per the ratio of wear life improvement.
Also a lot of time is saved that the engines are idling, however this effect is neglectable compared with the above savings.

8 CONCLUSIONS

VOSTA LMG / CWP / SANDVIK together have successfully developed a new tooth type for rotary dredge cutter heads which combines a several times longer life time with a unique self-sharpening effect called Duracore ® teeth. The benefits for the environment are huge especially when looking at the energy saved, due to much lower Q of teeth that have to be produced and the accordingly less transports, but also due to the improved efficiency of the dredger.
More testing is needed to get the maximum economical and environmental benefits out of this concept.

9 REFERENCES

K. Wijma (2005) "Third generation rock cutting system for cutter dredges with 3000-6000 kw cutter power - field results", proceedings WEDA Dredging days 2005, New Orleans, USA

K. Wijma and D. Petterson (1997) "Lowering the overall costs for the use of rock cutter head systems", Proceedings CEDA Dredging Days 1997, Amsterdam, The Netherlands.

ESTIMATING THE IMMEASURABLE: SOIL PROPERTIES

J. Braaksma[1], J. Osnabrugge[2] and C. de Keizer[3]

Abstract: The dredging process is characterized by the strong influence of soil properties, which vary with changing excavation locations. For optimizing the dredging production and energy consumption, it is necessary to know these properties. The problem is that a lot of these soil properties are not measured or very difficult to measure. By taking soil samples, it is possible to give a raw indication, but this does not cover the total dredging area.

Equipment for measuring the properties on-line are complex and, if available at all, too expensive to use. As an alternative, we use estimation methods. These estimation methods are based on knowledge obtained with the development of training simulators in the last decade. For these training simulators, sophisticated soil models, together with the dredging equipment, are modelled to simulate the dredging process dynamically. By using specific soil parameters, it is possible to forecast the dredging dynamics accurately.

In this paper we present a, for the dredging industry, novel approach which uses the models in an inversed way: using the models and the measurement data to estimate the soil type dependent parameters. To obtain this objective several advanced filters have been successfully implemented and tested in practice. Examples are recursive least squares filtering, linear Kalman filters and more complex techniques such as the extended Kalman filter and the Particle filter. In this paper four estimation examples will be described and the advantage for controlling the process control such as:

- estimating the mean grain size of the dredged soil
- estimating the overflow losses
- estimating the dredging forces
- estimating the anchor positions

The use in practice of the immeasurable will be described as well as future developments.

Keywords: Extended Kalman Filter, Particle Filter, Overflow Losses, Anchor Position, Dynamic Positioning and Dynamic Tracking, Trail Speed Control

[1] Engineer R&D, IHC Systems, Industrieweg 30, Sliedrecht, 3360 AA, The Netherlands, T: +31(0)184-431939, Email: jbraaksma@ihcmerwede.com

[2] Engineer R&D, IHC Systems, Industrieweg 30, Sliedrecht, 3360 AA, The Netherlands, T: +31(0)184-431932, Email: josnabrugge@ihcmerwede.com

[3] Manager R&D, IHC Systems, Industrieweg 30, Sliedrecht, 3360 AA, The Netherlands, T: +31(0)184-431573, Email: cdkeizer@ihcmerwede.com

1 INTRODUCTION

The dredging process is characterized by strong nonlinear system behaviour. This behaviour has been extensively studied and modelled (Jufin, 1966; Miedema, 1987; Matoušek, 1997; van Rhee, 2002) mostly with static models and lately also with dynamic models. In general, these models describe the physical behaviour and are parameterized in terms of the geometric properties and the physical properties. Usually, these models are used for predicting the system behaviour assuming that all the necessary soil characteristics are known or measured. Several laboratory or field experiments are available to obtain the parameters such as sieving a sample of sand or performing a penetration test.
For the purpose of control, these models can be used in a complete different manner. Instead of predicting the system behaviour based on complete knowledge of the soil properties, the soil properties are predicted/estimated by measuring the system behaviour, see figure 1.

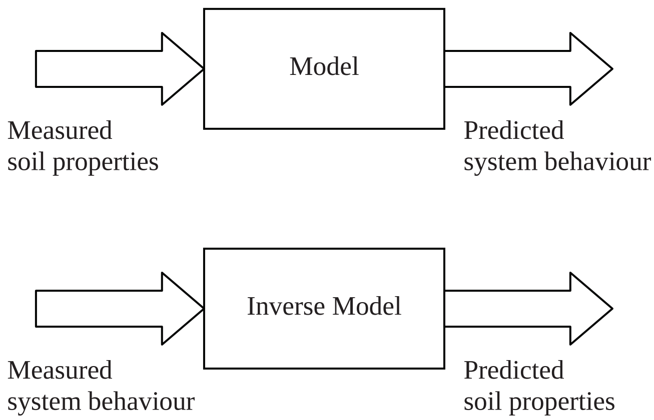

Figure 1. Two different applications of the same model. Top: predicting the system behaviour based on measured soil properties. Bottom: the model is uses inversely for predicting the soil properties based on the measured system behaviour.

Model-Based Control Design and Model-Based Control
Our goal is optimizing the dredging performance with the use of control and automation systems onboard of dredgers. During the operation of the ship, it is unknown which soil type is being dredged. This makes the use of the models impossible since the soil type parameters are unknown.
Why do we need models for controlling the dredgers?

- **Nonlinear system behaviour.** Due to the strong nonlinear system behaviour of the dredging process, the standard linear controllers such as a PID-controller do not give the desired performance. The design of advanced control techniques often rely on dynamic models. A common approach is *model-based control design* where the model is used for deriving the controller. Models can also be part of the controller (*model-based control*), which is the case in adaptive control.
- **Virtual sensors.** The dredging process is a hostile environment for sensitive equipment such as sensors. The normal of-the-shelf sensors must be ruggedized which make them expensive. Also some physical properties are very hard to measure reliably. Therefore when possible it is desirable to estimate the variable instead of measuring it. This requires an accurate model of the process.
- **Process optimization.** The ultimate goal for a dredger is maximizing the profit while respecting the constraints of the equipment and environment. The system behaviour can be predicted with the use of models. This enables us to find the optimal control strategy by calculating the effect of many possible strategies. This so-called Model Predictive Control (MPC) technique maximizes the performance of the dredger, see Braaksma (2008).
- **Decision support.** A decision support system can help the operator maximizing the performance by using models, see previous bullet. Furthermore, estimation of the soil parameters such as the grain diameter can be used for the development of advanced wear models of the pumps, pipes and valves. These wear models may be used for life time prediction in behalf of preventive/scheduled maintenance.

Most of these models need soil parameters for accurate prediction of the process. Therefore in order to use them online we need to estimate these parameters online. This paper presents a selection of estimation techniques that are implemented in our automation systems or techniques that will be implemented in the future dredging automation equipment.

2 OVERFLOW LOSS ESTIMATOR

Overflow losses play an important role in the dredging process of a trailing suction hopper dredger (TSHD). The losses have a negative influence on the dredging performance, therefore an operator must constantly monitor if the losses do not become too large.

Stricter environmental legislations require that the overflow losses must be limited especially in areas of fragile ecosystems. On the other end of the spectrum is agitation dredging where the overflow losses are kept intentionally high to discharge the fine grained fraction which can then be transported and permanently deposited outside the channel by tidal, river, or littoral currents.

Measuring the density and the mixture velocity in or near the overflow weir is a technical challenge. The turbulent mixture flow encapsulates air bubbles that distort the measurement. Moreover placing sensors in the hostile environment near the overflow requires much maintenance and a rugged housing. Since the density is usually measured with a radioactive measurements device, this requires qualified and skilled personnel and sufficient precautions to avoid accidents.

To overcome these difficulties, we developed an estimator for the overflow losses which only requires sensors already available on every modern hopper dredger. The method is a model-based approach based on only the balance equations. In the hopper a mixture with density ρ_i and flow-rate Q_i is discharged. This fills the hopper until the mixture level reaches the height of the overflow weir. Then, a mixture of sand and water flows out of the hopper through the overflow weir with density ρ_o and flow-rate Q_o. This is described with the following balance equations:

$$\begin{aligned} \dot{V}_t &= Q_i - Q_o \\ \dot{m}_t &= \rho_i Q_i - \rho_o Q_o \ , \end{aligned} \tag{1}$$

where V_t is the mixture volume and m_t is the total mass of sand and water in the hopper. Modern TSHD are equipped with draught sensors which are used to calculate m_t and level sensors in the hopper to calculate V_t. Furthermore, a sensor is available for measuring the incoming density ρ_i and a sensor for measuring the flow-rate Q_i. This means that in equation 1 only ρ_o and flow-rate Q_o are unknown.

2.1 The Estimation Problem

The estimation problem is to estimate the outgoing density and the outgoing flow-rate. For that we discretize equation 1 by using the Euler method:

$$\begin{aligned} V_{t,k+1} &= V_{t,k} + T_s(Q_{i,k} - Q_{o,k}) \\ m_{t,k+1} &= m_{t,k} + T_s(\rho_{i,k} Q_{i,k} - \rho_{o,k} Q_{o,k}) \ , \end{aligned} \tag{2}$$

where T_s is the sampling period. These state equations are augmented with a random walk model for ρ_o and Q_o. We assume the most general state-space model:

$$\begin{aligned} x_{k+1} &= f(x_k, u_k, \varepsilon_k) \\ y_k &= h(x_k, \varepsilon_{yk}) \end{aligned}$$

and define the augmented state, input and output vector:

$$x = \begin{pmatrix} V_t \\ m_t \\ Q_o \\ \rho_o \end{pmatrix}, \quad u = \begin{pmatrix} Q_i \\ \rho_i \end{pmatrix}, \quad y = \begin{pmatrix} V_t \\ m_t \end{pmatrix}.$$

The complete nonlinear state-space representation becomes:

$$\begin{pmatrix} x_{1,k+1} \\ x_{2,k+1} \\ x_{3,k+1} \\ x_{4,k+1} \end{pmatrix} = \begin{pmatrix} x_{1,k} + T_s(u_{1,k} - x_{3,k}) + \varepsilon_{x1,k} \\ x_{2,k} + T_s(u_{1,k}u_{2,k} - x_{3,k}x_{4,k}) + \varepsilon_{x2,k} \\ x_{3,k} + \varepsilon_{x3,k} \\ x_{4,k} + \varepsilon_{x4,k} \end{pmatrix}, \quad u = \begin{pmatrix} Q_i \\ \rho_i \end{pmatrix}, \quad y = \begin{pmatrix} V_t \\ m_t \end{pmatrix}.$$

This estimation problem is nonlinear, therefore we need to apply nonlinear estimation techniques such as the Extended Kalman Filter (EKF), Uncented Kalman Filter (UKF) or a Particle Filter (PF), see Welch, G. & Bishop, G. (2002) for a general introduction into Kalman Filters and Arulampalam et al. (2002) for a tutorial on the PF. It was found that an EKF or an UKF cannot simultaneously estimate ρ_o and Q_o see Babuška et al. (2006) and Lendek et al. (2008). Therefore a PF is used to solve the estimation problem, see Babuška et al. (2006). This algorithm is implemented in our Draught and Loading Monitor (DLM) software for online estimation of the overflow losses.
With the two estimations, the so-called `load efficiency' is calculated as follows:

$$Loadeff = \left(1 - \frac{m_0}{m_i}\right) \cdot 100 \quad [\%]$$

with

$$m_0 = \frac{\rho_0 - \rho_w}{\rho_q - \rho_w} Q_o \rho_q \text{ and } m_i = \frac{\rho_i - \rho_w}{\rho_q - \rho_w} Q_i \rho_q ,$$

where ρ_w is the density of water and ρ_q is the density of sand (quartz). This load efficiency indicates to the operator which percentage of incoming sand flows overboard. This enables the operator to monitor the instantaneous hopper load efficiency.

2.2 Measurement Results

The algorithm is firstly tested on a simulation model and tested with measured data. These results can be found in Babuška et al. (2006) and Lendek et al. (2008). This section shows the results of the filter working online on board of the medium sized hopper dredger during its first sea-trials.
The dredging cycle which is shown in these figures consists of three phases: no overflow phase, constant volume phase and constant tonnage phase. In the first phase, nothing is flowing overboard and thus the outgoing flow-rate is zero. Then, in the second phase material starts flowing overboard. During this phase the mixture volume in the hopper remains constant and thus on average the outgoing flow-rate equals the incoming as you can see in figure 2. Finally, in the third (constant tonnage) phase the overflow is lowered to maintain the maximum draught. In this phase the outgoing flow-rate becomes larger than the incoming flow-rate as the total mixture volume in the hopper decreases.

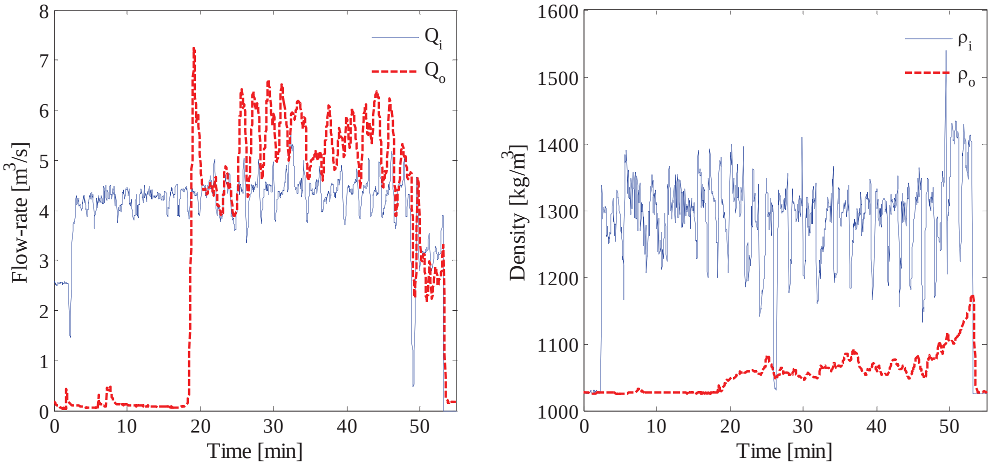

Figure 2. Results of the overflow loss estimator during the sea-trials of a recently built hopper dredger. Left: the incoming and the estimated outgoing flow-rate. Right: the incoming and the estimated outgoing density.

The soil type in the dredging area is medium/coarse sand, therefore the overflow losses are small. Figure 2 shows that in the beginning the outgoing density is approximately 1080 kg/m^3. The sand bed reaches the overflow height at the end of the dredging cycle. As a consequence the overflow density increases. When these losses become too large it is not economical to continue and the dredger should sail to the discharge area.

3 TRAIL FORCE ESTIMATION IN DP/DT AND THE TRAIL SPEED CONTROLLER

The dredging forces during the trailing of TSHD are mainly caused by the cutting force of the drag head. This cutting theory has been studied by Miedema (1987). The cutting force depends on the soil type, permeability and dredging depth. These parameters are not exactly known during the dredging process. Moreover, these properties vary from place to place. For a dynamic positioning and dynamic track controlling system it is of vital importance to know the dredging forces, therefore we use estimation techniques to accomplish this.

3.1 Smart Draghead-Pull-Sensor in Dynamic Positioning and Dynamic Tracking

During dredging, it is of major importance to keep your track and maintain the optimal dredging speed. The force caused by the drag head such as the cutting force pulls on the side of the ship. This dredging force may become so large that 100% of the available propulsion power is necessary whereas only 5 to 10 % is required for maintaining a ship speed of 2 to 3 knots without dredging. Dredging can lead to an increase of power up to 10 times.

An accurate Dynamic Positioning and Dynamic Tracking (DpDt) system requires measuring the dredging forces that act upon the dredging pipe and drag head. This measurement is then used in the DpDt system to immediately compensate these forces by adjusting the actuating propellers, rudders and bow-thrusters, before the track deviation or speed deviation is even measured. This improves the tracking performance significantly.

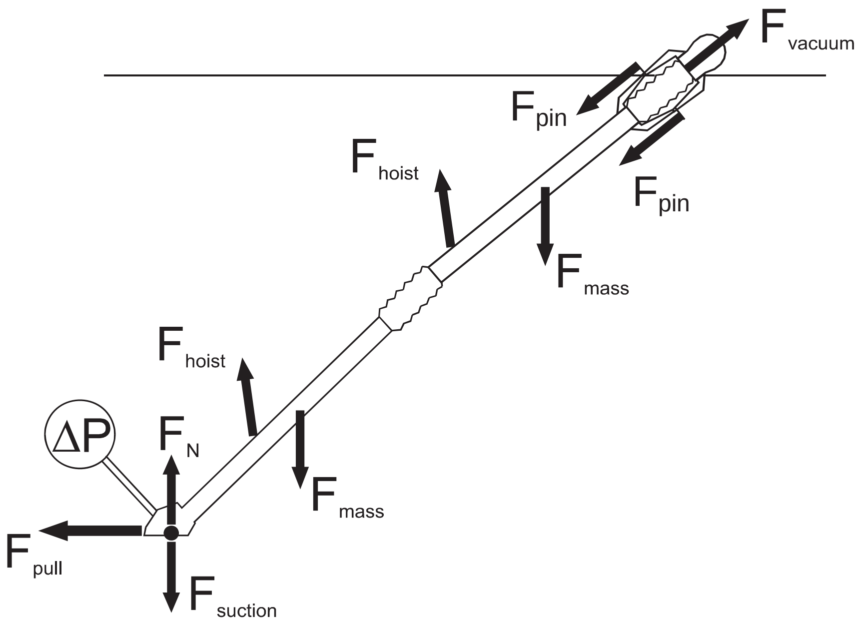

Figure 3. Forces acting on suction tube.

Unfortunately, the dredging forces are difficult to measure. Usually these are measured in the two pins of the upper hinge of the suction tube, see figure 3. This is not the actual pulling force as the figure shows. Calculating this involves many compensations e.g. for the weight of the suction pipe, the mass of the dredged mixture, tension in the hoisting wires etc.

These compensations make the calculation prone to sensor errors and sensor inaccuracy. Calibrating the sensors regularly helps preventing inaccuracy, but reliability is still an issue. As a consequence of dredging in a hostile environment the expensive force sensors need to be replaced regularly.

3.1.1 Current and Drag Head Force Estimation

We solved the reliability issue by combining advanced techniques such as model based estimation, filtering and adaptation to the changing dredging forces. An extended Kalman filter is used, which uses an accurate model of the dynamics of ship and the disturbances such as wind and current. Internally the estimates of the position, speed and heading are compared with the measurements. The error is used to adapt the estimates for the current and the dredging forces.

The patented adaptation algorithm makes a distinction between calibration errors and the disturbance forces such as the current and dredging forces. The distinction can be made because we use the prior knowledge that dredging forces vary rapidly and current forces vary slowly. High accuracy is guaranteed as is shown in (IHC Systems, 1996).

3.1.2 New Measurement Principle

Although the previous section described how we solved the reliability issue, the force estimation still relies on the measurement pins that are vulnerable and need to be changed regularly. This has been solved by a measurement principle that uses the differential pressure over the drag head (IHC Systems, 1997). Figure 4 shows a comparison between the differential pressure over the drag head (thin solid line) and the dredge force (dotted line).

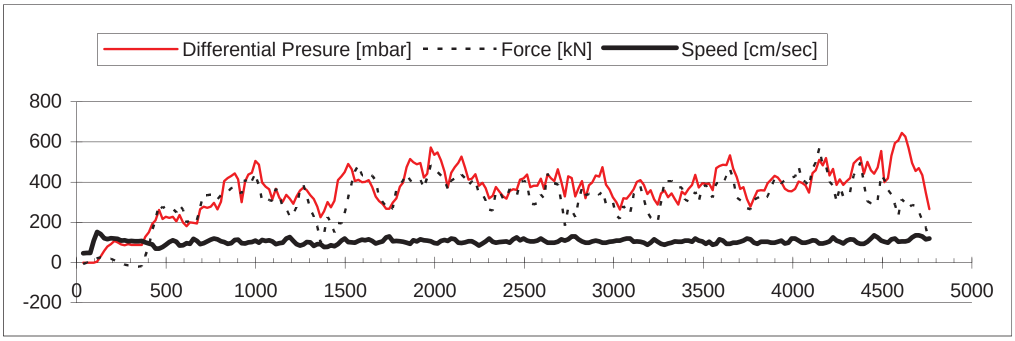

Figure 4. Relation between differential pressure and dredge head pull (time-scale = 5000 sec.).

At first glance the signals look similar, however, careful investigation shows that the relationship varies due to a varying soil type, the use of jet water, pumping speed and sharpness of the drag head teeth etc.
Fortunately the EKF of section 3.1.1 is robust enough to cope with the inaccuracy of using the pressure difference. Sea trials didn't show any noticeable performance degradation. And even if there were any differences, the increase in reliability, due to the absence of the measurement pins, favours the new approach.

3.2 Force Estimation in the Trail Speed Controller

The trail speed controller (TSC) is used to maintain a constant trail speed during dredging. Therefore, the ship navigator only needs to focus on navigating and monitoring the dredging process. This is especially the case on board of ships with a one-man-bridge. The second advantage is that the excavation height will be constant for a constant production-rate.

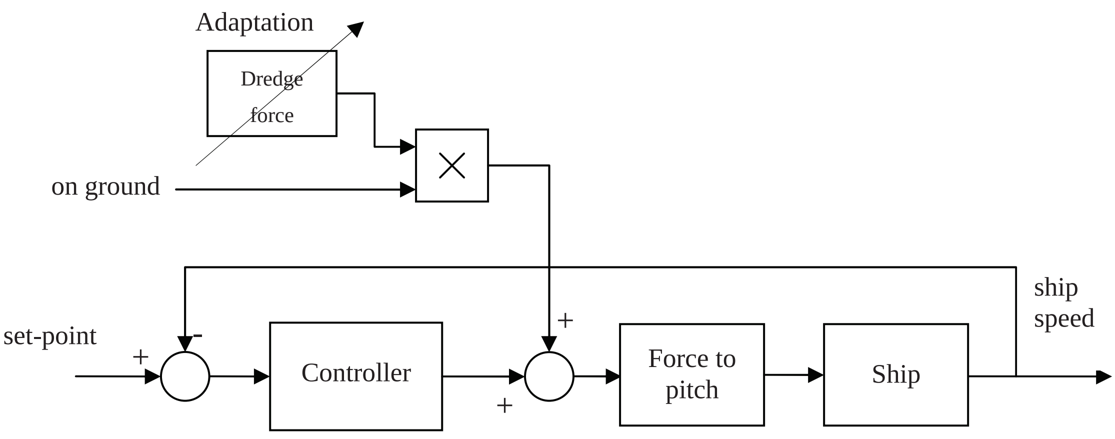

Figure 5. Schematic overview of the Trail Speed Controller.

The control problem for the TSC is much simpler than that of DpDt, because the TSC controls only the longitudinal speed. Therefore only the propeller pitches are actuated. Figure 5 shows a schematic overview of the control implementation. The controller structure is a classical combination of feedback and feed-forward. The estimation of the "Dredge force" is comparable with the method of section 3.1.

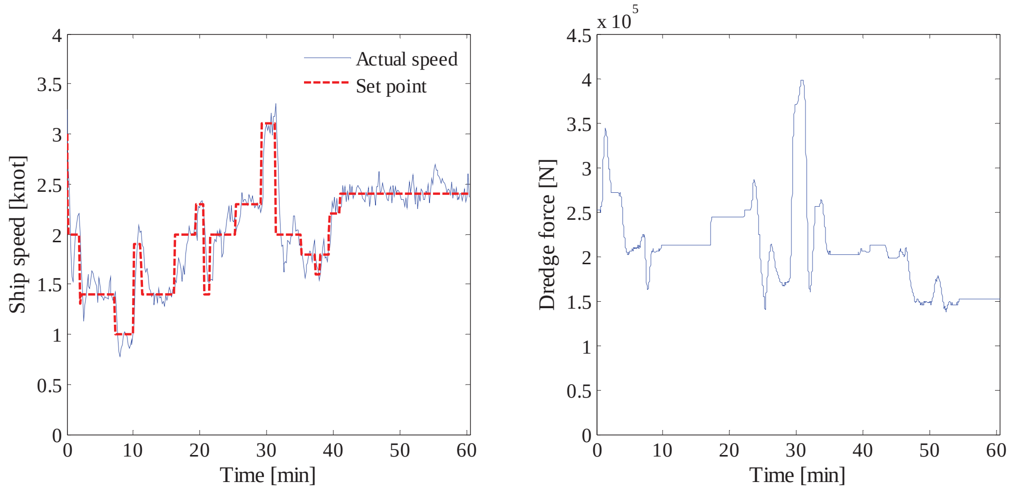

Figure 6.Measurement results of the Trail Speed Controller. Left: tracking performance, right: dredge force estimation.

Figure 6 shows the measurement results of a TSHD during sea trials. The left figure shows the tracking performance of the TSC and the right figure shows the dredge force estimation. When the drag head is lifted from the bottom, the estimation freezes which can be seen in the figure.

4 GRAIN SIZE ESTIMATOR

An important soil property for the dredging process, and in particular for the hydraulic transport process, is the mean grain diameter d_m of the dredged material. The behaviour of the dredge pumps and pipes are significantly influenced by the grain diameter. If we know the grain diameter we can for example optimise the production of the discharge process see Braaksma (2007) part 2. Furthermore the grain diameter can be used for the development of advanced wear models of the pumps, pipes and valves. These wear models may be used for life time prediction in behalf of preventive/scheduled maintenance and also for improving the design of pumps and pipes.

In this section, we describe how to estimate the mean grain diameter online by means of a simple model of the discharge process. In this model, a nonlinear behaviour is introduced by the pressure-losses in the pipelines. Such losses can be thought as a linear combination of homogeneous and heterogeneous losses, by means of a weighting factor α. In the model we have introduced, there are only two parameters to be estimated: the factor α and the grain diameter d_m. For the estimation of such unknown parameters, an Extended Kalman filter (EKF) has been designed. The EKF has been chosen, since it has a recursive formulation, which makes it an efficient implementation, and it naturally handles the uncertainties in the process itself and in the measured signals. The only measurements needed for the EKF are mixture flow, mixture density and the discharge pressure. The tests, carried out onboard several cutter suction dredgers (CSD), have proven the effectiveness of the proposed estimation scheme.

4.1 The Estimation Problem

A simplified model of the discharge process in the pipeline is given by the following equations:
The evolution in time of the flow in the discharge-pipeline can be described by the second-law of dynamics as

$$\dot{Q} = \frac{S}{\rho L} \cdot \left(H_{disc} - \Delta H_l - p_0 \right)$$

The pressure-losses in the discharge-pipeline can be reasonably expressed as a weighted average of *homogeneous losses* ΔH_{hom} and *heterogeneous losses* ΔH_{het}, by means of a weighting factor α, which takes values in the range $[0,1]$.

$$\Delta H_l = \alpha \Delta H_{\text{hom}} + (1-\alpha) \Delta H_{het}$$

Both homogeneous and heterogeneous losses can be conveniently expressed as a function of the losses due to pure water flowing into the pipeline

$$\Delta H_w = 0.5 \lambda \frac{L}{Xd} \rho_w v^2$$

by using a proper correction factor. For homogeneous losses, such a factor depends on the mixture density

$$\Delta H_{\text{hom}} = \frac{\rho}{\rho_w} \Delta H_w$$

whereas, for heterogeneous losses, it depends on the critical speed v_{kr} according to the formula of Jufin-Lopatin (Jufin, A. P. & Lopatin, N. A., 1966)

$$\Delta H_{het} = \left[1 + 2 \left(\frac{v_{kr}}{v} \right)^3 \right] \Delta H_w$$

The *critical speed* is given by

$$v_{kr} = \sqrt[3]{\frac{1}{2} \cdot C_T \cdot 33000 \cdot (g \cdot d)^{\frac{3}{2}} \cdot \frac{d_m}{d}}$$

where C_T is the *transportation coefficient* and is defined as

$$C_T = \frac{\rho - \rho_w}{\rho_g - \rho_w}$$

From the previous equations, a continuous-time state-space representation of the discharge process can be determined, if we make the following positions

$$x_1 = Q \qquad x_2 = d_m \qquad x_3 = \alpha \qquad z = x_1 = Q \qquad u_1 = H_{disc} - p_0 \qquad u_2 = \rho - \rho_w$$

It can be noticed, that the state vector of the system (first-order dynamics in our case), has been extended, by including the unknown parameters in the system model.
The continuous-time state-space representation must be discretized, in order to design a proper estimation scheme. The discrete-time state-space model can be written in the general form

$$\begin{aligned} x_1(k+1) &= f_1\left(x(k), u(k), w_1(k)\right) \\ x_2(k+1) &= f_2\left(x(k), u(k), w_2(k)\right) \\ x_3(k+1) &= f_3\left(x(k), u(k), w_3(k)\right) \\ z(k) &= h\left(x(k), v(k)\right) \end{aligned}$$

Given a process that can be described by a linear stochastic discrete-time model, the Kalman filter represents the optimal recursive solution to the discrete-data linear filtering problem. In other words, the Kalman filter provides an optimal estimate of the state of the system, given the measurements of the input and output signals. The filter estimate is optimal in the sense that it minimizes the estimate error covariance.
Since the model of the process is nonlinear in the state and input variables, the design of a Kalman filter, for the estimation of the state, cannot be directly accomplished. As a preliminary step, it is necessary to linearize such a model around the most recent state estimate. Then, the filter can be designed with respect to the linearized system. This design procedure is known as *Extended Kalman Filter (EKF)*. Compared to other estimation schemes, the Kalman filter has several advantages: (i) it is computationally efficient due to its recursive formulation; (ii) it has a simple and intuitive structure in the form of a predictor-corrector; (iii) it directly takes into account model uncertainties and noise.

In the model of the discharge-pipeline we have been using, the mean density in the discharge pipeline has been considered as input. However, we cannot directly measure the mean density in the pipeline, but only the density injected at the beginning of the discharge pipeline. The problem is, then, how to determine the mean density in the pipeline, given the density of the mixture which enters the discharge pipeline. In such a calculation, the phenomenon of density propagation along the discharge-pipeline must be taken into account, because, for the typical lengths of the pipelines (several km) and the typical speeds of the flow (4-7 m/s), the corresponding time-constants are not negligible.
The propagation can be taken into account in different ways (first-order filter, second order delay-model with three time-constants, “finite-element-like” approach). The simulations and experimental results suggest, that the effectiveness of the proposed approach based on Kalman filtering is, to a certainly extent, independent from the model used for the density propagation.

4.2 Experimental Results

The experimental data have been recorded during a dredging session on the CSD *Rubens*, while working in the *Deurganckdok (nearby Doel, Belgium)*. The pipeline is made up of three segments with the following lengths and diameters:

- Segment I (SB pump to driver): $L_1 = 100\text{m}$ $d_1 = 850mm$
- Segment II (driver): $L_2 = 660\text{m}$ $d_2 = 850mm$
- Segment III (pipeline on land): $L_3 = 7060\text{m}$ $d_3 = 900mm$

For the dredged soil a mean diameter of about $285\mu m$ has been measured. Since for this data-set, we were not provided with the measurements of the losses, when pumping only water into the pipeline, we have assumed for the friction coefficient the value $\lambda = 0.01045$.

In figure 7, we have reported the recorded tracks of the discharge pressure H_{disc}, the flow Q, and the density injected into the pipeline ρ_m. These quantities represent the measured signals used by the Kalman filter for the estimation of the mean-grain-diameter.

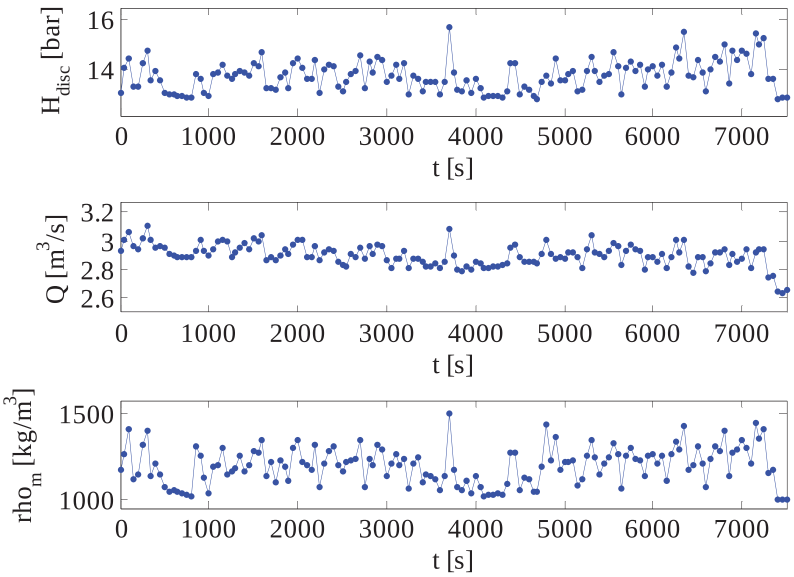

Figure 7. Measured signals used by the Kalman filter.

Here we have reported the evolution in time of the estimate of the mean-grain-diameter (and the corresponding estimation error), as provided by the extended Kalman filter. From figure 8, we can see that the estimate nicely converges to a boundary region around the measured value of the grain diameter. We can also notice that the convergence is quite slow, but this is something we cannot go around, since it is due to the slow dynamics of the discharge pipeline itself (this was also evident from the simulation results). Of course, with a different tuning of the user-defined parameters of the Kalman filter (covariance matrices), we can affect the convergence properties of the filter, but not change them dramatically.

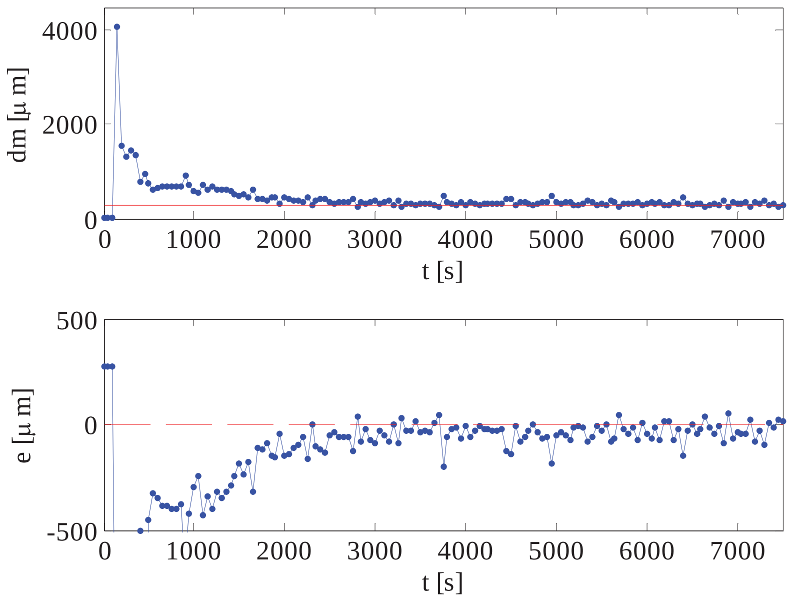

Figure 8. Measured value of the mean grain diameter (continuous constant value) and the estimated mean diameter (continuous lines with dots), and the corresponding estimation error for Ts = 50 s.

We can better see from table 1, what is also suggested by figure 8: the extended Kalman filter is able to achieve a good accuracy (the results are comparable to those achieved in simulations).

Table 1. The table presents the real mean diameter [µm], the estimated mean diameter [µm] and the relative percentile error [%] averaged over the last 10 samples (=500s).

Real mean diameter $[\mu m]$	Estimated mean diameter $[\mu m]$	Relative error $[\%]$
285	312	9.4

Subsequently, we have also run the Kalman filter without down-sampling the data (T_s = 5s), and with a different tuning for the covariance matrix of the measurements (a higher value has been used, in order to have a smooth estimate). It can be seen from figure 9, that the estimate converges very close to the real mean grain diameter, also with this different setting. This is also confirmed by the relative error.

Table 2. The table presents the real mean diameter [µm], the estimated mean diameter [µm] and the relative percentile error [%] averaged over the last 100 samples (=500s).

Real mean diameter $[\mu m]$	Estimated mean diameter $[\mu m]$	Relative error $[\%]$
285	309	8.4

Comparing figure 8 and figure 9, we can notice that the overshoot is definitely less pronounced in the second case.

For the available experimental data, it has been found that the estimated value of the weighting factor α is very small (as we have also found in simulation). As a consequence, a simplified model, considering only the heterogeneous losses can be conveniently used. However, it is likely that, under different experimental conditions (different grain diameters), the model based on both homogeneous and heterogeneous losses will outperform the simplified model based only on heterogeneous losses.

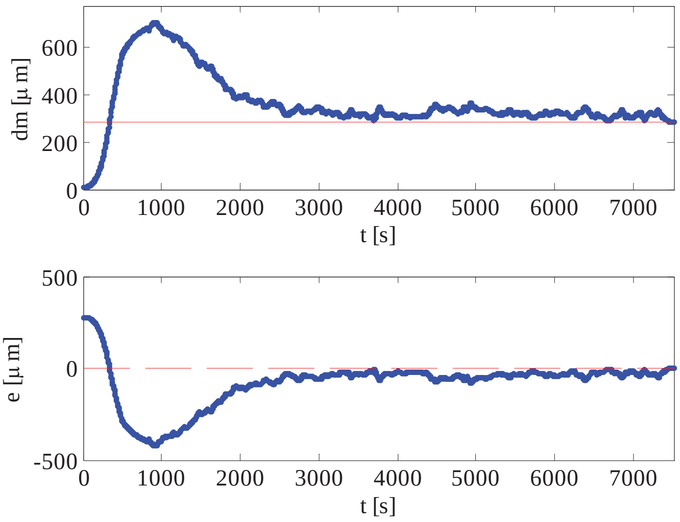

Figure 9. Measured value of the mean grain diameter (continuous constant value) and the estimated mean diameter (continuous lines with dots), and the corresponding estimation error for T_s = 5 s.

For the considered experimental data the performance of the extended Kalman filter was satisfactorily. Regarding the performance the following remarks are important:

- The pipeline layout (pipe lengths and diameters, geometric height difference) should be well known.
- The accuracy of the estimated friction coefficient is a critical factor, since it deeply influences the outcome of the mean grain diameter estimation. Moreover, during dredging generally it is not common to pump water into the discharge-pipeline, if not at the end of the dredging session, when it is needed for cleaning the pipeline. This obviously limits the availability of data, for the estimation of the friction coefficient.
- The used equations are only valid for sand with a maximum grain size of 2 a 3 mm. For other soil types or grain sizes the estimated grain diameter will not be reliable anymore.
- Furthermore, the used equations are only valid if no or less sedimentation is present in de pipeline. A significant amount of sedimentation in the pipeline will result in a higher estimated grain diameter.

5 ANCHOR POSITION ESTIMATOR

Regarding the dredge process of a CSD the anchor positions are of great importance. If the anchors lie too far backwards of the dredger the angles of the side winches will be unfavourable and the effective side winch force will be limiting the swing speed (i.e. the production). Especially at the end of the swing the CSD can get stuck due to the worse angle of the hauling side winch. Furthermore, when the local ground condition at the bottom around the anchor is poor the anchor can not get enough grip and will move during the swing movement of the dredger (i.e. dragging of the anchor). It is important the dredge master quickly notices this dragging.

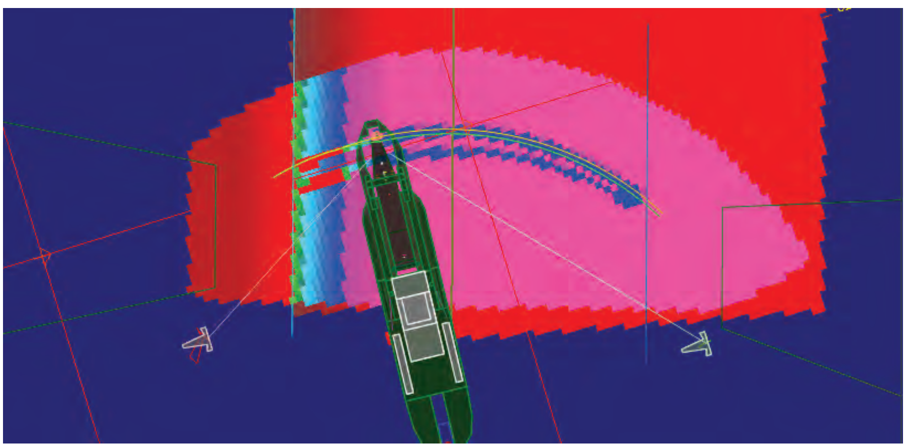

Figure 10. Top view of the dredger with the estimated anchor positions as presented to the dredge master.

In this section the online estimation of the anchor positions is discussed. The anchor position estimator is implemented and in use onboard several CSD. The estimator gives an advice to the dredge master when to reposition the anchors and also detects dragging of the anchors. Figure 10 shows a top view of a CSD with the estimated anchor positions as presented to the dredge master.
The anchor position estimator computes the position of the anchors in a polar coordinates system, with the main spud as origin, and the angular position evaluated with respect to the centre line, see figure 11. The choice of such a reference system can be convenient, since the swinging motion can be naturally described with the same polar coordinates.

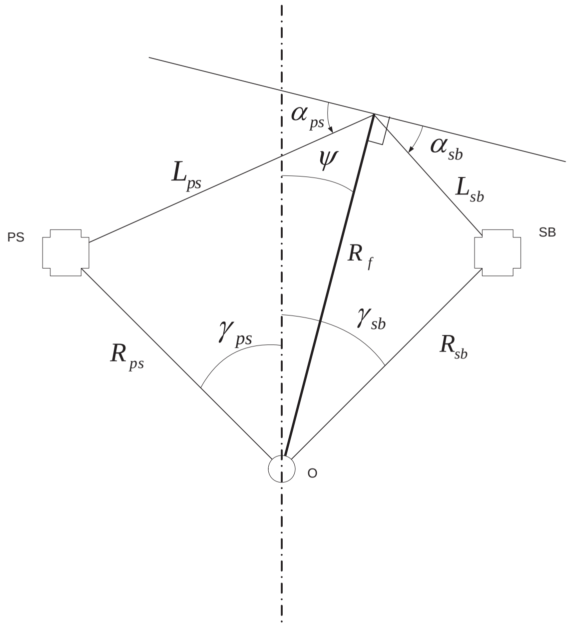

Figure 11. Reference system Anchor position estimator.

The computations are based on a batch algorithm which tries to minimize the mean square error (MSE) between the measured L_i and estimated $\hat{L}_i$ length of the side winches, over a prescribed number of samples N_s as defined by the size of the batch.

$$MSE = \frac{1}{N_s}\sum_{k=1}^{N_s}(L_i - \hat{L}_i)^2$$

The estimated wire length calculation is based on the following geometric relations:

$$\hat{L}_i = \sqrt{R_i^{\,2} + R_f^{\,2} - 2R_f R_i \cos(\gamma_i \mp \psi)}$$

where i = sb, ps and R_i, γ_i are the polar coordinates of the considered anchor, R_f is the swing radius (distance between the main spud and the wire sheaves on the ladder) and ψ is the swing angle.

The minimization algorithm has been implemented in an approximated form. At each time step, first, a regular grid of points around the current estimate of the anchor position is determined. The grid shape may be circular or square. Next, the mean square error is evaluated for each point of the grid, and the point with the lowest error provides the new estimate for the anchor position, see figure 12.

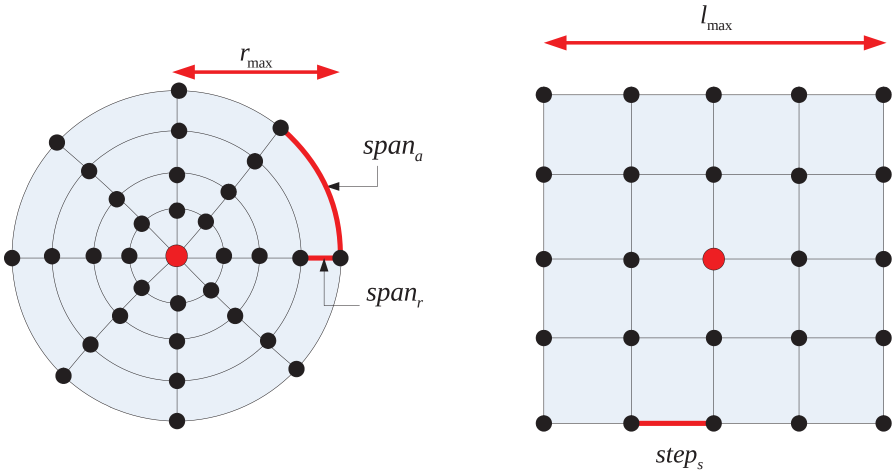

Figure 12. A circular and square grid of points for the approximated minimum search.

The knowledge of the anchor positions can be used not only for detecting possible dragging of the anchors, but also for the calculation of the side winch angles α_{sb} and α_{ps}. The side winch angles are used for the calculation of the effective side winch forces and for the calculation of the forces acting on the main spud due to the side winches.

6 FUTURE DEVELOPMENTS

In order to make dredging even more efficient there is still the need for more advanced estimators and accompanying process models. Some of these estimators will only be a small part of an advanced control strategy. Others will be used as decision support to the dredge master. Some examples of ongoing research topics in this area are:

- Estimating the pressure drop over the drag head and jet penetration depth to optimize excavation process.
- Estimating pump wear and predicting the moment for replacement of the impellor.
- Estimating the grain size based on the pump behaviour. The present grain size estimator is based on the discharge pipeline and as a result the estimated grain size is an average of the total pipeline. By also using the pump behaviour the grain size estimate will be faster updated.
- Estimating the settling velocity of particles in the hopper and sand bed height.

7 CONCLUSIONS

Modelling the dredging process has enabled us to develop advanced control algorithms that optimize the dredging efficiency. Most of these models contain parameters that depend on the soil properties. None of the advanced control algorithms would have been implemented without the use of estimation techniques described in this paper. We described an overview of estimation techniques which are developed during the last years and presented briefly the future developments.

An overflow loss estimator based on a particle filter has been developed and implemented in the latest releases of the DLM software. This estimator can support the operators in the decision making when to stop dredging and warn in case of excessive losses. It can also be used for agitation dredging where the goal is to increase the overflow losses.

The tracking and positioning performance for the DpDt system has been improved by an extended kalman filter. Moreover the reliability is increased by exchanging the force sensor pins in the upper hinge by a virtual dredge force sensor based on the pressure difference over the drag head. This has also been implemented in our newly developed trail speed controller.

For the discharge process, we have described a simple nonlinear dynamical model in the pipeline of a cutter suction dredger. Based on this model, a recursive estimator (extended Kalman filter) has been designed for the estimation of the unknown parameters in the models, namely, the weighting factor α and the grain diameter d_m. The experimental results prove the feasibility and the effectiveness of the proposed estimation scheme.

Finally this paper presented an anchor position estimator which has been succesfully implemented on board of several cutter suction dredgers. This system can give an early warning to the operators when the anchor is dragged over the bottom.

8 NOMENCLATURE

C_T	transportation coefficient	v	speed in the discharge-pipeline
d	discharge-pipeline diameter.	v_{kr}	critical speed in the discharge-pipeline
d_m	mean-grain diameter.	V_t	total volume of sand and water in hopper
e	error	x	state
f	state transition function	X	number of segments
g	gravity acceleration	y	output
h	measurement function	α	weighting factor
H_{disc}	discharge pressure	α_{ps}	angle of port side winch
k	discrete time step k	α_{sb}	angle of starboard side winch
L	discharge-pipeline length.	ΔH_{het}	heterogeneous pressure losses
L	discharge-pipeline length.	ΔH_{hom}	homogeneous pressure losses
L_{ps}	measured length port side winch	ΔH_l	pressure-losses in the discharge-pipeline
L_{sb}	measured length starboard side winch	ΔH_w	losses in the discharge-pipeline for water
m_t	total mass of sand and water in hopper	ε_k	Process noise
p_0	atmospheric pressure	ε_{yk}	Measurement noise
Q	flow in the discharge-pipeline	λ	friction coefficient
Q_i	incoming flow in hopper	ρ	mean-density in the discharge-pipeline.
Q_o	outgoing flow through overflow weir	ρ_g	mean-grain density.
R_f	swing radius	ρ_i	incoming density of mixture in hopper
S	discharge-pipeline section.	ρ_o	outgoing density through overflow weir
T_s	Sample time	ρ_w	water density.
u	input	ψ	swing angle

9 REFERENCES

Arulampalam, S.; Maskell, S.; Gordon, N. J. & Clapp, T. (2002), 'A Tutorial on Particle Filters for On-line Nonlinear/Non-Gaussian Bayesian Tracking', *IEEE Transactions on Signal Processing* 50, 174-188.

Babuška, R.; Lendek, Zs.; Braaksma, J. & de Keizer, C. (2006), Particle Filtering for On-Line Estimation of Overflow Losses in a Hopper Dredger, *in* 'Proceedings of the 2006 American Control Conference, Minneapolis', pp. 5751--5756.

Braaksma, J.; Osnabrugge, J.; Babuška, R.; Keizer, C. & Klaassens, J. B. (2007), Artificial Intelligence on Board of Dredgers for Optimal Land Reclamation, *in* 'CEDA Dredging Days 2007'.

Braaksma, J. (2008), 'Model-Based Control of Hopper Dredgers', PhD thesis, TU Delft.

IHC Systems (1996), 'IHC Systems and LIPS supply a new integrated Dynamic Track Keeping system on the "Pearl River"', *Offshore Visie* 13(3), 18-19.

IHC Systems (1997), 'New sensing system for measuring draghead pull', *Offshore Visie* 14(3), 35-36.

Jufin, A. P. & Lopatin, N. A. (1966), 'O projekte TUiN na gidrotransport zernistych materialov po stalnym truboprovodam', *Gidrotechniceskoe Strojitelstvo*, 49-52.

Kalman, R. E. (1960), 'A new approach to linear filtering and prediction problems', *Transactions of the ASME-Journal of Basic Engineering* **82**(1), 35-45.

Lendek, Zs.; Babuška, R.; Braaksma, J. & de Keizer, C. (2008), 'Decentralized estimation of overflow losses in a hopper dredger', *Control Engineering Practice* 16(4), 392-406.

Matoušek, V. (1997), 'Flow Mechanism of Sand-Water Mixtures in Pipelines', PhD thesis, TU Delft.

Miedema, S. A. (1987), 'Calculation of the Cutting Forces when Cutting Water Saturated Sand', PhD thesis, TU Delft.

van Rhee, C. (2002), 'On the sedimentation process in a Trailing Suction Hopper Dredger', PhD thesis, TU Delft.

Welch, G. & Bishop, G. (2002), 'An introduction to the Kalman filter', Technical report, Department of Computer Science, University of North Carolina at Chapel Hill, NC.

THE FEHMERN BAELT FIXED LINK

"The longest tunnel trench in the world will be asking for new dredging tools"

Steen Lykke, Project Director, Tunnel[1], Claus Iversen, Project Manager, Marine Works, Tunnel[2] and Stephen Pearson, Lead Engineer, Marine Works, Tunnel[3]

ABSTRACT: Following the signing of a Treaty between Denmark and Germany in September 2008, the Fehmern Baelt Fixed Link, connecting Scandinavia (Denmark) with the European Continent (Germany), finally got off the ground and has since then started moving into the initial Conceptual Design phase. This phase is the first step of a 10 year design and build process.

The fixed link will carry four lanes for road traffic as well as two tracks for railway traffic. A cable stayed bridge is the preferred solution and an immersed tunnel is the preferred alternative. An immersed tunnel will by far be the longest and the biggest immersed tunnel ever constructed. Conceptual design of both solutions is now being prepared as parallel activities.

The Fehmern Baelt Strait is approximately 19 km wide and the water depth varies between 20 and 30 meters within the heavily trafficked navigational channel, which covers approximately 50% of the total width. The expected construction period for both solutions is 7 years – with approximately 5 years allocated for the dredging and reclamation works – which in itself calls for a number of new innovative construction solutions.

Obviously the two alternative schemes involve some comprehensive but also rather complex marine operations and construction works – starting with dredging of the 19 km long and 11 – 14 meter deep tunnel trench – or alternatively with a series of up to 15 m deep pits for the foundation of bridge piers. Dredging and reclamation volumes vary between 20 million m3 for a tunnel trench and approximately 4 million m3 for a bridge solution. The maximum dredging depths will for both solutions be in the order of 45 m.

The paper will give a general description of the two alternative solutions – bridge or immersed tunnel – but will focus on major challenges for the dredging works in terms of dredging depths, expected techniques and capacities needed to meet the tight construction schedule. The works must be executed under strict environmental control in soil conditions varying from soft soil to hard formations of clay till in the northern section of the Strait. As much as possible of the dredged materials can be expected to be transformed into engineered fill in purpose build reclamation basins

Also the need for import of up to 15 million m3 of quality fill for backfilling of the tunnel trench and/or reclamation of anchor block islands for the bridge will be addressed.

[1] Femern A/S, Vester Soegade 10, DK-1601 Copenhagen V, Denmark, T: +45 33 41 63 00, F: +45 33 41 63 01, e-mail sly@femern.dk, www.femern.dk

[2] Femern A/S, Vester Soegade 10, DK-1601 Copenhagen V, Denmark, T: +45 33 41 63 00, F: +45 33 41 63 01, e-mail civ@femern.dk, www.femern.dk

[3] Tunnel Engineering Consultants (TEC), Barbarossastraat 35, NL-6522 AC Nijmegen, The Netherlands, T: +45 45 98 62 17, F: +45 45 98 67 00, e-mail spearson@runbox.com

INTRODUCTION

The present article deals with the planned design and construction of the Fehmern Fixed Link, which comprises a fixed road and rail link between Denmark and Germany. The link is planned to cross the Fehmern Baelt between Rødbyhavn, located some 180km south of Copenhagen on the island of Lolland in Denmark, and Puttgarden located on the island of Fehmern on the north coast of Germany. The crossing of the Fehmern Baelt will form a further link in the chain linking Scandanavia with the western European mainland after the construction of the fixed road and rail links across the Storebaelt (in 1998) and the Øresund (in 2000). All considerations made in this article are based on preliminary and not yet confirmed information about the geology and geotechnical characteristics of the soils involved. The plan is to have such information confirmed or adjusted by performing boring campaigns during the years 2009 and 2010 with following laboratory tests.

The Fermern Baelt Project is aligned with the ideals of the STRING-cooperation (Southwestern Baltic Sea Transregional Area Inventing New Geography), to which Denmark and Germany regional authorities are partners. This emphasises the value of the Fehmarnbelt project in terms of meeting key EU and regional transportation targets.

The Femern A/S (the Client) of Denmark is responsible for the development and implementation of the Fehmern Baelt Fixed Link and is a subsidiary of Sund & Bælt Holding A/S. The latter company is responsible for the operation and maintenance of the fixed link across the Great Belt and owner of half of the consortium responsible for the operation and maintenance of the Øresund fixed link.

Fehmern Baelt Construction Site.

BRIDGE OR TUNNEL

Two options are currently being considered for the fixed link; a bridge and a tunnel. The Ministers of Transport of Denmark and Germany have agreed that a cable stayed bridge should be considered as the preferred technical solution and an immersed tunnel as the preferred alternative solution for future investigations. Both solutions are to be developed for a four-lane motorway and a twin-track railway.

Notwithstanding the foregoing, a suspension bridge solution is also being considered within the scope of ongoing navigational studies and the choice between a cable stayed bridge solution and a suspension bridge solution will await the results of the navigational studies and the conclusions/recommendations from the maritime authorities. The Plan Approval process in Denmark and in Germany shall therefore on a parallel basis include both a bridge solution, as well as an immersed tunnel solution in order to place the winning concept in perspective compared to the relevant technical alternative.

The dredging and reclamation works for the bridge option comprise a series of up to 15 m deep (below seabed) bridge piers with a total volume of 4 million m3

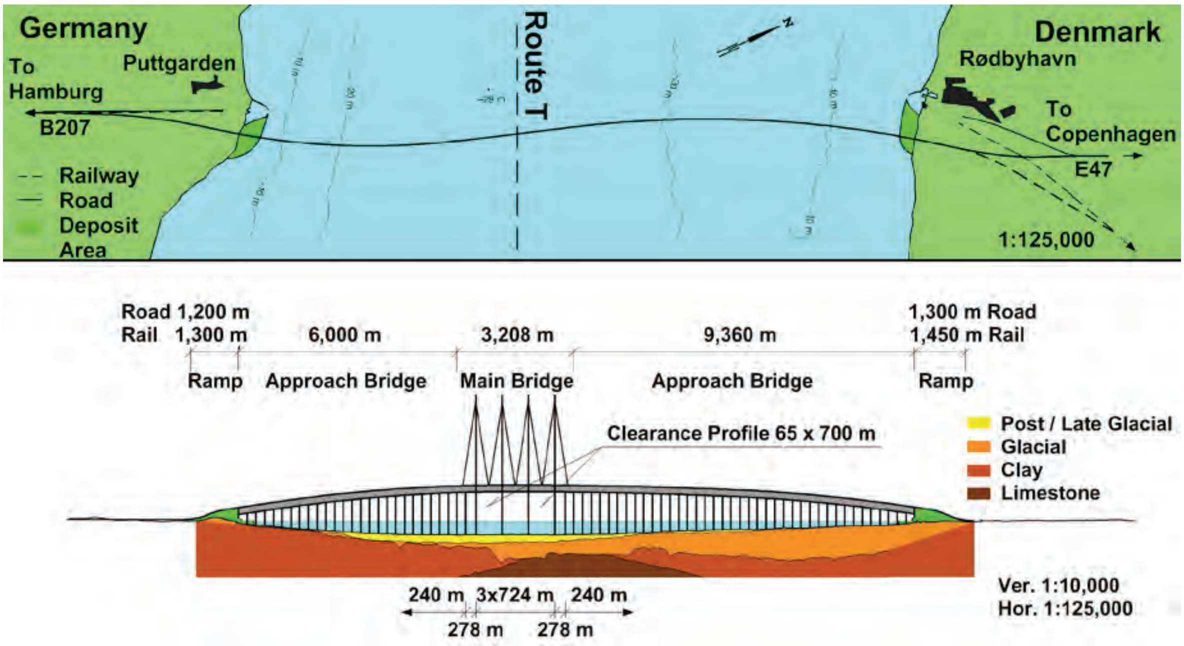

Potential Bridge Alignment

The dredging and reclamation works associated with the immersed tunnel solution comprise dredging of an 18.5 km trench some 12 – 15 m deep and 40 – 50 m wide between Rødbyhavn and Puttgarden, backfilling the trench after installing the immersed tunnel, construction of ventilation island(s) in approx. 25 m of water and the creation of land/marine disposal areas. Further dredging works might be required such as the sourcing of marine sand and the creation of casting basins or temporary marine storage areas for tunnel elements as they leave the fabrication sites.

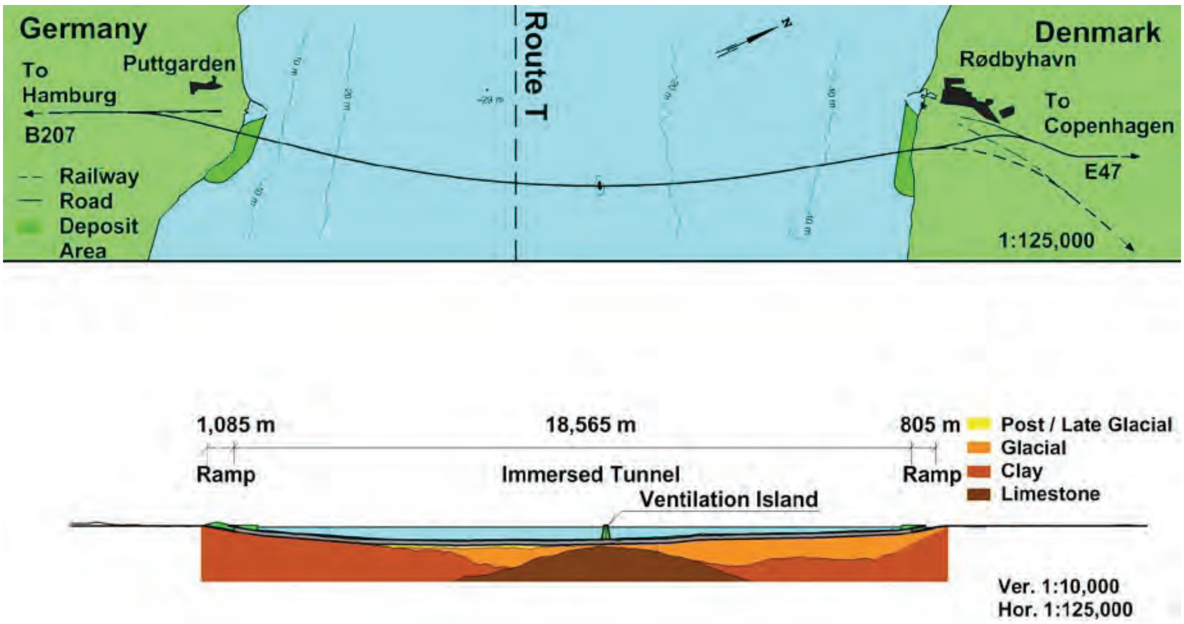

Potential Tunnel Alignment

A total of some 20 million m^3 of soils will be dredged from the trench and some 12 million m^3 will be required for backfilling the trench. It is unlikely that all dredged material will be suitable for backfilling the trench which means there will be in excess of 10 million m3 of dredged material to be disposed of in an environmentally sustainable and responsible way.

The dredging and reclamation/disposal works associated with the construction of a fixed link will pose major dredging challenges irrespective of whether a bridge or tunnel solution is finally selected. In the next few pages the major dredging challenges will be identified and discussed.

MAJOR DREDGING CHALLENGES

The construction of a fixed link across the Fehmern Baelt will pose major dredging challenges in terms of the depth to be dredged, the varying types of soils and soils/rocks to be dredged, the strict environmental control and the need to meet tight construction schedules.

The existing seabed profile between Puttgarden in the south and Rodbyhavn in the north comprises two nearshore areas that gently slope (1:150 on German side and 1:300 on Danish side) down from 0 to -25 m and subsequently form a central basin with water depths reaching almost -30 m.

The geological setting comprises Quaternary deposits of a few metres to more than 50m in thickness overlying a very thick layer of Paleogene clays, which in turn covers a cretaceous formation in the form of chalk to a level of approx. -400 m. Towards the northern extent of the basin a deep lying salt dome has lifted the chalk through the Paleocene clays such that the apex of the chalk has pierced through the Paleogene clays and reached a level of -50 m.

The trench will cross a variety of soil conditions. On the Danish nearshore the material to be dredged comprises sand deposits of 1 to 2 m thickness overlying hard to very hard clay tills with undrained shear strengths varying from 700 kPa to 2 MPa and containing stones and boulders (some up to several metres in diameter). On the German nearshore the material to be dredged comprises a layer of post-glacial sands and gyttja of 2 – 10 m thickness covering thick deposits of Paleogene clay with undrained shear strengths in the region of 100 – 200 kPa. The material to be dredged in the basin comprises a layer of gyttja covering glacial deposits of sands, silts and clays.

Dredging depth

Dredging for the immersed tunnel solution will need to produce a trench with a bottom level some 12 – 15 m below the existing seabed, which implies a maximum dredging depth of some -45 m. Trenching work on the German and Danish nearshore up to a depth of approx. -25 m may be possible with large sized conventional dredging equipment. However, dredging depths beyond -25 m may with todays existing technology preclude the use of most large sized conventional dredging equipment with the exception of Grabs and Trailing Suction Hopper Dredgers (TSHDs). The relatively flat nature of the basin and its transitions to the adjacent nearshore areas means that a dredging depth of -25 m and deeper is not just restricted to a small area, but extends over more than 65% of the total length of the tunnel.

Soils

The soils on the Danish foreshore mainly comprise extremely hard clay-tills (with 40 – 60% sand content) with an expected medium to high boulder content (to be confirmed). The undrained shear strength of the clay-till is expected to be so hard (0.7 – 2 MPa) that dredging by mechanical means can be considered, but will probably result in low production rates that might compromise the construction schedule. Dredging by mechanical/hydraulic means i.e. Cutter Suction Dredgers (CSDs), could prove to be more effective as far higher production rates can be achieved and hydraulic transport of the material would lend itself better to engineering the clay-till i.e. separating the granular material from the fines in a confined reclamation area, in order to be re-used as backfill material. However, the expected medium to high content of boulders in the clay-till will provide real problems to CSDs as they can only handle cobbles/stones with a maximum size of approximately 300mm.

The gyttja and post-glacial sands on the German nearshore should not pose any real dredging problems, but the underlying deposits of stiff to hard fissured Paleogene clays, which exhibit very high plasticity and lie relatively close to the seabed, will pose challenges both with respect to dredgeability (high adhesion) and pumpability (clay balling). The clays could have a beneficial use and be considered for use as cover layer material for the ventilation island and or providing the core of containment dikes for disposal areas.

In the central basin there are post-glacial deposits of gyttja, sand, silt and clay located in water depths below -25 m. The dredgeability of these materials should not pose any real problems for large sized Trailing Suction Hopper Dredgers (TSHD's) provided there are not any hard layers of clay.

Seabed Features

Seismic surveys have initially revealed the possible presence of sand waves (up to several metres high) on the Danish nearshore which could be active and might create problems during dredging and immediately prior to installation of tunnel elements. Furthermore, some possible wrecks and boulder fields have been detected on the seabed in the north and the south and may prove time consuming to remove before more productive dredging units can operate in these areas. There are also indications that the post glacial sediments on the German nearshore contain gas at a depth of approximately -25 to -30 m and as a result any hydraulic dredging units operating in this area would probably require suitable de-gassing installations. Magnetometer surveys have also revealed a presence of some metal objects which could also prove to be ordnance.

Environmental contraints

Environmental constraints will also pose real challenges to dredging. There was only limited opposition to the compensation dredging for the Store-baelt crossing as the environmental impacts were not serious. However, in the case of the Oresund crossing where much of the dredged material was limestone and clay – the potential environmental problems had come more into focus and the public awareness was intense.

Clamshell dredger "Kanyu" dredging the tunnel trench in the Bosphorus Strait

The materials to be dredged from the Fehmen Baelt will comprise similar materials to that dredged on the Oresund, but the distribution of the soils will be much different and total quantities for a tunnel solution will be in the order of 2½ times that dredged on the Øresund. Strict environmental control will likely include as a minimum carefully planning, monitoring and documentation of operations such as hopper and barge overflowing, discharges from disposal areas, turbidity and sediment plumes.

Benefical use of dredged material

A major challenge on the project will be to re-use as much as possible of the 20 million m^3 of dredged materials in a beneficial way because the disposal of such large quantities of soil into the marine environment may prove to be unacceptable. While an obvious use for the dredged material would be the backfilling of the trench and construction of one or more ventilation islands, it would only account for perhaps a little more than half of the material should the material be deemed suitable for this purpose.

The selection of the right type of dredging equipment and working methods will prove instrumental in maximising the re-use of dredged materials. The clay-tills on the Danish foreshore could be engineered to produce grannular backfill for the tunnel while the clays on the German foreshore could be used as cover layers for ventilation islands and core material for containment dikes and internal bunding of disposal areas.

Construction Schedule

In the early stages of the project there are many different dredging and reclamation activities which will be on the critical path and will require timely completion. These activities include performing many investigations (bathymetric, topographic, soil, magnetometer surveys etc.) and the removal of potential ordnance, creating stockpiles of construction materials, removal of boulder fields from the seabed, construction of dredge disposal areas, construction of temporary work harbours and construction of basins for fabrication of tunnel elements at multiple sites.

The construction and immersion of tunnel elements will also be on the critical path and therefore dredging and backfilling activities will also lie on the critical path. The construction of an immersed tunnel is envisaged to take some 5 years to complete and in that time some 125 large scale tunnel elements will have to be immersed which implies a continuous construction sequence whereby a tunnel element is immersed every 2 to 3 weeks. Dredging operations will have to be interfaced very closely with the immersion process and progress at a similar rate.

CLOSING REMARKS

The Fehmern Baelt Fixed Link is a unique project and the design and construction of the associated dredging and reclamation works for both the bridge and immersed tunnel solutions will raise many new challenges. Conventional dredging equipment and techniques will be able to deal with many of the challenges the project has to offer, but will have difficulty dealing with the dredging of stiff and hard materials at depths exceeding 30 metres and reaching a maximum dredging depth up to approxiamtely 45 metres. Serious consideration needs to be given to modifying existing equipment (custom-built equipment) and to developing innovative techniques to deal with all the cutting edge project requirements and challenges.

A suitable dredging and reclamation spread will have to be developed that is flexible in terms of the soils it can dredge, is capable of dredging stiff to hard material to depths of -45m, can keep the environmental effects within reasonable and acceptable levels and provide sufficiently high capacity to meet the demands of the construction schedule.

However, the authors are confident that the dredging and construction industry will be able to meet the challenges described above and develop both dredging equipment and innovative techniques which will be instrumental in completing the works on time, within the required quality and within budget.

FUTURE DREDGING TOOLS MADE FROM 'NEW' MATERIALS

H. H. Bugdayci[1], F.W.P. Smeets[2], T.A. van Opstal[3]

Abstract: In the late 1960s the development of fiber composites has been spurred by the space - and aircraft industries. Because of its unique characteristics this material has also found its way in other industries since then; e.g. wind turbines, high performance sports goods and yachting.
Fiber composites are materials where a fiber is embedded in a matrix material. Depending on the requirements specific fibers, usually carbon or glass can be chosen and orientated according the loads. Using these possibilities much lighter constructions can be accomplished than in steel while maintaining the same functionality or even adding improvements in the functionality.

In the dredging industry fiber composites are not widely used yet. On a couple of vessels fiber composite jet piping has been used but other than that most dredging equipment on dredging vessels is still made of steel. This could change soon; some recent studies on fiber composite and other plastics applications on dredging equipment show there are major advantages to be gained. Some of these include the reduction of weight, increasing the productivity and added functionality.

Recently at IHC Merwede some dredging equipment has been designed in fiber composites. For instance a telescopically extendable suction tube has been designed from scratch and a new design has been made for the outer casing of a double walled dredge pump also in fiber composite. Use of these new materials created new possibilities not possible in steel.
This paper describes these designs and some other studies showing the possibilities of fiber composite and other plastics application in the dredging industry.

Keywords: composites, fiber reinforced, carbon fiber, glass fiber, plastic, dredge pump, double-walled dredge pump

[1] Manager Innovation & Development, IHC Parts & Services, P.O. Box 50, 2960 AB, Kinderdijk, The Netherlands, +31 (0)78 6910 842, hh.bugdayci@ihcmerwede.com
[2] Innovation & Development Engineer, IHC Parts & Services, P.O. Box 50, 2960 AB, Kinderdijk, The Netherlands, +31 (0)78 6910 720, fwp.smeets@ihcmerwede.com
[3] Innovation & Development Engineer, IHC Parts & Services, P.O. Box 50, 2960 AB, Kinderdijk, The Netherlands, +31 (0)78 6921 754, ta.vanopstal@ihcmerwede.com

1 INTRODUCTION

At the end of the nineteenth century the first steps were taken in the development of plastics. The first plastic which was ‘discovered’ was celluloid. This invention / discovery would start a whole range of new materials; varying from the early Bakelite to the more recent discoveries of high tensile polystyrene strands. This development led to a whole range of products made from plastic; ranging from toys to telephones to most of our home appliances to the interior of our cars. Actually the list is so comprehensive it would not be possible to be complete. The success of plastics can be partly found in the versatility of the material. Especially nowadays for every application and requirement a specific plastic can be found and the inventions and discoveries continue.
Industrial applications can be found in piping or profiles or plating, all types of construction elements and so on. Most of these applications are moderately loaded though. When the loads and stresses of a component or product are higher and the requirements increase the main characteristics of the plastics will not suffice and it will be needed to be reinforced. This is usually carried out with the use of strong fibers made from carbon or glass. The material which is made this way is called fiber reinforced composite.

The development of fiber reinforced composite products started seriously during the Second World War. The first product was glass fiber composite housing for radar equipment. Because of the scarcity and the high price for glass fibers the applications were restricted to the defense and space industries these days. After the war the first commercial fiber reinforced boat hull was produced. This can actually be indicated as the start of the fiber composite industry.
The accidental discovery of carbon fibers in the mid fifties of the twentieth century gave another boost to fiber reinforced composite products. Carbon fibers are made from pure carbon and are among the strongest and stiffest materials for their weight. The first applications of carbon fiber composites can be found in high speed aircrafts.

From a human perspective these developments, inventions and discoveries are still very young. But still both developments have had a big impact in our lives.

There are some application of high performance composites and plastics in the dredging industry. For instance jet pipes in some of the larger dredging vessels are made from fiber reinforced composites. The benefits are its lightweight structure and resistance to corrosion. There are also some applications of dredging pipes made from plastics which have reasonable wear resistance.

Figure 1 Fiber reinforced composite jetpipes.

In general the main dredging components are still made from steel and iron. Since the wear resistance of composite materials is still less than that of cast iron or steel for that matter, the usual material for use in parts which are in direct contact with mixture will not be composite or plastic. For structural components though this is not the case. The properties of fiber composites can actually be a great advantage for use in this type of components and can probably lead to a lower cost per cubic meter of dredged material.

Recently several design / feasibility studies have been conducted to fiber composite and plastic components for dredging vessels. Applying fiber composites to these components resulted in possibilities which would not have been feasible in traditional steel or iron design.

This paper first describes the properties and characteristics of fiber composites in more detail. After which three cases of plastic applications in the dredging world are presented. Finally the conclusions are summarized in the last chapter.

2 HISTORY OF COMPOSITES

Composites materials are materials which are made out of two different types of materials and where the combination of the two creates a stronger material than of the individual parts separately. Wood is a typical example of a natural composite; cellulose fiber combined with lignin. The cellulose gives the wood its strength while the lignin bonds and stabilizes the cellulose fibers.
The first examples of manmade composites are the mud-bricks used by the ancient Egyptians. These mud-bricks, which are still being used in some parts of the world, are made from a mixture of clay mud and straw. The mixture is shaped using a mal and left to dry in the sun. The straw fibers hold the clay mud together while the load on the bricks is carried by the dried mud. This combination is stronger than either the clay or the straw.

Figure 2 Mud bricks; an example of ancient composites

Nowadays composites are still used for building housing and the construction industry in general; steel reinforced concrete. The steel reinforcements in the concrete give the composite its strength while the concrete itself adds rigidity. The combination of the two materials creates a composite which is ideal for building large rigid structures.
Another recent example of a common composite product is a typical car tire. In a car tire a combination of rubber with steel, nylon or other fibers are combined. The fiber reinforcements are hold together by the rubber matrix while also making the tire airtight. The fiber reinforcements give the tire the required strength.

The composite materials we will be discussing are composite materials which have a structure where synthetic fibers are combined with a polymer matrix material; Fiber reinforced composites (FRP). The matrix material usually does not have great mechanical properties but are chosen for their ease of processing and their ability to be easily formed in complex shapes. Fibers have excellent mechanical properties, but only in one direction. The matrix material distributes the loads evenly to all fibers and protects the fibers from abrasion and damage from external objects.
The properties of the composite will be a combination of the properties of the matrix material and the fiber properties. Furthermore the amount and orientation of the fibers inside the composite will determine the properties of the composite product greatly.

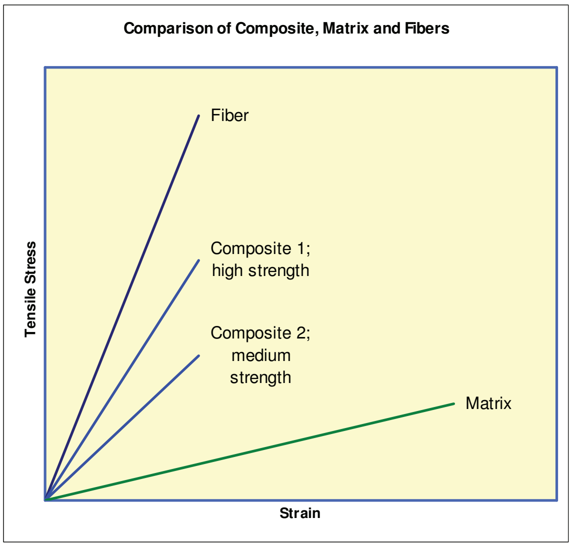

Figure 3 Comparison of composite, matrix and fibers

3 CHARACTERISTICS OF COMPOSITES

3.1 Synthetic fibers

There is a long list of types of fibers which can be used in composites, with new inventions and developments the list gets longer by the day. The most common types of fibers are glass -, carbon - and aramid types of fibers; the mechanical properties of the most commonly used fibers of these three types are shown in the following graph; compared with some metals.

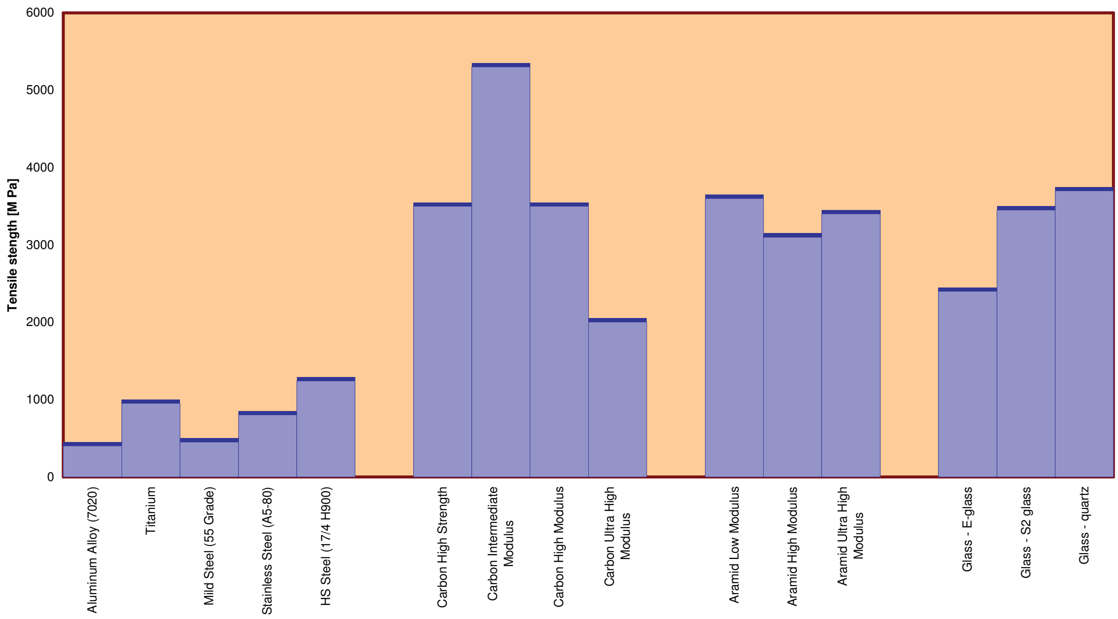

Figure 4 Tensile strength of composites compared

Apart from the difference in mechanical properties these types of fibers also differ in some other characteristics like impact resistance, thermal insulation capacity and the price, see the table below. The choice for a certain type of fiber depends on the application and the required characteristics.

Carbon fibers have high mechanical properties like strength and stiffness but are relative low on impact resistance. Glass fibers have good fire resisting and electrical insulation capabilities and have a low price compared to the other types. Aramid fibers have good impact strength and give good insulating capabilities.

Table 1 Characteristics of different fibers compared

Characteristics	Carbon	Glass	Aramid
Strength	High	Medium	Medium
Stiffness	High	Low	Medium
Compression	High	Medium	Low
Flexural strength	High	Medium	Low
Impact	Low	Medium	High
Density	Low	Medium	High
Fatigue resistance	High	Low	Medium
Fire resistance	Low	High	High
Thermal insulation	Low	Medium	High
Electrical Insulation	Low	High	Medium
Thermal Expansion	High	High	High
Cost	High	Low	Medium

Conditions where impact loading is also to be expected composites with carbon fibers are usually combined with glass and aramid fibers. The glass and/or aramid fibers are placed on the surface areas where it will act as a protective layer for the carbon fibers.
Conditions where only impact loadings are expected aramids will be the best choice, hence the use of aramid fibers in bullet proof vests. Glass fibers on the other hand are more common in large structures where moderate loads are expected and large quantities of fibers are required. Locations where high loads are expected can be strengthened with carbon fibers.

3.2 Polymer matrix

Most common types of materials used for composite matrix are epoxy, vinyl ester and polyester resins. In Figure 5 a comparison of the mechanical properties of these materials is given.

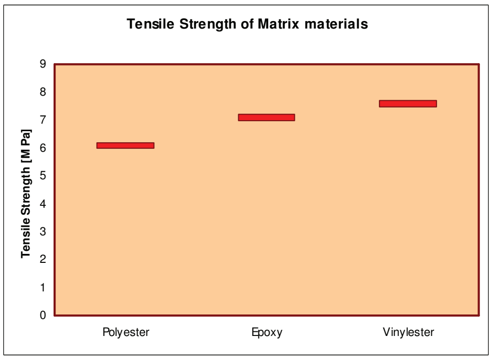

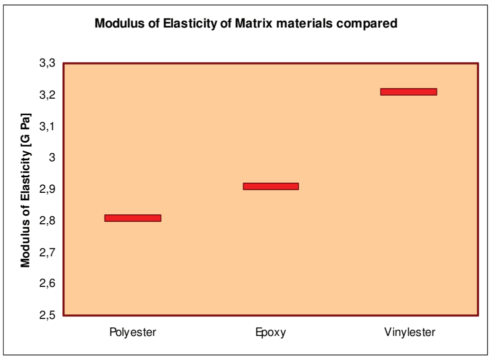

Figure 5 Tensile strenght and modulus of elasticity of common matrix materials

Polyester resins are the most commonly used resin types. There is a whole range of polyesters available. Small boats and yachts are commonly made with polyester resin.

Vinyl ester resins are similar to polyester resins but can withstand higher loads and have a better resistance against water and chemicals. Piping and chemical storage are typical applications where vinyl ester is used.

Epoxy resins have the best properties of the available resins nowadays and show very little shrinkage when curing. This is why they are often used in demanding applications. Epoxy resins need a hardener to be cured.
Most of the significant characteristics of the resin types are summarized in table below.

Table 2 Characteristics of typical matrix materials

Characteristics	Polyester	Epoxy	Vinylester
Mechanical properties	Low	High	Medium
Adhesive properties	Low	High	Medium
Fatigue resistance	Medium	High	Medium
Shrinkage	7%	2%	7%
Water resistance	Low	High	Medium
Temperature resistance	Medium	High	Medium
Chemical resistance	Medium	High	High
Ease of use	Good	Difficult	Medium
Cost	Low	High	Medium

3.3 Core materials

When flexural stiffness is required in a component enlarging the thickness is one of the options an engineer can apply. This method is commonly applied with composite components. The thickness of a composite component is enlarged by enlarging the core of a composite component with special core materials. Most common core materials are foam type materials and honey comb structured materials. Depending on the application the appropriate core material can be chosen.

Figure 6; Example of a sandwich construction with an aluminum honeycomb core.

Mechanical properties of steel components are mainly determined by the properties of the raw material. These properties are mostly fixed and only little influence can be exerted during the manufacturing process to the properties of the finished product. One could argue that the mechanical properties of steel components are mainly determined by the raw material manufacturer.
Contrary to steel components mechanical properties of composite components are mainly determined during the manufacturing process of the composite product itself. Since the manufacturing process of composite components is so important in the next chapter we will look at the different possibilities of the manufacturing process.

4 PRODUCTION OF COMPOSITE COMPONENTS

As mentioned before the production process of fiber composites greatly determines the (mechanical) properties and the abilities to carry loads of the component. Although there are some similarities with conventional production methods of metal components production of fiber composites is quite different. Generally the fiber materials and the resin have to be combined in a way that they bond well together. And specifically all fiber materials have to be placed as was designed by the engineer for the component. The fiber orientation has to be such that the required and designed (mechanical) properties of the component can be realized.

Some of the most used production methods of composite components are hand lay-up and vacuum injection.

Hand lay-up
With the hand lay-up method the composite component is manually fabricated with the use of a mould. Fiber fabrics are placed on a mould taking into account the orientation and amount of the required fibers. The fiber package is then manually impregnated using a brush or a roller; see Figure 7. The composition can then be cured under atmospheric conditions.

Figure 7 Hand lay-up

Vacuum injection
The vacuum injection method is very well applicable for large composite components. With vacuum injection the fiber stack is placed in the mould on top of a plastic sheet. After all fiber fabrics and possible core materials and other reinforcements are correctly placed the plastic sheet is closed airtight.
One side of the thus created vacuum bag is connected to a resin reservoir. And on the opposite side of the connection to the reservoir vacuum is applied to the bag with the use of a vacuum pomp. This operation will then draw the resin from the reservoir into and through the fiber pack. After all fibers are sufficiently impregnated the composition can be cured either under atmospheric conditions or in an autoclave.

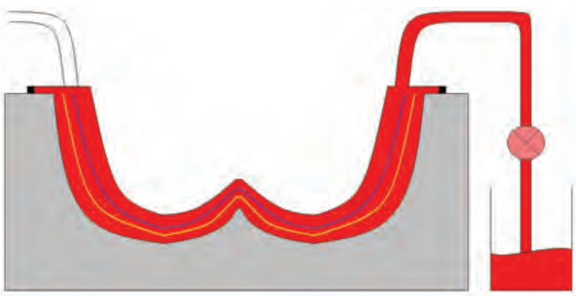

Figure 8 Vacuum injection

4.1 Life Cycle impact of composites

It is very well possible to recycle metal products and components. For fiber composite components this can be quite different. The extent to which fiber composites can be recycled depends greatly on the type of matrix material that is used. If thermoplastic matrix material is used the matrix material will have a melting temperature. This characteristic can be used to separate the matrix from the fibers. Thermosetting matrix materials have a non-reversible hardening process and heating above a certain temperature will make it disintegrate.
Unfortunately thermoplastics do not have high mechanical properties as do thermosetting materials making the thermosetting materials much more suitable for high performance components. Recent developments have made thermoplastics available with increasing mechanical properties.

5 APPLICATION OF PLASTICS AND COMPOSITES IN THE DREDGING INDUSTRY

The dredging industry has thus far been reluctant to the use of plastic materials, although there are some application of high performance composites and plastics in the dredging industry. For instance the composite jet pipes that were already shown in the beginning of this article, see Figure 1. The benefit of composite materials for this part lies in its lightweight structure and resistance to corrosion. There are also some applications of dredging pipes made from plastics which have reasonable wear resistance.

On the next pages three cases are illustrated where composite and plastic material can be used in the dredging industry and how it can lead to solutions not possible in steel.

6 THE LIGHTHOUSE

One of the most important components of the dredge system is the dredge pump. In many ships the IHC double walled pump is installed. The last year a new design for the outer casing of the double walled pump has been developed: the Lighthouse.

Double walled pumps are fitted with an external pump casing which allows the internal pump casing to be made in extra wear-resistant material. The outer pump casing serves as a support structure for the inner pump casing. This means a larger part of the inner casing is available as wear material. The outer casing also offers optimal security. In case of fracture of the internal pump housing, due to excessive wear or a sudden fracture, the outer housing prevents flooding of the pump room. To allow easy access to the wear parts inside the pump, the outer housing is split into two parts, see Figure 9; the cover plate and the outer casing.

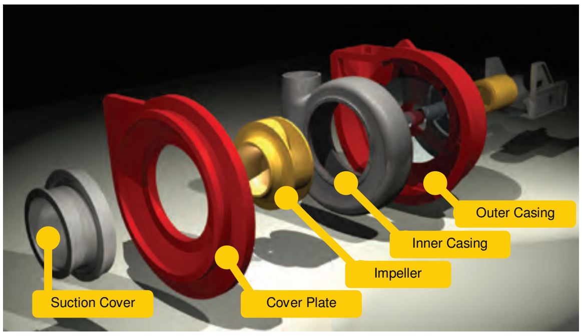

Figure 9 Definition of the parts in a double walled dredge pump

6.1 Objective

In project Lighthouse IHC did not look at the pump separately, but to the pump as a component of the dredging system in the ship. To get the ‘outside the box’ solutions, some challenging goals were set as depicted in Figure 10:

- Mass reduction of 50 % of the outer housing.
- Significant Reduction of build-in length.
- Significant Reduction of the replacement time of the wear parts.

For quantifying the goals and comparing different concepts, the design was based on the 262 pump. This pump has an impeller diameter of 2620 mm and is one of the largest pumps available, used in some of the jumbo hoppers in the world.

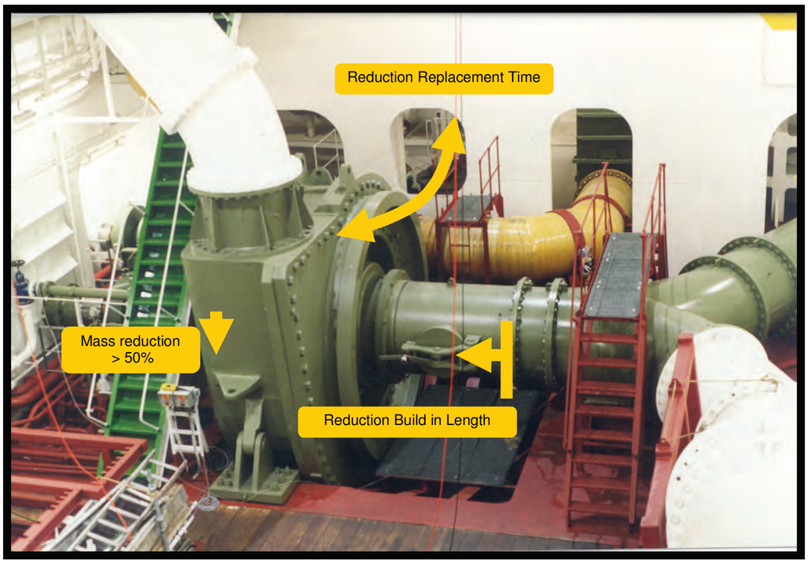

Figure 10 Goals of Lighthouse

Due to the functional split present in the current design of the pump, the outer housing does not have contact with the abrasive mixture. As discussed earlier these structural parts can also be made from fibre reinforced composites.

The different functions of the outer housing were defined as:

- *Providing access* to the wear parts
- *Supporting* the inner casing
- *Connecting* the two parts of the casing
- Watertight *sealing* of the outer casing parts

With these functions in mind several concepts were defined which were evaluated systematically. The result was a new design for a double walled dredge pump construction which was named the Lighthouse.

6.2 The Lighthouse Concept

In the new design the spiral shape of the pump is used for opening of the casing. This opening mechanism, as illustrated in Figure 11, reduces the number of bolts significantly. Therefore it is possible to open the case much more quickly. With the complete cover opening faster, the need for a separate suction cover is eliminated. This results in a reduction of the build in length and a further reduction of the mass. In the final design glass fibre is embedded in a thermosetting plastic. Some critical parts are additionally strengthened by carbon fibres.
In steel this design would not be possible, because the single part cover would be too heavy to handle efficiently and would require large and heavy lifting equipment inside the pump room.

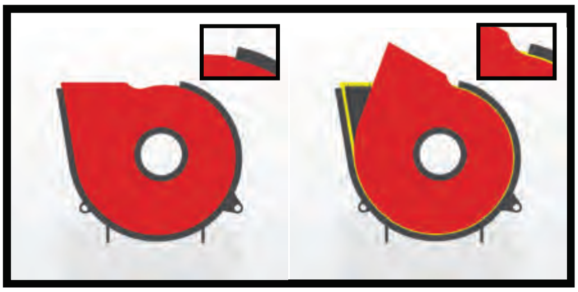

Figure 11; Spiral shape as a solution for opening

Figure 12; Impression of the LightHouse

Some sections of the housing are made in a sandwich construction with a very light core material, see Figure 13. This results in stiffness equal to the traditional steel housing. A special seal system is used to seal the two casing parts watertight. The advantage of this sealing mechanism is that no pre-tension is needed. The cover plate is guided by a support frame to ensure a correct alignment and to speed up the replacement time.

In this design a mass reduction for the outer housing of over 70% is accomplished. In addition both the build in length and the replacement time are reduced significantly. These advantages would not be possible without the use of fibre reinforced composites. For the lighthouse three patents are pending. Besides the spiral shape also the construction method used for the reinforced composite housing and the fibre reinforced cover plate are patented.

Due to the size and mass of the components a low temperature production process is desirable. To get a maximum quality out of the material, a process under vacuum conditions is the best choice. All processes need a mould. For these products a single sided mould will be sufficient. The mould material used must be able to cope with the process temperature, must be able to carry the material and must be unimpaired by the vacuum process. There are several production processes which meet these conditions of which the Pre-Preg or vacuum injection seem to be the best options. The connection with steel parts is done with several different types of inserts. A more detailed description of these production methods and the use of inserts are mentioned in the previous chapter discussing the production of composite components.

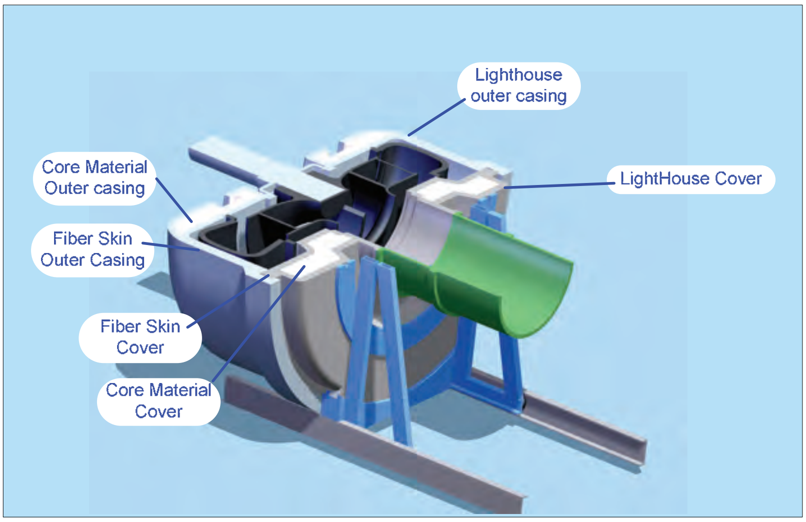

Figure 13; Crosssection of Lighthouse

Without fiber reinforced composites it would not be possible to create this much lighter pump with a shorter build in length and a shorter build in time. These improvements result in a gain of up-time and a gain in capacity. Requirements that ultimately lead to a substantial gain in overall output and, with that, a reduction of exploitation costs.

7 THE TELETUBE

The continuing desire to be able to dredge deeper is a recurring evolution that leads to pioneering development of on board equipment for trailer suction hopper dredgers. Dredging ships became bigger and longer and the depth dredgers can reach to, has been tripled over the last two decades. Not only became dredgers longer to be able to carry more load, but they also grew to be able to accommodate the long dredge installation that is needed for reaching these depths. There are even cases where dredging vessels are lengthened to carry a longer dredge installation. After all, the length of a dredge installation is directly linked to the space available on board of a dredger. There is a demand for dredge installations which can reach great depths, but still fits on the traditional dredging vessel without the need for lengthening the ship. This demand lead to the start of a project of designing a telescopically extendable suction tube: the Teletube.

7.1 Objective

With this project, IHC Merwede has set itself a high target when it comes to meeting the customers' demand. That demand characterizes the need to be able to dredge deeper at mostly specialized jobs without the need to lengthen the ship. The lengthening of a ship is a costly and drastic operation. The focus or this project was therefore on existing ships. To make such an operation attractive and competitive compared to the lengthening of the ship, the new design had to be a plug and play unit. The new design had to be able to fit on a ship with little or no changes required to the ship itself. This would dramatically reduce downtime compared to lengthening the ship and adding a longer conventional suction tube.

7.2 Systematic Analysis

Extensive and profound research has resulted in a number of concepts including a flexible suction tube, a hinged tube and a telescopically extendable tube. Further research proved a telescopically extendable tube, or TeleTube, to be the best competitor. Because of the difference between standard circumstances and the abrasive circumstances in a dredging environment, high demands were set to the suitability and the

durability of the new design. The wearing circumstances, the great forces and the functionality of an extendable system had to be fit in a design that is robust, durable, user friendly and exchangeable with the existing installation.
The new design had to fulfill the following three main functions:

- transportation of the mixture
- positioning of the draghead
- handling of the forces during the process.

In the current installation all these generic functions are all filled by the tube.

7.3 The Concept

For the new design the aforementioned functions are translated to different specific solutions. The function of transporting the mixture is now filled in by two suction tubes with a different diameter that can slide in and out of each other.
The function of handling the forces is filled in by two frames that also slide in and out of each other and which are positioned on and around the same axis as the suction tubes, see Figure 15. This decision was made to keep the new design as compact as possible.
The function of positioning the drag head and the linking of the drag head to the rest of the installation is also filled in by the frameworks.
To reach the goal of being able to position the drag head deeper a drive based on a winch has been developed. The hydraulically driven winch is directly connected to the frames and indirectly to the suction tubes. In between the frames a glider system has been engineered that makes the system slide in and out of each other. An additional advantage of this system is that the suction tubes can function as wear parts while the frame parts are the structural components.
The complete package results in a plug and play unit that is exchangeable with the existing suction tube that is positioned in between the drag head and the cardan. The only addition that has to be made to the ship is adding more cable length to cater for the extended depth.

Figure 14 Impression of the TeleTube

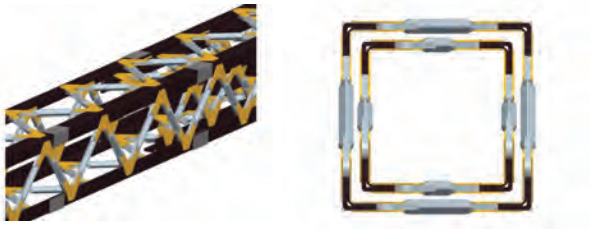

Figure 15; Close up view and cross sectional view of carbon fiber composite Teletube frame.

7.4 Using composite materials and other plastics

A phenomenon that often goes hand in hand with a separation of functions is the increasing of mass. Calculations showed that the new design would become too heavy when using steel compared to the original design of the dredge installation that it would replace. Creating a plug and play unit would not be possible in steel because of the much higher weight of the newly designed system. The only possible option would ne the use of composite and plastic parts.

The first step in achieving this result was realized by cutting the weight of the frame. By using reinforced composites, the required stiffness would be realized while keeping the weight of the frame acceptably low. This was done by designing the frame in reinforced carbon fiber which can be manufactured by vacuum injection.
The second step was to use plastic wear parts. Plastic with high wearing resistance usually has low specific strength. Due to the functional separation this would not be a problem for the Teletube since the suction tubes are not included in the interplay of forces and loads. Critical points and linked elements are made from steel to guarantee the durability of the Teletube and to cater for the possibility of mounting and demounting of the Teletube.

IHC Merwede has created a new alternative solution that can compete with the option to lengthen a ship. Because of the possibility to exchange the Teletube with the existing part of the dredge installation, without adjustments to the ship downtime and cost is reduced significantly.
Without the use of composite frame and plastic tube the Teletube would not be possible. The weight of the extendable installation in steel would exceed the conventional installation greatly. IHC Merwede has managed to achieve the highly set goals thanks to the use of composites instead of traditional steel.

8 PLASTIC SHEAVES

In the world of mobile cranes plastic sheaves have been successfully used for several decades, but for some reason the dredging industry has thus far been reluctant to use these sheaves.

In a crane the key advantages are the following:

- reduction of boom weight
- a significant increase in cable lifetime due to a more even distribution of the loads on a cable.

The above mentioned advantages are not big advantages in the dredging industry. The weight of the sheaves is not so much an issue and the cable in a dredging vessel is more harmed by corrosion because of the hostile environment than the wear on the sheaves.

Still, IHC P&S together with a strategic partner in engineering plastics decided to see if a plastic sheave could be used in the dredging world and what its advantages would be. The first question that needed to be answered was if it would be technically possible to use a plastic sheave in these harsh conditions.

The loads that the sheave has to withstand on a dredging vessel are well within the material limits. In the crane industry, the lifetime of the plastic sheaves is at least equal to the lifetime of the traditional steel sheaves.

8.1 Testing on a Beaver

Plastic sheaves become more cost effective if the mold can be used multiple times. For Beavers, IHC Merwede's standard series of cutter dredgers, the application of plastic sheaves looks promising. The first step is to test the plastic sheaves in practice on one of the new Beavers. The main question that needs to be answered is if the sheave can cope with the dredging environment. The question that needs to be answered is what the effect of sand will be on the lifetime of the sheave.

Figure 16 Plastic sheave on a beaver for testing

The sheaves on this new type of Beaver will have a diameter of about 450 mm. One advantage of the reduced weight is that the mounting of the sheaves is much easier because the sheaves can now be easily carried by just one man. At the time of writing this article the first Beaver equipped with plastic sheaves is starting its first trials.

Nylon sheaves can structurally very well replace the traditional steel sheaves. The main advantages of a plastic sheave will be the cost effectiveness on a dredging vessel.

9 CONCLUSIONS

Fiber composite products are widely used in several industries. The dredging industry is still reluctant to implement composite products. In this paper three possible applications of composite products for the dredging industry are discussed. The products discussed in the case here are examples which show that composite products can bring benefits to the dredging industry.

10 REFERENCES

Bugdayci, Ir. H.H.; ir. F.W.P. Smeets; LightHouse, the development of the next generation double-walled pumps, Ports & Dredging E168, IHC Merwede, Autumn 2007
A Beacon to aim for; Dredging and Port Contruction, P38-39, February 2008
Guide to composites; Gurit Services AG

CO_2 INDEX: MATCHING THE DREDGING INDUSTRIES NEEDS WITH IMO LEGISLATION

R.G. van de Ketterij[1], D.Stapersma[2], C.H.M.Kramers[3], L.T.G. Verheijen[4]

Abstract: The European Union (EU) has set very challenging targets for reduction of energy consumption and related emission of greenhouse gasses. This is one of the key drivers for the Maritime Environmental Protection Committee of IMO to develop measures to reduce the emission CO_2. One of the tools is the development of a CO_2 index as means to indicate the CO_2 emissions of merchant ships. This index was renamed at MEPC 58 into energy efficiency design index (EEDI).

IMO is forced to produce an integrated package of measurements to reduce CO_2 emissions from ships, including an operational index, a design index and a market-oriented tool imposing some sort of tax on CO_2 emissions. As a result of policy by EU an energy efficiency design index will become effective in short notice. This can be a derivative of the EEDI as proposed last year, but if IMO fails to produce and adopt regulation in 2009, EU will come up with her own index in short notice.

The effects of these developments are significant. In the near future shipowners will obtain limited CO_2 emission rights per annum, which will strongly decrease in time. Costs of acquiring emission are significant, effectively increasing fuel costs, and will progressively increase in time. It is also likely that EEDI will determine where and when dredgers are allowed to operate in the EU and other important dredging sites. An EEDI that reflects the actual fuel consumption by a dredging activity is therefore of the upmost importance.

The EEDI which is subject of discussion within IMO does not reflect energy consumption of most vessels that are being constructed in Western Europe in general and of dredging equipment in particular. Even worse, the EEDI may have a negative impact on attempts to improve energy efficiency onboard dredgers!

As a result of several efforts dredgers have been excluded from the EEDI during MEPC59 which is on the table at IMO. Moreover, the EEDI formulation underwent important changes. In this paper we first describe how an EEDI for dredgers may be built-up, based upon the actual energy consumption of most important consumers. The dredging cycle plays an important role in energy consumption. In the paper we will first describe the economic impact of CO_2 emission trade. Next we focus on the EEDI, explain the proposal of 2008, submitted during MEPC58 by IMO and our objections. We will also discuss the 2009 adoptions during MEPC59. We finally describe our proposal for a Trailing Suction Hopper Dredger specific EEDI, including a 'standard' dredging cycle that we propose to be used for comparison of the energy efficiency of different trailing suction hopper dredger designs. We aim at an EEDI that can be used by both builders and dredging companies.

Keywords: CO_2 index, levy, energy consumption, dredging cycle

[1] Manager Knowledge Development, MTI Holland B.V. Smitweg 6, Kinderdijk, 2961 AW, The Netherlands, T: +31 78 6910321, F: +31 78 6910331, E-mail: r.vandeketterij@mtiholland.com, www.mtiholland.com

[2] Professor – Delft University of Technology and Nederlandse Defensie Academie- Mekelweg 2 2628 CD Delft, the Netherlands, T: +31 – 0152783051, E-mail:D.Stapersma@wbmt.tudelft.nl

[3] Manager Product Development, IHC Dredgers B.V., Smitweg 6, Kinderdijk, 2961 AW, the Netherlands, T: +31 78 6910742, F: +31 78 6910331, E-mail: CHM.Kramers@ihcmerwede.com

[4] L.T.G. Verheijen – Manager Design and Cost Estimating Department - IHC Dredgers BV, P.O. Box 1, 2960 AA Kinderdijk, The Netherlands, T: +31-78-6910532, E-mail: ltg.verheijen@ihcmerwede.com

1 INTRODUCTION

1.1 BACKGROUND

At Kyoto governments of an important number of countries agreed to reduce CO_2 emissions significantly in the period up to 2010. These agreements where laid down in the Kyoto and Kyoto II agreements. However, shipping and aircraft where excluded from these agreements. At the Bali summit of 2007 governments agreed to include both shipping and aircraft during the Copenhagen summit in December 2009 (COP15 conference). This forced IMO into action and IMO started procedures to come up with an Energy Efficiency Design Index (CO_2 index) for ships. Such an index will probably be used by (port) authorities in the tender process for maintenance and land reclamation.

Irrespective of such an index and the consequences it may have for ships operations, the upcoming agreements from the COP15 conference will result in limited CO_2 emission rights for ship owners, and significant costs for excess of CO2 emission limits. These emission rights will be limited progressively in time. CO_2 emissions must be reduced by 20 % in 2020 with respect to the emissions in 1990. It is expected that emissions reduction targets for 2050 amount 50 %. It is therefore utmost important that the CO2 index calculated according to IMO norms correctly reflect the energy consumption and energy efficiency of out ships.

1.2 MARKET ORIENTED INSTRUMENTS

Basically two different instruments are possibly. Firstly, a trade system can be implied, enabling ship owners to trade in emission rights on the free market. The second instrument is a levy based system: shipowners have to pay a levy that is brought into a fund that will, hopefully, be used for initiatives to reduce CO_2 emissions.

Complicating factor is that both the Kyoto and the Bali agreements mention the "common but differentiated" principle. The agreements hold for both developed and developing countries, but the developed countries need to make more efforts than developing countries. This may work well in the industry, but in shipping industry such principle could easily lead ship-owners to sail under the flag of a developing country.

Costs involved with market based instruments are significant. Internet sites like the site of Pointcarbon (www.pointcarbon.com) provide a good overview of market prices of CO_2. On 13th of May, 2009 trading prices were 15.11 €/ton for December 2009, rising to 17.52 €/ton for December 2012. Forecasts for 2020 ranged from a high € 79/ ton last year to a low € 38 in May of this year (Source: Research group of 'Société Générale'). On average, about 3.1 tonne of CO_2 is emitted per ton fuel. Effectively fuel cost would therefore increase to 46.84 €/ton in December 2009, rising to 54.31 €/ton in December 2012, and to some €120/ton fuel in 2020.

Although trading prices decreased strongly over the last few months when less CO_2 was emitted due to the financial crisis it is to be expected that emission costs will rise sharply as soon as the world economy starts improving. We should therefore account for an effective fuel price increase of around 75 €/ton of fuel used in excess of the emission rights.

Figure 1: CO2 trading prices in Europe (Prices in Euro's / tonne. (Source: Pointcarbon: www.pointcarbon.com).

1.3 IMPACT ON OPERATING PERMISSIONS

More important than the cost impact is the decision of several authorities not to allow dredgers with insufficient energy efficiency. Both state and (private) port authorities like the Port of Rotterdam consider this option. Where the market based instruments 'only' influence cost price of dredging, this may severely jeopardize operability of the dredging fleet if the EEDI does not correctly represent actual energy consumption \.

2 EEDI PROPOSED BY IMO

2.1 PROPOSAL OF 2008, MEPC58

The formula below shows the EEDI index as proposed during the MEPC58 conference of IMO [IMO, 2008].

$$\frac{\left(\prod_{j=1}^{M} f_j\right)\left(\sum_{i=1}^{nME} SFC_{MEi} P_{MEi} C_{FMEi}\right) + P_{AE} C_{FAE} SFC_{AE} + \left(\sum_{i=1}^{nPTI} P_{PTi} - \sum_{i=1}^{nWHR} P_{WHRi}\right) C_{FAE} SFC_{AE} - \left(\sum_{i=1}^{neff} f_{eff} P_{eff} C_{Feff} SFC_{MEi}\right)}{Deadweight\, V_{ref}\ f_W}$$

where P_{AE} is the required auxiliary engine power, determined according to the following formula:

$$P_{AE(MCR_{ME}>10000\,\mathrm{kW})} = \left(0.025 \cdot \sum_{i=1}^{nME} MCR_{MEi}\right) + 250 \text{ if main engine power exceeds 10000 kW}$$

$$P_{AE(MCR_{ME}<10000\,\mathrm{kW})} = \left(0.05 \cdot \sum_{i=1}^{nME} MCR_{MEi}\right) \text{if main engine is below 10000 kW}$$

2.2 COMMENTS ON THIS FORMULA

The kernel of the formula is: $EEDI = \dfrac{\left(\sum_{i=1}^{nME} C_{FMEi} SFC_{MEI} P_{MEI}\right) + P_{AE} C_{FAE} SFC_{AE}}{Deadweight\, V_{ref}}$.

First of all, benefits of many ship types cannot be expressed in terms of speed and deadweight, simply because it is not the mission of these ships to transport weight from A to B, or to sail at a certain speed, or both. For ships like tugs or well intervention vessels, deadweight is not a measure for the profitability of the ship. Therefore, the formula does not distinguish between energetically ‘good’ and ‘bad’ ships. As a result the energy (CO_2-) index will not be the driver for reduction of the emissions of the ship. For a tug the product of bollard pull and free sailing speed could be a good term for the nominator (profit of the vessel).

The ’benefit to society’ of a dredger is loosening and horizontal transport of soil. The design index of a trailing suction hopper dredger (TSHD) could be calculated by above formula, but benefit to society is not reflected by the product of deadweight and reference speed. For a cutter suction dredger sailing speed is not a dominating design element: most CSD’s even don’t have a sailing speed. On most CSD’s deadweight is limited to fuel, lubricating oil, water and spare parts, and is not significant. With deadweight close to zero and sailing speed equal to zero, the EEDI would become infinitely high for this type of ship.

It is our firm believe that any CO_2 index described with the aim to facilitate reduction of the emissions of a ship type should have the ‘benefits to society’ for which this ship type has been developed as profit in the nominator. This has already led to separate formulation for passenger vessels and it should also lead to a separate formulation for specialized vessels such as dredgers, tugs and offshore supply vessels.

For many ship types activities other than sailing determine the proper functioning of the vessel. These other activities often require a significant part of the total energy consumption. An energy index based only on the free sailing power consumption can not distinguish either between ships that do fulfill these mission related activities energetically cheap and ships that don’t. For all these vessels implementation of mentioned energy index will not be a driver for optimization of the total ship. The attention on free sailing energy consumption is too high, and can even be at the expense of energy consumption at the other parts of the mission. This can lead to sub optimisation or even a deterioration of the overall energy consumption. As an example, for TSHD’s the formula neglects energy consumption during dredging and when discharging, so any attempt to decrease energy consumption of dredging equipment, increasing overall efficiency, is neglected.

A third objective considers the auxiliary power consumption. In the formula the auxiliary engine power is a function of main engine power only. Main auxiliary consumers, like dredge pumps, driven by small diesel engines will therefore not result in a higher EEDI. If same users were driven by an electromotor, fed by a shaft generator from one of the main engines, main engine power could increase (dependent on the main power balance of the ship). This increases the EEDI both by an increase of main engine power and by consequent increase of rated auxiliary engine power. A ship with diesel driven dredge pumps therefore has a much lower design index than an equivalent ship with electrical driven pumps, even if actual power consumption of the latter is lower.

We observed large variations may occur in EEDI’s between TSHD’s with equivalent deadweight (see figure 2). As (port) authorities might consider the EEDI of dredgers in the tendering phase, this would be totally unacceptable for the dredging industry.

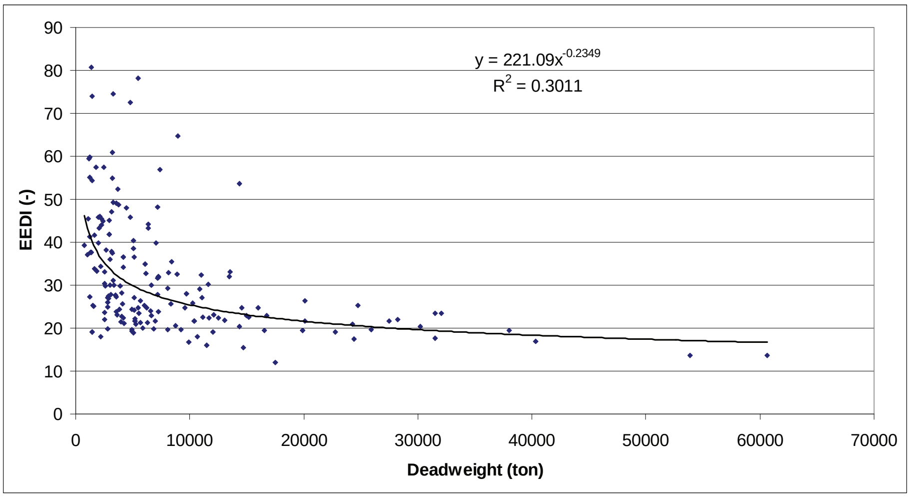

Figure 2: Energy Efficiency Design Index of 178 TSHD's calculated using the formula of MEPC58

Fortunately, dredging industry is not the only stakeholder having objectives to the index. Tug owners, offshore companies, and many stakeholders owning special vessels objected to some or more parts of the EEDI. The Netherlands expressed these worries in a document presented at the MEPC59 conference in April this year [Anink, 2009]. Anink analysed 1150 ships built in the Netherlands between 1978 and 2008, and came to worrying conclusions, especially for ships with deadweight below 15000 ton deadweight (roughly equivalent to 10,000 m^3 of hopper volume).

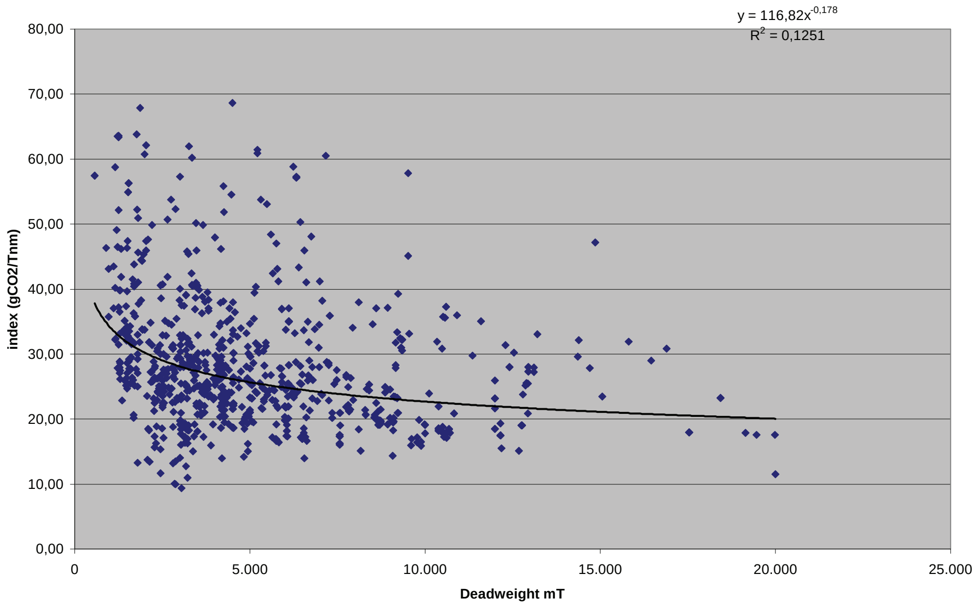

Figure 3: EEDI of ships built in the Netherlands between 1978 and 2008 [Anink, 2009].

2.3 PROPOSAL FOR 2009, MEPC59

At the MEPC59 conference member states recognised the deficiencies in the formula and the fact of a single formula for all vessel types and sizes being impossible. The formula was restricted to a limited number of ship types (excluding dredgers) and ship sizes, excluding ships smaller than 15000 tons deadweight. Moreover, the formula itself was adopted, accounting for visions as laid down above.

Auxiliary power (P_{AE}) is now defined as the required auxiliary engine power to supply normal maximum sea load including necessary power to supply power for machinery, systems, equipment and living on board when the ship is engaged in a voyage at the design speed under the design loading condition. Any power needed for thrusters only used to manoeuvre in port, cargo gear, cargo pumps, ballast pumps etc. as well as power to sustain cargo is excluded from the 2.5 % P_{ME} +250 / 5 % P_{ME} rule and should be accounted for separately.

This gives the dredging industry the opportunity to come up with an energy efficiency design index for our own ships. Such an EEDI proposed by the dredging industry should provide a practical performance indicator that rewards environmentally friendly dredging.

3 ENERGY CONSUMPTION OF A TRAILING SUCTION HOPPER DREDGER

The CO2 index of ships is based on the energy index, which has been introduced by Gabrielli and von Karman [Gabrielli, 1950], in a famous article. In this article they compared power consumption of various transport means, made dimensionless by dividing it by the transport capacity (see also figure 4). The latter was expressed as the product of weight and speed: $I = \frac{P}{w \cdot v}$.

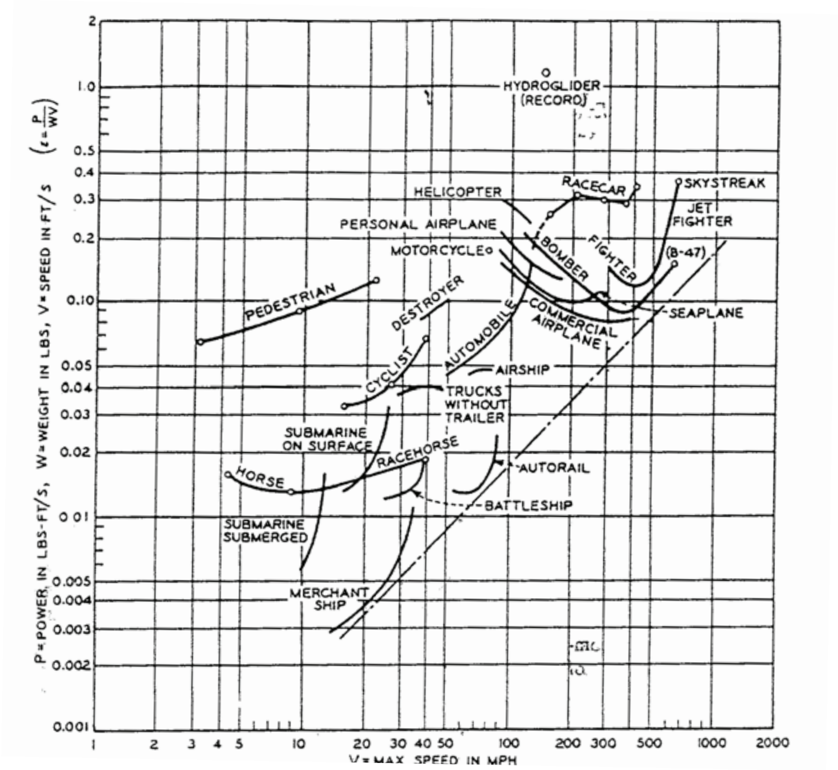

Figure 4: power consumption of various transport means (taken from [Gabrielli, 1950]).

When multiplying power consumption with a specific CO2 emission per produced KWh, we obtain a CO_2 index. We follow the calculation methods of IMO to arrive from power consumption to CO2 emissions. We focus on the determination of the energy consumption, i.e. the power terms. We do not focus on correction factors for ice reinforcements. The proposal for calculation of the auxiliary by MEPC59 is acceptable for us, so we do not further elaborate on auxiliary power consumption in this paper.

The mission of a TSHD, is to transport soil horizontally. This transport is effectuated in four phases.

1. Sailing empty to the winning location
2. Dredging
3. Sailing fully laden to the discharge location
4. Discharging

Here we neglect manoeuvring, still laying etc.

Energy consumption of each phase is of the same order of magnitude. When discharging energy consumption depends largely on the discharge method. When discharging by rainbowing or shore pumping, energy consumption is of the same order of magnitude as during free sailing. When dumping through the bottom doors, energy consumption is almost negligible.

In order to capture the entire dredging process in the energy index, energy consumption of all four phases of the dredging cycle should be incorporated; herewith we obtain a technical-operational index.

$$E_{tot} = \left[P_{empty} \cdot t_{empty} + P_{dredging} \cdot t_{dredging} + P_{full} \cdot t_{full} + P_{disch} \cdot t_{disch} \right] \Big/ 3600 \, .$$

We propose to only consider power required for driving the propellers, dredge pumps, jet pumps and hydraulic pumps (used for the ships hydraulics: this can be a significant portion). For use in the energy index, we return to a power term (as used in the MEPC proposals) by division with the Total time required for the dredging cycle, where: $t_{cycle} = t_{empty} + t_{dredge} + t_{full} + t_{disch}$

A simple summation of the energy-index of all four individual phases, normalized by division with the total cycle time, won't work. During dredging and discharging sailing speed is very low. Division with the sailing speed of these terms leads to a strong overestimation of the contribution of these parts of the cycle to the total energy index.

The energy index is then described by formula below:

$$I_{TSHD} = \frac{P_{empty} \cdot \frac{t_{empty}}{t_{cycle}} + P_{dredging} \cdot \frac{t_{dredging}}{t_{cycle}} + P_{full} \cdot \frac{t_{full}}{t_{cycle}} + P_{discharge} \cdot \frac{t_{discharge}}{t_{cycle}}}{DWT \cdot g \cdot v_{dr}}.$$

The only question that needs to be answered is how to define the speed *v*.

We propose to define this speed (in m/s) as sailing distance full divided by cycle time: $v_{dr} = \frac{a_{full}}{t_{cycle}}$. This is the purest representation of the ships' mission (horizontal transport of soil). We neglect the distance traveled during dredging , as sailing a certain distance during dredging is generally not part of the ships' mission. On the other hand, time required for dredging and discharging does influence the overall capacity, and therefore should be taken into consideration.

Mentioned energy index represents according to us an objective measurement to determine the energy efficiency of different TSHD's for a given dredge job.

By using a standardized dredge cycle, a comparison of the energy efficiency of different dredgers can be made, but this does not say much about the energy efficiency for a specific dredge job, as optimum sailing speed and dredging output varies with sailing distance and discharge method.

Further elaboration to a CO2 index can be done in the same way as with conventional ships. Concluding we come to the following EEDI for dredgers:

$$\frac{\left(\sum_{i=1}^{nMEDr} C_{FMEDri} SFC_{MEDri} P_{MEDri}\right)_{empty} \cdot \frac{t_{empty}}{t_{cycle}} + \left(\sum_{i=1}^{nMEDr} C_{FMEDri} SFC_{MEDri} P_{MEDri}\right)_{dredging} \cdot \frac{t_{dredging}}{t_{cycle}}}{DWT \cdot g \cdot v_{dr}} +$$

$$\frac{\left(\sum_{i=1}^{nMEDr} C_{FMEDri} SFC_{MEDri} P_{MEDri}\right)_{full} \cdot \frac{t_{full}}{t_{cycle}} + \left(\sum_{i=1}^{nMEDr} C_{FMEDri} SFC_{MEDri} P_{MEDri}\right)_{disch} \cdot \frac{t_{disch}}{t_{cycle}}}{DWT \cdot g \cdot v_{dr}} +$$

$$\frac{P_{AE} C_{FAE} SFC_{AE} + \left(\sum_{i=1}^{nPTI} P_{PTi} - \sum_{i=1}^{nWHR} P_{WHRi}\right) C_{FAE} SFC_{AE} - \left(\sum_{i=1}^{neff} f_{eff} P_{eff} C_{Feff} SFC_{MEi}\right)}{DWT \cdot g \cdot v_{dr}}$$

4 PROPOSAL FOR A STANDARD DREDGING CYCLE

Dredging cycles vary enormously. Therefore, we should agree on some sort of standard dredging cycle, we consider typical. We should discuss the following factors:

- Soil type
- Dredging depth
- Sailing distance
- Discharge distance when shore pumping
- Breakdown into dumping, rainbowing and shore pumping
- Times to be used in the dredging cycle

Soil type

As soil type we propose medium fine sand, as defined by table 1. This sand is sufficiently fine to show differences between ships where overflow design and lay-out of loading boxes has been well designed to decrease overflow losses, improving the dredging performance, and ships where these investments have not been made. Also, this soil type has been used in the specifications of many ships.

D_0	D_{10}	D_{20}	D_{30}	D_{40}	D_{50}	D_{60}	D_{70}	D_{80}	D_{90}	D_{100}
0.400	0.307	0.283	0.261	0.244	0.232	0.221	0.209	0.197	0.171	0.090

Table 1: grain size distribution of medium fine sand

Dredging depth

We have two considerations to calculate the dredging depth. First of all the dredging depth that should not become too deep, so it can be reached by the vast majority of vessels. The dredging depth should also be sufficient to highlight the improved dredging performance that is obtained by the use of a submerged pump. We would therefore propose a dredging depth of 25 meters. Ships that can not reach this depth should use a calculative figure: as if they were dredging at 25 meter water depth. Calculation method can be verified at maximum dredging depth of said vessel.

Sailing distance

We propose to take as sailing distance the distance the ship can sail in one hour, when fully loaded in deep water with a smooth surface (wind force less than 2 Beaufort).

Discharge distance

Some ships do not have the possibility to discharge either by rainbowing or by pumping ashore. The EEDI of these ships could be calculated either by removing the terms related to shore pumping / rainbowing or by using a theoretical figure.

As shore pumping or rainbowing requires a lot of energy, disregarding these discharge options would have a disproportional beneficial effect on these ships. We therefore propose to use a calculative figure for ships without a shore pump / rainbow possibility, based upon the following basic principles.

- Discharge time shore pumping: 60 minutes
- Discharge time rainbowing: 50 minutes
- Power consumption dredge pump in both cases: maximum power on the pump shaft
- Power consumption jet pump in both cases: maximum power on the pump shaft
- Power to the propellers: 10 % of maximum power on the propeller shaft

If a ship has shore pumping facilities we propose a discharge pipe length of 1000 meter.

Breakdown into dumping, rainbowing and shore pumping

Dredge operators typically attempt to continue discharging via the bottom doors as long as possible. After that they continue discharging by rainbowing, which takes more time and energy. Only when rainbowing is not possible anymore, dredge operators will continue rainbowing.

We therefore propose the following breakdown:

- Dumping: 50 %
- Rainbowing: 30 %
- Shore pumping: 20 %

Times to be used in the dredging cycle

We consider the following parts of the dredging cycle:

- Sailing fully loaded to the discharge location
- Discharging
- Sailing empty to the dredging location
- Dredging

This ignores time to manoeuvre into position, for connecting to a discharge pipe, and waiting time to pass crowded areas, locks etc. We propose to ignore these activities in the standard dredging cycle for the design index, as they are dominated by operational conditions and do not require significant amounts of energy.Table 2 lists proposed time required for the different parts of the dredging cycle.

Cycle part	Time required
Sailing fully loaded	1 hour
Discharging: dumping	10 minutes
Discharging: rainbowing	Calculated figure*
Discharging: shore pumping	Calculated figure**
Sailing empty	Calculated figure***
Dredging to maximum draught	Calculated figure****

Table 2: time required for the different parts of the dredging cycle

* When no rainbowing installation is available, we propose to use 50 minutes

** Assumptions: maximum available power to the dredge pump, with 10 % of the maximum propulsion power in spare for propulsion, at a discharge distance of 1000 meter

*** Sailing distance: equal to sailing distance fully loaded

**** Assumptions: stores sufficient for one week operation, and no spare parts on board

5 CONCLUSIONS

The paper discusses two ways in which authorities will attempt to reduce the energy consumption of dredgers. The market based instruments will very likely be applied on all ship types, raising serious financial implications. IMO attempts to define an index that indicates the energy efficiency of ships. It is important that such an index correctly reflects energy efficiency as (port) authorities will use such index for harbour dues etc. The original formula proposed by IMO had important deficiencies for smaller ships in general and special ships such as dredgers in particular. The new IMO proposal overcomes part of these shortcomings. Moreover, the IMO proposal will only apply for a limited set of large ships, leaving space for the dredging industry to define an index for dredgers.

A CO_2 index for dredgers should correctly reflect social benefit, and the costs in terms of power cosumption required to attain this social benefit. For a trailing suction hopper dredger this means that all parts of the dredging cycle have to be considered separately. Moreover, the dredging industry has to decide on a 'standard' dredging cycle to calculate the CO_2 index upon. To start the discussion we defined a possible standard dredging cycle.

6 LIST OF SYMBOLS

P_{MEi}	= 75 % of the MCR of main engine	[kW]
P_{empty}	= propulsion power consumption sailing empty to the winning location	[kW]
P_{full}	= propulsion power consumption sailing loaded to the discharge location	[kW]
P_{dredge}	= power consumption of dredging related components, including propulsion power, during dredging	[kW]
$P_{discharge}$	= power consumption dredging related components, including propulsion power, during discharging	[kW]
P_{MEDr}	= Power consumption of each consumer required for the dredging process, including dredge pumps, jet pumps, propulsion, bow thruster, hydraulics etc. required from the main diesel engine, including losses of gear box, transmission from mechanical to electrical energy	[Kw]
SFC_{MEDri}	= Specific fuel consumption of each engine at 90 % MCR	[g / kWh]
$_{empty}$	= time required to sail empty to the winning location	[s]
t_{full}	= time required to sail loaded to the discharge location	[s]
t_{dredge}	= time required for dredging	[s]
t_{disch}	= time required to discharge	[s]
t_{cycle}	= time required for the dredging cycle	[s]
E_{tot}	= total energy consumption	[kWh]
I_{TSHD}	= energy index trailing suction hopper dredger	[-]
DWT	= deadweight	[ton]
g	= gravitational acceleration	[m/s^2]
a_{full}	= sailing distance fully loaded	[m]
v_{dr}	= reference speed TSHD	[m/s]
f_j	= corrections to account for ship specific design elements (such as ice class)	[-]
C_F	= conversion factor between fuel consumption and CO2 emission	[-]
SFC	specific fuel consumption at 75 % of the rated installed power (MCR)	[g/kWh]
nME	= number of main engines *i*	[-]
f_w	= coefficient to account for the decrease of speed in representative sea conditions	[-]
P_{WHR}	= rated electrical power generation of waste heat recovery system at P_{Mei}	[kW]
P_{Pti}	75 % of the rated power consumption of shaft motors	[kW]
P_{eff}	main engine power reduction due to innovative energy efficient technology	[kW]
P_{AE}	required auxiliary engine power	[kW]
D	grain diameter	[mm]

Subscripts are defined as follows:

ME	main engine
AE	auxiliary engine
ref	reference

7 REFERENCES

Anink, 2009 **D.Anink, and M. Krikke** "The IMO Energy Efficiency Design Index A Netherlands Trend Study", report nr. 3064 of the Centre for Maritime Technology and Innovation", Zoetermeer, January 7th, 2009.

Gabrielli, 1950 **G, Gabrielli and T. von Karman**, 'What price speed? Specific power required for propulsion of vehicles', Mechanical Engineering, ASME, Volume 72, Number 10, (1950), p775–781

IMO, 2008 **IMO** circular MEPC/58 WP.8 "Prevention of air pollution from ships", Report of the Working Group on Greenhouse Gas Emissions from Ships, London, October 9th, 2008

IMO, 2009 **IMO** circular MEPC/59 "Prevention of air pollution from ships", Report of the Working Group on Greenhouse Gas Emissions from Ships, London, February 2009, Annexes A and B.

PHOSPORITE MINING: A BRIDGE BETWEEN DREDGING AND DEEP SEA MINING

L.J. de Jonge[1]; B. Hogeweg[2]

Abstract: This paper discusses the proposition:

The dredging industry cluster has all opportunities (with their knowledge on soil/rock excavation and vertical transportation) to become an essential partner for the offshore/deep sea mining industry and boost its development by offering and creating the essential crossovers in technology and establish crossover industry consortiums.

A new wave of attention for deep sea resources has arisen in the last decade, mainly for SMS, phosphorites and Methane Hydrates deposits. Due to technical, economical, legislation and environmental developments this new attention opens up the prospects as never before. However the offshore/deep sea mining industry is not yet a matured and fully developed industry. No matured centre players can be identified, although key candidates can be found in the offshore oil and gas industry or the mining industry. In these two industries players with the right volume, turnover, and processing and distribution channels are present. The dredging industry, both in technology and equipment as well as contractor partners, can become essential players in this industry.

Keywords: deep sea mining, offshore mining, remotely operated vehicles, energy

1 Technical Manager, IHC Merwede Deep Sea Dredging & Mining, Smitweg 6. Kinderdijk, 2961 AW, The Netherlands, T: +31 78 6910911; Email: lj.dejonge@ihcmerwede.com; www.ihcmerwede.com.

2 Mining Consultant, Dredging Advisory Services, MTI Holland, Smitweg 6. Kinderdijk, 2961 AW, The Netherlands, T: +31 78 6910911; Email: b.hogeweg@mtiholland.com; www.mtiholland.com.

1 OFFSHORE DEEP SEA MINING: OPPORTUNITIES FOR THE DREDGING INDUSTRY

In the world's seas and oceans a vast potential of mineral and energy resources is available. The mineral resources range from diamonds on the beaches of Namibia to manganese nodules at 4000+m water depth. In between there is aggregates, phosphorites, manganese crusts, SMS (Seafloor Massive Sulphides) and many yet unknown deposits. Gas hydrates on the seafloor form a huge potential energy source, if retracting methods can be found.

Up until now the exploration of these resources has been limited, with barriers on technical, economical, legislation and environmental aspects. In many of these aspects new developments and improvements have been made. Found difficulties are the diversity of the resources, soil and rock behaviour, the local environment and remote locations. For each deposit a specific technical and logistical approach is required.

Another barrier is that the offshore/deep sea mining industry has not yet matured into a fully developed industry segment. Missing in the centre are full grown offshore/deep sea mining companies, with the know-how and helicopter view to oversee all above aspects of offshore/deep sea mining. In a circle around these companies the chain of specific equipment suppliers, specific contractors and other supporting companies are not yet fully focused on the opportunities offered.

Clear candidates for the centre position should be found in the offshore oil & gas and the mining industries. The oil & gas industry can offer a lot of technology and development power, however it is mainly focused on the vertical, drilling, approach and on the distribution of energy resources. The mining industries can offer processing and distribution channels for the mineral resources but their main focus is on onshore technology and developments; their specific offshore knowledge is limited.

The obvious gap exists in the steps from subsea extraction to transport towards the onshore destination. These are typical aspects that have close relation to dredging: cutting, gathering, vertical transport and horizontal transport of material in large volumes. In the complete chain of steps these cannot be seen independent of other aspects that are offered by the offshore and mining industries: material processing, deepwater technology, handling equipment, transport logistics, distribution channels etc.

In this exciting, challenging and highly innovative world of offshore/deep sea mining there are still many challenges, but it is clear that there can be important roles for the dredging industry cluster:

- Supplier of know-how and experience in
    - project and process development
    - large volume cutting and pumping
    - dredging technology
- Supplier of equipment
- (Sub)Contractor in mining operations
- Or even as an independent mining company

This leads to the following proposition, focusing on the technological aspects:

> *The dredging industry cluster has all opportunities (with their knowledge on soil/rock excavation and vertical transportation) to become an essential partner for the offshore/deep sea mining industry and boost its development by offering and creating the essential crossovers in technology and establish crossover industry consortiums.*

In this paper this proposition will be explored by looking what the offshore/deep sea mining industry is requesting, what the dredging industry can offer and which steps can be taken towards boosting offshore/deep sea mining towards a mature industry in which the dredging cluster has an important role.

As a case study phosphorite mining offshore Namibia will be discussed since this is a good example where all the challenges seem to be within reach, but are not yet fully developed.

2 FUTURE RESOURCES: THE POTENTIAL IN THE DEEP SEA

The mining industry will be most interested in the mining potential that can be found all over the world and the fact that major resources of aggregates, copper, zinc and tin are abundant. In the majority of these deposits, traces of gold, silver and other precious metals are found, significantly adding value to these deposits. Phosphorites, important for fertilizer production, are also abundant in many areas in the world, as they are deposited on the seafloor on the margins of the continental shelf.

The oil & gas industry will be mainly interested in the gas methane hydrates. These are potentially one of the largest energy resources in the world. There are estimates that these hydrates hold enough methane to cover the world's energy needs for the next 1500 years.

Definition of deep

The definition of deep differs for the various industries and applications, for example:

- Offshore drilling and pipe laying industry: 3 km barrier is in sight
- Offshore installations: 2 km water depth are no exception
- Pipe burial: 2 km can be done
- Rock dumping: 1 km (Beginning of 2011: up to 2 km)

For dredging with conventional equipment:

- Sand/aggregates dredging with TSHD (Trailing Suction Hopper Dredger): 150m
- Rock dredging with CSD (Cutter Suction Dredger): 50m

From this perspective a depth of 200-300m for offshore/deep sea mining can already be considered deep, since no conventional dredge equipment can be used.

Important progress in preconditions

Important steps for the creation of legislation handling the rights of the deep sea have been the signing (1982) of the United Nations Convention on the Law of the Sea (UNCLOS) and the establishment (1994) of the International Seabed Authority, with responsibility for controlling all deep sea mining in international sea waters. The first legislative achievement of this intergovernmental organization was the adoption (2000) of regulations for prospecting and exploration for polymetallic nodules.

Another important step has been the establishment and recognition of EEZ (Exclusive Economical Zone) areas, which clarifies the ownership of resources within the 200 mile zone of the coast. As a side-effect however international ownership disputes have arisen around rocks and atolls in the oceans, where the potential resources are the treasure to be hunted, as has happened for instance in the Indian Ocean. The recent muscle play around the North Pole is another example.

Figure 1 shows the oceans potential as a resource base for minerals. The map also shows the proximity of the majority of the deposits to continents, making part of the adjacent country's EEZ.

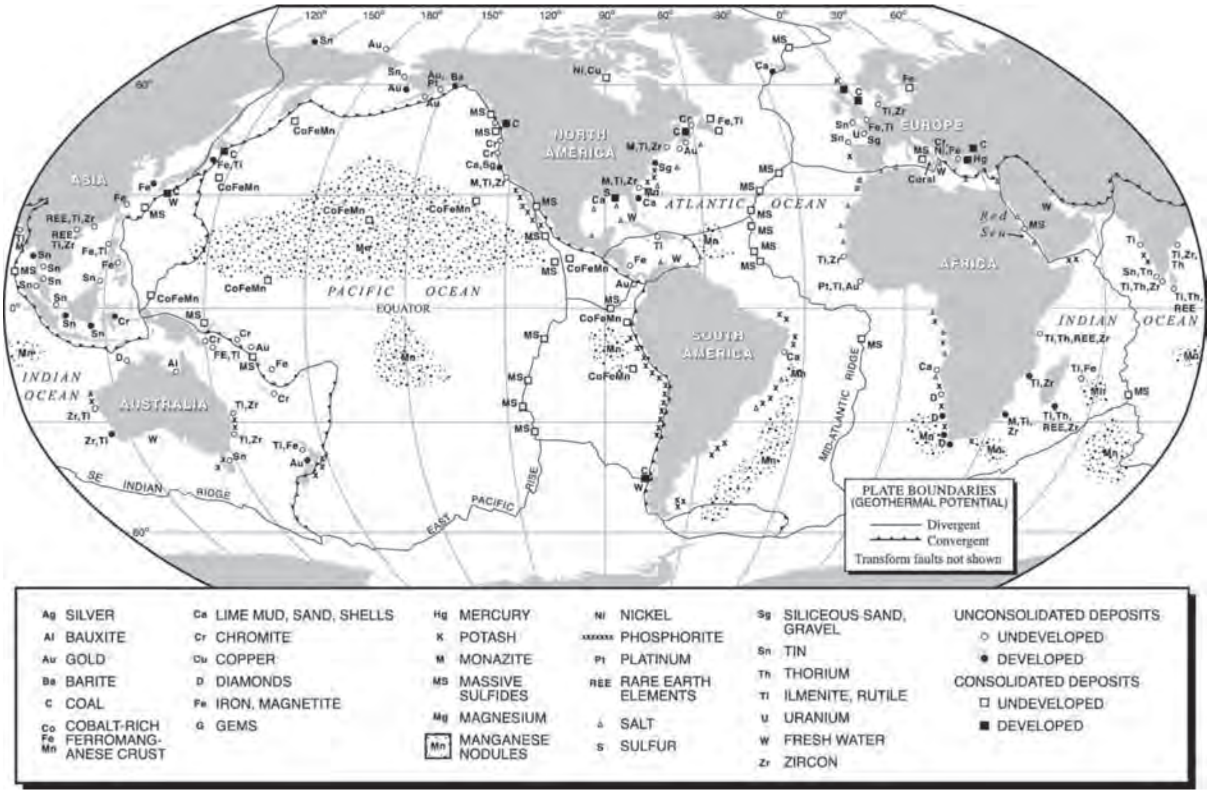

Figure 1: Overview of offshore mineral deposits (Rona 2008).

Examples of current offshore mining activities that have proven to be technical and economical feasible are, but not limited to:

1. **Marine aggregates dredging**,
   In the Channel and the North Sea by DEME (DBM) and HANSON Aggregates.
   For instance with TSHDs to a maximum of 60m (potentially 150m). Processing/sizing on board with fixed screening. Figure 2 shows an example of a gravel dredger.
2. **Tin dredging**,
   By PT Timah in Indonesia.
   With large bucket ladder dredgers to 50m, also resources at larger depths On board processing plant. An example is shown in figure 3.
3. **Offshore Diamond mining**,
   By De Beers Marine offshore Namibia and South Africa.
   With Remotely Operated Vehicles (ROV) or Subsea Dredge Crawlers to a maximum of 150m (potential of ROV 250m, resources go to 500+m). On board processing only, tailings go directly overboard, only diamonds are shipped.

Figure 2: DBM's Charlemagne, gravel hopper dredger, mining aggregates on the North Sea.

Figure 3: A bucket ladder dredger with on-board processing plant, owned and operated by PT Timah, offshore Indonesia.

All activities at this moment are within the normal reach of conventional dredging equipment. However here already specialized equipment is used which shows an important aspect of mining: the specific conditions of the deposit like the soil and sea conditions, and the need for processing, require specialized equipment. This will be discussed in the next paragraph.

Most promising deposits
Besides the already mentioned deposits of diamonds, tin and aggregates, the most promising deposits are:

1. **Phosphorites**
   a. Typical water depth 300-500m (some less concentrated at 150m)
   b. Different types consisting of soft layers a few meters thick to harder materials in the form of loose rock.
   c. Basis for fertilizer which is a strategic resource.
   d. Important are transport distances to processing factories, depending on distance, offshore offloading required.
   e. Processing/Improvement of material on board limits transport of less concentrated material
2. **Seafloor Massive Sulphides**
   a. Typical water depth 1500-2500m
   b. Deposits build up in chimneys by volcanic activity on the edges of tectonic plates, rich of copper, zinc, traces of gold and many other metals.
   c. Hard to very hard material (5-40MPa on the surface), rough bottom surface and slopes.
   d. Potentially all over the world, individual areas can be enough for more than 10 years of mining.
   e. Hyperbaric effects in rock cutting, all material to be cut.
   f. Processing on the surface limited, to be kept wet during transport to prevent degrading through oxidation
   g. FPSO (Floating Production Storage and Offloading facility) like offloading required for horizontal transport.
3. **Gas Methane Hydrates**
   a. Typical from 425 to 2000+ m
   b. Exceeding all other carbon based energy resources seen as the fuel of the future.
   c. Methane trapped in ice crystal like structures, in meters thick layers on most ocean seafloors.
   d. Relatively soft material, that needs to be kept under pressure, to prevent the uncontrolled escape of the methane into the atmosphere. Methane is at least an order of magnitude more effective as a short-term greenhouse gas than carbon dioxide.
   e. FPSO like systems with Offshore Oil & Gas restrictions and rules

3 CAN THE NEW MINERAL RUSH BE JUSTIFIED?

Several enthusiastic “mineral rushes” have been flowing through the marine and mining industry. Best known is the quest for manganese nodules in the sixties and seventies. Although attracted by the seemingly “golden” opportunities, in most cases the enthusiasm ceased because of barriers on technical, economical, legislation and environmental aspects.

It cannot be ignored that the deep sea still forms a very challenging and in many ways unknown environment with its depth, the pressure and the impossibility for local presence for operation and control.

What new developments would justify this new surge to go for mining in the deep sea?

Legislation (UNCLOS):
The United Nations Convention on the Law of the Sea and the definition of the EEZ areas define the rights for countries and provides a legal basis.

Economics:
Energy and base metal prices have risen over the past decades and demand is expected to continue to increase when China and India will continue their economic growth. Although the current economic crisis is now disturbing this growth, the tendency over the last decade still shows an incline. Figure 4 shows the ten year price graph for copper, demonstrating this tendency.

Figure 4: A 10 year price graph for copper, showing the current positive trend.

Environmental:
In the present, the environmental aspect could be an even more important aspect than in the past. It is governed not only rational decision, but also very strongly controlled by politics. The cradle to cradle principles can act as an interesting benchmark for comparison of offshore/deep sea mining with conventional mining practices. Some advantages:

- Floating mine equipment can be refurbished and used all over the world
- Limited overburden, most deposits on surface,
    - no energy required to move useless material
    - Limited impact on direct surroundings
- Direct loading in transport medium that can be transported all over the world

Technological steps:
Two main development paths are leading the way for offshore/deep sea mining: the huge steps in computer technology and the move to deeper waters by the Offshore Oil & Gas, actually paving the path. These have led to improvement and development of:

- Automation, control and remote control
- Surveying techniques
- Remotely operated vehicles
- New materials

- Development of deep sea auxiliary

Development of dredging industry

The dredging industry matured in the last decades and is willing to adapt new technologies:

- New technology can create new opportunities and markets, examples of the past
    - Submerged motor → deeper operation possible
    - Scale increase, certainly in TSHDs → made land reclamation profitable
    - Flexible spuds → better behaviour in waves for CSDs gives an increased availability
- Huge increase in level of automation and information technology has improved the knowledge and quality of dredging
- Search for greater depths >150m

Mature supporting shell of companies

The outer shell of supporting and supplying industries to the Oil & Gas offshore industry is already used to going to greater depth, a focus towards mining and dredging required.

The steps made in the paste decades have proven that with dedication and of course a lot of investments, slowly, but steadily the deep sea is being explored. However for offshore/deep sea mining there are still some specific challenges left.

4 EXCITING TECHNOLOGICAL CHALLENGES

A lot of technology can be borrowed or adapted from the offshore industry. Pipe burial with crawlers and ploughs to 2000m is already common practice. An example is shown in figure 5. Top side equipment is also available, in the form of launch and recovery systems, umbilical winches, heave compensations etc. Figure 6 shows a handling winch system for deep sea equipment. On component level there are some new requirements but those should be left with the specialists in the market.

Figure 5: Deep sea plough for pipe burial.

Figure 6: Handling system for deep sea equipment.

Focus for the dredging industry should be on the key issues that are vital for the development of deep sea mining equipment:

1. Cutting of soil and rock - with special attention to hyperbaric effects on rock
2. Vertical transport - critical process and largest energy consumer

Both act in high volumes. Along with these two key issues, two other issues evolve:

3. Integral system design - system architect
4. Energy supply - generation, transport and transformation

Separation of functions

The separation of functions opens a range of possibilities for the development and application of new dredge mining equipment. Conventional dredging equipment is limited to depth and working in swell and waves: TSHD (150-200m), CSD (50m). Dynamic limitations are mainly due to the rigid connections between the supporting vessel and the seafloor dredging tool (draghead or cutter). To overcome these limitations more flexible connections are required.

Cutting of soil and rock
The cutting of soil is where it all starts: what is not coming in cannot come out. Only material that is loosened, gathered and slurryfied can be transported to the surface. The efficiency of these processes will determine the output of the system. At a first glance, for a lot of soil types this looks much the same as for conventional dredging. However there are some typical aspects:

- The seafloor dredging tool has a flexible connection with the support vessel and is limited in size and weight
- Cutting forces are limited to the maximal transfer of forces by the seafloor dredging tool
- Bearing capacity of the seafloor is limited by the weight of the used tool.
- Local propulsion capabilities determine the propulsion speed
- Production depends on the soil or rock and can be limited by cutting capabilities or by the volume the seafloor dredging tool can cover. This volume is determined by the cutting profile (cutting height and width) and the area that can be excavated per hour

In loose and soft soils the propulsion will be a limiting factor, in hard soils the actual cutting forces will be the limiting factor. Each deposit must be evaluated for its soil and rock characteristics, proposed mining plan and the production requirements. It is clear that many parameters determine the requirements and layout of the total system.

Phosphorites and gas hydrates are relatively soft and might have layers were erosion through suction is enough, but propulsion and transfer of forces however might be the determining factor through their different bearing capacities. Gas hydrates on the other hand may become unstable and release their methane uncontrolled.

A different order is the cutting power required for SMS material. Cutting under hyperbaric conditions at 1500-2500m can make rock ductile, requiring an increase in cutting power and energy. Production per unit could decrease significantly.

IHC Merwede is carrying out a research program in which this hyperbaric rock cutting process is investigated. Significant results are being collected with cutting tests in hyperbaric tanks. These will be evaluated and compared with numerical models. Understanding this process is essential for further development of offshore deep sea mining activities, certainly in SMS material.

Vertical transport
Another important issue is the vertical transport of multiphase fluidums (gas, slurry, solids) to the surface. Of course this is depending on depth and on the required production. Mining phosphorites is probably the closest to state of art dredging technology, since depth is limited and could be within reach of extended conventional equipment. Gas hydrates have to be kept under pressure to maintain solid and are also requested in large quantities, so top side processing requirements can be a factor as well. SMS material has in comparison a low production but has to come from deep waters.

Again many parameters determine the most suitable system and with a choice of centrifugal pumps, gas lifts, positive displacement pumps, hybrid systems, etc. etc., it is not easy to choose the most economic, reliable and technical best solution. Understanding the processes is again essential, including hardware (pumps, risers etc), the topside (processing) and downside (cutting, seafloor dredging tool) requirements.

IHC Merwede has started up special research program to get more insight in many of these matters, certainly on the process side, to understand the typical behaviour of multiphase slurries in these long pipes and with the different types of pumping systems. This program will lead to a better understanding and design of the vertical transport systems.

Energy supply
Both processes, cutting and vertical transport, require a lot of energy. The layout of the system determines at what depths specific types of energy is required. Other processes also require energy, but it is not so straightforward to bring 3 MW, 10 MW or even 50 MW to a depth of 2000m and distribute it to all systems.

An industry wide research program is setup to investigate this issue on three aspects: generation, transport and transformation. It is tempting to focus on electrical diesel power first, but considering the environment and CO2 production, other energy sources or carriers should be investigated as well, like (water) hydraulics, wave/current energy, nuclear energy, fuel cells and all other sustainable methods.

Normally energy generation would be done on the supporting vessel and the electrical energy is transported through an umbilical to the seafloor. This is state of art practice and can be supplied turn key. However losses and physical barriers in the umbilical raise the question if local (seafloor) more environmental friendly power generation is possible, like wave/current energy or maybe even the usage of temperature differences etc. This would make the system more efficient.

Transport of electrical energy in large quantities over large distances in a flexible manner under water is not state of art technology. The umbilicals become to heavy and thick. Other methods and carriers are under research as well.

When the energy is supplied, it needs to be transformed into the right type. Having a plug with the capability to supply 50MW is not sufficient. It needs distribution to consumers of different types like pumps, cutters, propulsion, cylinders etc.. Depending on the function these consumers are continuous, start-stop, require peak supply, or need to be controllable. The transformation and distribution of energy is a major issue. Part of the research program is dedicated to this aspect as well.

Integral systems design

Three observations:

1. *There is a need for specialized equipment that meets the wide range of specific requirements of the different deposits, for each case a through evaluation is required.*
2. *A delicate balance in the game of capacities is required, to optimize all links in the mining chain.*
3. *Interface management between all systems is crucial.*

This means that integral system design, or a system architect, is required. However the risk, sheer size and required specialist know-how, implies that development of these systems cannot be left with a single party. Only cooperation between industries and bringing together of the existing know-how in the world can bring these projects to a good end. This implies a very good interface management as well.

If system design and single subsystems are so dependent on deposit characteristics and the interfaces with other systems, it becomes essential to be involved as early as possible in the gathering of information of the deposit and the overall system design.

In the Mining and Oil & Gas industry, each single deposit is carefully examined and evaluated for the best technical and economical solutions. At this stage the emerging deep sea mining companies are doing the same, however being in the early stages and not yet full grown, these investigations are more focused on WHAT can be found, so bankable resources, than on HOW to extract.

If involved at an earlier stage, equipment designer and contractor together are able to advise what valuable information is required for optimal design. In figure 7, this is illustrated in a chart that was developed by IHC's Deep Sea Dredging and Mining (department of IHC Dredgers B.V.):

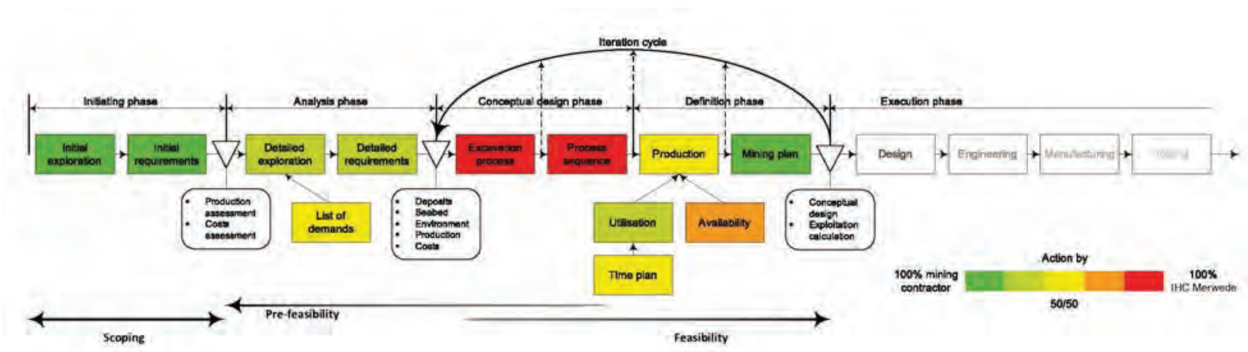

Figure 7: Flow chart for the development of deep sea mining equipment.

5 CASE STUDY: PHOSPHORITES OFFSHORE NAMIBIA – SOUTH AFRICA

A large deposit of phosphorites exists offshore Namibia. Phosphorites contain of phosphate and occur as small precipitation grains on the sea floor. The phosphate content of the phosphorites makes them a suitable raw material for the production of fertilizer. MTI Holland investigated the possibilities to dredge mine the deposit.

The deposit of interest covers an area of 8000 km^2 and has a thickness of about 3 meters. This results in the gigantic potential deposit volume of 24,000,000,000 m^3, roughly equalling 45 billon tons.

The successful mining of the offshore phosphorites is bound by a number of constraints that have a direct impact on the technical and economical feasibility. The main constraints are described below.

The first important constraint is the required dredging depth. The deposit is located at a depth of 270 meters. Current dredging technology, using TSHDs, can reach a dredging depth of 155 meters, although it is expected that a much deeper dredging depth can be reached with an adjusted suction pipe. Remotely operated vehicles have a proven record of operation at much greater depths; however the experience of using ROVs for mining is limited to about 150 meters.

The locations of the deposit and the processing facilities onshore create a very long transportation distance to be covered. From the deposit, offshore Walvis Bay, Namibia, it is a 1350 nm (2500 km) sail to the port of Richards Bay, South Africa. At Richards Bay, processing facilities are present that can handle the phosphorites. This long transportation distance requires that a choice has to be made between either the combination of the mining and transportation system or the separation of these functions.

The rough sea state at the deposit location limits the workability of conventional dredging equipment. The wave and swell action has to be overcome to allow (accurate) dredging. Ways to overcome this action can include swell compensators, common on modern TSHDs, but also a semisubmersible platform that through its volume and mass acts as buffer against the motions.

Finally, the processing requirements of the phosphorites have a significant impact on the operation. To be able to process the material (and such to earn money from it), the undersize of 150 micron and the oversize of 850 micron will have to be removed form the dredged bulk. Both fractions are estimated to account for 10% of the bulk each. Preferably, the processing is done immediately when the dredged material comes to the surface. This would optimize the profitable load that has to be transported over the large distance.

Based on the project constraints, equipment can be selected for the dredge mining and transport operation. For the dredging of the material, two options can be regarded: a TSHD and a ROV. A TSHD has the advantage of being a relatively cheap option, when compared to a ROV that has to be equipped with surface support facilities, apart from the ROV itself. The downturn of the TSHD is the potential problems that arise from the dredging depth, compared to the proven technology of ROVs operating at larger depths. As mentioned, the choice of equipment to cover the long transport distance is between either a combination of the transport and mining system and the use of separate, dedicated mining and transport vessels. A TSHD is a typical example of a vessel that combines a mining and a transport system, where the use of a ROV with a support vessel and dedicated transport barges separates these functions. From the discussed equipment, multiple scenarios can be made combining the different kind of tools to design the optimal dredge mining operation.

This case demonstrates that offshore mining of deep deposits can be made technical (and economical) feasible when (proven) technology of the dredging, oil & gas and mining industry are combined. An integral approach is necessary to be able to make this combination.

6 CONCLUSION

Offshore/deep sea mining offers many challenging opportunities for the next decades to come. The developments in legislation, economics and technology aspects, allows for new optimism that successful projects will be launched into the water.

In the introduction the following proposition was posed:

The dredging industry cluster has all opportunities (with their knowledge on soil/rock excavation and vertical transportation) to become an essential partner for the offshore/deep sea mining industry and boost its development by offering and creating the essential crossovers in technology and establish crossover industry consortiums.

In the last decades the dredging business has proven to be able to extend its barriers, develop, adapt and make use of new technologies to cope with the challenges of new market opportunities.

The dredging industry can form the link between the innovative and deepwater challenging Offshore Oil & Gas industry and the rather conservative, onshore based Mining Industry. If one of these industries can be persuaded to become a central player in the Offshore/Deep sea Mining industry, the dredging industry can boost these challenges by filling in the gaps in technology and take up their traditional role as contractors.

The market potential is such that cooperation in this market can be more profitable for the dredging industry as a whole than to fight each other.

It is clear that the key technologies can only be developed in consortia made up of the main players in the specific fields of technology.

The mining of phosphorites can be the first step to the development of an offshore/deep sea mining industry when cooperation of industries and technologies can be achieved.

REFERENCES

Anon. (2008). New opportunities – IHC Merwede technology supports offshore diamond mining. Ports and Dredging, Vol 170, Autumn 2008.

Anon. (2009). The revival of an old passion – IHC Merwede moves into Deep Sea Mining. Ports and Dredging, Vol 171, Winter 2009.

Hogeweg, B.; Ketterij, R.G. van de; Bloois, J.W. van (2008). Continued research efforts for the development of deep sea mining equipment. 38th Annual Meeting of the Underwater Mining Institute, Oxford MS, USA, Nov 17-22 2008.

Muijen, H. van; Allworden, S. von; Boer, T. de (2007). Sustainable inland and offshore aggregate production requires modern dredging equipment. CEDA Dredging Days 2007, 7 - 9 November 2007, Ahoy' Rotterdam, The Netherlands.

Rona, P.A. (2008). The changing vision on marine minerals. Ore Geology Reviews, Vol 33, pp 618-666

Slagmolen, S. (2009). Economic analysis of deep sea mining operation and conceptual design of mining machine. MSc thesis, Delft University of Technology/MTI Holland (unpublished), 189 pp.

Vercruisse, P.M. (2007). Developments in the dredging industry. Hydrotransport 17. The 17th International Conference on the Hydraulic Transport of Solids, The Southern African Institute of Mining and Metallurgy and the BHR Group, 2007.

TOWARDS AN LCC APPROACH IN THE DREDGING INDUSTRY

J.J. Paauw[1], M. Alvarez Grima[2], J.D.P.A. Peters[3], M. De Boom[4], S. Claessens[5], J.C. van Dijk[6]

Abstract: Nowadays there are very high demands with regards to dredging capacity. One approach to meet these demands is by creating extra capacity; another way is by optimising the exploitation of the current dredging fleet capacity. This article focuses on the latter strategy.

Prior to an offer, the total expenditure for that particular project is determined. To determine the turnover of a project, an estimate is made of the /m^3, which is highly dependent on the operational expenditures of the project. The operational expenditures can roughly be classified in production and maintenance costs. Production costs are the costs due to the production system being in operation, like fuel and personnel costs. Maintenance costs are mainly made due to wear of the components in the dredging system and the transition from the operating state to the down state.

To reduce maintenance costs and to optimise the availability of a dredger, it is necessary to move from a corrective maintenance strategy to a preventive maintenance strategy. To determine when maintenance is necessary one needs to know how and when the dredging equipment fails. This can be done by collecting real-time data from the field using a Condition Based Maintenance (CBM) system, designed by IHC Merwede and DEME. Besides real-time data, the necessary manual input is mainly gathered by inspection plans also set up by IHC Merwede in close cooperation with DEME. The CBM system monitors the actual condition of the dredging equipment, including pumps, cutters, pipes and valves on board.

One of the key factors that determine maintenance costs of dredging equipment is wear caused by the transported slurry. MTI Holland has developed wear prediction models to estimate the lifetime of pipes and pumps. These models will be implemented into the CBM system. However, not all the components of the dredging system can be predicted by the current analytical models of MTI. To determine the other failures on board, all maintenance tasks can be registered in the CBM system. This enables the determination of the condition of these components. Using this information MTI Holland and DEME will develop new models based on analytical and statistical principles. By knowing the condition of these components at all times, it is possible to plan the correct maintenance tasks and provide the dredger with the necessary spare parts when they are required.

This article highlights techniques to collect and analyse failure data. These data can be used to determine the lifecycle costs (LCC) and finally can be used to improve planning of maintenance and inventory control to improve the production availability and simultaneously reduce LCC; ultimately leading to an improvement in economical feasibility of dredging projects.

Keywords: lifecycle costs, maintenance costs, wear, failure data

[1] Dredging consultant, MTI Holland BV, P.O. Box 8, 2960 AA, Kinderdijk, The Netherlands, +31 (0)78 6910326, j.paauw@mtiholland.com

[2] Project manager, MTI Holland BV, P.O. Box 8, 2960 AA, Kinderdijk, The Netherlands, +31 (0)78 6910190, m.alvarezgrima@mtiholland.com

[3] Product manager, IHC Systems BV, P.O. Box 41, 3360 AA, Sliedrecht, The Netherlands, +31 (0)184 431950, jdpa.peters@ihcmerwede.com

[4] Manager Technical Department, Dredging, Environment & Marine Engineering (DEME) NV, B 2070, Zwijndrecht, Belgium, de.boom.marc@deme.be

[5] Project engineer research, Dredging, Environment & Marine Engineering (DEME) NV, B 2070, Zwijndrecht, Belgium, claessens.stijn@deme.be

[6] Maintenance engineer, IHC Parts & Services, Technical Services. P.O. Box 50, 2960 AB Kinderdijk, The Netherlands, +31 (0)78 6921818, jc.vandijk@ihcmerwede.com

1 INTRODUCTION

The Life Cycle Cost (LCC) analysis is an economic evaluation technique to determine the total cost of owning and operating a system over a period of time. If LCC analysis is executed for a project, the deterioration of dredging equipment is mainly caused by wear. For every project the wear can be considerably different, because of the different kinds of soil dredged. This has results on the maintenance cost and downtime of the equipment.

A LCC analysis can be used in decision making. The decision model to establish a LCC analysis is illustrated in figure 1. In the figure the information flow between the contractor and the original equipment manufacturer (OEM) is illustrated.

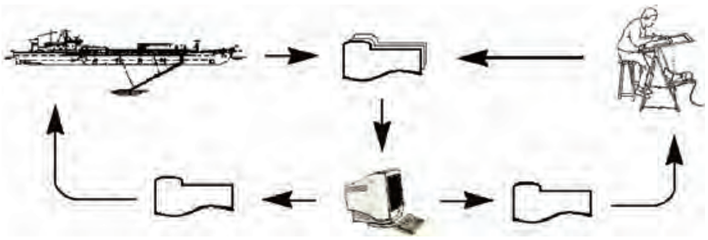

Figure 1. The information flow

To establish a LCC analysis cost related data is required from the dredging vessels and from the OEM. The cost related data is information on the performance of the technical system. To understand the performance of the technical system, it has to be examined. The OEM and the contractor are capable to provide this information. The technical system is set up by several equipment units. The dredging equipment units are designed and produced by the OEM. Maintenance manuals are provided with the equipment. In the maintenance manuals the owner of the dredging vessel can find the required maintenance activities including the required spare parts.

The cost related data on the performance of the technical system, have to be provided from the crew aboard of the dredging vessel and from service engineers ashore. This data concerns reliability, maintenance and inventory data. Reliability data concerns information of failures occurred aboard. This is the most important data source to collect, because maintenance and inventory control is a direct consequence of failures. However it is quite difficult to retrieve, because the data has to be recorded and has to be trustworthy. Both maintenance and inventory control are major cost drivers. Modeling with incorrect reliability data results in correct timing in the model of maintenance activities and inventory control and thus higher total LCC will be obtained.

Having collected all the data the Life Cycle Cost can be predicted for a project or for the total life cycle. The data can also be used for decision making in the operational process of the technical system. It can be used for example in maintenance planning/scheduling, inventory control or design considerations. By providing this information back to the dredger or to the OEM optimization will be obtained.

In the dredging industry there are two ways to look at a life cycle cost analysis. First the life cycle cost analysis can be performed for the life cycle of a particular product. Second the life cycle cost analysis can be performed for the life cycle of a project. A better name for such an analysis would be project life cycle cost analysis. This analysis is similar to the life cycle cost analysis for a particular product, but now for only one period of the life cycle. In dredging industries this project life cycle cost analysis is better applicable, because a lot of information is only known for one project ahead. This information is related to soil type, dredging depths, transporting distances. And it is always the question what is going to happen after that specific project.

A powerful tool for this LCC analysis is the Condition Based Maintenance (CBM) system developed by IHC Merwede in cooperation with DEME. The CBM system collects all the data related to deterioration of the pipes, valves, pumps and cutter due to wear by the dredged soil. MTI Holland and DEME will develop new models for the prediction of wear in these components. The CBM system will be installed and tested on the cutter suction dredger D'Artagnan. All the photos of wear in this paper were not taken on the D'Artagnan or on other vessels of DEME.

Figure 2. D'Artagnan at work

2 GENERAL ASPECTS OF WEAR

Wear is the progressive loss of material from a surface occurring as a result of relative motion at the surface. There are several types of wear mechanics, like abrasive wear, adhesive wear, corrosive wear, fatigue wear, fretting and fretting corrosion. In dredging industries the components are mostly subjected to abrasive wear.

Wear is inevitable with the hydraulic transport of dredged soil. Several components of a cutter suction dredger are therefore subjected to wear. The components taken into account in the project are the dredge pipes, dredge valves, submerged pump, inboard pumps and the cutterhead. The wear is influenced by the soil type, hydraulic transport and the dimension and material hardness of the components.

2.1 Wear effect of the soil type

The soil type is an important factor for the wear of the dredging components. The effects of the soil type on wear are influenced by the grain size, the grain shape, the grain hardness and the specific gravity.

An increasing grain size will result in an increasing wear rate by similar mixture concentration and mixture velocity. For every soil sample a grain size distribution can be obtained with the median grain size (d_{50}) and the average grain size (d_m). In practice it has been found that the abrasive wear rate increases linearly with the particle size up to 10 mm. Above that the effect of the particle size on abrasive wear will become less. But the impact wear becomes predominantly.

A sharper grain shape will produce a higher wear rate by similar mixture concentration and mixture velocity. Thus angular particles will cause more wear in comparison with rounded particles. In general angular particles will have twice the wear rate in comparison with rounded particles, although this is related to the hardness of the soil particle in relation to the material hardness. The grain shape can be classified according to Russell and Taylor for 0 to 1 as depicted in figure 3.

Figure 3. Grain shape classification according to Russell and Taylor

Soil with a higher grain hardness and/or higher specific gravity will have a higher wear rate by similar mixture concentration and mixture velocity. This counts for both abrasive wear and impact wear in pipes and pumps.

For more details regarding the effect of soil properties on wear the reader is referred to Kawashima et al. (1978).

2.2 Wear effect of the hydraulic transport

The effects of the hydraulic transport on wear are mixture velocity, mixture concentration and flow angle.

A major influence on the wear is caused by the mixture velocity at which the mixture passes through the hydraulic transport system. The function for wear has a polynomial order related to the mixture velocity with the exponent varying between 2.5 and 3 as indicated in Cornet (1975).

As the mixture concentration increases also the wear will increase. At low concentrations (till 10% of the weight) the wear will be linear to the amount of particles impacting on the surface area. At higher concentrations the frequency of impacts tends to decrease though, because of mutual interaction between particles.

The impingement angle has an influence on the wear as can be seen in Finnie et al. (1992). In case the flow angle is 0 to 10 degrees abrasive wear will occur by shearing, which will result in the formation of grooves, lines and scratches on the surface. The shape and mixture velocity are important parameters for the wear, but also the relation between the hardness of the grains and the surface. In case the flow angle is 90 degrees impact wear will occur, which causes plastic deformation in the form of depressions, craters and a flaky surface. Between these two extremes a combination of both types of wear will appear. In this region the highest wear will occur.

2.3 Dredge pipes and dredge valves

Dredge pipes and dredge valves deteriorate by abrasive wear. In bends, Y-pieces or T-pieces also impact wear does appear. The selected material determines the lifetime of the dredge pipes. This is twofold, namely the type material has a result on the wear rate and on the minimum wall thickness. The minimum wall thickness of a pipe depends on the strength of the material and the pressure in the pipe.

The wear of the pipes is influenced by the material hardness, the effects of the soil and the hydraulic transport. The wear is most considerable at the bottom of the pipe, where the heavier parts will be transported. At the top the lighter parts are transported, but with a higher velocity. The heaviest wear appears just besides the bottom of the pipe. Therefore it is worth turning the pipes, so the total pipe can wear equally. Also the inclination of the pipe has an effect on the wear. An inclined pipe with going up slurry will wear more considerably at the bottom, while an inclined pipe with going down slurry will wear less at the bottom. If hydraulic pipes are long the soil grain degradation will occur. This means that grain size will be reduced so in longer pipelines the wear will decrease against the length. When two flanges are not placed correctly wear will occur as illustrated in figure 4. Also the curve of a bend has an effect on the wear as illustrated in figure 4.

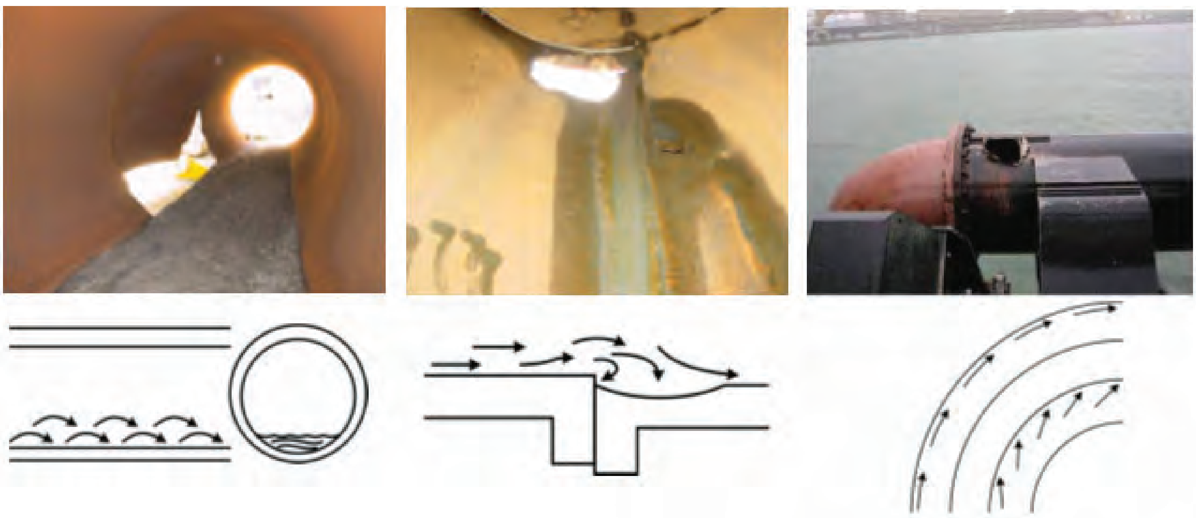

Figure 4. Wear in pipes

2.4 Dredge pumps

Several parts of a dredge pumps are vulnerable for wear, like the casing, impeller, Liquidyne seal, wear plates, lipseal.

The impeller deteriorates by three wear mechanisms, which are abrasive wear, impact wear and cavitation erosion as depicted in figure 5. Abrasive wear is the result of sliding of soil against the surface of the impeller blades. This type of wear occurs when pumping sand. Impact wear is the result of material loss of the impeller by repeatedly impacting of the soil against the impeller. This type of wear occurs when pumping large particles such as gravel and rocks. Another type of wear is cavitation erosion. Cavitation is the formation of vapor bubbles of a flowing liquid in a region where the pressure of the liquid falls below its vapor pressure. When these vapor bubbles implode, cavitation erosion will occur on the inlet of the blades.

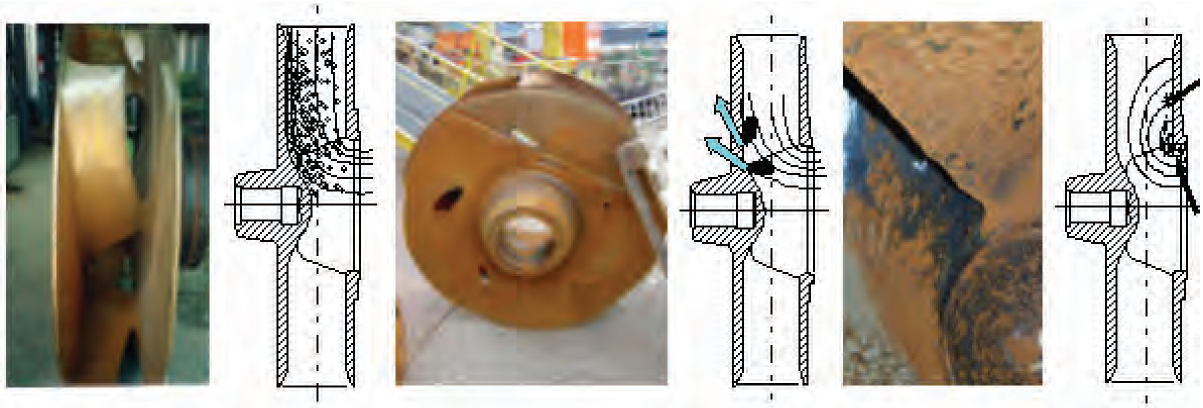

Figure 5. Wear in impellers

Because of wear the efficiency of the pump will decrease in time. To have the lowest wear it is required to work in the best efficiency point. In this point there will be the lowest energy losses, so less energy will be absorbed by wear. Also it is the point where the flow is more uniform in the pump casing. Not working in the best efficiency point will have effects on the wear of the cutwater. Working below the BEP will result in wear at the inner side of the cut water due to eddy formations, while working above the cut water will result in wear at the outer side of the cutwater as can be seen in figure 6.

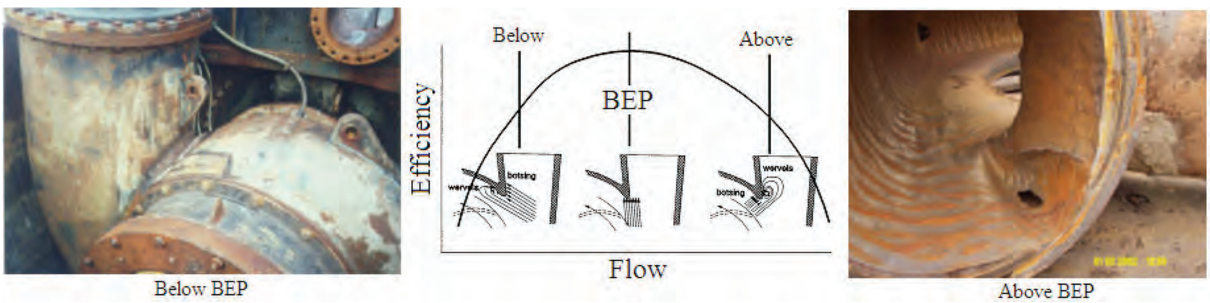

Figure 6. Wear in pump casings

2.5 Cutterhead

The most wearable parts of the cutter are the cutter teeth. These parts have a low cost but a high demand and therefore have a relative high share in the total cost due to wear. The teeth are fitted on the cutterhead via an adaptor. The forces on the teeth are used to cut the soil. During dredging it is required that all the teeth are of equal length. If for instance one new tooth is installed between all worn teeth, this new tooth might break off, because the new tooth is longer, and all forces are concentrated on this tooth.

Several parameters influence the wear rate/lifetime of the teeth namely the strength of the soil/rock and the amount of abrasive minerals present in the material. Abrasive wear is the typical tooth wear, but in case of operating in strong rocks breakage of the tooth can also take place. In that case the wear is characterized by mechanical deformation and fatigue. The occurrence of abrasive wear and/or breakage will depend on the characteristics of the rock mass (i.e. massive rock mass or fracture rock mass) along with the strength of the material.

3 CONDITION BASED MAINTENANCE SYSTEM

The Condition Based Maintenance (CBM) system basically consists of a data logger, a computer for performing the model calculation and a SCADA workstation for the necessary user interaction. Data from the PLC is stored in the data logger and used by the CBM system.

The wear prediction models developed by MTI and DEME are programmed into the model computer. On certain moments the models are triggered and an actual wear rate is calculated. The soil type is of great influence on the calculated wear rate and because of that it is very important to know the soil conditions. Therefore the system is connected to the Dredge Track Presentation System (DTPS) computer. If soil conditions are known, they can be stored in the DTPS and retrieved by the CBM system. If soil conditions are not known, the system makes use of the grain size estimator developed by IHC Merwede. Using certain process information, the grain size estimator can make an accurate estimate of the actual soil type. This estimation can be used as an input for the wear prediction models. Together with process information like pressure, velocity and concentration all the information is there to calculate an accurate wear rate.

The output of the system is the condition of most of the components, for example pumps, pipes, bends, valves and the cutterhead on board of the dredger. The condition of these components is visualized on various user-friendly SCADA pages, enabling the crew not only to monitor the condition of all the components, but also to enter manual measured data. Both the manual entered data, for example measured wall thickness of a pipe piece, and the estimated values for that wall thickness are depictured in graphs. If the models are correctly tuned, the measured wall thicknesses are the same as the predicted thicknesses by the models. The result is that less manual measurement are necessary and maintenance costs are reduced.

If, according to the CBM system, maintenance is necessary, a work order is generated to the Computerized Maintenance Management System (CMMS). When the work is done the performed maintenance action needs to be given in into the SCADA system. In that way the CBM system is lined up with the changed situation and new wear predictions can start!

All in all, an user-friendly system is in development that continually monitors the condition of almost all the components on board of the dredger and outputs the necessary work orders.

4 WEAR MODELLING

For several components in the hydraulic transport line of a cutter suction dredger wear models are in development for determining their wear rate and/or lifetime. The components taken into account in the project are the dredge pipes, dredge valves, submerged pump, inboard pumps and the cutterhead. The inputs of the models are the soil type, hydraulic transport and the dimension and material hardness of the components. The output of the models gives the wear for dredge pipes in millimeters for one million cubes soil. For the pumps the lifetime is given in the amount of soil pumped in cubes, because the wear of pumps is not linear over time. New models for cutterheads and valves still have to be developed.

These wear models have been developed in the past by MTI in cooperation with other IHC business units. These models can be applied for softer soils (i.e. sand and gravel) but not for hard materials such as rock. These models combine laboratory experiments and data collected on board and they are applicable for the estimation of wear in pipes and pumps only.

In a further joint cooperation between DEME and IHC-MTI the existing models will be validated and new models will be developed for rock.

Two modeling approaches are foreseen, based on either analytical methods or in combination with statistical modeling. The selection of methods will depend on the complexity of the wear process, the amount of data available and the know-how of the DEME crew and staff.

As these new models are key in predicting life expectation of the various components, they will form the kernel of the new CBM system. They will form an essential part of the CBM designed by IHC Merwede.

5 CONCLUSIONS

The CBM system gives added value for lowering the LCC in the dredging industry. The measured wall thickness and lifetime data can be used for lowering the number of manual measurement and can be used for the prediction of the wear cost of a new dredging project. By this information maintenance can be planned on a convenient moment and spare parts can be acquired on time, which result in lower maintenance cost and a higher production availability, which is beneficial for the total life cycle cost of a dredging project.

REFERENCES

Alvarez grima, M. (2001). Wear process in centrifugal pumps, TID Lecture Notes

Alvarez Grima, M., C.H. van den Berg, A.C. Korving, H. Zochling (2003) Performance and wear analysis of the CSD Beaver Martina, Port & Dredgers 159

Alvarez Grima, M., C.H. van den Berg, T. Gochilashvili, M. Gelenidze (2008) Analytical wear prediction model for heavy duty centrifugal pumps, 14th International Conference on Transport and Sedimentation of Soil Particles

Berg, van den, C.H. (1992). Slijtage van baggerpompen, TID lecture notes Nederlandse cursus centrifugaal pompen

Berg, van den, C.H. (2000). Grain shape effects on wear, Port & Dredging E152

Cornet, R. (1975) Wear in dredgers, The dock & harbour authority May 1975, pp 10-12

Jacobs, B.E.A., J.G. James (1984) The wear rates of some abrasion resistant materials. 9th International Conference on Hydraulic Transport of Solids in Pipes

Finnie, I., G.R. Stevick, J.R. Ridgely (1992) The influence of impingement angle on the erosion of ductile metals by angular abrasive particles. Wear 152, pp 91-98

Kawashima, T., T. Yagi, T. Ise, E. Sato, H. Washimi, A. Yokogawa (1978). Wear of pipes for hydraulic transport of solids. Fifth International Conference on the Hydraulic Transport of Solids in Pipes

Paauw, J.J. (2006). Data collection & analysis for performing a Life Cycle Cost analysis in the dredging industries, MSc Thesis Erasmus University Rotterdam

Russell, R.D., R.E. Taylor (1937). Roundness and shape of Mississippi River sands, Journal of Geology 45, pp 225-267

TURBIDITY MEASUREMENTS: A TOOL FOR ENVIRONMENTAL DREDGING UNDER STRICT ENVIRONMENTAL CONTROLS CASE STUDY: PORT OF MARINA DI CARRARA , ITALY, SITE OF NATIONAL INTEREST (SIN)

I. Melito[1], ***Port Authority of Marina di Carrara,***
B. Capuozzo[2], ***Jan de Nul Italia S.p.A.*****, C. Boeri**[3], ***Jan de Nul Italia S.p.A.,***
B. Callaert [4], ***Envisan NV, Member, CEDA,*** **and S. Herman** [5], ***Envisan NV, Member, CEDA***

Abstract: The Port of Marina di Carrara (Italy) is well known for the export of the Carrara marble. The port is situated into the National Interest Site (SIN) of Massa Carrara (Law 426/98, , Decree of 21st December 1999 Decree of 18th October 2001, No. 468 – Environment Ministry), so dredging activities are strictly regulated. This paper describes in the detail the monitoring activities conducted during the environmental dredging campaign 2008.

Based on the environmental plan and data collected, we can conclude that the impact of environmental dredging on the turbidity is negligible in comparison to other factors and other operations going on around the area, such as commercial navigation traffic.

Keywords: dredging, environmental monitoring, turbidity

[1] Engineer, Port Autoriry of Marina di Carrara,Viale Colombo, 6 - Marina di Carrara (MS), Italy, Tel. +39-0585-782501, Fax +39-0585-78.25.55, E-mail: info@autoritaportualecarrara.it , www.autoritaportualecarrara.it

[2] Project Engineer, Jan De Nul Italia S.p.A., Via Matteucci, 38F, 56124, Pisa, Italy, Tel. +39-050-54.24.35, Fax +39-050-97.39.03, E-mail: barbara.capuozzo@jandenul.com, www.jandenul.com

[3] Project Engineer, Jan De Nul Italia S.p.A., Via Matteucci, 38F, 56124, Pisa, Italy, Tel. +39-050-54.24.35, Fax +39-050-97.39.03, E-mail: carlo.boeri@jandenul.com , www.jandenul.com

[4] Engineer, Envisan NV, Tragel, 60, Aalst, 9308, Belgium, Tel. +32-53-731.652, Fax +32-53-772.855, E-mail: bart.callaert@envisan.com , www.envisan.com

[5] Project Engineer, Envisan NV, Tragel, 60, Aalst, 9308, Belgium, Tel. +32-53-731.652, Fax +32-53-772-855, E-mail: sofie.herman@envisan.com , www.envisan.com

1 BRIEF DESCRIPTION OF THE PROJECT

The Port of Marina di Carrara is located in Massa Carrara, in Tuscany Region (fig. 1).

Figure 1 Location of the Port

The port of Marina di Carrara is well known for the exportation of the Carrara Marble. The port is part of the National Interest Site (SIN) of Massa Carrara (Law 426/98, Decree of 18th October 2001, No. 468, Decree of 21st December 1999 –Environment Ministry). This means that dredging activities must be performed using all possible environmental precautions.


Figure 2 Areal view Port of Marina di Carrara

Vessels that currently call the Port of Carrara (fig 2 – Areal view Port of Marina di Carrara) are bulk-cargo carriers, ro-ro, tankers and containers having LOA over 200 m, beam up to 40 m, draft up to 10 m, and cargo capacity up to 30.000 tons.

The entrance channel of the Port has been subject to different dredging interventions in order to maintain the depth of the access channel and therefore to assure a safe access condition for the vessels entering and leaving the port.

The dredging project was carried out on behalf of the Port Authority of Marina di Carrara . The total surface to be dredged is 35000 m2 up to a level of -10.5 m MSL for a total in situ volume of 25.000 m^3 of dredged material (Fig.3)

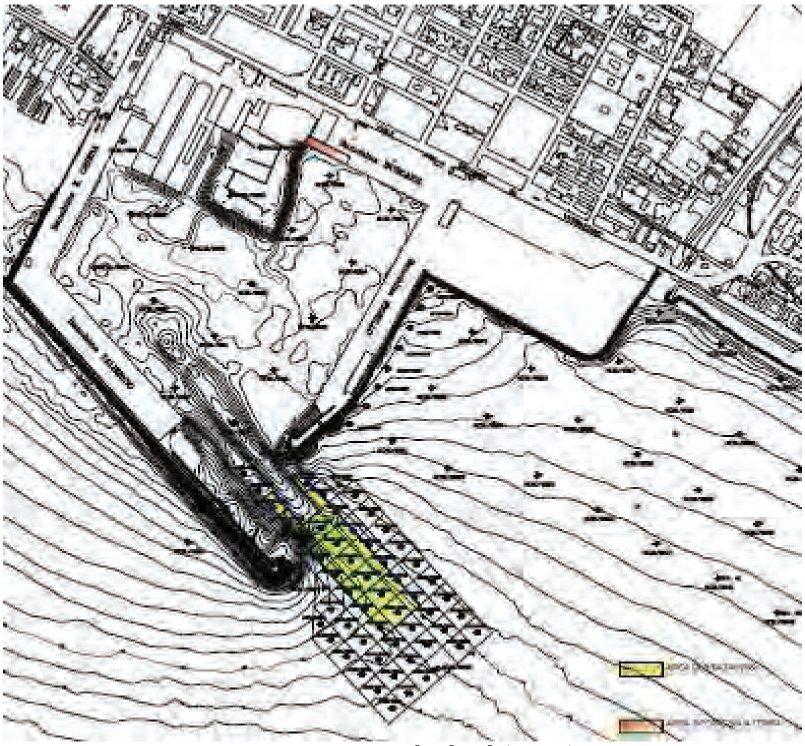

Figure 3 Area to dredged (green)

2 MITIGATION MEASURES

The dredging activities were carried out by using an environmental bucket in order to minimize the turbidity and to avoid spill from the dredging operation. Due to the nature of the material (silt /sand), dredging could be done using this kind of equipment.

3 ENVIRONMENTAL MONITORING

A complete monitoring plan was set up in accordance with the specific site requirements.
The monitoring plan consists of two types of analyses; i.e. continuous and discontinuous analyses.

3.1. Continuous monitoring
For the continuous analyses multi parameter probes were installed around the dredging area. The type of probes used for this project was called “Troll 9500” (fig 4).

Figure 4 Multi- parameter probe

With these probes the following parameters were recorded: water temperature, barometric pressure,Turbidity, pH and DOC (Dissolved Oxygen Conductivity).
The probes S1, S2 and S3 have been located near the port breakwater, while probe S4 has been installed on an off shore buoy (Fig. 5 a -b).

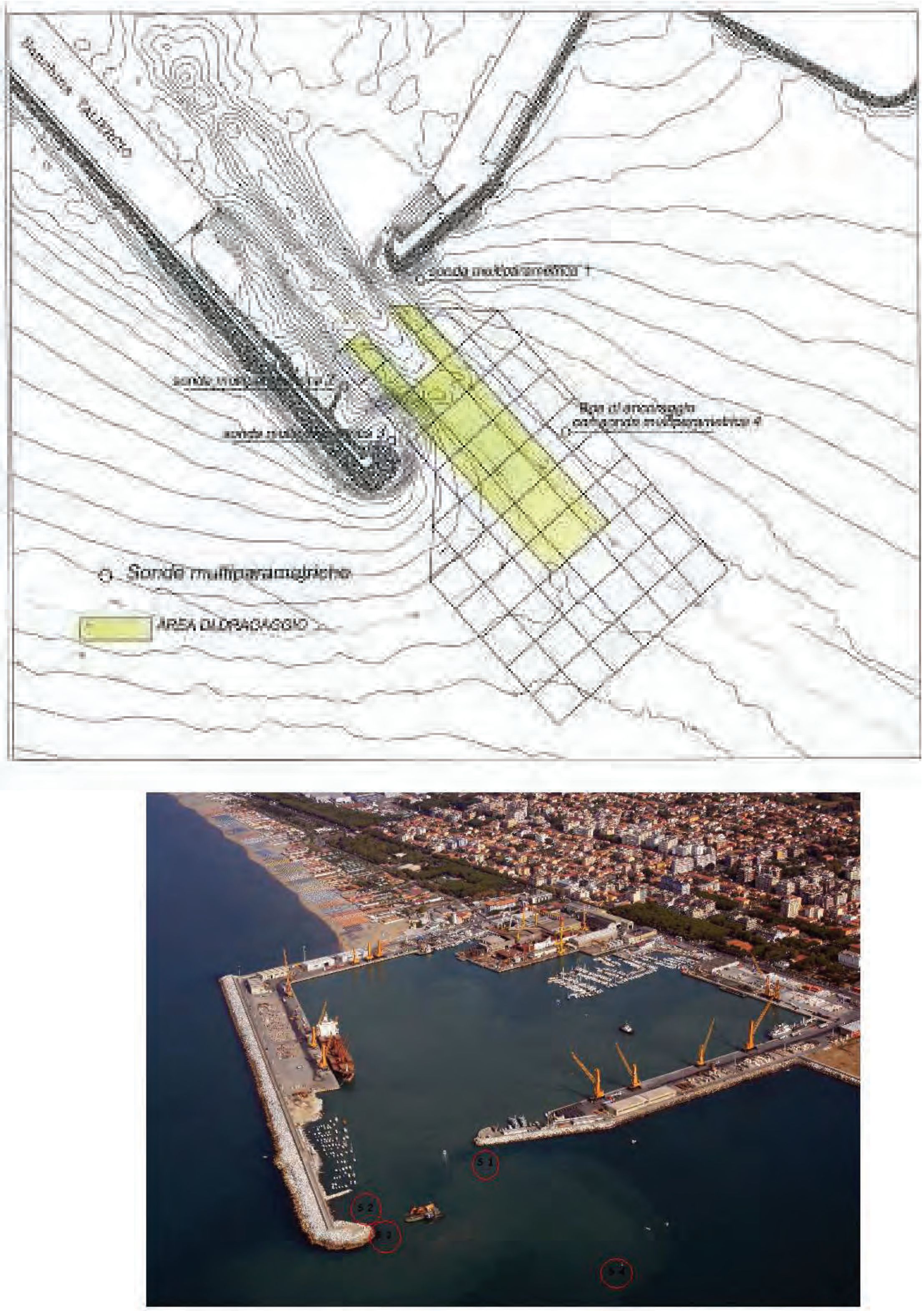

Figure 5 Location of the multiparametrical probes

All probes were installed at a depth of 4.5m below sea level. The data were downloaded on a portable computer for further evaluation and interpretation.

3.2. Discontinuous monitoring:
On a regular basis water samples were taken by an independent laboratory. These samples were taken at different depths by means of a Niskin bottle (Fig 6).

Figure 6 Niskin Bottle

These samples were sent to a local laboratory and the following parameters were analysed: Mercury, Lead, Nickel, Copper, DDT, Naphthalene and total Solids

3.3. Monitoring before, during and after the dredging activities:
Before the start of the dredging activities, monitoring (continuous and discontinuous) was performed in order to obtain some basic reference information During the dredging campaign monitoring was performed on a daily and weekly basis. Based on the gathered information and data, some conclusions and recommendations could be made.

4 DATA AND RESULTS

4.1. Data gathering:
The data were collected in six different phases. These phases are described in the table (Fig 7) – below.

Figure 7 Different Phases during the execution of the project

Phase of work	Period	Nr of days	Activity
1	4 /05/2008-30/05/2008	26	Before commencement of the work
2	31/05/2008-10/06/2008	10	During dredging activities
3	11/06/208- 21/06/2008	10	No dredging
4	22/06/2008-8/08/2008	16	During dredging activities
5	9/08/2008-24/08/2008	15	No dredging
6	25/08/2008- 26/09/2008	31	During dredging activities

The four probes (S1 till S4), registered variable and irregular turbidity values as show Fig 8; which gives the impression that the values seem to be independent from the dredging activities.

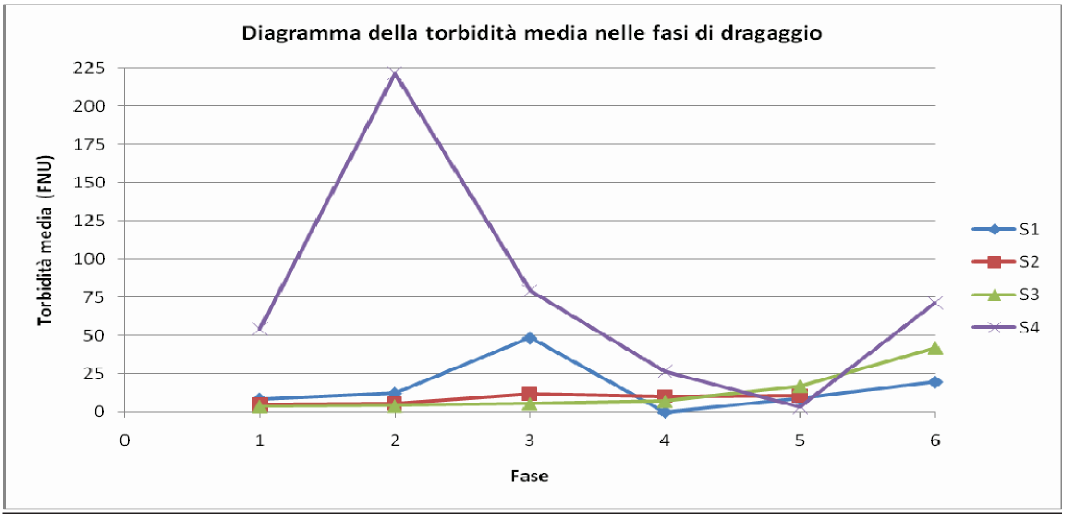

Figure 8 Diagram of summary of average turbidity in six phases of the work

Probe S2 did not register data in the last phase (phase 6) due to technical problems with the probe.

4.2. Results - Interpretation and correlation:
Fig 9 below gives a general overview of the different probes. Different calculations have been performed based on the data of ship movements through the entrance channel.

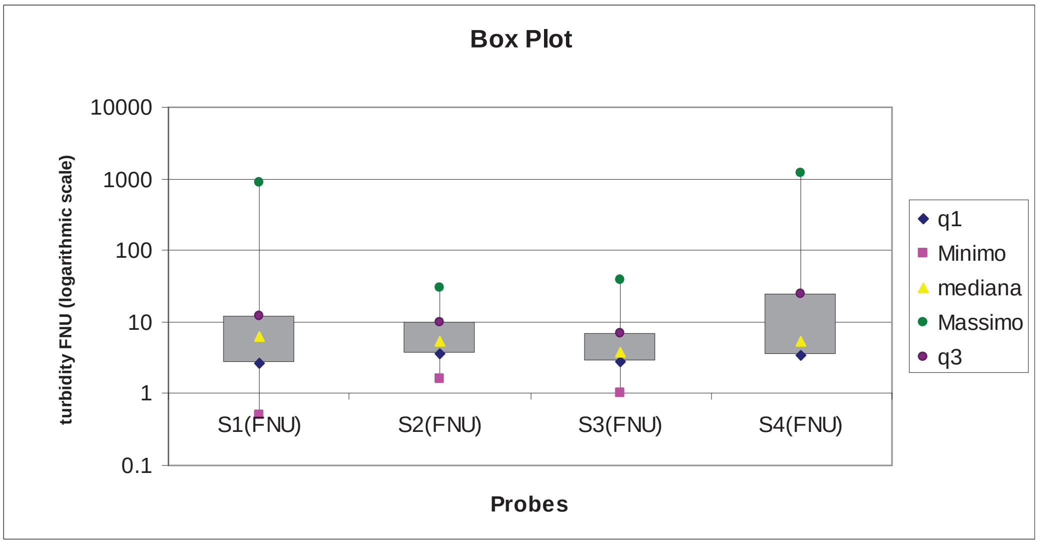

Figure 9 Box plot of the turbidity in the four probes

Probes S1 and S4 present more extreme values. There is a good correlation between S2 and S3. These probes show a uniform behaviour, due for sure to their close proximity.

5. CONCLUSION

The turbidity measured in the access channel of Marina di Carrara does not seem to be effected by the environmental dredging activities. During different phases of the project, data (continuous and discontinuous) were collected and interpreted. The continuous gathering with the multi parameter probes made it possible to check the influence of the dredging activities and compare it with normal port activities. (Ships entering and leaving the port). Different evaluations have been made and there was no significant impact of the dredging activities on the turbidity in comparison with the ship movement, of course depending on the number of ships entering and leaving the port. On the other hand it was not possible to make any correlation between the continuous and discontinuous monitoring executed; this is probably due to the limited number of samples taken during the discontinuous monitoring.

A SPECIAL UNIT FOR WATER INJECTION DREDGERS

Mr. Gert de Vries[1], B.Sc. and Mr. Jorne Beyen[2], B.Sc.

Abstract:

Over the years, the water injection dredger (abbreviated as WID) has found its way in the dredging world.
For smaller dredging projects, this type of dredger has become a highly appreciated piece of equipment.
However, in practice we see that these dredgers are equipped with many tools, especially designed for various types of jobs: they are also used for other purposes. For example, water injection dredgers are also used for levelling of sand barriers, etc. This has often consequences for the structural design of the water jet ladder and ladder hinges, especially in relation to strength.
Water injection dredgers are mostly small vessels with good manoeuvrability. Sometimes they are used for other tasks. So why not modify work vessels with good manoeuvrability and sufficient deck space into a water injection dredger. In this way, the idea arose to design containerized units, which could be easily mounted on suitable existing vessels with only small permanent adaptations.

Keywords:
Flexibility, multi functional, simplicity.

[1]Vuyk Engineering Rotterdam B.V., P.O. Box 1, 2900 AA Capelle aan den IJssel, The Netherlands,
T: +31 10 4502500, F: +31 10 4587245, gdv@vuykrotterdam.com, www.vuykrotterdam.com.

[2] DEME, Haven 1025, Scheldedijk 30, B-2070 Zwijndrecht, Belgium,
T: +32 32505211, F: +32 32505650, beyen.jorne@deme.be, www.deme.be.

1 INTRODUCTION

The water injection dredger is a relatively recent development in dredging equipment.
Water injection dredging is a technique where water is injected in the top layer of sedimented mud.
The generated slurry becomes a fluid with a higher density than (sea)water and flows away from the dredging site. This method is a very cheap way of taking away sediment in unwanted locations; it has the ecological advantage that it does not disturb the sediment balance of watercourse. The method is most suitable in mud and fine sand beds and has been used successfully in port areas.
However, the technique requires very specific environmental conditions, mainly regarding the composition of the mud and the bed topography. Careful assessment must be made of the likely destination of the turbid water.
Originally, Water Injection Dredging is a patented technology. However, the patent has expired and since that date, the water injection technology is taken in use by several dredging contractors.

In this article, the design of a special water injection dredging unit is described.
The modular unit can be installed on suitable multi-purpose work vessels. Before coming to the final design of the unit, the ideas and prototypes have been tested on two work vessels of a dredging contractor. Also, a lot of attention has been paid to the way of mounting of such a unit and the dimensions of it.

In addition, some specific design criteria to workability of water injection dredgers will be discussed, like calculation of ship's motions to design roll and heave compensators for the WID equipment.
The mounting on board of the unit, the consequences for the existing design and the key activities during the time at the yard will be described.
Finally, the performance during operations and the other possibilities of the vessel are mentioned.

The most prominent feature of a water injection dredger is its long injection beam underneath the vessel. Through this hollow injection beam, large quantities of water are injected into the bottom under low pressure.
The sand / mixture, created in this way, flows away to the sides under the influence of gravity.
This type of dredging results in a trench in the bottom.
Water injection dredging is a cost-efficient way to carry out maintenance dredging in silted up navigation channels and ports.
Executed in a professional way and under the right conditions, it offers an economical alternative for maintenance dredging.

2 TYPES OF WATER INJECTION DREDGERS

For explaining how the design was created, it is necessary to know about the existing designs of water injection dredgers, because the modular unit design is based on the experiences with this kind of arrangements.
When we look at the present fleet of water injection dredgers, we mainly see two types as new designed ships. The converted vessels are based on these ideas.

<u>TYPE A</u>
Type A is a dredger with a well at centreline and a central ladder with spreader pipe at the stern side.
The hoisting gantry is bridging the two hull parts, over a certain length of the hull, and the water pumps are located inside the hull. Of course, the hoisting wire is also equipped with a wave compensating system. Sometimes the pump drives are combined with the ship's propulsion. This layout demands two propellers.
The design of the water injection pipe is nicely protected within the ship's hull form.
This type of water injection dredger is schematically shown in figure 1.

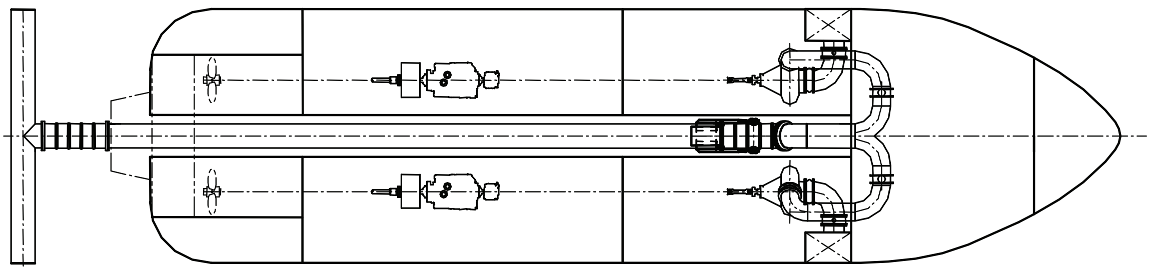

Figure 1 – WID with centreline well

When we look at a centre well design, a logical step is a catamaran design. This design is very suitable for modular execution, as shown in figure 2. This is a completely dismountable containerized execution.
The hull form will give more resistance, so speed will be reduced in free sailing conditions.
The two propulsion units can be positioned at stern side or one at stern side and one at bow side. Due to the container dimensions, this design has its limitations, especially with respect to freeboard and propulsion.
The propulsion has to be indicated as auxiliary propulsion; in this way reducing the Class requirements when building under survey.

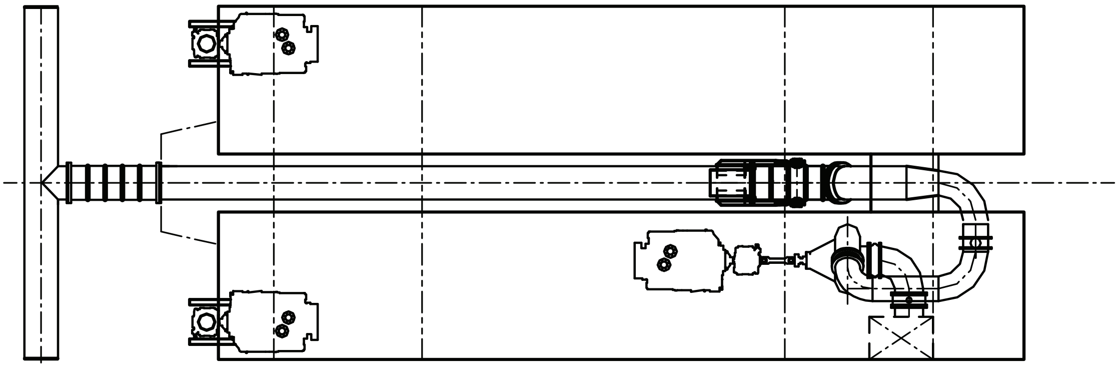

Figure 2 – WID in catamaran-like execution

<u>TYPE B</u>

This design has a complete hull with the water injection pipes in a U-shaped unit.
The water supply is at both sides of the vessel, also with the pumps inside the hull.
In this arrangement, one propulsion unit is possible, but for manoeuvrability, two units will be better.
A combination of pump and propulsion drive is possible. The outside position of the water supply pipes increases the risk of damage when ships are passing by and under mooring conditions.
This layout permits a wider spreader beam thus more working area, compared to type A, based on the same ship's breadth (see figure 3).
Looking at vessels to be converted into a water injection dredger, the type B is most suitable.
Constructing a centreline well in an existing vessel is obviously more complicated than creating suction and delivery inlets for water injection pumps.

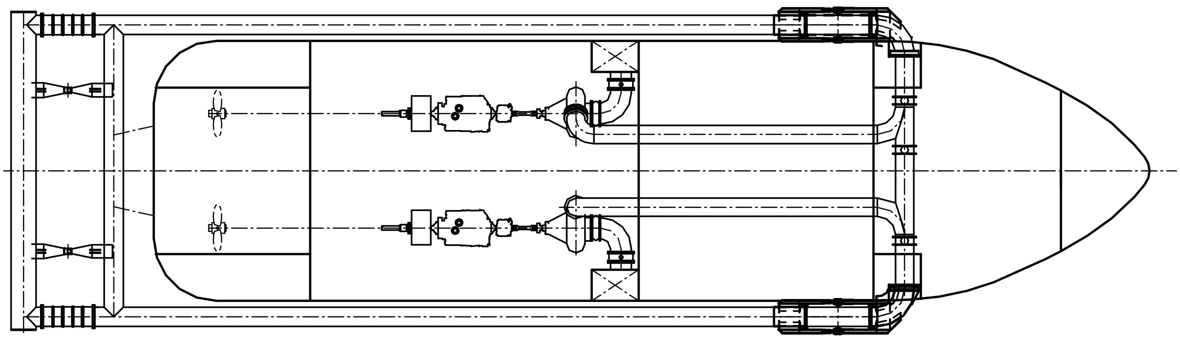

Figure 3 – WID with water injection pipes in a U-shaped unit

As indicated in the abstract, this kind of dredging tool is also used for other purposes in practice like using as equipment with a dozer blade. This has consequences for the design, especially for the water injection pipe structure.
Originally, the hinge points on hull sides were executed as turning glands. This proved to be not strong enough. Also, leakage occurred at the seals.
Creating horizontal hinges with rubber hose was already a better solution.
However, over the horizontal shaft, this was still a stiff arrangement. Finally, a double hinge (cardanic hinge) was the best solution.

3 PREDECESSORS

Looking at modified work ships, two vessels can be mentioned as predecessors for the design of the water injection dredging unit. This concerns the dredging plough vessel Alligator (fig. 4) and the diesel-driven tug Geer (fig. 5).
The Alligator is a multipurpose vessel, which can be equipped with a sweep beam or a dredging plough.
The dimensions of the vessel are:

Length o.a.	33,55 m
Breadth o.a.	10,38 m
Depth	3,50 m
Maximum draft	3,20 m
Bollard pull	about 25 ton
Installed power	about 2300 kW

Figure 4 – Multi-purpose work vessel Alligator

Figure 5 – Tug Geer

The idea for the unit arose when jet water supply to the plough was required to improve efficiency. A modular diesel jet pump was installed on the work deck. The water supply to the plough was effected by means of a long rubber hose.

The tug Geer is an old single-screw tug (built in 1954 – output 868 kW), operating in Western African waters. For a specific job, a plough has been installed, with jet water supply and jet water pump unit on the aft deck. Also, a hydraulic power pack and a hoisting winch had to be installed.
The dimensions of the tug Geer are:

Length o.a.	26.40 m
Length b.p.p.	24.00 m
Breadth o.a.	6.90 m
Depth	3.45 m
Draft	2.33 m
Bollard pull	11.5 ton
Main engine	868 kW

For water injection dredging, also water supply is necessary, however with lower pressure of 150 kPa (1.5 bar).
So the water supply is the link between plough jetting and water injection dredging.
The pump unit can be placed on deck. The gantries for hoisting can also easily be mounted.
Hinges and pipe structure are more complicated, but the idea for the unit was born.

4 DESIGN OF WATER INJECTION DREDGING SET

From all above indicated items, is has become clear, which design conditions are relevant for the WID unit and for the vessel.

For the WID unit:
* Modular design
* Reduced weight
* Self-priming pump
* Separate hydraulic power pack for winches and eventually wave compensator

For the vessel:
* Sufficient deck space
* Good manoeuvrability
* Space for gantries and winches
* Rigid hull connection
* Pontoon-shaped hull form

A multi-purpose work vessel could match these conditions. The tug Geer did not;. for that reason, extra floaters have to be added at the stern to carry the weight of the pump set and plough, as also mentioned under Predecessors.

A containerized pump set could be placed on board the PARAKEET; container fittings were already integrated in the main deck plating. The unit could be considered as deck load, to be temporarily on board.
In that case, the classification society had no objections. For permanent installation onboard, a new stability booklet including inclination test has to be submitted to the classification society.
The introduction of the suction inlet is the only serious modification of the hull. This inlet has to be integrated into the hull's structural design. For this reason, the PARAKEET had to be dry-docked.
The inlet had to be based on a pump capacity of approx. 1,306 m³/s (4.700 m³/h) at a delivery head of 150 kPa (1,5 bar).

As the PARAKEET was already equipped with high-power tractive winches on deck, these winches could be used for hoisting the WID pipe unit. Figure 3 is the best arrangement as already mentioned in “Types of water injection dredgers”. The hoisting gantries can be positioned on the stern. These can also be used for plough dredging.
With some WIDs, the hinge points are constructed as turning glands. Because these dredgers are also used "in practice" for dozer like activities, the hinge points do not have sufficient strength. For this reason, the hinges are designed as cardan hinges. See figures 6 - 7.

Figure 6 – Aft view on WID

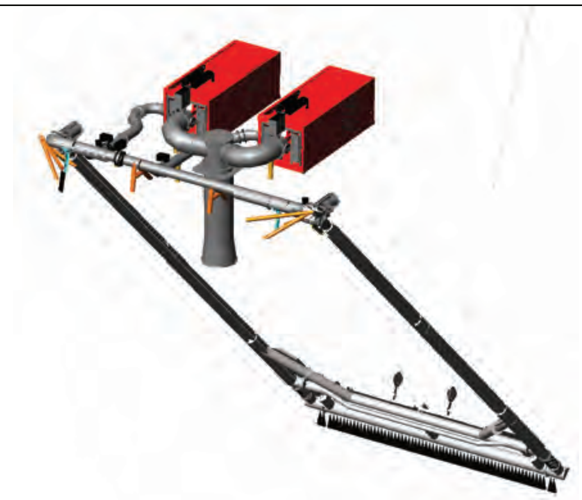

Figure 7 – Arrangement for WID

So what we see now is a quite simple design and because of its modular structure also maintenance friendly.

4.1 Seagoing conditions

The workability in seaways of current WID designs is limited due to the risk of touching of the WID head on the seabed (see figure 8). During operation, the roll motions of the water injection dredger result in touching the seabed of WID head's tips, which might results in structural failure of the equipment.
Studies are in progress to compensate the roll and heave motions of the WID ladder structure.
With the help of motion calculation software (like AQWA) a clear insight can be gained about the vessel's motions in operating position with WID equipment. From the results of the motion analysis and the required operating sea state, the technical specifications of the motion compensation equipment can be determined, such as stroke of the heave and roll compensation. Also the reaction forces in the supports, created by the drag of the WID equipment, can be calculated in this way. From the above can be concluded that with the insight in vessel's motions and workability, the design of water injection dredgers can be optimized and workability improved.

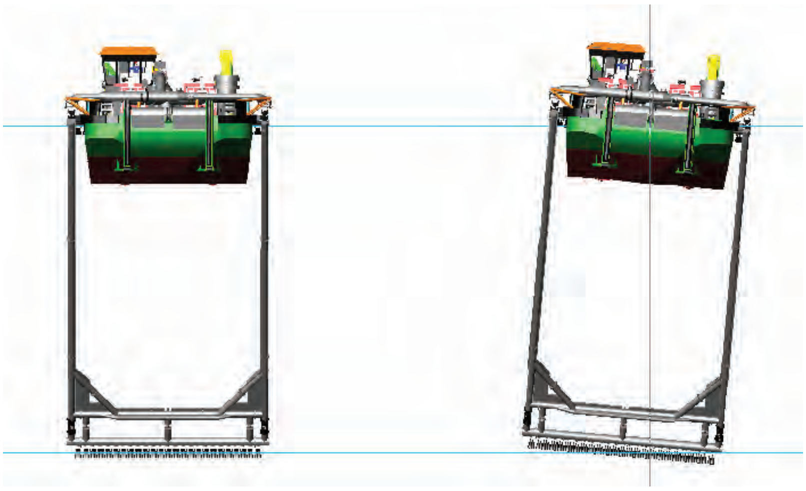

Figure 8 – Touching of the WID head during roll motions

5 CONVERSION FROM MULTICAT TO WATER INJECTION DREDGER

Following description of events is a testimony of how simple this kind of conversion can be executed in any part of the world.
The multipurpose vessel PARAKEET sailed to Visakhapatnam to be converted into a water injection dredger.
Due to the lack of dry dock capacity, a local fisherman dry dock (figure 11) was chosen to perform the conversion.

Figure 11 – the fishermen dry-dock of Kakinada

All critical equipment was shipped from Europe to India.
The 'conversion kit' arrived in two 40-foot (12,19-m) long containers, enabling the dredging contractor to perform a time-effective conversion (see figure 12). The shipyard had to perform only assembly and some welding, as most equipment was pre-fabricated in Europe. The purpose of the kit was to have a flexible solution. Simplicity in different aspects!

Figure 12 – The 'conversion kit' arrives by truck in containers

Next to the containers, two diesel driven high volume, low pressure pump sets arrived at the Yard.
Before entering the dry dock, the conversion already started at the quay wall to meet the tight delivery schedule.
Because of the flexibility inherent to the design, this way of working caused no hindrance at all.
First of all the hard wooden deck was removed to enable welding on deck and to locate the spot where the suction pipe should be installed.
Installation of the A-frames could be done with the cranes of the multi purpose vessel itself.
A part of the outer frame was assembled on the quay wall, to be lifted onboard later with the A-frames of the PARAKEET. This simple procedure prevented the use of expensive, high-capacity mobile telescopic cranes.
In this way only a small crane was sufficient (see figure 13).

Figure 13 – Lifting of outer frame's aft part

With the front and aft part installed, the connection between these parts could be made easily (see figure 14). In this way the assembly of the outer frame was completed. Hydraulic piping was already mounted on the separate pipes. Only the pipes needed to be connected and the hydraulic system was operational.

Figure 14 – Assembling the outer frame

Entering dry-dock with the outer frame already mounted (figure 15). The only structural work to be done, was making a moonpool or suction pipe through the entire hull.

Figure 15 – In dry-dock with mounted outer frame

First an opening was made. The most suitable spot was the fore ship, as in this location almost no interference with the ship's other systems occurred (figure 16).

Figure 16 – The hull opening for the central moonpool

The central suction pipe was lowered in the opening and welded to the ship's structure. Afterwards the pumps could be installed together with the connecting parts.

Figure 17 - Installation of the central suction pipe, fabricated on India's west coast

A passive heave compensation system has been installed to cope with the swell and to regulate the ground pressure of the jet bar (figure 18).

Figure 18 – the passive swell compensation system

Finally the assembly was ready and the testing procedures could start.

Figure 19 – testing in progress

Without going to much in detail on the water injection dredging technique itself, some figures and experiences are given.
The pump curve (figure 20) shows the measured pump characteristic at 32,5 Hz (1950 rpm).
This figure shows that a total flow rate of approx. **1,306 m^3/s (4700 m³/h)** can be expected, resulting in approx. 0,0372 m^3/s per nozzle (134m³/h per nozzle)

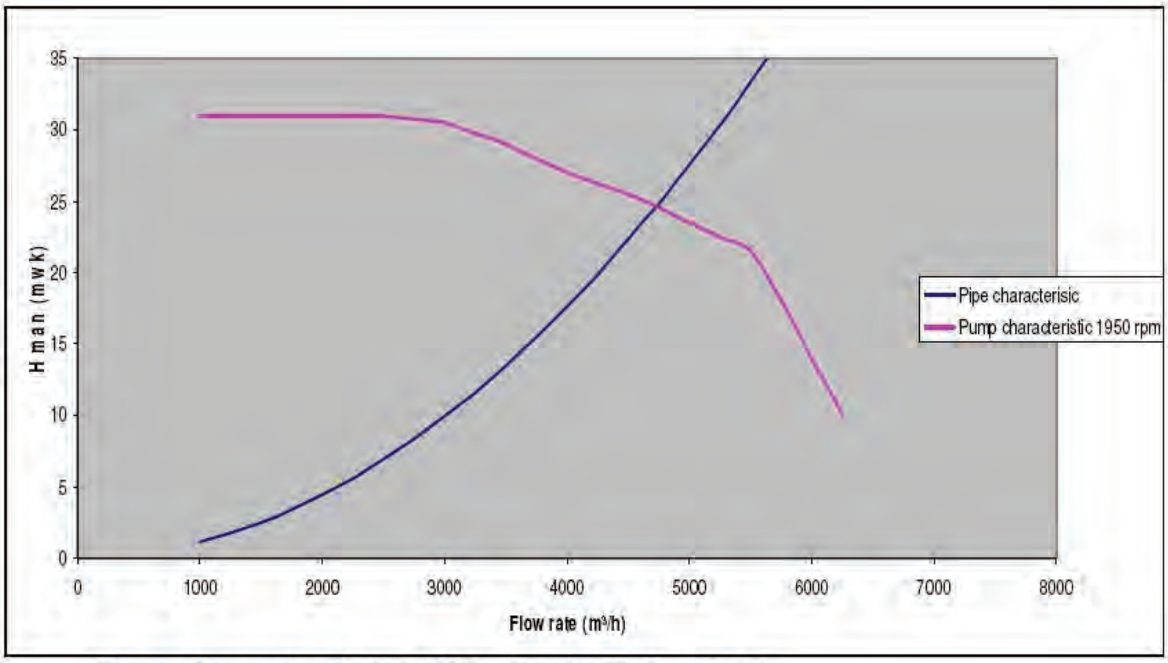

Measured pump characteristic (B&E), pipe ("load") characteristic

Figure 20

Water flow within the WID piping

On figure 21 is shown that all the water runs through the outboard frame. The frame has two functions, a structural and transport function.

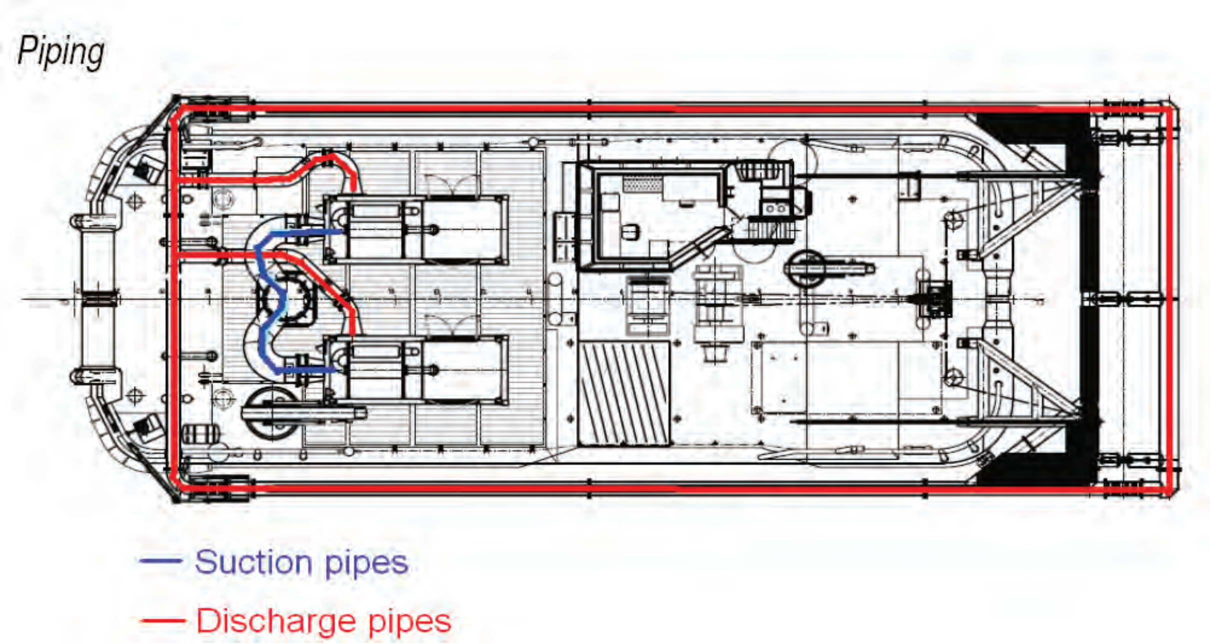

Figure 21 – Piping diagram

Detail of jet bar with the nozzles

The nozzles should be very near to the bottom. It is experienced that nozzles should not be further than 0,3 m away from the seabed. Toughing the seabed seems to be very effective in some areas.

Figure 22 – Jet bar with nozzles

6 RESULTS OF WATER INJCETION DREDGING

The figures 23 and 24 of a survey show the immediate effect of water injection dredging after 6 and 105 hours dredging. The material has been transported elsewhere.

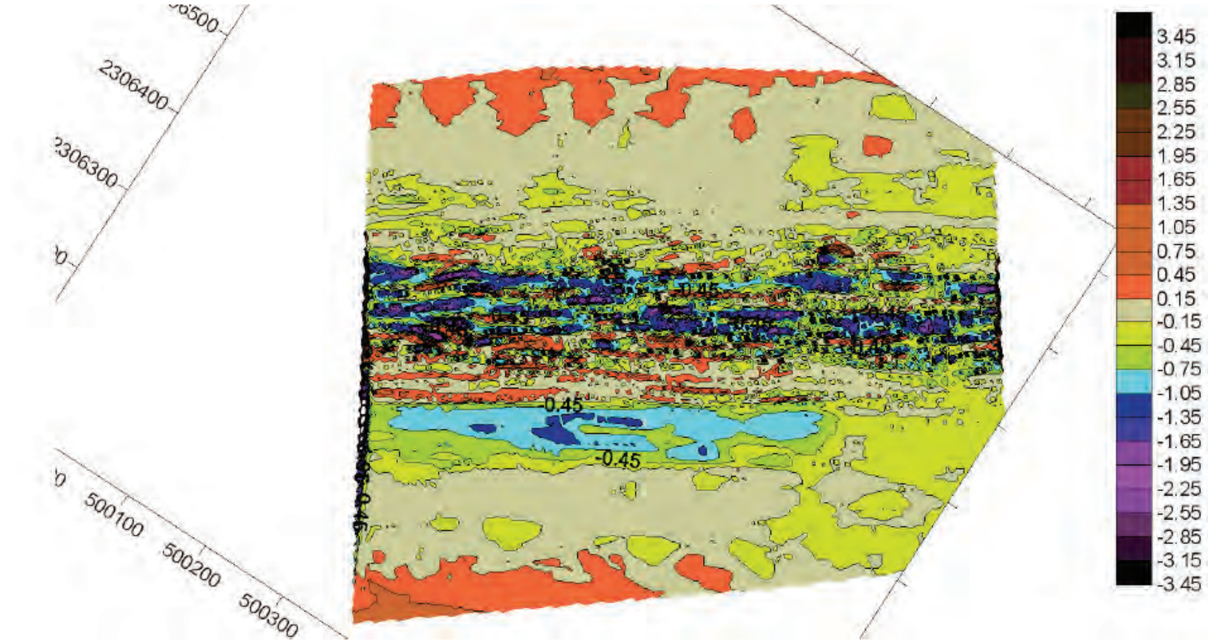

Figure 23 – Difference chart after 6 hours dredging

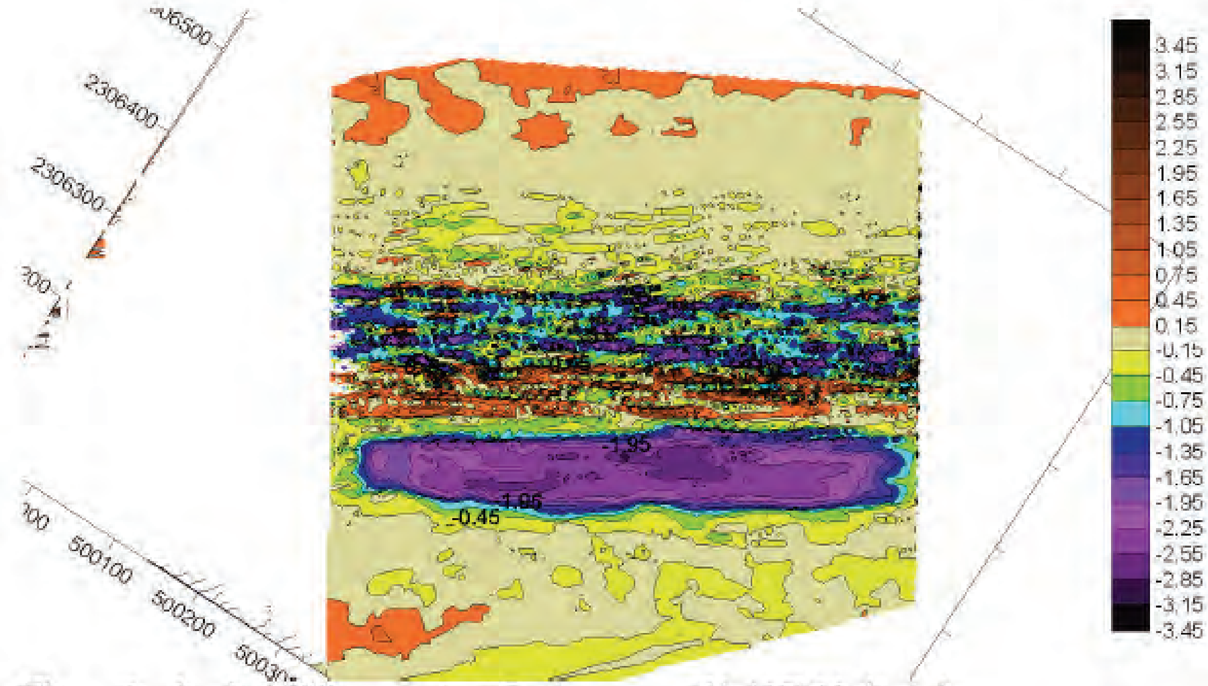

Figure 24 –Difference chart after 105 hours dredging

Conclusions after the first tests:
* Large layers can be removed with the water injection dredger.
* Production drops when in deeper layers stiffer clay is being encountered.
* The dredging speed is between 0,514 and 1,029 m/s (1 and 2 knots).

* Layers between 0,05 m and 0,10 m are normal.
* Productions of more than 0,278 m^3 per second (1000 m^3 per hour) are possible, depending on the slope and material to be removed.
* Some material settles in deeper laying areas and some material has disappeared with the current. This way no re-handling has to be performed by other dredgers.
* Material from outside the dredge zone has been removed; this supports the density current theory.
* Production drops when more compacted clay is encountered.

7 SUMMARY OF ADVANTAGES AND LIMITATIONS:

Advantages of water injection dredging:
* Simple to operate
* Increased manoeuvrability
* Few manning / limited fuel consumption
* No active transport of sediment
* Limited wear
* Operating hours / week

Resulting in low cost alternative for appropriate locations
- Maintenance dredging ports,
- Badly reachable areas (near quay walls, under jetty's, etc.)
- High spot hunting

Limitations of water injection dredging.
* Material should be mainly silty
* Material should not be polluted
* Disposal should not be too far away
* Estimating production is sometimes difficult to determine
* Transport distance is difficult to determine

8 CONCLUSIONS:

The principle of water injection dredging is already known for a while. Patents date from 1984 and since then several water injection dredgers were made and used worldwide. Notwithstanding the existence of the water injection dredging technique for decades, new applications can be considered. One of them is the temporary application of the water injection dredging technique on multipurpose vessels. These vessels accompany the dredging fleet anyhow.
The mix of advantages and limitations could suggest the water injection dredging technique can be utilized at several dredging projects. Therefore a flexible solution seems to be a good solution.

A flexible to mount, easy to mobilise conversion kit to be installed on a multi purpose vessel is such solution. When for the dredging contractor, because of the limitations inherent to this technique, no water injection dredging can be used; the kit can be dismounted and sent to another place.
This will certainly reduce mobilisation costs. With modest mobilisation costs for the kit, the water injection technique could become more and more cost-effective on smaller projects.

Water jets surrounded by an air film

F.R.S. Vinke[1]; A.J. Nobel[2] and A.M. Talmon[3,4], *Member, CEDA*

Abstract:
The effect of introducing an air film around a water jet is examined in laboratory experiments. The objective is to reduce the friction forces between the water jet and the ambient fluid, making a jet potentially more effective at a larger distance. The test were conducted at a physical scale comparable to dredging practise, contrary to earlier experiments reported in the literature, where small scale jets were tested. During the tests the development of the jet was measured in axial and radial direction. The jet pressure and air discharge were varied, leading to a number of combinations of jet pressures and air discharges. The results showed that also at this scale the development of the water jet is influenced by the air film, although not as much as in the earlier experiments. Governing parameters have been established. Examples are the volume, mass and momentum ratios between the air flow and water flow. The ratios of the air flow and water flow were not in the same order if the comparison is made between the large and small scale water jets. Relatively less air was added in our tests. A description of the results of a water jet surrounded by an air film with a nozzle diameter of 3 cm is formulated based on the description of a submerged water jet according Rajaratnam (1976) and a description of water jet with an air film with a nozzle diameter of 2 mm according Yahiro and Yoshida (1974).

Keywords: Water jets, air film, experiments

Nomenclature:

c	= shift of theoretical line	[m]
c_1 ,c_2	= scaling parameters	[-]
D_n	= nozzle diameter	[m]
L	= length of potential core	[m]
p	= stagnation pressure	[bar]
p_0	= exit pressure of the jet	[bar]
$Q_{air,in}$	= air discharge added to the jet	[m^3/s]
$Q_{air,netto}$	= amount of air used to create air film	[m^3/s]
Q_{entr}	= amount of entrainment	[m^3/s]
u	= velocity at the centre line of the jet	[m/s]
u_0	= exit velocity of the jet	[m/s]
x	= distance to the nozzle	[m]

[1] Ir. F.R.S. Vinke, Delft University of Technology, The Netherlands
[2] Ir. A.J. Nobel, Boskalis, Rosmolenweg 20, Papendrecht, 3350 AA, The Netherlands, T: +31 78 6969441,
Email: A.J.Nobel@boskalis.nl, www.boskalis.com
[3] Dr. Ir. A.M. Talmon, Delft University of Techonology, Mekelweg 2, Delft, 2628 CD, The Netherlands, T: +31 15 2783717,
Email: A.M.Talmon@tudelft.nl
[4] Deltaris, Rotterdamseweg 185, Delft, 2629 HD, T: +31 88 3358174, Email: Arno.Talmon@deltares.nl

1 Introduction

1.1 Problem definition:

In dredging practice jets are used to excavate soil. To excavate soil a minimum stagnation pressure (in clay) or jet velocity (in sand) is needed. The jet velocity and stagnation pressure of a submerged jet decreases as a result of ambient fluid that is entrained into the jet. So, the distance over which soil is excavated is limited.
By introducing an air film around the jet the amount of entrained water will decrease, resulting in larger velocities, making the jet more effective at larger distances.
Previous research, Ginniken et al (2006), on water jets surrounded by an air film showed in comparison to water-in-water jets an increase of the potential core from 6 up to an axial distance of 36 nozzle diameters. The potential core is defined as the distance over which the stagnation pressure at the centerline equals the exit pressure, of the jet. The experiments of Ginniken et al were conducted with a nozzle diameter of 3 mm. This scale is small relative to the scale of dredging practice, ca. 3 cm. Until this research no other research has been carried out to examine the effect of an air film around a water jet at the scale of 3 cm.

1.2 Objectives:

This research has been carried out to examine the effects of an air film around a water jet at the scale of 3 cm. The velocities were measured in axial and radial direction at a number of positions to examine to what distance the effect of an air film is observed. The objective is to determine the amount of air required to create an effective air film and to examine if there is an optimum air discharge. Quantification is made of the thickness of the air film and the distance over which the air film is present.

2 Experimental setup

A schematic overview of the setup in the flume is given in Figure 1. The numbers in the figure corresponds with 1) water discharge meter 2) jet pressure transducer 3) air discharge meter 4) orifice plate 5) Pitot tube 6) array of conductivity probes 7) EMS.

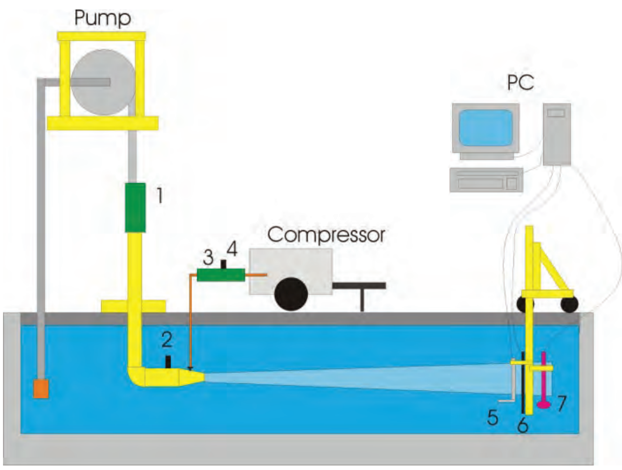

Figure 1 Schematic overview of the setup in the flume

The measurements were conducted in a flume with dimensions 30*2.4*2.2 m (L*W*H). The experimental setup consists of two main parts: the construction of the jet with air film and the carriage with measurement probes. The construction of the jet with air film is connected via hoses to a pump and a compressor.
The discharge of the water flow was measured by a discharge meter, while the air discharge was measured via an orifice plate. The air discharge was regulated by a valve. During the experiments two compressors were used, with a maximum total air discharge of 90 l/s. This air discharge is given for atmospheric conditions. The water depth in the flume was 1.8 m and the nozzle was situated 0.75 m above the bottom of the flume. In the direction perpendicular to the flow the nozzle was situated at centerline of the flume.

The dimensions of the nozzle are:
The diameter of the nozzle is 30 mm

The inner diameter of the annular air slit is 36 mm
The outer diameter of the annular air slit is 44 mm

Figure 2 is a drawing of the nozzle and annular air slit.

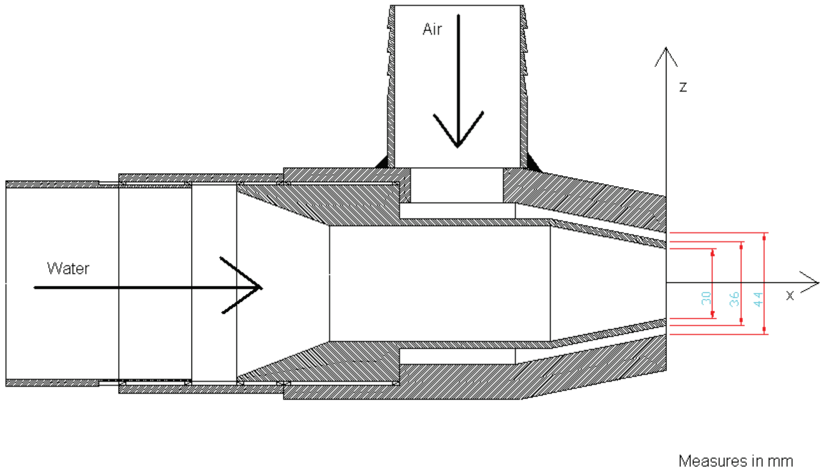

Figure 2 Drawing of the nozzle and coordinates

Since the rail bounded carriage could be positioned at any position above the flume, the measurement probes could be placed at different axial distances. For the measurement of the velocity profiles in radial direction the frame with the measurement probes could be shifted in vertical and horizontal direction.
The measurement probes mounted on the frame are: pitot tube, EMS and an array of conductivity probes. A technical drawing of the frame with the measurement probes is given in Figure 3.

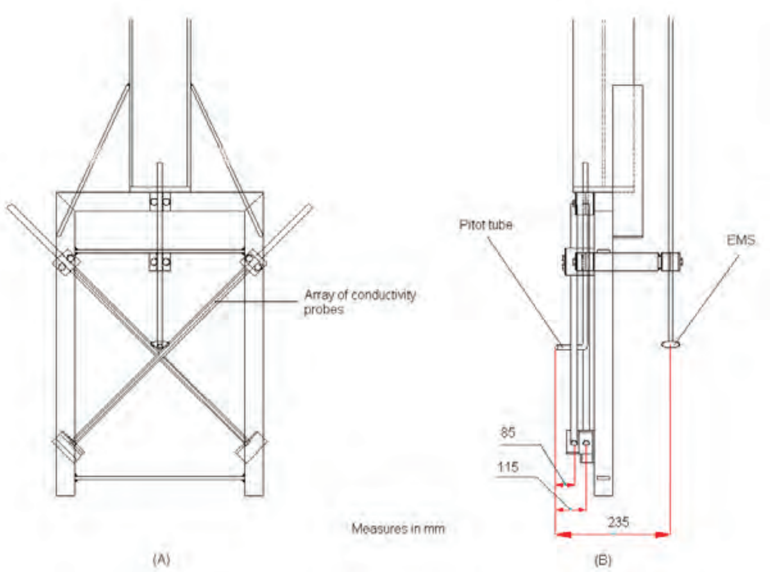

Figure 3 Frame with the measurement probes

The dimensions of the pitot tube were: inner diameter=3mm, outer diameter= 10 mm. To be able to determine the velocities from the measurements with the pitot tube the density of the air-mixture has to be known. The density of the air-water mixture is determined by an array of conductivity probes. The distance between the pairs of probes was 40 mm. The velocity range of the EMS was too small. So, the measurements with this device are not used in the elaboration and analysis of the data.

3 Results

During the experiments a part of the air added to the water jet was ascending to the water surface, as a result not all the air is used to create an air film. The air ascending to the water surface was collected in a large upside-down bucket. In this submerged bucket the pressure was measured to determine the amount of escaped air that was not available to create an air film. Figure 4 shows the amount of air used to create an air film ($Q_{air,netto}$: $Q_{air,in}$ minus the air discharge ascending to the water surface) as a function of air discharge ($Q_{air,in}$) for a number of jet pressures. The amount of air in the air film increases with increasing jet pressure and air discharge added to the jet.

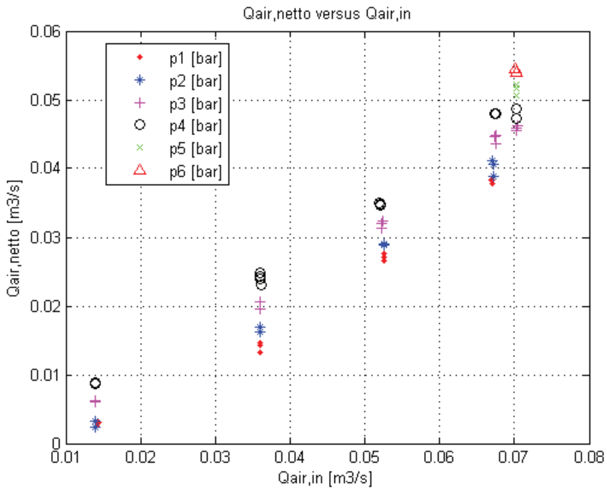

Figure 4 Qair,netto versus Qair,in[5]

Figure 5 is a plot of the velocities at a number of axial distances for one jet pressure and different air discharges. The measured velocities at the centerline for jets without an air film are almost similar as the expected velocities incase of a jet without air film. The expected velocities are described according Rajaratnam (1976):

$$u = 6.3 * u_0 * \frac{D_n}{x} \tag{1}$$

wherein u is the velocity [m/s], u_0 is the exit velocity of the jet [m/s], 6.3 is a scaling parameter [-], D_n the nozzle diameter [m] and x the axial distance to the nozzle [m].

If the air discharge is varied for a constant jet pressure, the velocities at the centerline increase in the domain between 6 and 36 nozzle diameters. Beyond the axial distance of 36 nozzle diameters the axial velocities at the centerline of the jet are smaller than expected for a jet without an air film.
For larger air discharges, the increase of the velocities at the centerline of the jet is smaller with increasing air discharge.

[5] Because of competitive interests of Boskalis, certain values have been omitted'

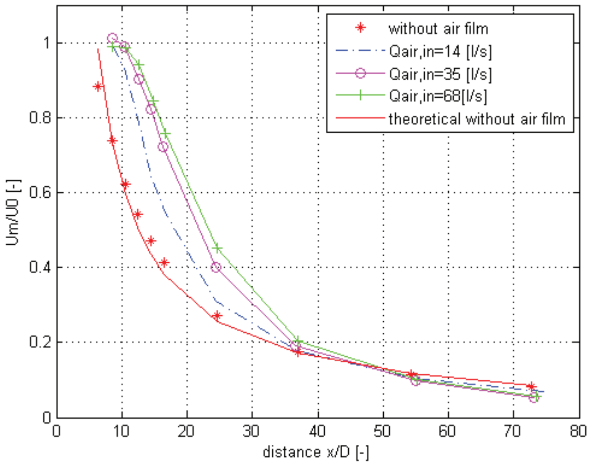

Figure 5 Normalized velocities versus axial distance for a number of air discharges

Figure 6 is a plot of the normalized axial velocities at the centerline of the jet if the air discharge is constant and the jet pressure is increased. As shown in the figure the influence of the air film increases with jet pressure. The jet pressure of the jet of Ginniken et al is 10 times larger than the jet pressure used in our tests. The air discharge added to the in the test of Ginniken is 7 l/s. The plot shows in case the jet of Ginniken et al an increase of the velocities at the centerline of the jet up to larger distances.

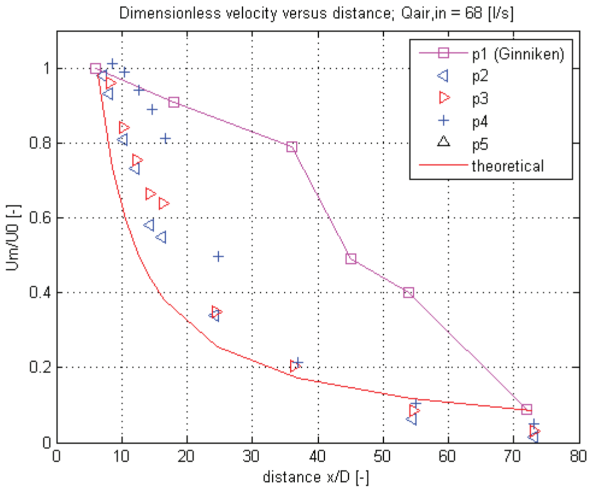

Figure 6 Normalized velocity versus axial distance for a number of jet pressures

For a number of axial distances the air discharge is increased to examine if a minimum and an optimum exists.
In Figure 7 an increase of the velocity at the centerline is observed for air discharge up to 40 l/s at an axial distance of 12 nozzle diameters. Beyond this air discharge, at an axial distance of 24 and 36 nozzle diameters an increase of the velocity at the centerline of the jet is still observed.

So for large axial distances a minimum air discharge is required to create an effective air film.
Beyond the air discharge of 40 l/s the velocity at the centerline of the jet at a distance of 12 nozzle diameters reached a maximum value. At a distance of 24 nozzle diameters a maximum of the velocity at the centerline of the jet is reached at an air discharge of 50 l/s. At an axial distance of 36 nozzle diameters no maximum velocity is observed.

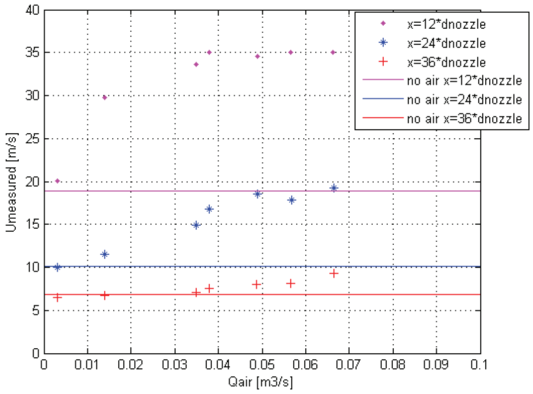

Figure 7 Velocity versus air discharge at a number of axial distances

Velocity profiles were measured at axial distances of 8, 12, 24 and 38 nozzle diameters. The velocity profiles are plotted in Figure 8. The measured velocity profiles are different in comparison to the expected velocity profiles of a jet without an air film.

The velocity profiles measured for a jet with an air film have a larger peak velocity at the centerline and the width of the profile is narrower. This is observed at an axial distance of 8, 12 and 24 nozzle diameters. At a distance of 36 nozzle diameters the velocity profile is almost similar to the expected velocity profile for a jet without an air film.

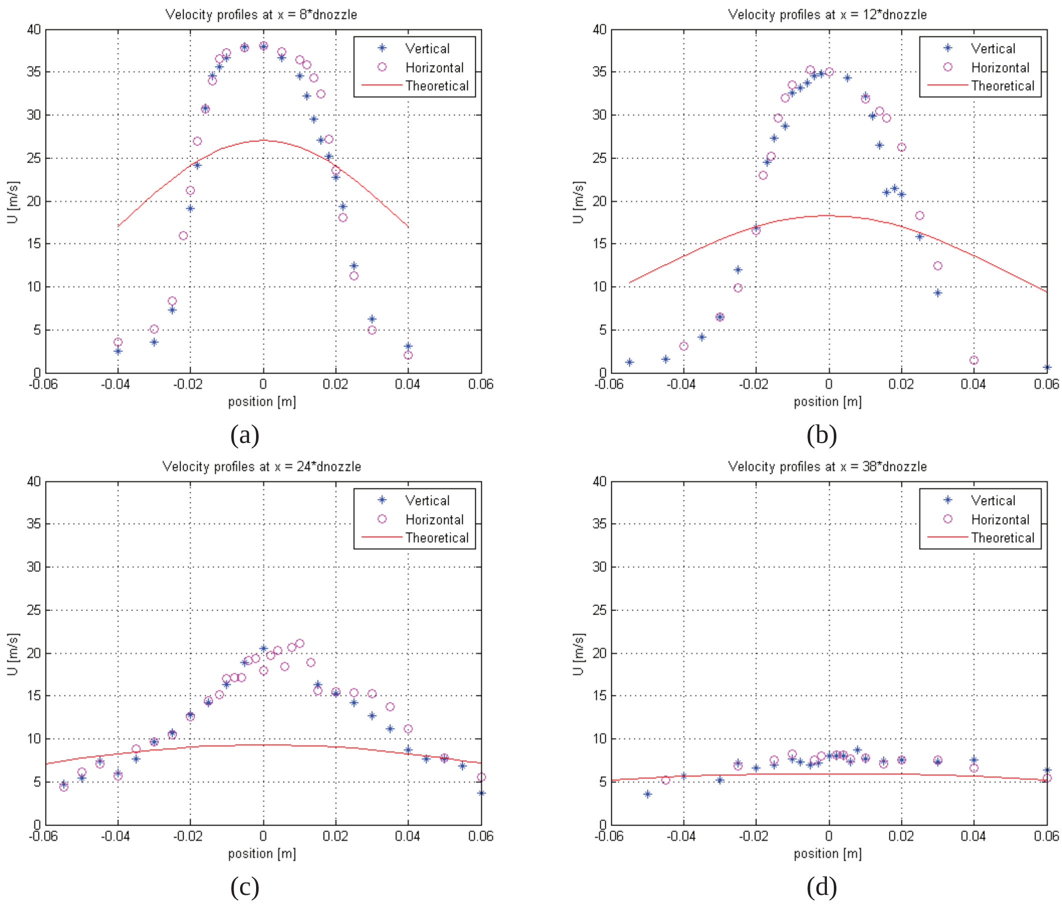

Figure 8 Horizontal and vertical velocity profiles at x=8*D_n, x=12*D_n, x=24*D_n, 38*D_n.

The densities measured at the centerline of the jet are given for two jet pressures and a constant air discharge (see Figure 9). Both jet pressures show a drop in the density over a certain distance. The drop of the density of the higher jet pressure is larger and the axial extent of this drop is also larger than the lower jet pressure. The distance over which air is trapped at the centerline of the jet is larger for higher discharges.
So, a jet with higher pressure is capable to drag the air film over a longer distance.

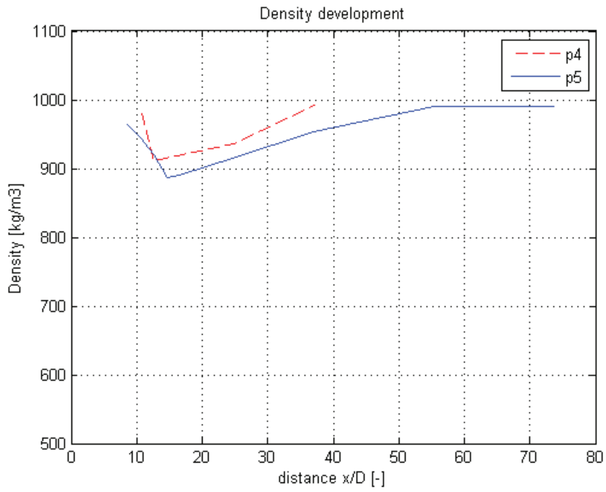

Figure 9 Density at the centerline of the jet in axial direction

The density profiles are measured at the axial distances of 8, 12, 24 and 38 nozzle diameters (see Figure 10). At the axial distances of 8 and 12 nozzle diameters the presence of an air film is observed as a drop in the density profile between 35 mm and 60 mm in radial direction from the centerline of the jet. At 24 and 38 nozzle diameters the densities are between 900-1000 kg/m^3 and no drop below 900 kg/m^3 is observed.

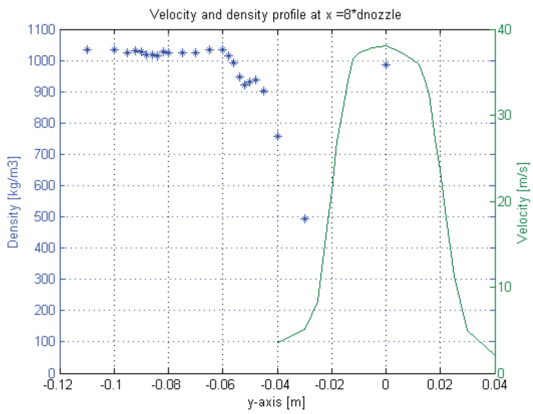

(a)

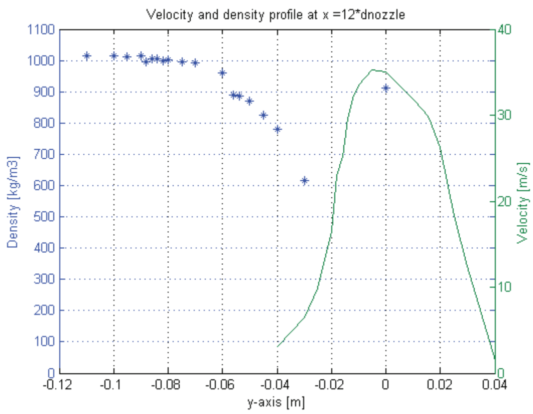

(b)

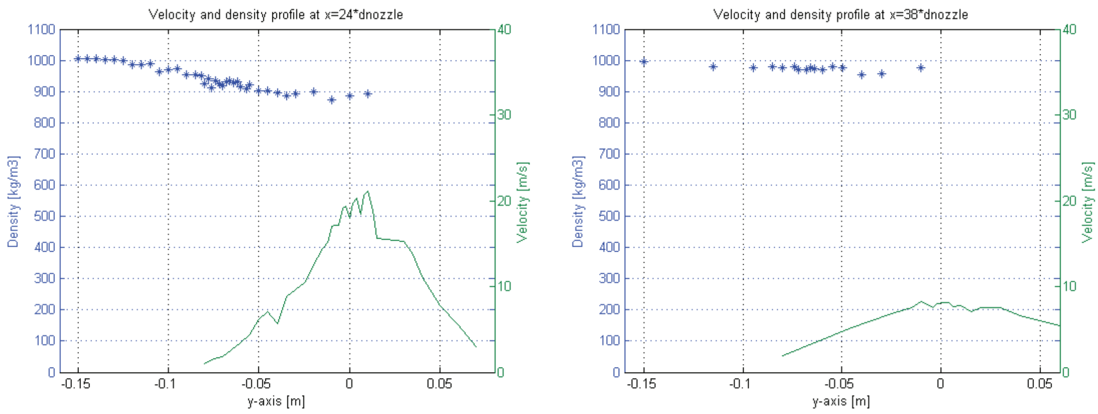

(c) (d)

Figure 10 Density and velocity profiles at distances (a) x=8*D_n; (b) x=12*D_n; (c) x=24*D_n; (d) x=38*D_n

4 Analysis

As seen from the results the introduction of an air film around a jet leads to an increase of the velocities at the centerline of the jet in a certain domain of axial distances. The velocity profiles measured for a jet with an air film has a higher velocity at the centerline and the width of the velocity profile is narrower.
However, for the nozzle of 3 cm, the domain wherein the velocities at the centerline increases is smaller than the domain incase of an nozzle with a diameter of 3 mm.
A number of parameters were determined to examine a possible explanation for the different effects of the air film between the small and large scale water jets.

The main differences are: Dnozzle, pjet, Qair/Qjet and Qair/Qentr. In the last two parameters Q_{air} is the amount of air added to the jet, Qjet is the discharge of the jet and Q_{entr} is the amount of entrainment of the jet. In these parameters the amount of air are compared to the jet discharge respectively the entrainment discharge. Other parameters as Reynolds number, Weber number are of the same order.

The difference is found in the jet pressure and Qair/Qjet. In both tests the thickness of the air film was equal.

5 Description

A description of the result is based on two other descriptions: the description according to Yoshida and Yahiro (1974) of a water jet surrounded by an air film, based on measurements with a nozzle of 2 mm and the description according Rajaratnam (1976) of a submerged water jet.
The theoretical background of the description is that the air film acts as a separation between the jet and the ambient fluid and in ideal conditions the description of a submerged water jet is shifted over the distance over which an air film is present.
In the axial direction the domain is divided in two main regions for which one of the mentioned descriptions can be applied.

x/D = 6-24 $$p = p_0\, e^{c_1 (x-L)^{c_2}} \qquad (2)$$

x/D >24 $$u = 6.3 * u_0 * \frac{D_n}{x-c} \qquad (3)$$

with

p = stagnation pressure [bar]
p_0 = exit pressure of the jet [bar]
c_1 ,c_2 = scaling parameters [-]
u = velocity at the centre line of the jet [m/s]

u_0	= exit velocity of the jet	[m/s]
D_n	= nozzle diameter	[m]
x	= distance to the nozzle	[m]
c	= shift of theoretical line	[m]
L	= length of potential core	[m]

Typical values of the scaling parameters are c_1 =-0.002 to -0.05 and c_2 = 1.2 to 2.1.
The axial position of 24 nozzle diameters is chosen, because beyond this distance an air film is not present.
The factor c/Dn is the shift of the description of a submerged water jet according Rajaratnam (1976).
For example, for an air discharge of 68 l/s a shift c of 11 nozzle diameters is found. The description of the data is plotted in Figure 11. The data and description are almost similar to each other.

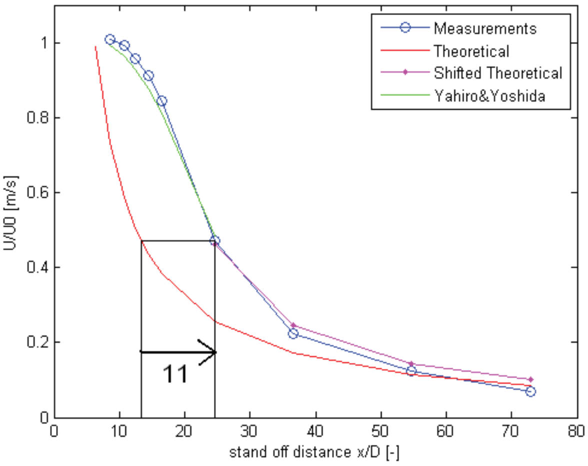

Figure 11Description of the data

6 Conclusions
The experiments have shown that the velocities at the centerline of the jet increases. The domain over which this increase is found is between 6 and 36 nozzle diameters. The air film is present up to a distance of 24 nozzle diameters.
The velocity profile of a jet with an air film has a higher velocity at the centerline of the jet and the width of the velocity profile is narrower.
The domain over which an increase of the velocities is observed at the centerline of the jet is smaller than the domain of the previous research of Ginniken et al (2006). An explanation is the amount of air added to the water jet and jet pressure. At the scale of a 3 cm nozzle relatively less air is added to the jet, than at the scale of 3 mm nozzle.
A description setup in this research gives similar results compared to the measurements. The description is based on two descriptions: a submerged water jet according to Rajaratnam (1976) and small scale water jets with an air film according to Yahiro and Yoshida (1974).

References

- **Ginneken R. et al** (2006). Verbeteren van de stuwdruk van een water jet onder water, BSc-thesis, 3ME, TU Delft, Delft.
- **Rajaratnam N.** (1976). Turbulent jets, Elsevier, Amsterdam
- **Yahiro T. and H. Yoshida** (1974). On the characteristics of high speed water jet in the liquid and its utilization on induction grouting method, second international symposium on Jet cutting technology, Cambridge.

USING FLOCCULANTS TO ENCLOSE SILT PARTICLES IN THE PORE VOLUME OF SAND

J.N.Mol[1,2], dr. ir. A.M. Talmon[3,4], ir. A.J.M. van Hemmen[5]

Abstract: Discharging dredged soil containing a large silt fraction (particle diameter d < 0.063 mm) into a reclamation area causes various problems at the fill area or surrounding environment. Typical problems are 1) exceeding of turbidity requirements with possibly environmental damage. 2) non-homogeneous soil properties of the reclamation area,

The settling behavior of a particle is partly a function of its size and density, the smaller the particle, the lower the settling velocity. Different settling behavior of the particles leads to a separation of particles out of the discharged soil-water mixture over the path of the process water flow between discharge pipeline and weir box of the reclamation area. Very small particles will escape with the process water through the weir box.

To create a homogeneous soil layer over the entire reclamation area the use of flocculants has been tested in a laboratory sand fill model. A solution of fresh water and an anionic or cationic flocculant ($1 \cdot 10^{-3}$ $^{kg}/_{L}$) has been added to the outgoing flow of the discharge pipeline. Doses flocculant per kilogram dry silt ranged between $5 \cdot 10^{-6}$ $^{kg}/_{kg}$ and $1 \cdot 10^{-3}$ $^{kg}/_{kg}$. The silt fraction flocculated and settled down between the larger particles of the mixture, resulting in a homogeneous soil layer. Due to the pore space of the flocks the permeability of the total soil layer increased compared with a soil layer containing silt pockets. The outgoing process water left the water box without any particles. The possibly environmental load according to the use of a flocculant depends of the type of flocculant used and the dose.

Keywords: dredging, reclamation, silt, environment, turbidity, flocculant

---

[1] MSc-student, Offshore Engineering, Delft University of Technology, j.n.mol@boskalis.nl
[2] Production Engineer, Royal Boskalis Westminster nv, Rosmolenweg 20, Papendrecht, 3356 LK, tel.: +31 (0)78 6969 574, email: j.n.mol@boskalis.nl
[3] Assistant Professor, Dredging Engineering, Delft University of Technology, Mekelweg 2, Delft, 2628 CD, tel.: +31 (0)15 278 3717, email: A.M.Talmon@tudelft.nl
[4] Senior Researcher, Deltares, Rotterdamseweg 185, Delft, 2629 HD, tel.: +31 (0)88 335 8174, email: arno.talmon@deltares.nl
[5] Senior consultant, Eijkmanstraat 5, Papendrecht, 3356BL, tel.: +31 (0)78 641 23 60, email: vanhemmen@zonnet.nl

1. INTRODUCTION

On reclamation dredging campaigns the issues 'handling fines' and 'turbidity conditions' grow stronger, driven by environmental, political, economical and practical developments. Dredged material containing a relative high silt fraction (with silt defined as particles with diameter $d < 63$ µm) can cause problems at or around the reclamation areas. Typical problems at the reclamation area are: relative huge dimensions of the settling basins, existence of silt lenses within the discharged soil layers, inferior soil mechanical quality and insufficient dewatering capacity. The problems around the reclamation area can be described as limit exceeding turbidity limit and inefficiency of the dredging works; the suspended silt volume causes turbidity. The dredging activities can be stopped temporary by the client or government if the turbidity values exceed prescribed limits and if the soil quality of the reclamation area doesn't meet the agreed standard. In such cases the dredging contractor needs more effort to improve the soil quality.

To handle siltation problems, several approaches already exist, like silt screens and settling basins. This research describes the search for a solution to catch the silt particles and enclose them in the pore space of the sand skeleton by means of flocculants [Mol, 2008].

2. COLLOIDS

2.1 Settling velocity of colloid particles

The settling behavior of a particle is partly a function of its size, the smaller the particle, the lower the settling velocity. Different settling behavior of the particles leads to a separation of particles out of the discharged soil-water mixture over the path of the process water flow between discharge pipeline and water box. Very small particles will escape with the process water through the water box.

Colloid particles with a nominal diameter $d < 10$ µm show a different settling behavior compared to larger particles due to electrostatic surface effects. Colloidal particles often carry an electrical charge and therefore attract or repel each other according to *Coulombs law*. If the gravitational forces on the colloids are small compared to the electrostatic forces acting on the particles, the colloids do not settle in vertical direction but will follow the Brownian motion. The Brownian motion is the seemingly random movement of particles suspended in a fluid (i.e. a liquid or gas), caused by collision or repulsion between particles. The charge of particles depends on the electro-chemical properties, size and shape of the particle.

2.2 Electro-chemical forces

The cohesion of fine clays is due to their electro-chemical properties. Fine clay particles are negatively charged at their face and they may be surrounded by a cloud of cations, whose concentration is very high in the Stern layer, immediately adjacent to the particle surface, and decreases in the outer Gouy layer; these together form the so-called diffusive double layer, Figure 1 (a). The double layer is characterized by the ζ-potential ζ_0 at the water/particle interface, which decreases proportionally to the ion concentration, Figure 1 (b). The thickness of the double layer can vary largely for different minerals and ion concentration in the medium, and also according to the balance between attractive electrical forces and diffusion within the medium [Maggi, 2005]. The interaction between two approaching particles is governed by the interaction of their double layer, Figure 1 (c): a first repulsive electrical force tends to separate the particles; if this is overcome at a certain distance, then collision may occur and the particles may be kept attached to each other by attractive forces.

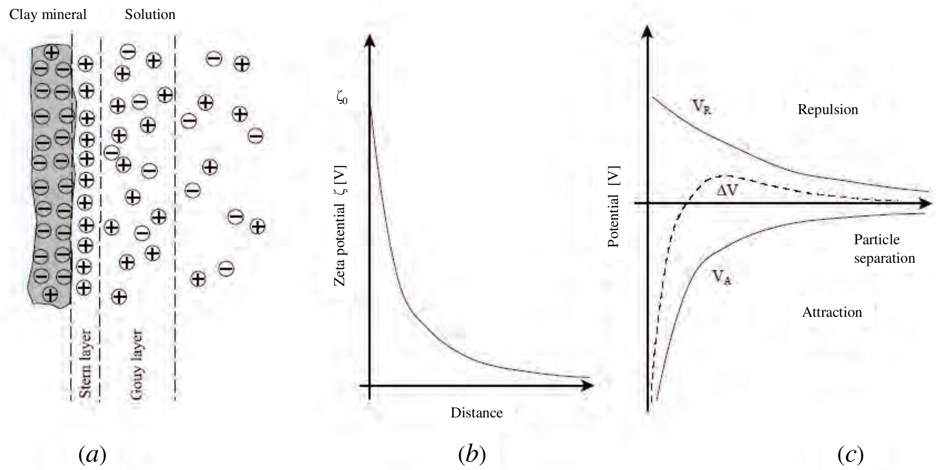

Figure 1. (a) schematic representation of the electric double layer surrounding the particles. (b) qualitative representation of the ζ -potential as a function of the distance from the surface of the particle. (c) potential energy corresponding to the double layer interaction for two approaching particles, where VR and VA are the potential energies associated with repulsion and attraction respectively, with ΔV the electrical barrier [Maggi, 2005].

The energy of the electrical barrier can vary widely as a function of ion concentration. The presence of salt in natural water produces free ions and cations that cause a decrease of the energy barrier, and ultimately an elimination for mid to high salt concentrations.

The addition of an opposite loaded polymer or electrolyte (i.e. flocculants) destabilizes the solution because the electrostatic load of suspended colloidal particles will be neutralized.

2.3 Flocculants

Flocculants, or flocculating agents, are chemicals that promote flocculation by causing colloids and other suspended particles in liquids to aggregate, forming a floc. Flocculants are used in water treatment processes to improve the sedimentation or filterability of small particles. Flocculation and sedimentation are widely employed in the purification of drinking water as well as sewage treatment, storm water treatment and treatment of other industrial wastewater streams.

Therefore, flocculants are often added to overcome the repulsive forces of the particles. The addition of flocculants is followed by low-shear mixing in a flocculator to promote contact between the particles, allowing particle growth through the sedimentation phenomenon called flocculant settling.

The three main types of flocculants are inorganic electrolytes (such as alum, lime, ferric chloride, and ferrous sulfate), organic polymers, and synthetic poly electrolytes with anionic or cationic functional groups.

The amount of flocculation that occurs depends on the opportunity for contact between particles, which will vary with the overflow rate, the depth of the settling basin, the velocity gradients in the system, the concentration of particles, and the range of particles sizes. The effects of these variables can only be accomplished by sedimentation tests.

2.4 Environment

The environmental load of the use of flocculants on a reclamation area depends on the flocculant type and dose, as well as the flocculation process. The flocculant should disappear with the silt particles as flocs into the pore space of the sand skeleton. It is up to responsibility of the dredging contractor to choose a suitable flocculant within the regulations of the (local) government. However organic polymers did not succeed during the tests, non-organic environmental friendly flocculant types were successful.

3 THE TESTS

Several flocculant solutions have been tested on seawater containing a range of silt volumes. To find an optimal flocculant dose for a silt/seawater mixture settling columns were used to observe the flocculation process and the settling velocity of the flocs. The silt fraction has been obtained by mixing of siltstone powder in fresh water. The siltstone originated from Bahrain and was provided by Boskalis.

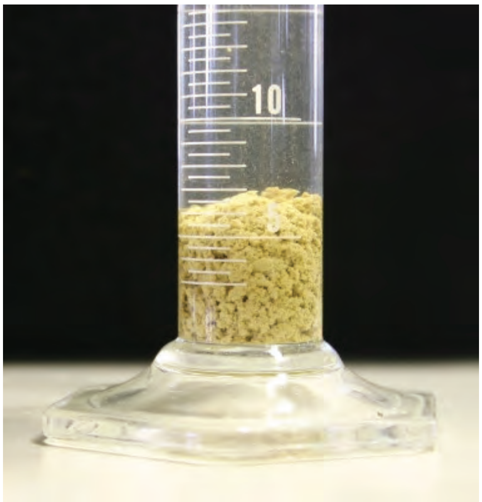

Figure 2. Example of settled flocculated silt, notice large pore spaces

3.1 Graduated glass tests

The search for an optimal flocculant type and dose to catch a given amount of suspended solids started in the laboratory. The effectiveness of different flocculant doses cleaning a range of turbidity levels has been compared in settling columns. A system of six settling columns has been used to test the effectiveness of one flocculant type and dose on six turbidity levels simultaneously. However a lot of tests were needed to find the right flocculant type and dose for a range of turbidity levels. Visual comparison gave a quick indication of the optimal result. Tests with a mixture of sand and silt pointed the same optimal flocculant type at the same dose but the average floc size was significant smaller.

The test showed no visible effect when the flocculant dose was too low. Injecting too much flocculant mixture showed a relative large filamentous floc structure while the turbidity in the settling column did not disappear.

3.2 Typical results of sand fill tests

To investigate the behavior of flocs in a sandfill, a 1-D sandfill model compatible to the TU Delft miniature slurry circuit was built [Cartigny et al, 2007]. Figure 3 shows a schematic overview of the slurry circuit.

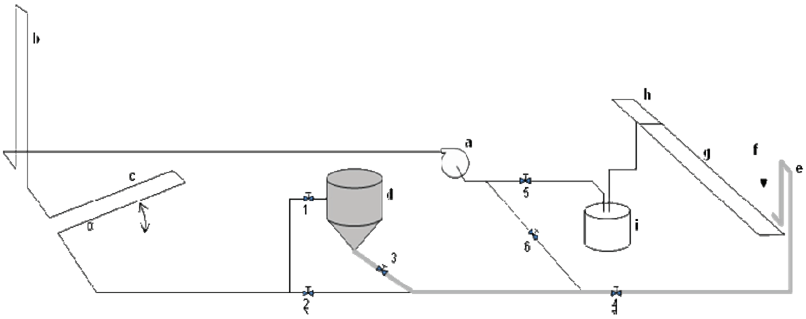

a	Sand pump
b	Vertical measuring column
c	Turnable test arm
d	Cyclone
e	Discharge pipe line
f	Flocculant supply
g	Sandfill model
h	Weir box
i	Buffer tank
1 … 6	Valve

Figure 3. Schematic overview of the TU Delft slurry circuit

The length of the sand fill model is 4.00 meter, the width is 0.12 meter. The model was equipped with a discharge pipe, perspex walls, and a weir box. The perspex slurry circuit was used to mix and to deliver the sand and silt mixture via a discharge pipe into the sand fill model. The process water ran through the weir box back into the slurry circuit. Tests with a sand and silt mixture, with no addition of flocculants showed a separation of sand and silt. The sand fraction settled, the silt fraction stayed in suspension and escaped through the weir box. In prototype this would cause considerable turbidity. Tests with addition of a flocculant mixture showed quick floc forming immediately after supply of the flocculant into the sand silt mixture. A solution of fresh water and an anionic or cationic flocculant ($1 \cdot 10^{-3}\ ^{kg}/_{L}$) has been added to the outgoing flow of the discharge pipeline. Doses flocculant per kilogram dry silt ranged between $5 \cdot 10^{-6}\ ^{kg}/_{kg}$ and $1 \cdot 10^{-3}\ ^{kg}/_{kg}$. The flocs settled between the sand particles and formed a homogeneous soil layer. The process water was visually clear.

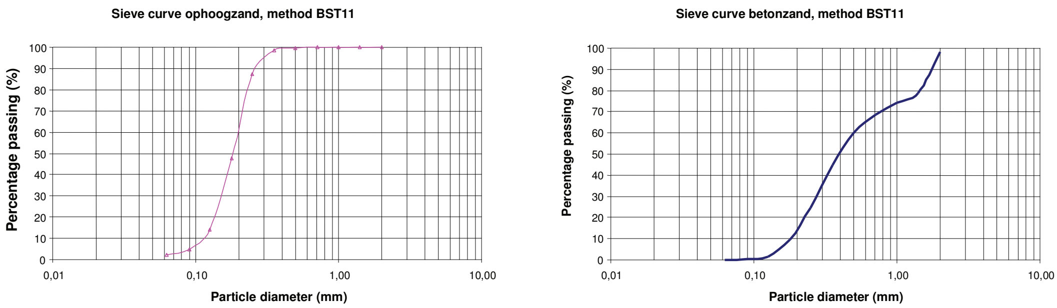

Figure 4. Particles distribution functions of sand 1 (left) and sand 2 (right)

To investigate the amount of silt enclosed in the sand pores, soil samples from 4 fixed positions equally divided over the length of the sandfill model have been analyzed in the laboratory. Location 1 was located at the discharge pipe line supplying the ‘dredged mixture’. Location 4 was located at the weir box and the locations 2 and 3 were located in between.

3.2.1 Typical results of sand fill tests

During the tests the sand/silt/water mixture entered the sand fill model by the discharge pipeline, see point A at Figure 5. This was also the location of the flocculant mixture injection. The turbulence caused contact between the flocculant mixture and the fine materials. Due to the turbulence level the particles and flocs did not settle during the transport at point B but settled at the talud in the low turbulence and low velocity zone located at point C.

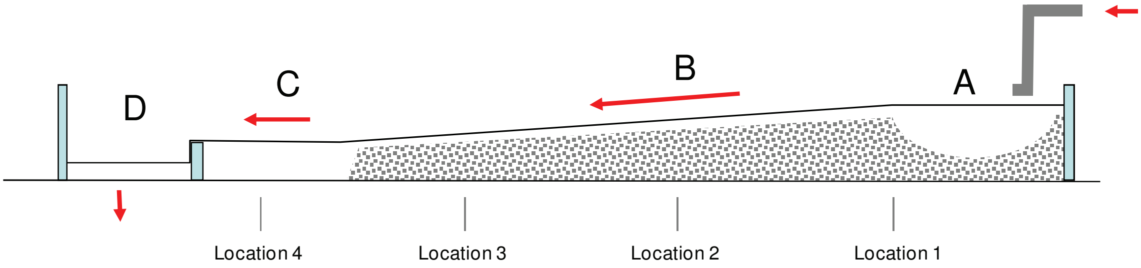

Figure 5. Schematic view of the sand fill model

Finally the process water entered the weir box at location D without particles (visually) and left the sand fill model.

This process is also demonstrated in Figure 6. This figure shows the development of the sand fill, for demonstration purposes showed with brown colored sand (d_{50} = 350 µm) and white sand (d_{50} = 120 µm). For particle distributions used during the flocculant tests, see Figure 4.

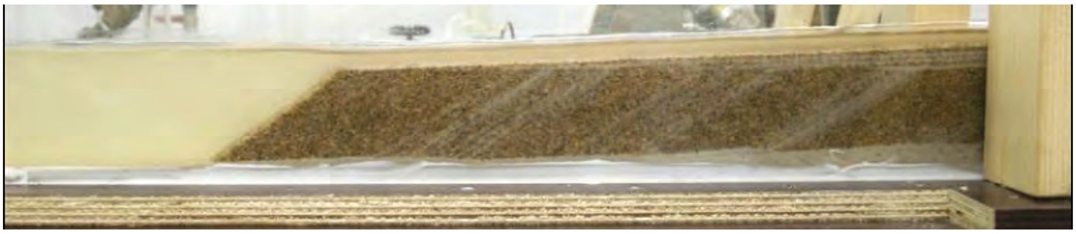

Figure 6. The settling process, for demonstration purposes showed with two different types of sand.

After transportation over the existing bed layer, the particles settled into the talud at the left side of the picture. A typical mixture flow during the test was 2.0 $^{L}/_{s}$. A typical flocculant mixture flow was 0.015 $^{L}/_{s}$.

The tests with the sand fill model showed that it is possible to enclose flocculated silt in the pore space of sand to obtain a homogeneous sand / silt layer. Figure 7 shows three different layers. The lowest layer is sand. The middle layer consists of silt flocs only and the upper layer is a homogeneous sand / silt layer. The three layers clearly showed a difference in color and structure. The shown result is from a test in which flocculant dosing and sand discharge varied in the beginning of the test, hence distinct horizontal layers were produced, well suited for illustration purpose. It is the objective to produce the homogeneous sand / silt layer, see Figure 8.

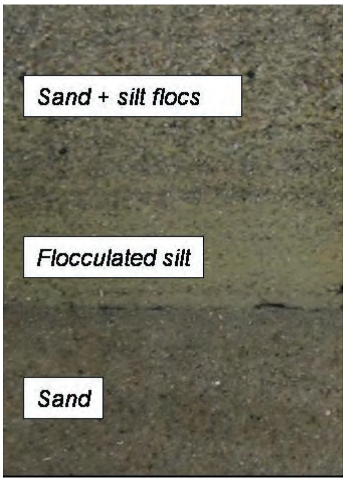

Figure 7. Different soil layers in the sand fill model.

Figure 8. The homogeneous sand / silt layer.

The dewatering properties of the homogeneous flocculated silt/ sand mixture became appearing after a test was finished and water drained from the depot. Compared with test conditions in which non homogeneous sand with silt lenses was produced, dewatering was faster. The relative density of the flocculated silt/ sand depot is lower than that of the relative density of the sand, which means that the pore space of the depot is larger. The usual compaction method as used on reclamation areas (e.g. compaction with bulldozers) is not taken into account.

A significant difference between using fresh water and sea water did not show up during the settling tests and the sand fill model test. One of the flocculants did not work in seawater. When an overdose of flocculant was supplied, the mixture showed the same phenomenon as seen during the tests with the settling columns.

The analysis of the soil samples provided additional information on the settling behavior of the sand silt mixture. The silt volume as percentage of the total sample volume is presented in Figure 9. Clear water discharged over the weir in these tests.

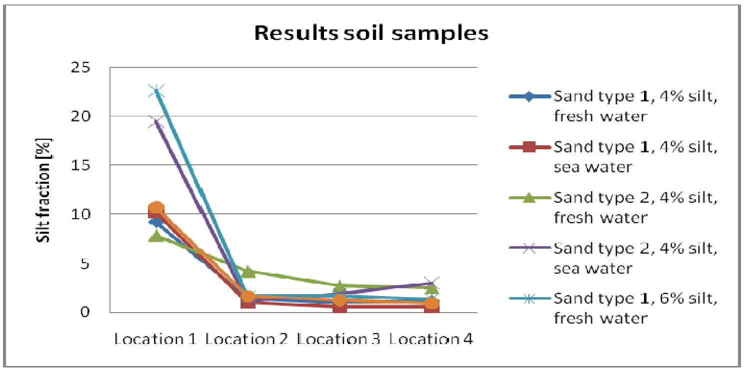

Figure 9. Results soil samples

However a percentage of 4% or 6% of silt (silt/sand ratio) was mixed through the sand of the slurry circuit, a percentage of up to 22.6% was found near the discharge pipe line of the slurry circuit.

Test:	Bore hole location 1 [% volume silt]	Bore hole location 2 [% volume silt]	Bore hole location 3 [% volume silt]	Bore hole location 4 [% volume silt]
Sand type 1, 4% silt, fresh water	9,19	1,36	0,99	1,15
Sand type 1, 4% silt, sea water	10,22	1,00	0,59	0,59
Sand type 2, 4% silt, fresh water	7,85	4,19	2,71	2,49
Sand type 2, 4% silt, sea water	19,46	1,17	1,89	2,97
Sand type 1, 6% silt, fresh water	22,63	1,66	1,65	1,34
Sand type 2, 6% silt, fresh water	10,69	1,62	1,24	0,92

Table 1. Measured silt content (silt/sand ratio)

The soil samples taken at location 1 (see Figure 5) structurally showed higher silt fractions than the soil samples from location 2,3 and 4 did. This did not agree with the visual observations during the sand fill tests. The silt as used in the tests contained undissolved siltstone particles with the size of sand particles which behaved like sand particles during settling into the sand fill model. These siltstone particles degraded to silt during the wet sieve tests in the laboratory. This effect has possibly affected the silt fraction as found at the sieve analysis. This implies that the silt-size fraction of the supply was lower than the 4% and 6% stated in Table 1 and Figure 9, and this implies that the results of the samples at location 2, 3 and 4 can not be quantitatively compared with the silt-size fraction of the supply flow.

4 CONCLUSIONS AND RECOMMENDATIONS

4.1 Conclusion

It is possible to enclose flocculated silt particles in the pore pace of a sand depot. The silt fraction flocculated and settled down with the larger particles of the mixture, resulting in a homogeneous soil layer. Due to the pore space of the flocs the permeability of the total soil layer increased compared with a soil layer containing silt pockets. The outgoing process water left the water box without any particles.

The possibly environmental load according to the use of a flocculant depends of the type of flocculant used and the dose. The injected flocculant type and dose depend on the silt fraction, the electro-chemical properties of the silt and the properties of the process water.

The tests have been influenced by:

- The silt as used in the tests must have contained undissolved siltstone particles with the size of sand particles which behaved like sand particles during settling into the sandfill model but still degraded to silt during the sieve tests in the laboratory. This effect has possibly affected the sieve analysis.

- Scale effects have not been taken into account because only the principle of enclosing silt in the pore space of sand has been taken into account, not the feasibility of the full scale use of flocculants.

4.2 Recommendations

The following recommendations are needed to improve the results and implement the concept of using flocculants to enclose silt particles in the pore space of a sand layer on a full scale project.

- In follow-up laboratory experiments, slurry preparation should be improved such that all silt-stone is disintegrated into silt-size particles.
.
- In such follow-up laboratory experiments, reference slurry samples should be taken of which the particle size distribution is to be determined by a less destructive method, such as the laser-diffraction method. Bed samples should be processed by the same method. The rheological properties of the flocculated slurry feed should also be determined as a basis for scale-up.

- Investigate dewatering and consolidation as well as the soil mechanical properties of sand / floc depots and the effect of usual compaction methods on the consolidation and dewatering properties.

- For optimization of the settling process of the sand/silt mixture, the flocculant dose and the controllability of floc forming related to the silt fraction in dredged material needs to be investigated.

- A feasibility study on use of flocculants on full scale dredging projects is needed.

REFERENCES

Cartigny M.J.B., Talmon A.M., Delfos R, Vlasblom, W.J. and Rosenbrand W.F., 2007, *On the relation between Hydraulic Losses due to Bends and Mixture Stratification,* Dredging Days 2007.

Huisman L., 1997, *Sedimentation*, Delft University of Technology.

Lu J. H., Wu L., & Letey J., 2002, *Effects of Soil and Water Properties on Anionic Polyacrylamide Sorption*, Soil Science Society of America Journal, VOL. 66, MARCH–APRIL 2002.

Maggi F., 2005, *Flocculation dynamics of cohesive sediment*, Doctoral Thesis for the Technical University of Delft.

Mol J.N., 2008, *Toevoegen van flocculant aan slibdeeltjes (eng: The addition of flocculant to silt particles)*, Patent number NL2001485 C1, Royal Boskalis Westminster nv.

Whitehouse R.J.S., Soulsby R.L., Roberts W. & Mitchener H.J., 2000, *Dynamics of Estuarine Muds, A manual for practical applications*, Thomas Telford Publications.

WORKING WITH NATURE

J. Brooke[1]

Abstract: Working with Nature, a recent PIANC position paper, calls for an important shift in thinking in our approach to navigation development projects. **Working with Nature** aims to help deliver mutually beneficial, 'win-win' solutions by promoting a proactive, integrated approach which:

- focuses on achieving the project objectives in an ecosystem context rather than assessing the consequences of a predefined project design;
- focuses on identifying win-win solutions rather than simply minimising ecological harm.

Keywords: ecosystem, win-win solution, stakeholder engagement, sustainable development

[1] Jan Brooke, PIANC Environmental Commission UK representative, 17 Suttons Lane, Deeping Gate, Peterborough, PE6 9AA, UK. T: +44 1778 345 979. E-mail: jan@janbrooke.co.uk

1 INTRODUCTION

During 2007 and 2008, PIANC's Environmental Commission (EnviCom), worked with their partner associations on EnviCom (particularly the Central Dredging Association (CEDA) and the International Association of Dredging Companies (IADC)) to prepare a position paper, the aim of which was to help the sector develop and deliver sustainable solutions to the provision of new navigation infrastructure. The **Working with Nature** position paper was thus prepared through an iterative process. It was submitted to PIANC's Executive Committee, and approved, in late 2008. CEDA and IDAC have also now endorsed the paper.

Working with Nature calls for an important shift in thinking insofar as it recommends considering the project objectives firstly from the perspective of the natural system rather than from the perspective of technical design. However, **Working with Nature** does not mean that we no longer achieve our development objectives: rather it ensures that these objectives are satisfied in a mutually beneficial way. Further, whereas it is acknowledged that a proactive approach such as **Working with Nature** should also be applied to the development of strategic plans and programmes, this position paper focuses particularly at the project level.

As well as describing the concept, the position paper discusses the extent to which **Working with Nature** can already be put into practice and some of the outstanding challenges. It is recognised that developing and delivering such win-win initiatives will take more innovation and imagination in some cases than in others. However, notwithstanding such challenges, PIANC is convinced that the rewards of **Working with Nature** will extend far beyond the natural environment into social and economic aspects.

The **Working with Nature** position paper is reproduced in Sections 2 to 5 below.

2 WHAT DO WE MEAN BY 'WORKING WITH NATURE'?

Maximising opportunities; reducing frustrations. **Working with Nature** is an integrated process which involves working to identify and exploit win-win solutions which respect nature and are acceptable to both project proponents and environmental stakeholders. It is an approach which needs to be applied early in a project when flexibility is still possible. By adopting a determined and proactive approach from conception through to project completion, opportunities can be maximised and - importantly - frustrations, delays and associated extra costs can be reduced.

Whilst the requirement to consider the potential environmental impacts of proposed projects for ports, navigation or associated infrastructure is well-established, the process of so doing is often complicated and difficult. If the design concept for a project has progressed before environmental issues are considered, the environmental impact assessment necessarily becomes an exercise in mitigation or damage limitation, potentially resulting in sub-optimal solutions and missed opportunities.

Working with Nature requires that a fully integrated approach be taken as soon as the project objectives are known – i.e. before the initial design is developed. It encourages consideration of how the project objectives can be achieved given the particular, site-specific characteristics of the ecosystem.

Working with Nature is about more than avoiding or mitigating the environmental impacts of a pre-defined design. Rather, it sets out to identify ways of achieving the project objectives by working with natural processes to deliver environmental protection, restoration or enhancement outcomes.

Fundamentally, therefore, **Working with Nature** means doing things in a different order:

(i) establish project need and objectives
(ii) understand the environment
(iii) make meaningful use of stakeholder engagement to identify possible win-win opportunities
(iv) prepare initial project proposals/design to benefit navigation *and* nature

A new way of thinking. **Working with Nature** thus requires a subtle but important evolution in the way we approach project development. We need to move towards an approach which:

- focuses on achieving the project objectives in an ecosystem context rather than assessing the consequences of a predefined project design;
- focuses on identifying win-win solutions rather than simply minimising ecological harm.

Working with Nature considers the project objectives firstly from the perspective of the natural system rather than from the perspective of technical design.

3 BUT CAN WE DO IT?

Working with Nature will undoubtedly pose significant challenges - in gaining acceptance of the concept and in ensuring that we have the scientific knowledge and understanding necessary to realise the potential benefits, whilst at the same time ensuring compliance with the ever-increasing national and international legislation and regulations. Nonetheless, it is important to recognise that significant progress has been made in a number of relevant areas over the past two decades, for example:

- we have achieved some important advances in technology, science and understanding, in modelling and design as well as in ecosystem functioning;
- we are starting to progress beyond documenting the natural state to understanding and predicting system dynamics;
- we are becoming better equipped to recognise and deal with uncertainty;
- we understand the importance of balancing economic, social, technical and environmental parameters, and of exploring the full range of potential solutions;
- we make more use of effective stakeholder engagement in contributing to a truly sustainable outcome.

Working with Nature represents a real opportunity for all future navigation-related developments. PIANC acknowledges that a concerted effort will be required to raise awareness of the concept and the benefits it offers. All parties potentially involved in development projects will need to be engaged in the transition: port and navigation authorities, governments and regulators, project developers, local communities, and environmental stakeholders. Some will undoubtedly find it difficult to accept or will be reluctant to accept the new way of thinking. Perseverance and patience will be vital. PIANC is convinced that **Working with Nature** is essential to future, sustainable, port and navigation development.

4 WHAT ELSE IS NEEDED?

Whilst technical and scientific knowledge and understanding has improved significantly over recent years[2], this does not mean that we have all the answers. **Working with Nature** requires an understanding of dynamic natural ecosystems. In some cases we already have a reasonable understanding, in others we do not. Although some research into ecosystem dynamics and cause-and-effect relationships is ongoing, more is needed. Data must be collected. Modelling tools need further development and verification. But these gaps in knowledge and understanding should not be used as an excuse to defer attempts to put **Working with Nature** into practice.

Many recent marine and inland water infrastructure projects have been delayed as a result of administrative procedures. Environmental regulations are not typically designed to stimulate development and innovation: indeed the relative lack of flexibility in the application of much environmental regulation could prove to be counter-productive insofar as the aims of **Working with Nature** are concerned. It will therefore become increasingly important to look to the intention of the legislation rather than taking a prescriptive approach to its implementation. A transition from a philosophy of ‘control’ to one of ‘management’ is needed and the cultural differences between ecologists, civil engineers, planners and politicians similarly need to be addressed if '**Working with Nature**' is to be embraced. Although these are real problems, they are not insurmountable.

5 WHY DOES IT MATTER?

Numerous research projects over recent years have highlighted the significant contribution aquatic ecosystems make to human economic well-being: e.g. water resources, nutrient cycling, food production, flood defence, recreation and tourism. The growth in world population, its increasing needs and the challenges of climate change are putting the natural environment under ever-increasing pressure. Notwithstanding the significant progress made in recent years, the current approach to assessing environmental impacts - no matter how well it is applied - typically results in an environmental loss. The approach is not, therefore, sustainable.

In the meantime, this growth translates into a global increase in trade and the associated need for new and/or more efficient waterborne transport infrastructure continues. We therefore need to use our improved knowledge and experience to begin to look at things differently - to facilitate the delivery of better environmental protection and/or enhancement alongside economic development; to reduce delays and frustrations; and to explore opportunities to provide local communities with much-needed amenity areas, recreational resources and improved landscapes.

Working with, rather than against, natural processes can result in less expensive and more sustainable solutions. Utilising natural processes rather than artificial means can offer viable, cost-effective long-term options. For example retaining dredged sediment within the estuarine system helps to sustain mudflats and salt marshes, and thus reduces the cost of flood defence maintenance. Exploring opportunities to use dredged material for beach nourishment is another well-established 'win-win' management option.

Working with Nature does not mean that we no longer achieve our development objectives: rather it ensures that these objectives are satisfied in a mutually beneficial way. Developing and delivering such win-win initiatives will take more innovation and imagination in some cases than in others, but PIANC is convinced that the rewards of **Working with Nature** extend far beyond the natural environment.

6 THE WAY FORWARD FOR PIANC

The **Working with Nature** position paper represents an important element of PIANC's future strategy: it will be actively promoted both within and outside the organisation as a necessary way to contribute to truly sustainable development.

[2] Recent projects which have sought to bring together some of this experience include: EMPHASYS (see www.estuary-guide.net/pdfs/emphasys_guide.pdf); Paralia Nature (see www.imieu.eu/index.php?option=com_content&task=view&id=47&Itemid=52); Building with Nature (see www.ecoshape.nl) and New! Delta (www.newdelta.org/navigatie/frameset.asp)

HINDERED EROSION OF GRANULAR SEDIMENTS

F. Bisschop[1], P.J. Visser[2], and C. van Rhee[3]

Abstract: In case of flooding of a polder, the inundation rate is one of the determining factors in predicting the resulting damage (casualties, damage infrastructure, economic damage, etc.). The inundation rate depends heavily on the flow velocity through the breach in the dike and the development of the breach in time, so on the process of erosion of the dike material. Existing sediment erosion formulae, like the Van Rijn formula (Van Rijn, 1993), overestimate the erosion rate of the breach in case of non-cohesive dike material. The same difference is encountered in dredging practice. Trailing suction hopper dredgers extract sand from the sea bed for reclamation purposes. As in the breaching process, the conventional erosion functions also overestimate the erosion rate during jetting.

Sediment erosion formulae like that of Van Rijn are basically pick-up functions of single particles in case of relative low flow velocities (0.5 tot 2.0 m/s). Flow velocities in dike breaches can increase to approximately 10 m/s. Typical flow velocities during jetting sand using a trailing suction hopper dredger are around 30 to 60 m/s. At these large flow velocities the erosion process is significantly influenced by the properties of the soil mass (non-cohesive particles). Governing parameters at higher flow velocities are dilatancy, permeability and the (un)drained shear strength of the soil. The sediment concentration in the water also influences the erosion process, especially in case of higher erosion rates.

Based on the concept presented by Van Rhee (Van Rhee, 2007) a simple analytical formula is derived that gives a clear insight into the parameters influencing hindered erosion. The concept of hindered erosion is explained by two properties of granular soils: dilatancy and permeability. This implicates that the erosion behaviour of granular soils cannot be described by the behaviour of single particles alone. The properties of the whole soil mass should be considered in predicting erosion at higher flow velocities. Results of a large-scale breach experiment performed in 1994 in the Zwin Channel (the Netherlands) are analyzed to evaluate the formula (Visser, 1998).

Keywords: erosion, granular sediments, breaching, jetting

[1] Senior Geotechnical Specialist, ARCADIS, Lichtenauerlaan 100, Rotterdam, 3062 ME, The Netherlands, T: +31 10 253 2222, F: +31 10 253 2194, E-mail: F.Bisschop@arcadis.nl, www.arcadis.nl and PhD Student, Faculty of Civil Engineering and Geosciences, Delft University of Technology, Stevinweg 1, Delft, 2628 CN, T: +31 15 278 4656, F: +31 15 278 5124, E-mail: F.Bisschop@tudelft.nl, www.tudelft.nl

[2] Associate Professor, Faculty of Civil Engineering and Geosciences, Delft University of Technology, Stevinweg 1, Delft, 2628 CN, T: +31 15 278 8005, F: +31 15 278 5124, E-mail: P.J.Visser@tudelft.nl, www.tudelft.nl

[3] Professor, Faculty of Mechanical Engineering and Marine Technology/Faculty of Civil Engineering and Geosciences, Delft University of Technology, Mekelweg 2, Delft, 2628 CD, T: +31 15 278 3973, F: +31 15 278 5602, E-mail: C.vanRhee@tudelft.nl, www.tudelft.nl

1 INTRODUCTION

In the Netherlands the safety level of a dike is expressed in terms of risk. Risk is defined as the product of the probability of inundation (failure of the dike) and the expected damage caused by the inundation (Visser, 1998). It is necessary to model the inundation process of the polder in order to be able to estimate this damage (casualties, damage infrastructure, economic damage, etc.). The process of polder inundation depends heavily on the flow velocity through the breach and the development of the breach width in time. The flow velocity in a breach is approximately 5 to 10 m/s. Due to these large flow velocities, the application of conventional sediment erosion formulae, like that of Van Rijn (Van Rijn, 1993), in breach models leads to significant overestimations of the breach growth.

The same difference is encountered in dredging practice. Trailing suction hopper dredgers extract sand from the bottom of the sea for reclamation purposes. A suction head is trailed over the sea bed and the granular sediment is loosened using water jets. Typical flow velocities are around 30 to 60 m/s (Van Rhee, 2007). As in the breaching process, the conventional erosion functions also overestimate the erosion rate during jetting.

2 TRADITIONAL EROSION FORMULA

Sediment erosion formulae like that of Van Rijn (Van Rijn, 1993) are basically pick-up functions of single particles. Particle movement will occur when the instantaneous fluid force on a particle exceeds the instantaneous resisting force related to the submerged particle weight and the friction coefficient. The incipient motion of a particle is related to the critical Shields parameter (θ_{cr}, Fig. 1):

$$\theta_{cr} = \frac{\tau_{b,cr}}{\left(\rho_s - \rho_w\right) \cdot g \cdot D_{50}} \tag{1}$$

in which:

$\tau_{b,cr}$	=	critical bed-shear stress according to Shields [N/m^2]
ρ_s	=	density of granular sediment [kg/m^3]
ρ_w	=	density of water [kg/m^3]
g	=	acceleration of gravity [m/s^2]
D_{50}	=	median particle diameter of granular sediment [m]

In (Van Rijn, 1993) the Shields curve is expressed in terms of the dimensionless mobility parameter θ and the dimensionless particle diameter D_*:

$$D_* = \left[\frac{(s-1)\cdot g}{\nu^2}\right]^{1/3} \cdot D_{50} \tag{2}$$

in which:

υ	=	kinematic viscosity of water [m^2/s]
s	=	relative density: ρ_s/ρ_w [-]

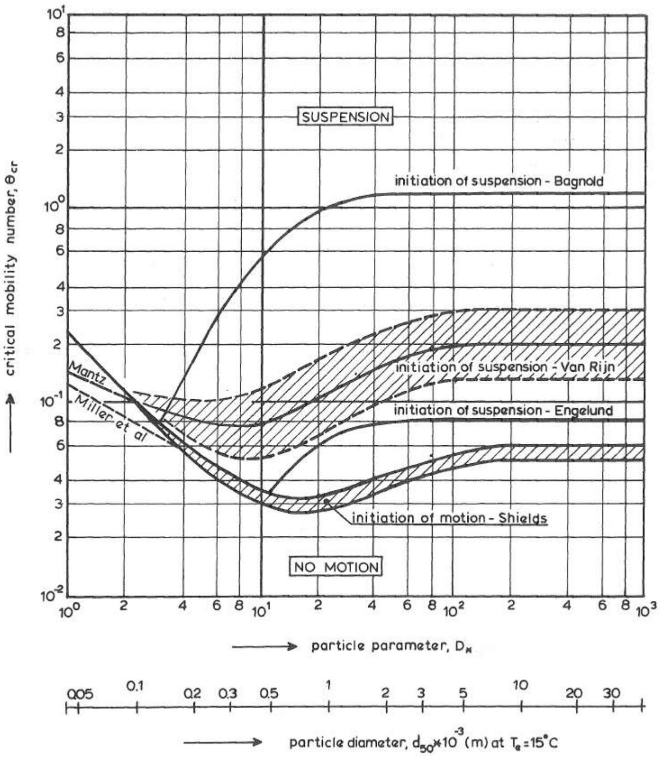

Fig. 1: Incipient motion and suspension for a flow over a plane bed (Van Rijn, 1993)

Van Rijn performed experiments to determine the pick-up rate of particles in the range of 130 to 1500 μm (Van Rijn, 1993). Tests were performed with mean flow velocities in the range of 0.5 to 1.0 m/s. Analysis of the experimental data yielded the following empirical pick-up function (E, see Fig. 2):

$$E = 0,00033 \cdot \rho_s \cdot \left[(s-1) \cdot g \cdot D_{50} \right]^{0,5} \cdot D_*^{\,0,3} \cdot T^{1,5} \tag{3}$$

$$T = \frac{\tau_b - \tau_{b,cr}}{\tau_{b,cr}} = \frac{\theta - \theta_{cr}}{\theta_{cr}} \tag{4}$$

$$v_e = \frac{E}{\rho_s \cdot (1 - n_0)} \tag{5}$$

in which:

E	=	pick-up rate in mass per unit area and time [kg/sm^2]
T	=	excess bed-shear stress parameter [-]
τ_b	=	bed-shear stress [N/m^2]
θ	=	dimensionless particle mobility parameter, see definition of θ_{cr} in formula (1)
v_e	=	erosion rate [m/s]
n_0	=	in-situ porosity [-]

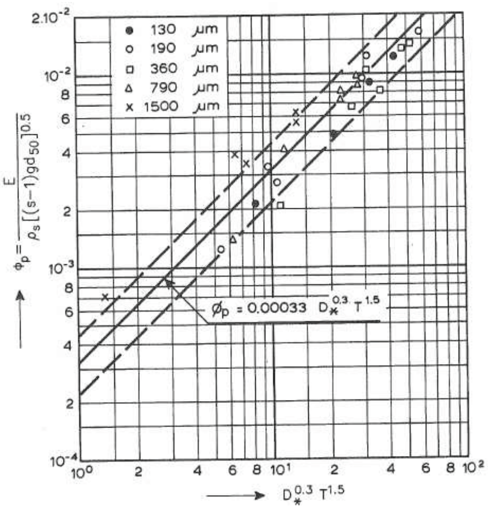

Fig. 2: Empirical pick-up function of van Rijn (Van Rijn, 1993)

3 HINDERED EROSION

The theory of hindered erosion is based on the assumption that the erosion is hindered by the properties of the soil mass, especially taking place at higher flow velocities. Van Rhee described the erosion at higher flow velocities (Van Rhee, 2007). To understand the theory of hindered erosion, two properties of a granular soil should be explained:

- dilatancy;
- permeability.

3.1 Dilatancy

At relative low flow velocities grains are picked up grain by grain. When flow velocity and erosion rate increase layers of grains are picked up at a time. The top layer of the sand bed is subject to shear (Van Rhee, 2007). During shearing the arrangement of the grains will change to enhance horizontal en vertical deformation. If the grains are loosely packed (as shown in Fig. 3) porosity decreases while shearing. This is called contractant behaviour. Normally sand is densely packed as shown in Fig. 4. During shearing the grains have to move upwards in order to enhance horizontal displacements. The porosity of the sand increases. The increase in volume needs to be compensated by the flow of water to the increased pore volume. This happens only if the pore pressure decreases in the sheared zone introducing a hydraulic gradient. The hydraulic gradient pushes the top layer on the bed and hinders erosion. This gradient will increase with the erosion rate and decreases with the permeability of the sand.

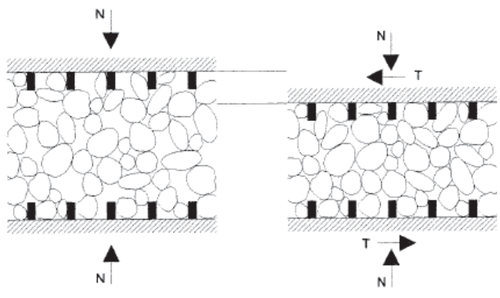

Fig. 3: Decrease of porosity during shearing of loosely packed sand: contractant behaviour (Lubking, 2004)

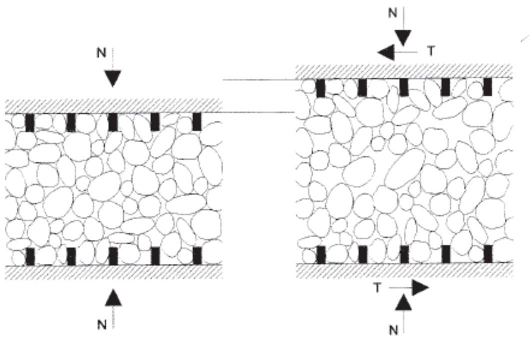

Fig. 4: Increase of porosity change during shearing of densely packed sand: dilatant behaviour (Lubking, 2004)

3.2 Permeability

The following three characteristics influence the permeability of fully saturated granular soils (Lambe and Whitman, 1969):

- particle size (distribution);
- void ratio or porosity;
- composition (mineralogy).

Particle size

Particle size is highly influencing the permeability because the smaller the soil particles the smaller the voids. The voids form the flow channels and thus the smaller the voids the lower the permeability. Experimental data proved that finer particles in a soil have the most influence on permeability. Based on these data experimental formulae have been developed based on the D_{10} (Lubking, 2004):

$$k = m \cdot D_{10}^{\;2} \tag{6}$$

with:

k	=	permeability [m/day]
D_{10}	=	grain size at which 10% of the soil weight is finer [mm]
m	=	factor approximately 1000 [-]

This relation assumes that the distribution of particle sizes is spread enough to prevent the smallest particles from moving under the seepage force of the flowing water. If the flow washes out the fines the permeability increases with duration of the flow.

Void ratio or porosity

Another factor but not highly influencing permeability is the void ratio (e). Related parameters are porosity and in-situ density. A mainly theoretical expression describing the permeability of porous media is the Kozeny-Carman formula including the effect of the angularity of grains (Lubking, 2004):

$$k = \frac{\rho \cdot g}{\eta} \cdot \frac{e^3}{1+e^3} \cdot \frac{1}{k_0 \cdot S_v^{\;2} \cdot f} \tag{7}$$

with:

k	=	permeability [m/s]
ρ_w	=	density water [kg/m^3]
η	=	dynamic viscosity water [kg/(ms)]
e	=	void ratio [-]
k_0	=	Kozeny-Carman constant [$k_0 \approx 5$]
S_v	=	specific grainsurface [m^2/m^3]
f	=	angularity factor of Loudon [1,1 -1,4]

Experimental data of sand (Lambe and Whitman, 1969) has shown that permeability is directly related to the factor $e^3/(1+e)$ implicating that an increase of the void ratio is related to an increase of the permeability. The permeability of a rather loosely packed granular material is approximately 3 times higher than of a densely packed granular material.

Composition/mineralogy

The last effect is the amount and mineralogy of the fines (particle size ≤ 2 μm). Smaller grains in between larger grains decrease the effective porosity and therefore the permeability (Fig. 5). If the particles between the larger grains are clay particles the permeability decreases significant. This is the result of the ability of clay particles to bind water. Due to their capacity in binding water the clay particles fill a relative large volume in relation to (inert) quartz particles of similar size. The amount of water which is bound depends on the mineralogy of the clay particles. A useful index to characterize the bounding capacity of water and resulting assemblage of soil particles are the Atterberg limits. The Atterberg limits for a soil are related to the amount of water that is attracted to the surface of the soil particles and therefore they determine the total volume of the clay particles and bounded water. Based on this knowledge Skempton (Lambe and Whitman, 1969) defined a quantity called activity:

$$A = \frac{PI}{\% \leq 2\mu m} \qquad (8)$$

with:

A	=	activity [-]
PI	=	plasticity index [%]

The plasticity index and amount of the clay fraction (≤ 2 μm) determine the activity and therefore the effect of the clay fraction on the permeability.

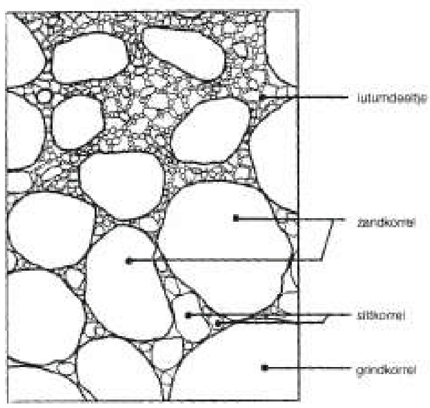

Fig. 5: Soil fabric of granular material containing fines (Lubking, 2004)

4 EROSION FORMULA FOR HIGH VELOCITIES

In (Van Rhee, 2007) a formula is derived including the effect of hindered erosion. The model is based on the effect of dilatancy and permeability of the soil. At relative low flow velocities the grains are picked up grain by grain by the current. At increasing flow velocities and subsequent erosion rates, the top layer of the soil is sheared. As a result of shearing the grains show dilatant behaviour when the soil is packed higher than its critical density, being normally the case. The porosity of the top layer increases and water has to flow into the sheared zone. This causes a hydraulic gradient pushing the top layer on the bed and "hinders" erosion. The hydraulic gradient (i) over the top layer is:

$$i = \frac{v_e}{k} \cdot \frac{n_i - n_0}{1 - n_i} \tag{9}$$

with:

n_i = porosity sheared layer [-]

A hydraulic gradient in a sandy slope has an effect on the stability of the slope in the material (Van Rhee and Bezuijen, 1992). An inward or outward directed hydraulic gradient exerts an extra respectively lower force on the soil particles. An inward flow in the slope increases the stability while an outward flow is decreasing the stability. This behaviour can be compared with the effect of dilatancy. Dilatancy causes an extra inward hydraulic gradient on the soil particles increasing the stability, or better increasing the resistance to erosion.

Practically this can be explained by a fictitious higher critical Shields parameter (θ_{cr}^*) including the effect of the inward hydraulic gradient. By Van Rhee this fictitious parameter is defined as, considering the soil mass as a continuum (Van Rhee, 2007):

$$\theta_{cr}^* = \theta_{cr} \cdot \left(\frac{\sin(\varphi - \beta)}{\sin(\phi)} + \frac{i}{(1 - n_0) \cdot \Delta} \right) \tag{10}$$

in which:

φ = angle of friction granular material/soil particles [º]

β = angle of slope [º]

Δ = relative grain density: $(\rho_s - \rho_{w)} / \rho_w)$ [-]

Substituting of (9), the hydraulic gradient (*i*) caused by dilatancy and the resulting flow of water, into (10) gives for a horizontal bed (β = 0) the following criterion:

$$\theta_{cr}^* = \theta_{cr} \cdot \left(1 + \frac{v_e}{k} \cdot \frac{n_i - n_0}{1 - n_i} \cdot \frac{1}{\Delta \cdot (1 - n_0)} \right) = \left(1 + \delta \cdot \frac{v_e}{k} \right) \cdot \theta_{cr} \tag{11}$$

with:

$$\delta = \frac{n_i - n_0}{1 - n_i} \cdot \frac{1}{\Delta \cdot (1 - n_0)} \tag{12}$$

Formula (11) includes the effect of hindered erosion.

The term T, including the effect of hindered erosion according to (11), is defined as (Van Rhee, 2007):

$$T = \frac{\theta - \theta_{cr}^{\ *}}{\theta_{cr}^{\ *}} = \frac{\theta - \left(1 + \delta \cdot \frac{v_e}{k}\right)\theta_{cr}}{\left(1 + \delta \cdot \frac{v_e}{k}\right)\theta_{cr}} \tag{13}$$

For flow velocities (u) of more than 4 m/s can be stated that:

$$\theta >> \left(1 + \delta \cdot \frac{v_e}{k}\right) \cdot \theta_{cr} \tag{14}$$

This means:

$$\theta - \left(1 + \delta \cdot \frac{v_e}{k}\right) \cdot \theta_{cr} \approx \theta \tag{15}$$

And at high flow velocities (u > 4 m/s):

$$\theta \approx \theta - \theta_{cr} \tag{16}$$

The simplification according to (16) is necessary to prevent the calculation of erosion rates below the critical Shields parameter (θ_{cr}). The denominator in formula (13) can be simplified, at relative erosion velocities (v_e/k) of more than 40, because:

$$\delta \cdot \frac{v_e}{k} \cdot \theta_{cr} >> \theta_{cr} \tag{17}$$

This leads to:

$$\left(1 + \delta \cdot \frac{v_e}{k}\right) \cdot \theta_{cr} \approx \delta \cdot \frac{v_e}{k} \cdot \theta_{cr} \tag{18}$$

The simplification according to (15), (16), (17) and (18) means for formula (13):

$$T = \frac{\theta - \left(1 + \delta \cdot \frac{v_e}{k} \cdot\right) \cdot \theta_{cr}}{\left(1 + \delta \cdot \frac{v_e}{k}\right) \cdot \theta_{cr}} \approx \frac{\theta - \theta_{cr}}{\delta \cdot \frac{v_e}{k} \cdot \theta_{cr}} \tag{19}$$

Combining (1), (3), (5) and (11) gives a formula in which the erosion rate is present in both sides (Van Rhee, 2007). The simplification of formula (13), presented in (19), leads to:

$$v_e^{\ 5} = \alpha^2 \cdot D_*^{0,6} \cdot \left(\frac{\theta - \theta_{cr}}{\theta_{cr}}\right)^3 \cdot \left(\frac{k}{\delta}\right)^3 \tag{20}$$

with:

$$\alpha = 0,00033 \cdot \frac{\sqrt{(s-1) \cdot g \cdot D_{50}}}{1-n_0} \tag{21}$$

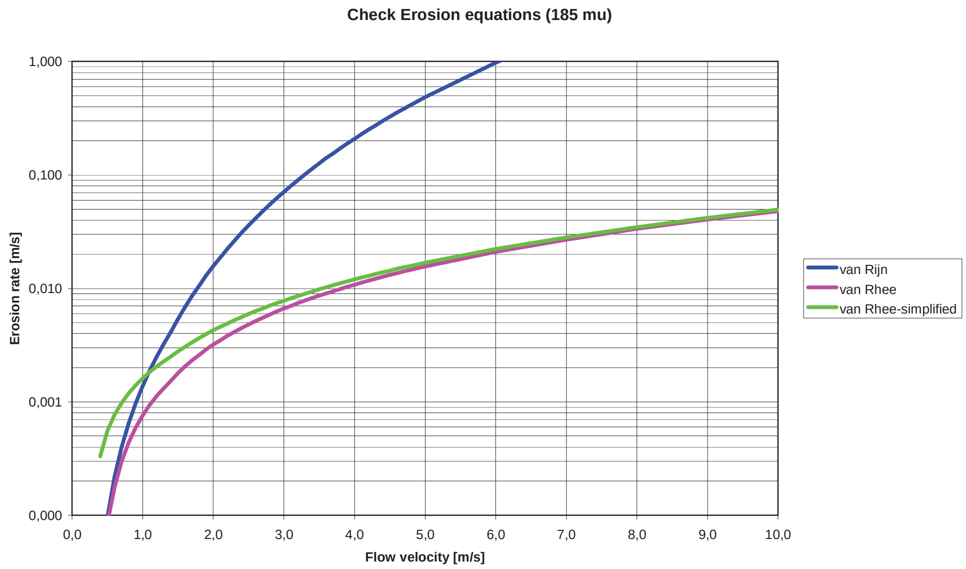

Fig. 6: Check simplification

The error due to the simplification is less than 10% for above mentioned values of the flow velocity and v_e/k (Fig. 6). For dredging practice (flow velocities of more than 30 m/s) the error is negligible (< 1%).

The factor δ used in formula (11) is defined as the dilatancy factor. A higher factor means that the porosity of the granular material needs to increase more to enhance shearing of the layer, causing a higher inward gradient during erosion.

Formula 13 gives a clear insight into the mechanism of hindered erosion:

- a lower permeability causes a lower erosion rate: the lower the permeability the higher the extra downward force due to the extra hydraulic gradient;
- for a material with a relative high in-situ porosity (low δ) a relative low increase of porosity is necessary resulting in less hindered erosion and therefore higher erosion rate;
- an increase of the critical Shields parameter leads to a decrease in erosion rate.

5 EVALUATION WITH DATA OF ZWIN'94-EXPERIMENT

To evaluate the theory, erosion data are necessary. No specific data are available in the literature of erosion rates induced by water jets (dredging at relative high erosion rates and/or dredging of granular material with a relative low permeability). To overcome this problem data were used of a large-scale dike breach experiment (Zwin'94-experiment). The Zwin'94 experiment was performed in 1994 in the Zwin Channel, a tidal inlet at the Dutch-Belgian border connecting the nature-reserve "Het Zwin" with the North Sea. On basis of the results of this field experiment the process of breaching of a sand dike was studied and a model was developed for the prediction of the breach growth and the discharge through the breach (Visser, 1998).

A sand-dike was built with local sand from the Zwin Channel and the beach. The total Zwin Channel was closed off by the sand-dike. Just before high tide a small pilot channel was made in the crest of the sand-dike to ensure breaching near the middle of the Zwin Channel. The results of the experiment are shown in Fig. 7 presenting the measured breach width (at the crest of the dike) versus time. These data are used to check the above presented model. On the basis of Fig. 7 the vertical erosion rate was determined:

$$v_e = \frac{1}{2} \cdot \frac{dB_{cr}}{dt} \cdot \tan\left(\gamma\right) \tag{22}$$

with:

B_{cr} = breach width at crest [m]

γ = side slope angle breach [°]

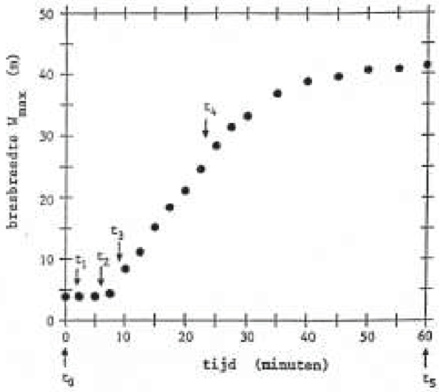

Fig. 7: Growth of breach during Zwin-experiment (Visser, Smit and Snip, 1996)

For the data only results are used of the breach growth in phase 4 (between t_3 and t_4) and phase 5 (after t_4) (Visser, Smit and Snip, 1996 and Visser, 1998). In these phases the breach has grown through the whole dike and has reached the base of the dike at t_3. In phase 4 the erosion process is rather constant in time. In phase 4 and 5 the erosion of the breach takes mainly place by vertical erosion of the side slopes of the breach (Fig. 8).

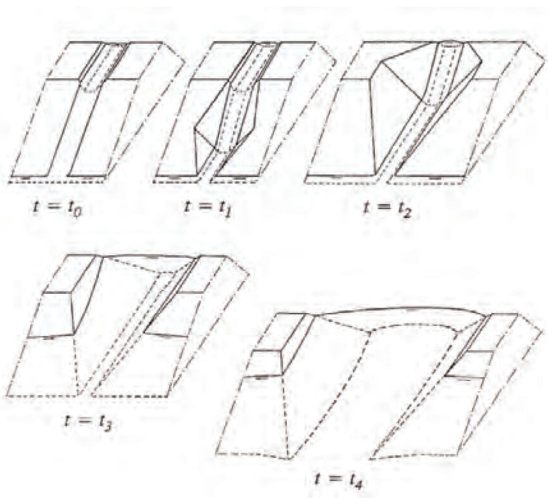

Fig. 8: Schematic illustration of breach growth in a sand dike (Visser, Smit and Snip, 1996)

On the basis of these results the erosion rate was calculated from the observations of the breach crest width and compared with the flow velocity through the breach (Fig. 9). These observed erosion rates are compared with the erosion rate calculated with the simplified van Rhee-model. Two components of the data set of the Zwin'94 experiment are rather unknown:

- grainsize of the sand: the sand dike was built with material from the Zwin Channel and from the beach. These materials showed large differences in grainsize (table 1). Calculations of the erosion rates for both materials were made (Fig. 9);
- side slope angle of the breach: to determine the vertical erosion rate from the experimental data the side slope angle should be known. This angle was not measured during the Zwin'94 experiment, but both photos and videos taken during the experiment show that this angle was rather large, say approximately 60°. The sensitivity of the calculated erosion rate as function of the slope angle was determined for three side slope angles (see Fig. 9).

Type of sand	D_{10}	D_{50}	D_{90}
[-]	[μm]	[μm]	[μm]
Original sand from Zwin Channel	155	185	285
Beach sand	215	315	600

Table 1: Grainsize sand

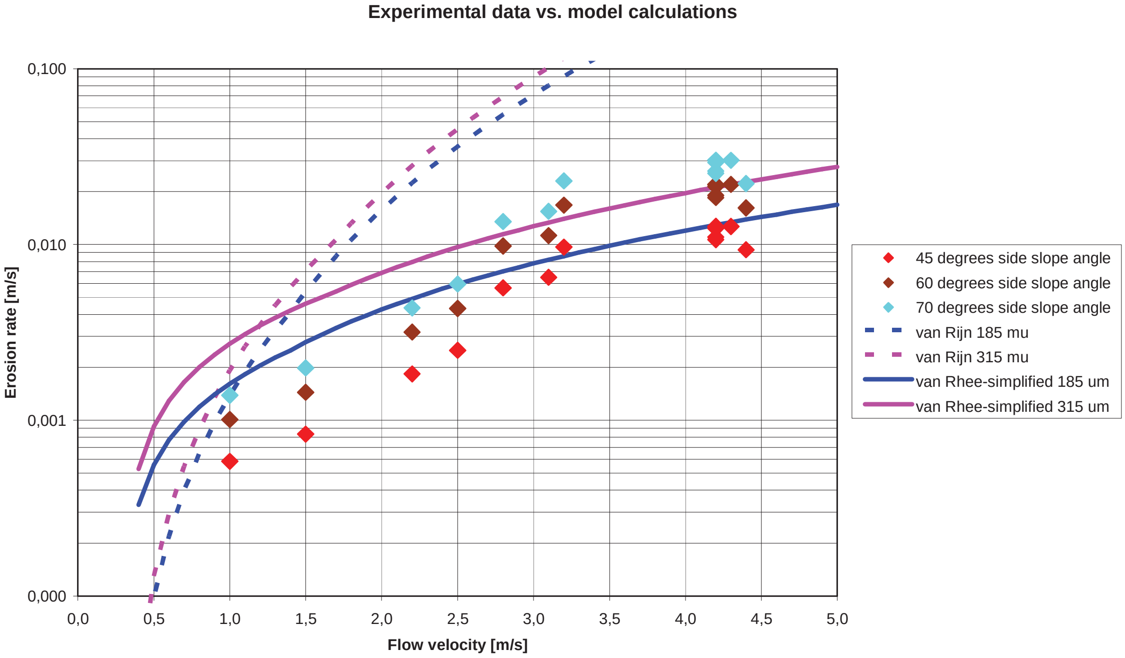

Fig. 9: Erosion rates for Zwin'94-experiment

Fig. 9 shows that the erosion model of Van Rijn (Van Rijn, 1993) overestimates the erosion rate at flow velocities of more than 1 m/s and values of v_e/k being larger than 5. At higher flow velocities the simplified Van Rhee-model gives better agreement with the data. Especially this model gives a rather good prediction of the erosion rates in phase 4, while the model overestimates the erosion rates in phase 5 (flow velocity smaller than 3 m/s). For flow velocities smaller than 3 m/s the Van Rhee-model according to (Van Rhee, 2007) should be used. Other possible causes for these differences could be the variable nature of the material used in the sand dike and/or changes in the side slope angle during the breach process.

6 CONCLUSIONS

Erosion of granular materials is not only influenced by the properties of the single particles (grain diameter: D_{50} and density: ρ_s) but at higher flow velocities (higher than 1.0 m/s) the erosion process is significantly influenced by the properties of the soil mass. Governing parameters at higher flow velocities are dilatancy, permeability and the (un)drained shear strength of the soil mass. Based on the concept presented by Van Rhee (Van Rhee, 2007) a simple analytical formula is derived for hindered erosion, in which the erosion process is also influenced by two extra properties of the soil mass: dilatancy and permeability. The model shows that the erosion rate is directly related to the permeability ($k^{0,6}$) and the amount of dilatancy. A relative high volume increase during shearing (the higher the amount and factor of dilatancy) causes a relative low erosion rate.

The model was compared with the data of a large-scale breach experiment performed in 1994 in the Zwin-channel. The agreement between model predictions and experimental data is rather good, especially for high flow velocities (higher than 4 m/s). This makes the model useful, especially for dredging.

ACKNOWLEDGEMENT

The financial support of the SSB (Stichting Speurwerk Baggertechniek, which includes Royal Boskalis Westminster Dredging BV and Van Oord Dredging and Marine Contractors BV), IHC Merwede BV and the Dr. Ir. Cornelis Lely Foundation (Rijkswaterstaat) is gratefully acknowledged.

REFERENCES

Lambe, T.W., Whitman, R.W. (1969), Soil Mechanics, John Wiley & Sons.
Lubking, **P.** (2004), Handboek Zandboek, CROW, Ede.
Rhee, C. van (2007), Erosion of granular sediments at high flow velocity, Hydrotransport 17, The 17th International Conference on the Hydraulic Transport of Solids, The Southern African Institute of Mining and Metallurgy and the BHR Group, pp. 551-560.
Rhee, C. van, Bezuijen, A. (1992), Influence of seepage on stability of sandy slope, Journal of Geotechnical Engineering, vol. 118, no. 8, pp. 1236-1240.
Rijn, L.C. van (1993), Principles of Sediment Transport in Rivers, Estuaries and Coastal Seas, Amsterdam, the Netherlands.
Visser, P.J. (1998), Breach Growth in Sand-Dikes, PhD thesis, Delft University of Technology, Delft, the Netherlands.
Visser, P.J., Smit, M.J., Snip, D.W. (1996), Zwin ’94 Experiment: Meetopstelling en overzicht van alle meetresultaten, TU Delft.

STORAGE CAPACITY OPTIMIZATION OF TAILING PONDS BY MEANS OF MECHANICAL DEWATERING

S. Pensaert[1], and Ken Van de Velde[2]

Abstract: Up till now it is common practice for mining and metallurgical companies to store mineral residues, such as tailings, in large ponds without any (pre)treatment. As most of these residues are pumped to the ponds hydraulically this has resulted in huge dumpsites with a high volume of water. Nowadays this procedure is no longer considered as environmentally sustainable. Lack of space, difficulties in permitting additional storage capacity, lixiviation of pollutants, stability issues etc. demonstrate the need for more efficient storage. The same problem applies for dredged sediment storage ponds. Efforts towards optimisation of storage capacity and minimisation of disposal costs are the key elements of the development schemes for new technology.

New developments in combined dredging and mechanical dewatering offer a cost-efficient solution to reduce the mass and volume of the mineral residues or dredged sediments in existing ponds. Dewatering followed by controlled backfill of the ponds can increase the storage capacity of the pond seriously.

DEC (DEME Environmental Contractor) is currently carrying out a full scale dewatering of two metallurgical tailing ponds in the Belgium. The largest pond is pond contains about 1,500,000 m³ gypsum precipitate residue from the neutralisation of spent hydrosulphuric acid of zinc leaching. The smaller pond contains 500,000 m³ of goethite, a residue from hydrometallurgical zinc refining. The goethite is extremely corrosive which required special attention in the design of the whole treatment process.

A full scale dewatering plant was being designed, built, and is nowadays being operated, based on two large membrane filter presses. Residues dredged from the ponds as well as freshly generated residues from the metallurgical plant are pumped to the dewatering installation, which has a total capacity of 150,000 tons of dry matter per year. The stable filter cakes are backfilled in a controlled way in the already dredged areas of the ponds. The project has started in 2006 and will take 10 years.

With this project a volume gain of about 100 % (50 % volume reduction) will be achieved, enabling a new storage capacity of another 40 years.

Keywords: mechanical dewatering, sediment, tailings

[1] Process and R&D Manager, DEC NV (DEME Environmental Contractors), Haven 1025 – Scheldedijk 30, 2070 Zwijndrecht, Belgium, T: +32 3 250 54 11, F: +32 3 250 52 53, E-mail: pensaert.stany@deme.be, www.decnv.com

[2] Process & R&D Engineer, DEC NV (DEME Environmental Contractors), Haven 1025 – Scheldedijk 30, 2070 Zwijndrecht, Belgium, T: +32 3 250 54 11, F: +32 3 250 52 53, E-mail: van.de.velde.ken@deme.be, www.decnv.com

1 INTRODUCTION

In the past far most of the dredged sediments from waterways and ports have been stored in sediment ponds. This practice resulted in large surfaces of land which were made unsuitable for reuse due to the geotechnical poor quality of the stored sediments.

Similar ways of storage can be found in mining, metallurgy, etc. Here huge amounts of tailings, precipitates, or other residues have been stored in large ponds. Mostly these residues were pumped to the ponds again resulting in large areas unsuitable for development.

This practice is not longer considered as environmentally sustainable, and there is a lack of space in densily populated countries such as Belgium and the Netherlands. For this reason it is getting more and more difficult to obtain permits for new sediment or residue ponds, or for the vertical or horizontal extension of existing ones.

For this reason stakeholders are looking into 'preventive' techniques to reduce the volumes of these sediments to be stored, such as partially recycling (e.g. by desanding if appropriate) or in-situ dewatering. However also 'curative techniques' can be chosen, such as re-excavating or dredging followed by on-site dewatering the historically stored sediments in order to gain extra space assuring further exploitation of the ponds.

2 VOLUME REDUCTION OF EXISTING TAILING PONDS

2.1 Some theoretical considerations first

Dewatering can be considered as the main volume reduction concept for wet sediments or residues. This is illustrated when one calculates, starting from the properties of the initial sediment, the theoretical mass and volume reduction in function of the dry matter content of a dewatered sediment. Figure 1 illustrates this for a typical dredged sediment, initially at 40 % DM content and grain density of 2.55 kg/dm³, for various higher dry matter contents. For instance if this sediment is dewatered to 65 % dry matter content (a typical value obtained by mechanical dewatering with a filter press), a volume reduction of about 50 % is obtained compared to the initial volume of sediment. Dewatering up to 80 % DM content (a value obtained by natural dewatering in the open air) can even reduce the initial volume by 65 %.

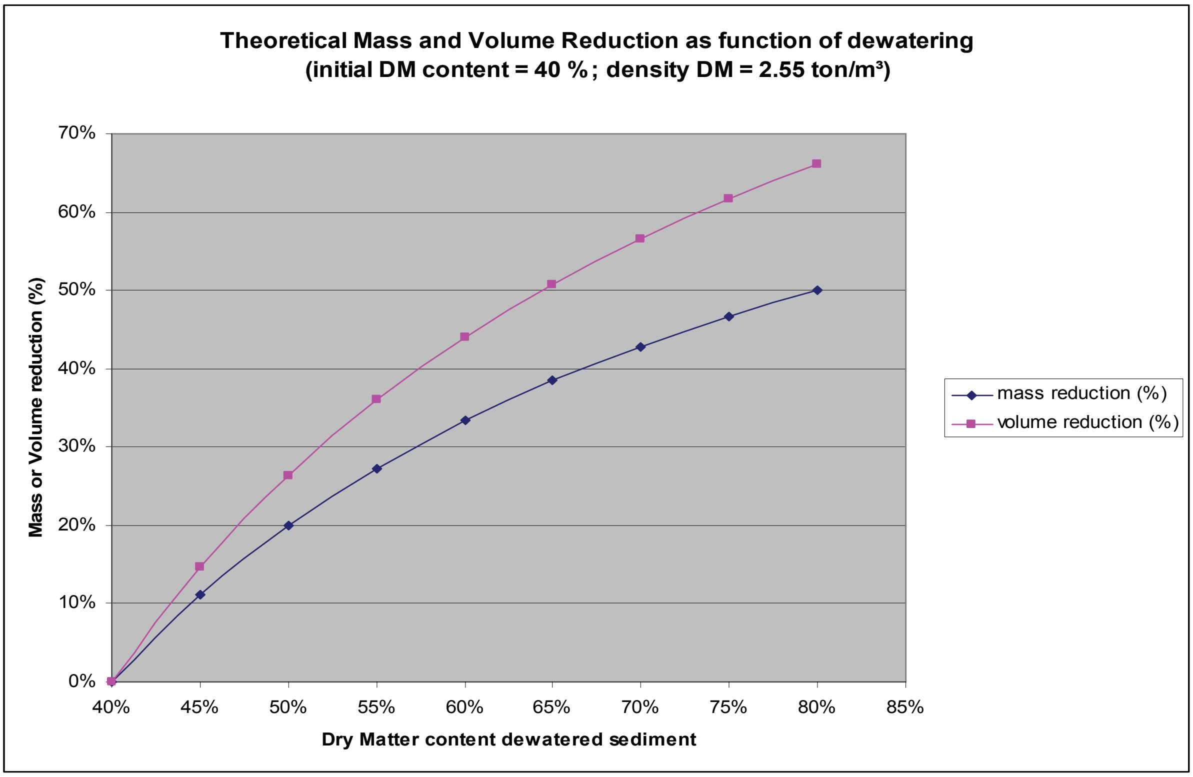

Figure 1: theoretical mass and volume reduction of a sediment as function of the final dry matter content

However, these are only theoretical calculated values based on the fact that the dewatered sediments are fully water saturated. In practice however, the actual obtained volume reductions can be much less than expected from design output, if not sufficient care is taken for certain boundary conditions such as pretreatment of the sediments, flocculation prior to dewatering, variability in the sediments, and last but not least optimal compaction of the dewatered material in its final disposal area. The most optimal volume reduction can only be obtained by seeing all steps of the process, as shown schematically in figure 2, in a general way.

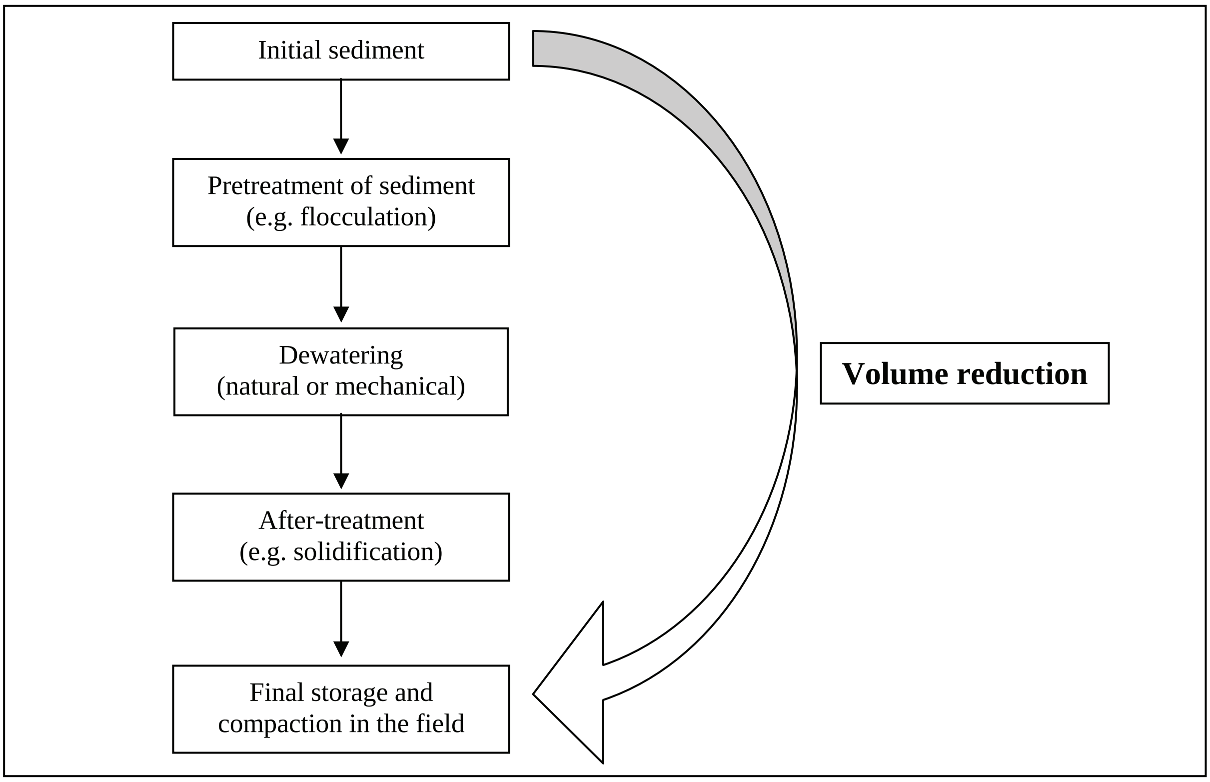

Figure 2: The volume reduction from initial sediment to final stored sediment is a function of all process steps in between

One of the most important steps shown in figure 2 is the last one: the backfill and compaction of the dewatered sediments. It is known from soil mechanics that the volume of any backfilled material is inversily proportional to its dry density γd. In order to obtain a minimal volume the maximal dry density should be obtained. Theoretically the maximal dry density for a certain water content is obtained when the material is fully saturated, i.e. no air voids are present. This maximal dry density curve is shown on figure 3. It can be seen that the highest theoretical dry density can be obtained at a zero water content.

However it is known that these theoretical dry densities can never be obtained in practice. In order to find the maximum obtainable dry density of a certain material, at a certain compaction degree, a Proctor curve is developed.

Figure 3 shows the Proctor curves of two sediments: a lagooned sediment and a mechanically dewatered sediment (flocculated with quicklime). The compaction energy applied to develop this curve was a so-called Standard Proctor Compaction.

One can see that for the lagooned sediment the so-called optimum Proctor dry density is about 1.65 kg/dm³ which can be obtained at w = 18 % (= DM Content of 85 %). The actual water content of lagooned sediment however is w = 25 % (= DM content of 80 %) where only a dry density of 1.40 kg/dm³ can be obtained.

Theoretically however, if complete saturation could be obtained, i.e. at a perfect compaction degree, the dry density at this water content of 25 % would be 1.55 kg/dm³. The difference between the obtained dry density and the theoretical is as expected: the lagooned sediment is less plastic and by consequence more difficult to compact.

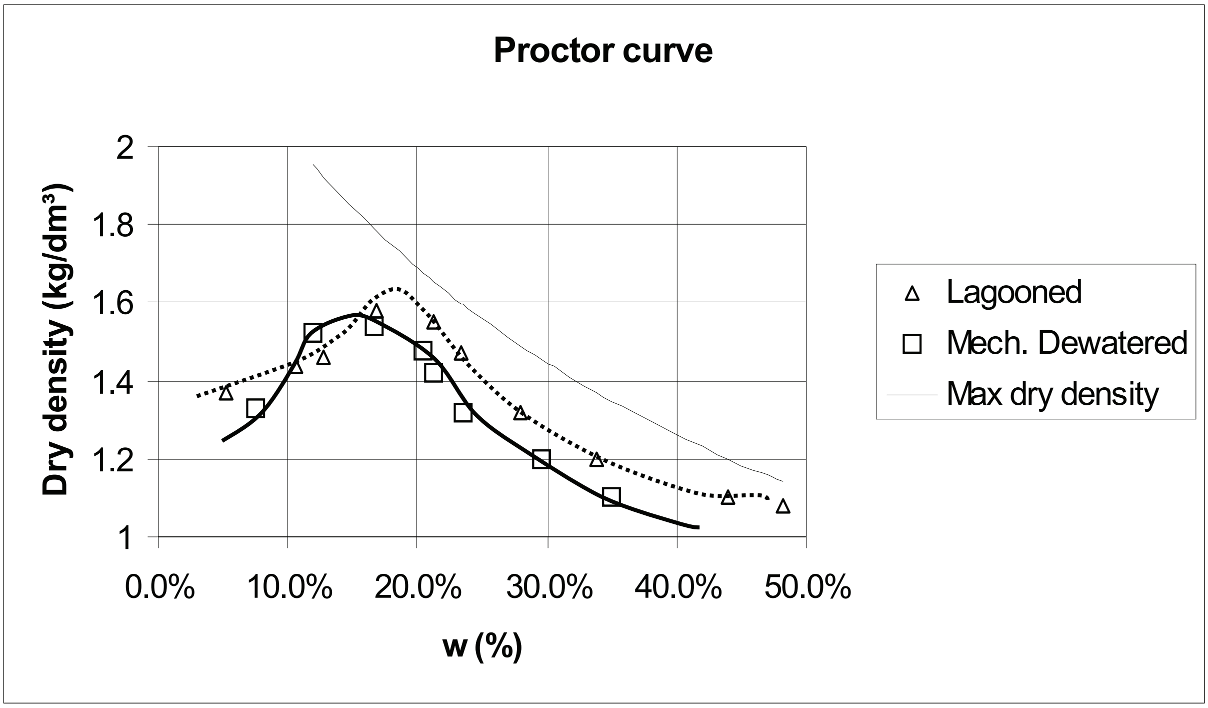

Figure 3: Proctor curve for sediments (Standard Proctor compaction energy), w(%) is the water content of the sediment.

A similar illustration can be done with the mechanically dewatered sediment. Here the optimum Proctor dry density is 1.55 kg/dm³ obtained at w = 15 % (= DM Content of 87 %). The actual water content of the filter cakes is only w = 54 % (= DM Content of 65 %) where only a dry density of about 1 kg/dm³ can be obtained. The theoretical dry density for these filter cakes at complete saturation and at this water content of 54 % would be 1.07 kg/dm³. The fact that the obtained dry density of the filter cakes is close to the theoretical maximum is obvious: the filter cakes are fully saturated and can be quite easily compacted as they are still very plastic at this water content.

2.2 The importance of compaction

The imperfect compaction has a serious consequence with respect to the volume reduction that can be obtained. This is again illustrated in table 1 for the examples used above. The following observations can be made from this table:

- One can see that for both dewatered sediments the initial volume could be reduced to about one third if the most optimal condition could be obtained, i.e. dewatering to the optimal Proctor water content (w = 15 to 18 %) followed by maximal compaction.
- It is also noticed that as compaction can never be perfect, the volume reduction by dewatering is overestimated with about 4 to 5 %.
- It is however clear that dewatering should be done to as close as possible to the optimum Proctor Content. The knowledge of the optimum Proctor point and the selection of the appropriate technique is therefore very important.

Table 1: Theoretical and real volume balance

	Initial relative volume (sediment before dewatering at 40 % DM content or w = 150 %)	Theoretical volume after dewatering (lagooning or mech. Dew.)	Real obtainable volume for standard compaction at water content	Minimal obtainable volume for standard compaction at optimum Proctor
Mechanically dewatered sediment	100	49	53	34
Lagooned sediment	100	34	39	32

2.3 The impact of pre-treatment or after-treatment on the volume reduction

On top of this, various other aspects have a (negative) impact on the volume reduction that can be obtained:

Pre-treatment (flocculation) of the sediments: the use of lime as a flocculant instead of poly-electrolytes can increase the theoretical cake volume up to 5 %, due to the addition of the lime itself which contributes to the dry matter volume.
Lime addition will also alter the geotechnical behaviour of the filter cakes as it will shift the optimum Proctor water value to a higher water content (about 5 to 10 %) and the obtainable dry density to a lower value (often 0.1 kg/dm³ lower). The latter is due to the more open matrix structure obtained by the lime treatment.
The compaction in the field can be far beyond the compaction applied in the laboratory when determining the Proctor curve.

In particular the use of lime as a flocculant during mechanical dewatering can have a serious impact. The advantage is that it does indeed shift the optimum Proctor point towards a higher water content, hence closer to the water content obtained by a dewatering technique. In addition it stabilises the dewatered sediment which improves the geotechnical quality of the stored sediment. However due to the addition of the lime itself (order %) and to the lower dry density that can be obtained in the filter cakes, the volume reduction can be around 10 % less than when no lime would be used.

Again all these considerations illustrate the need to look into the volume reduction approach in a holistic manner.

3 STORAGE CAPACITY OPTIMISATION OF THE TAILINGS POND AT UMICORE BALEN

Since decades two main residues from Umicore’s zinc smelter at Balen have been pumped into a 27 hectare tailing pond within the plant’s premises. The residues mainly consist of the so-called neutralization sludge (mainly gypsum based) arising from the neutralization of spent acid leaching solutions, and goethite (iron hydroxide) arising as residue from the leaching process.
A picture of the ponds can be seen in figure 4.

Umicore wanted to extent the content of its tailings ponds in order to gain extra storage capacity for another 40 years of production, The initial idea was to increase the height of the existing dyke by more than 10 meters to create the needed volume. This concept was rejected during the planning application, so other solutions had to be studied.

MWH came up with the idea of creating volume in the existing ponds by dewatering the already stored materials, as well as all newly produced residues to be stored in the future. Based on the above described holistic procedure DEC (DEME Environmental Contractor) offered Umicore to design an optimal volume reduction technology that was able to achieve the requirements of the client.

Based on pilot scale filter press dewatering and compaction tests it was possible to design a large dewatering plant that can cope with at least 150,000 tonnes of dry matter a year. The plant has two identical membrane chamber filter presses of 20 m³ cake volume each (see figure 5). A major boundary condition in the design was that both presses in the plant have to be able to dewater both alkaline gypsum residue as well very acidic hence corrosive goethite. It was not allowed to neutralise the goethite as Umicore recycles the filtrate that is rich in heavy metals.

After the design and construction in 2007 the full scale dewatering of the tailing pond is currently being carried out. The pond contains about 1,500,000 m³ of neutralisation sludge which has to be dewatered over a period of about 10 years. The filter cakes are then compacted and stored in the same ponds again.

In parallel the freshly produced goethite is dewatered at a rate of minimal 75,000 tonnes of dry matter a year. The filter cakes from the goethite are highly contaminated with heavy metals, and are mixed just after dewatering by means of quicklime. The quicklime immobilises the heavy metals from leaching, also increases the geotechnical properties of the cakes, but unfortunately reduces the degree of compaction that can be achieved in the field.

All filter cakes are backfilled in a controlled way in the already dredged areas of the ponds. The project will take 10 years.

With this operation a volume gain of about 100 % (50 % volume reduction) will be achieved, enabling the required storage capacity of another 40 years. The presentation will outline the whole project. The experience gained in this project can be applicable on capacity optimisation of existing sediment lagoons.

Figure 4. View on the tailing ponds and the dewatering plant

Figure 5. View on filter presses

4 CONCLUSIONS AND RECOMMENDATIONS

Disposal sites of dredged sediments, metallurgical tailings,… are often not optimized in terms of maximum storage of dry matter. Due to various restrictions, such as environmental issues, lack of space,… planning permissions for extension of these sites or construction of new sites are difficult to obtain.

However logistically not simple, re-excavation or dredging of these sediments or tailings combined with large scale mechanical dewatering can significantly decrease the volume present in the disposal site, and will increase its geotechnical stability. Volume reductions of over 100 % of the initial volume stored can be achieved, which enables further storage of the materials in the same ponds. However, close attention should also be paid to all other aspects that influence the volume reduction, in particular the recompaction of the filter cakes in the disposal site.

5 REFERENCES

Detzner H.D. (1995) The Hamburg Project MEtha: large scale separation, dewatering and reuse of polluted sediments. European Water pollution control, vol 3, no 5, sep 1995.

Pensaert S., Pashkin I., Elskens F., and Dutilleux D. (2003). Treatment of dredged sediments on the Mobidec service pontoon. Coasts and Ports 2003 – Australian Conference, Auckland, New Zealand, September 9th – 12th.

Pensaert S., and Burton O. (2003) Experience with mobile dewatering of dredged sediments. 2nd Conference on remediation of contaminated sediments, Venice, September 30th to October 3rd.

Nevejans B. (2003). Treatment of contaminated dredged material in harbour areas, review on 10 years experience. 2nd Conference on remediation of contaminated sediments, Venice, September 30th to October 3rd..

Pensaert S. (2004). Mobile dewatering of dredged sediments: a case study from Belfast. Wodcon XVII, Hamburg, Germany, 27th September – 1st October.

P**ensaert S., Nevejans B., D'Haene S., and Van de Velde K.** (2005). Mechanical dewatering of hydraulically excavated and stored sediments. Reused, Budapest, May.

MAASVLAKTE 2 : CONSTRUCTION PROGRESS AND ASSOCIATED ENVIRONMENTAL MONITORING

Tiedo Vellinga[1], Wil Borst[2],

Abstract : In September 2008 the start of Maasvlakte 2 was officially celebrated.
In January 2009 the fist TSHD started her activities. At the end of 2009 a large portion of the sand volume required for the construction will be put in place. It is anticipated that at that time 6 to 8 TSHD will be working around the clock (7/24 format). The extensive baseline surveys and studies, carried out prior to the start of the works, are followed by actual monitoring. Some findings and details of ongoing monitoring will be presented. Underwater sound in front of the future MV2 near the entrance to the Port of Rotterdam was measured in 2008. In the fall of 2009 all specific stages in the working cycle of the TSHD's will be measured, resulting in so called source levels. Prior to the start of the project baseline studies were carried out; Benthic, Silt profiling, Juvenile Fish. In 2009 and the years thereafter Benthic and Silt profiler surveys will be carried out again. Not all monitoring will be physically in the field, as the use of numerical models and data assimilation with remote sensing is carried out as well. A new development program was started at he end of 2008 as a follow up of the pilot project : ToTSM : Integration of Remote Sensing and Modelling of Total Suspended Matter in the Dutch coastal zone, Deltares& IVM. The state of the art with respect of the modelling for MV2 and the integration of the field data will be discussed and presented.

Keywords : Baseline studies
Silt profiling measurements
Data assimilation – Ensemble Kalmann Filtering
Ecological impact monitoring
Mismatch algae bloom, silt concentrations & cockle growth

[1] Director Environmental Monitoring Maasvlakte2
Rotterdam Port Authority, P.O. Box 6622, 3002 AP, Rotterdam, The Netherlands, , Tel. +31102521010, t.vellinga@portofrotterdam.com, Mobile +31653911594, www.maasvlakte2.com
Associate Professor Ports and Environment, Civil Engineering and Geosciences, Delft University of Technology.

[2] Project Manager field measurements and (environmental) modelling for MV2
Rotterdam Port Authority, P.O. Box 6622, 3002 AP, Rotterdam, The Netherlands, Tel. +31102521010, wil.borst@portofrotterdam.com, Mobile +31651395687, www.maasvlakte2.com
Netherlands Dredging Consultants BV & Partner of Blue Pelican Associates BV, www.bluepelican.eu

1 INTRODUCTION.

After a long preparation period (more than 15 years) the construction of Maasvlakte 2 (MV2) finally started in September 2008. The works were tendered as a “Design & Construct” contract. The contractor has to comply with the specification provided by the Client Maasvlakte 2 Project Organisation (PMV2) of The Port of Rotterdam.

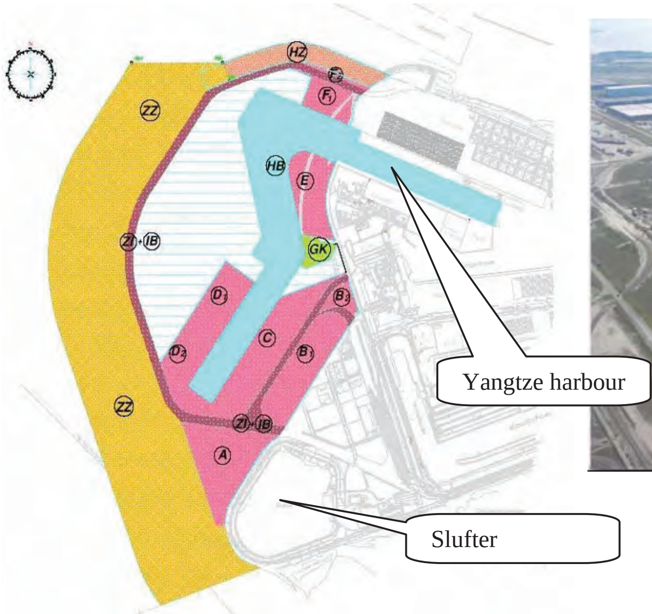

Figure 1: First phase of MV2 project

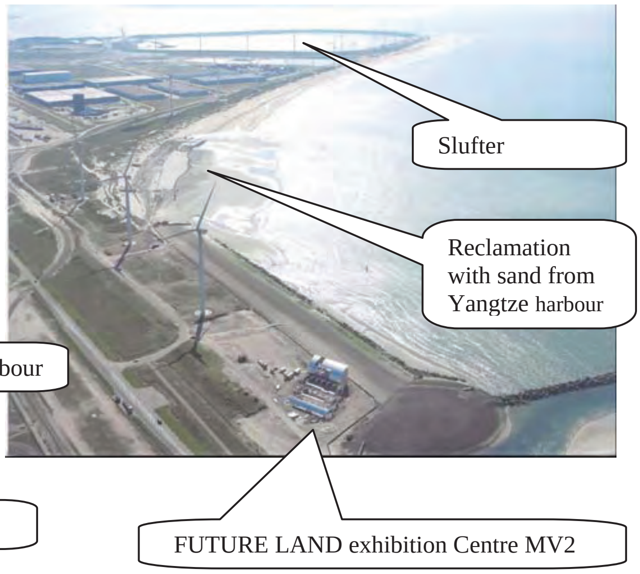

Figure 2*:* Start of project September 2008, sand from Yangtze harbour on beach area Maasvlakte

The first m3 of sand were dredged from the Yangtze harbour (Euromax container terminal) and deposited by pipeline on the sandy beach in front of the existing Maasvlakte.
The bulk of the sand needed for the construction of MV2 however has to come from an offshore located borrow area approx. 10 – 15 km from the Maasvlakte.
The sand extraction by trailing suction hopper dredger (HAM-316) started on 13 January 2009.
Gradually over time the number of TSHD bringing sand to Maasvlakte 2 increased.
In June 2009 ten (10) TSHD were deployed by PUMA, the Contractor, being a joint venture between Boskalis and Van Oord. The number of dredgers working for MV2 changes constantly. In June 2009 approx. 29 million m3 of sand, of the required 220 million from the offshore borrow area, was already put in place.

The whole MV2 project is based on a business case approach as the POR (Havenbedrijf Rotterdam NV) is and operates as a private company. The first concessions for a new container terminal on MV2 were awarded before the construction started. Hence a fixed milestone was present: first containers through the terminal in 2013. This mile stone is leading in the whole design and construction schedule of the project.

In order to comply with the miles stone many activities had to be carried out parallel instead of sequential. While the studies and the drafting of the Environmental Impact Assessment (EIA) was still underway the tendering procedure was started. Two groups of dredging companies Jan de Nul & DEME versus Boskalis & Van Oord bid for the job and worked out their respective designs (2006 – 2008).
In 2008 POR made their final choice for the combination Boskalis & van Oord working under the name PUMA. PUMA offered the best value for money and complied with all the requirements stipulated in the Program of Requirements

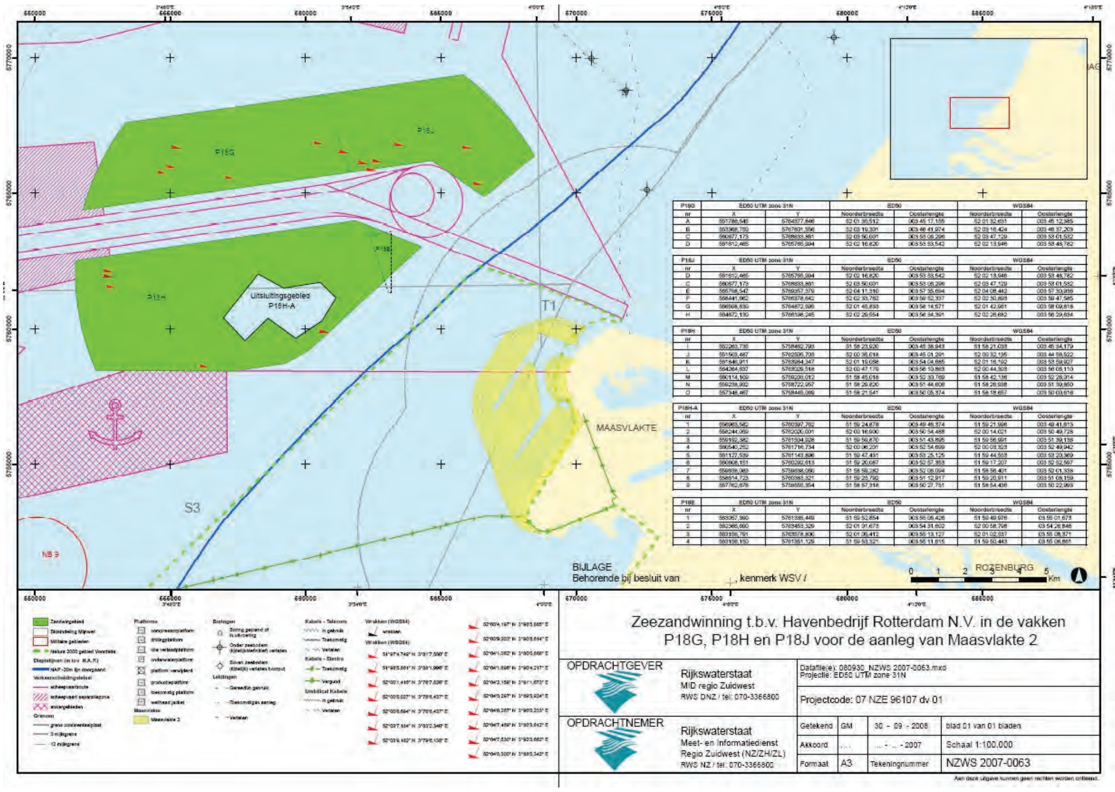

Figure 3: Drawing of the sand borrow area's North and South of the entrance channel (Euro Maasgeul) to the port of Rotterdam (source: Permit for sand borrowing from RWS-DNZ). Sand borrow area's are indicated in green. The light blue part in the southern borrow area is excluded (clay layers).

Due to the nature conservation regulations the EIA needed to be based for its impact analysis on worst case scenario's. Furthermore the EIA should take into consideration all possible (and feasible) operational aspects the Contractor may come up with during tendering and in his final offer, as the 5 major permits needed to start the project, would be based on the EIA. Much effort has been put in the EIA to make sure that the contractor would not be limited in its operations and could indeed achieve the best possible solution(s).

Prior to the start of the project a number of baseline studies were carried out, some even after the start the project as they were not critical in time (e.g. underwater sound measuring).

2. PROGRESS MV2 CONSTRUCTION: JUNE 2009

2.1 General

The sand extraction offshore started in January 2009 with one TSHD : HAM-316.
Gradually the number of trailers increased and in June 10 trailers were working for MV2. In table 1 all the dredgers that work on MV2 so far (June 2009) have been listed. The project is on schedule and progressing smoothly. Figure 4 (on the next page) shows the intended progress and the various stages defined by PUMA.

At the end of June already more than 29 million m3 of sand was put in place as is clearly visible on the photo (figure 5).
Table 1 lists all the TSHD that worked for MV2 in the period January through June 2009.

Trailing Suction Hopper Dredgers (Period January – June 2009)

Name	Owner	installed Power (kW)	Dredge mark (m)	Dredging Depth (m)	Hopper volume (m3)
Amazone	Baggerbedrijf de Boer	3,747	5.00	28.0	2,680
Barent Zanen	Boskalis	12,658	8.81	49.0	8,116
Cornelia	Boskalis	7,805	7.45	36.4	6,388
Crestway	Boskalis	6,075	7.10	33.0	5,600
Geopotes 14	Van Oord	11,326	8.66	41.7	7,422
Geopotes 15	Van Oord	12,445	9.07	53.0	9,962
HAM311	Van Oord	5,317	5.68	29.6	3,510
HAM312	Van Oord	5,436	5.68	30.0	3,512
HAM316	Van Oord	11,650	9.05	40.3	8,473
HAM317	Van Oord	6,132	7.12	37.1	4,407
Hein	Van der Kamp	5,410	5.00	40.0	3,653
IJsseldelta	Van der Kamp	4,000	4.50	30.0	2,034
Oranje	Boskalis	19,500	12.02	90.0	15,961
Ostsee	Van Oord	6,090	5.51	25.0	3,906
Prins der Nederlanden	Boskalis	19,500	12.02	90.0	15,961
Seaway	Boskalis	12,819	10.55	57.0	13,255
Shoreway	Boskalis	6,075	7.10	33.0	5,600
Utrecht	Van Oord	23,807	10.38	60.0	18,282
Volvox Olympia	Van Oord	6,542	7.19	32.0	4,750
Volvox Terranova	Van Oord	29,563	11.75	101.5	20,015
Vox Maxima	Van Oord	31,200	14.50	125.0	31,136
Waterway	Boskalis	6,365	6.58	28.0	4,906

Table 1: List of dredgers working for MV2 from the start in January till June 2009

Figure 5
Arial photograph of reclamation, showing the start of the landfill for the first container terminal and, in the background, the outer contour of the MV2 constructed as a soft beach structures (similar to existing Maasvlakte)

2.2 Quantities - Volumes

Dredge volumes are recorded automatically on board of each trailer as they are equipped with a MARS-system. MARS is a black box (developed by RWS DNZ) to monitor all process related signals on board of the trailer and allow monitoring and supervision from "a distance". PUMA also carries out manual measurements for each trip. Both volumes are reported in daily log files, weekly and monthly report to POR and are given to the authorities to check compliance with the obligations mentioned in the sand extraction permit. According to the permit the Contractor may extract sand resulting in a pit with a new seabed on an average level ranging between NAP – 25 to -40 m with a maximum local depth of NAP -20 meters below the existing seabed. The depth limitations are to prevent anaerobe areas near the bottom of the pits.

2.3 Quality of the sand

Form each trip sediment samples from the hopper are collected. The quality of the sand, expressed as D50, is established by PUMA onboard of the trailer for each trip as the design required sand of various qualities to be deposited per location and variable in time. In order to comply with the permit also 10% of the samples, randomly chosen, are analysed in a certified laboratory according to the Dutch & EURO Norms.

The D50 of the sand taken from the borrow area's ranges between 180 and 450 µm. The permit stipulates that sand with a D50 beyond 450 µm and having a sufficient thickness (for commercial applications) shall be left in place. It is the government intention to make accessible area's with coarse sand near the surface to facilitate the making of so called : Concrete & Masonry" sand. For which a sufficient percentage of sand with a D50 over 450 µm is needed. In the north-eastern part of the southern borrow areas there is such a level at approx. NAP – 35 m. In the Contractors plan of execution this aspect has been worked out and was approved by the authorities for Phase 1 of MV2.

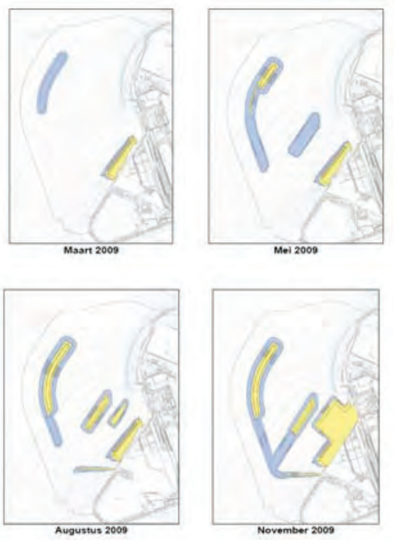

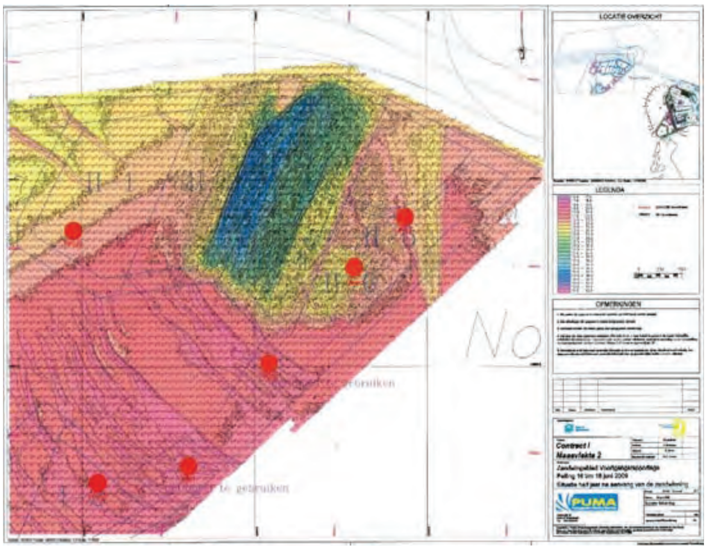

Figure 6 : left : Various building stage of the reclamation
Figure 7 : right : Excavation progress (~ 29 million m3) in the southern borrow area, June 2009

The coarser the sand the better the quality as the sustainability of the new sandy dunes embankment (soft outer contour) shall require minimal maintenance during it life span. This is one of the criteria of the Port's program of requirements. For the bulk of the reclamation a lesser D50 is quite acceptable as long as settlements are minimal and overall stability is guaranteed.

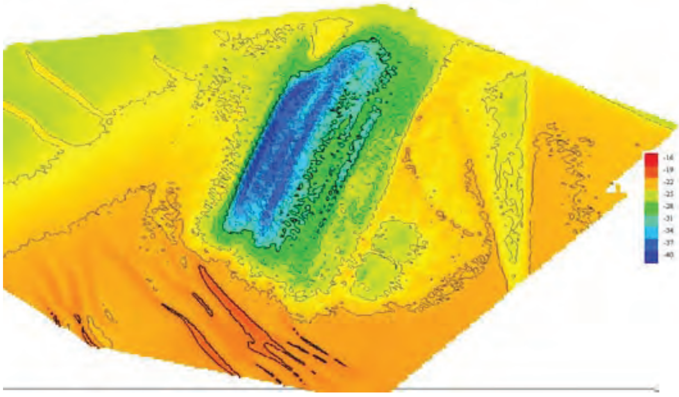

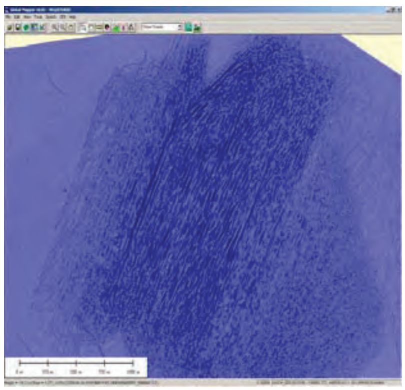

Figure 8 : Left : depth contours of the borrow area. Depth in m NAP .
Right t : details of tracks in northern area (bifurcation point north due to non removable channel marking buoy).

3. MONITORING SETUP : OVERALL SCHEME

The MV2 project is part of a total concept for the development of Rotterdam-Rijnmond, in which three objectives are combined. The 3 objectives are: the sustainable expansion of the Rotterdam Port by construction of MV2, the creation of 750 ha. new green areas and recreational facilities in the greater Rotterdam Area and the re-development, re-allocation and improved efficiency of the exiting port.

To implement the above the Project Mainport Rotterdam (PMR) was created in 1999, as a combined effort of the Port of Rotterdam, The Municipality of Rotterdam and some National & provincial Government agencies : Ministry of Transport, Ministry of Agriculture, Fishery, Nature and Food safety and the Provincial Public Works Departments.

For MV2 only there are 5 major permits: Excavation permit, Concession permit, Nature Protection Act, Flora & Fauna Exemption Act & Public Works Act (permission to work in or on the seafloor). These are issued by two different ministries (RWS & LNV). Each permit has its own MEP and underlying Monitoring Program (MP) to The MP shall provide the necessary input for answering the question to allow the evaluation of the actual effects registered through monitoring (and further analysis). The MP is delegated through the permits to POR. The evaluation remains the responsibility of the Authorities. Hence the combined and integrated approach under the PMR umbrella, to safeguard uniformity and unambiguity in the evaluations, as shown in figure 9 (unfortunately only available in the Dutch language).

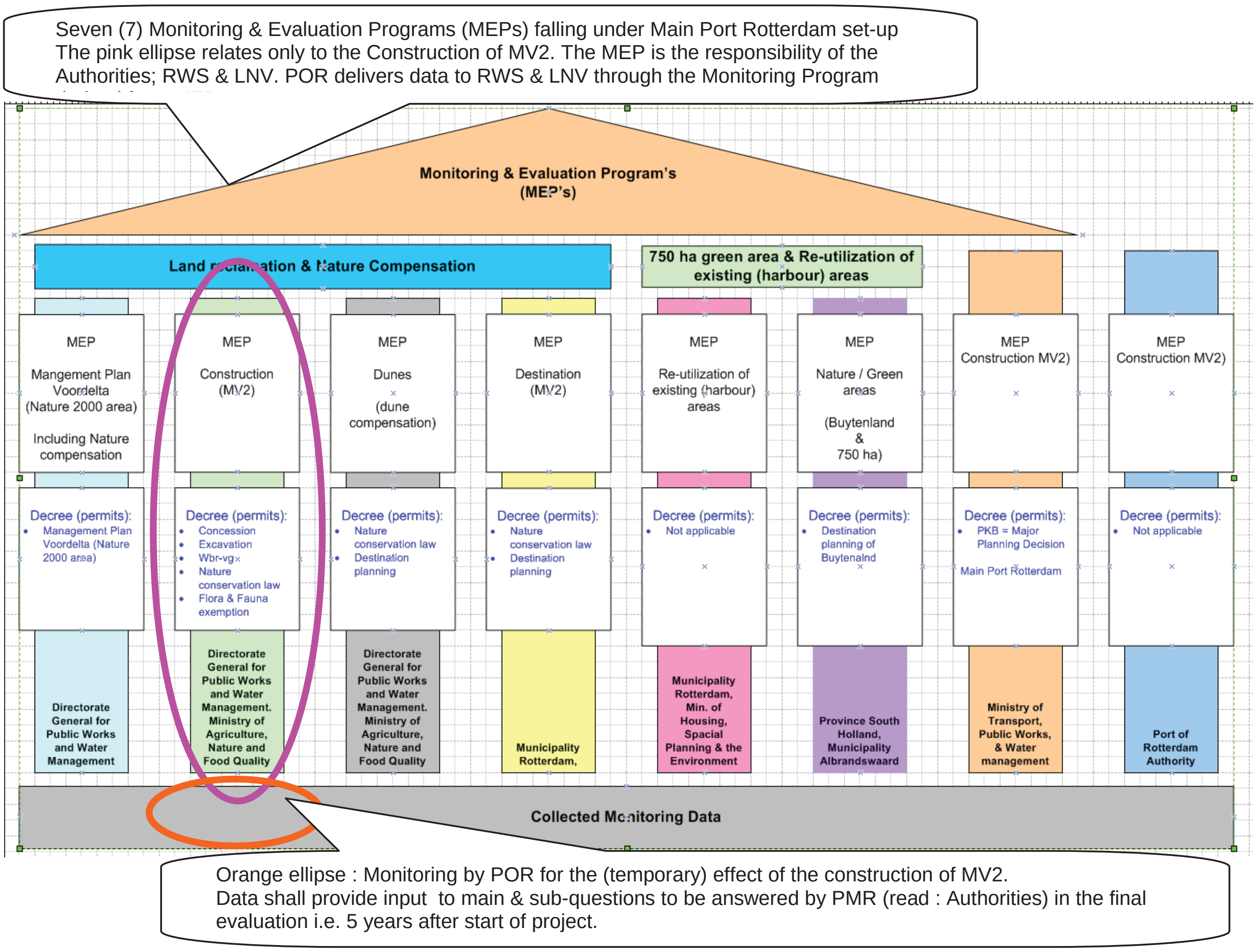

Figure 9 : Organisational setup to bring all MEP's under one umbrella as many MEP are intertwined and provide data to more than one program (pillar) which may have different stakeholders.

In general only effects, although small, that can not be neglected or are potentially significant require monitoring. Effect analysis is based on the BACI (Before-After–Control-Impact) assessment.
For the construction of MV2, apart from the covering up of existing sea bottom, the driving force for the possible impact is the extra silt (fine fractions) brought in suspension in the water column. The fine fraction emerges as wash-out of the dredged sediment being released with the excess transport water through the overflow of the TSHD when dredging sand from the borrow area.

All possible effects chains have been worked out and were reported in the EIA (MER-Aanleg MV2 ; Ref literature list). Leading in formulating the main questions (topics) to be addressed in the evaluation of the PMR projects, in our case the MV2 construction and presence, were the EIA, the so-called Appropriate Assessment for the effects on Nature 2000 area's and the 5 main permits. The permits contain directives for monitoring, either in a very concrete and explicit format (RWS) or in a more general sense (LNV).

All separate projects for which monitoring are required are brought under one integrated umbrella (figure 9). Under the umbrella, in concert with all parties concerned, the ultimate questions to be answered in the evaluation of the impact of MV2 construction, MV2 presence, etc. have been formulated. The question can be found in the various MEP's. From each main-question sub-questions, if relevant, have been derived. The monitoring results shall provide answers so that the main and sub-questions can be answered after a 5 year period.

Hereinafter an eexample of one of the typical evaluation questions of the MEP is given

Subject :	Construction MV2 – borrow area
Main question:	How will the quality of the seabed (benthic communities) develop in the borrow areas after construction of MV2 w.r.t. to the original benthic community in and around the excavation pits.
Sub questions:	What benthic community was present before the start of MV2 What are the soil properties of the top layer in and around the designated borrow areas What is the quality and the variability of the original benthic community What benthic community will come back (re-colonization) How long will it take before re-colonization will take effect What will be the quality and variability of the new community

The scheme (figure 10) illustrates the monitoring for just the construction and the presence of MV2. The whole schema comprises only (!) the purple ellipse from figure 9 above. The path in the middle of the figure 10 (coloured in orange) are done by the POR, as a MP obligation laid down in the applicable permits. Other monitoring is done by the central government (RWS) or third parties. The interrelation and dependencies are clearly shown. The real evaluation takes place after 5 years of monitoring in 2013. Although the scheme is only available in the Dutch language, (and difficult to read) it clearly shows the complexity of the MP and the many dependencies.

The actual monitoring for the construction Phase of MV2 will continue after 2013 as some after effects may occur e.g. due to buffering of silt in the seabed, being released again into the water column by storms, i.e. by wave induced water - bottom interaction. (Ref : van Ledden at all)

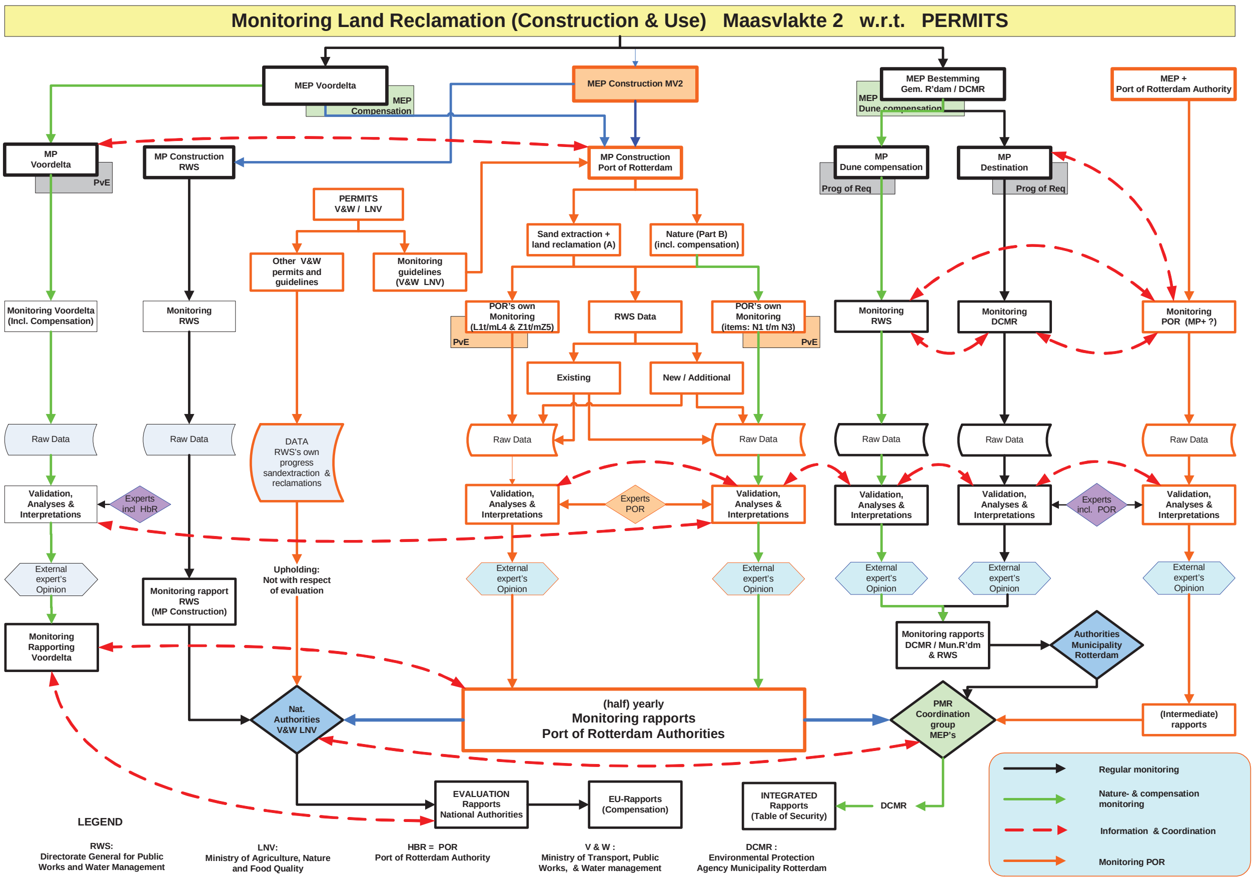

Figure 10 : Monitoring for MV2 construction & presence, all aspects needed for answering the MEP shown in figure 9, the pink ellipse.

4. EIA- BASELINE MONITORING SURVEYS & STUDIES

4.1 General

Even before the EIA was released (2008) it was evident that some baseline studies were needed regardless of the outcome of the EIA, the permits and the final Monitoring & Evaluation Program (MEP).

4.2 Benthos studies

In 2006 an extensive benthos survey was carried out along the Dutch coast stretching from IJmuiden till the Kop of Goeree (150 km) with a width of approx. 50 km. The benthos survey comprised 300 point, of which 257 were actually done. The remainder could not be done due to a limited time frame and bad weather delays.

The benthos baseline study was repeated in 2008, but the area was adapted to incorporate the results of worst case scenario modelling runs for the silt dispersion along the coast as a result of the variations in: slit contents of the sand, extraction rates, location of the borrow pits, wind & wave conditions. Furthermore reference areas needed to be included as well for comparison purposes.
The area now stretches from Petten till Vlissingen (250 km) and has a width of approx. 35km. Again 300 point were defined. All points were sampled this time.

The benthos study consists of three elements; i.e. boxcore sampling (ø 32 cm, height 20 – 30 cm), benthic sledge sampling (~ 15 m2) and sediment sampling from the boxcore (~ 10 cm3 from two consecutive layers : 0-5 cm and 5-10 cm of seabed).

4.3 Seabed composition: silt fraction of top layer.

The seabed composition of the top layer (0-5 cm & 5-10cm) has been determined from samples taken from the box core during the benthic surveys.

The composition is thus established for the strip along the Dutch, conform the benthic surveys as it concerns the same locations. Again this monitoring will be continued as long as benthic surveys are required to be carried out.

Two data sets are now available i.e. April-June 2006 en April-July 2008, with 257 and 300 locations sampled respectively. The benthic survey of 2008 was from IJmuiden till the Kop van Goeree (width ~50 km). The second survey (2008) from Petten till Vlissingen, maximum width ca. 35 km.

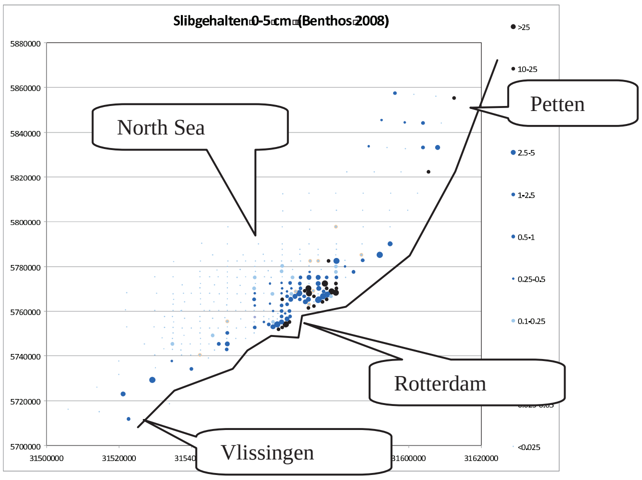

Figure 11: silt distribution top layer along Dutch coast
The bigger/ darker the dot the more silt (%) is present

More recently June – July 2009, the re-colonisation survey was carried out giving a third data set consisting of 100 locations in- & around the borrow areas. The idea is that any changes in benthic communities shall be related to the “extra” amount of silt brought in the system by dredging. This extra amount of silt shall manifest itself the most prone in and around the sand extraction pits. The earlier described monitoring set–up for the benthic re-colonisation anticipates on this development, hence the 4 squares approach in combination with the section approach. In the section the change of silt continent to and from the borrow area should be visible.

De 2006 en 2008 benthos surveys were carried out, after European tendering, by the combination of IMARES & NIOO. NIOO was responsible for the box core sampling and analysis, whereas IMARES for the over all coordination and the benthic sledge sampling and analysis.

The sediment samples were analyses by a laser particle sampler, volume from the box core ~11 cm3 for each layer. The silt was divided in the following fraction

<2 µm	<4 µm	<8 µm	<16 µm	<32 µm	<50 µm	<60 µm

From the sediments that remained on the 60 µm sieve the following was obtained:

<63 - <125 µm	<125 - <250 µm	<250 –<500 µm	> 500µm

The figure show the percentage of fines (particles < 60 µm) for the result obtained in 2008. Known locations with high silt contents are clearly visible in the distribution along the coast.
Likewise the data sets for 2006 and 2009 are available and will be used as input for the MoS2 modelling and used for correlation purposes with other measurements e.g. silt, juvenile fish etc.

4.4 Juvenile Fish study

In 2007 a juvenile fish survey was carried out. The area investigated was similar to the one described above for the adapted 2006 2nd benthos baseline survey. This fish survey was carried out in the same area in conjunction with the Port’s silt survey (same area and statistically speaking the same points). The fish survey and the silt survey comprised of 100 locations, 20 section perpendicular to the coast and approx. 5 point per section. The 100 locations are intertwined with the benthos 2008 baseline locations (statically speaking the “same“ coordinates).

The juvenile fish survey consisted of catching bottom fish with a 2m width beam trawl and pelagic juvenile fish with a plankton net. The survey was carried out in April, July and in October 2007. Approx. 65.000 fish from the bottom trawl have been weighted and measured in order to establish their condition.
More than 52 species were identified in the catches. From the juvenile fish samples were taken and deep frozen. The idea was to compare their stomach contents in case the condition of the juvenile fish established during the construction of MV2 (effect of the extra silt from the borrow area on juvenile fish larvae) would be found. The

stomach content should indicate if silt particles would be the reason. In the permits and later when the final MEP was available the effect on juvenile fish was considered negliable and difficult to prove due to the variability of the system.

As the juvenile fish larvae were still stored it was it was decided in 2008 to carry out a further analysis on the stomach contents of the frozen juveniles. The environment parameter and constraints will be taken into account when analysis and interpreting the results. The report on the findings is pending.

4.5 Silt measurements

As mentioned above in 2007 three silt survey campaigns were carried out by POR, i.e. in the same time frame and on the same locations. The sampling route and locations was randomised as much as possible taking into account the available contract time, the sailing distances, the tidal conditions (not all shallow samples at low tide), etc.

In the silt survey the measurement were taken by a silt profiler being owned by the Port.
The investigated parameters over the vertical profile were measured with the following devices:

- Optical backscatter probe: 2 no. With different ranges depending on the TSM (total suspended matter) concentrations encountered.
- Transmission probe, idem TSM concentrations
- Conductivity : results in salinity after computations using a.o. the temperature
- Chlorophyll probe
- Pressure sensor
- Temperature sensor
- Niskin water samplers (3 no. ; volume 1,6 litre.)

After the silt measurement baseline study of 2007 it was decided to improve the measurements by building a new profiler. Mid July 2009 the new profiler was tested and put in operation in the survey of July and thereafter.

Figure 12 : The new silt profiler (designed & constructed 2009, owned by POR)

The new profiler has apart from the old one the following extra sensors and probes:

- A Wetlab ACS probe, capable of providing for each 10 cm of water layer (depending on the lowering speed) a continuous colour spectrum to measure the quality and the amount of dissolved substances of the North Sea water.
- A LISST probe, also capable of measuring for each 10 cm layer a particle size distribution of that layer, including the concentration of the TSM
- An altimeter (echo sounder) to be able to close the bottom Niskin water sampler precisely on a pre-determined height (say 50 cm) above the seabed.
- A probe to measure current speed and direction.

Part of the equipment is also a dedicated dGPS system, a detachable acoustic Doppler Current Profiler (ADCP), a portable TRIOS sensor (watercolour, incoming and reflected spectra of sunlight). The validation, elaboration and further analysis of the gathered data are done by PMV2 staff in concert with external specialists.

All of the above gathered silt profiles are input for the numerical model (MoS2) and the data assimilation by remote sensing of satellite

4.6 Underwater sound (noise) measurements.

There is not much data available in the public domain on underwater noise created by TSHD during the various stages of the dredge cycle. The permit for the sand extraction stipulates that the POR shall make available sound source levels for the distinct stages : dredging, sailing full, placing of sand through bottom doors or valves , rain bowing, pumping ashore and sailing empty back to the borrow area again.

A background (baseline) underwater sound measurement survey in front of the entrance to the port of Rotterdam and Maasvlakte was initiated and carried out in September 200 prior to the dredging activities at location Z
The measurements were carried out with two hydrophones positioned 2 and 7 meter above the seabed in 14m water depth. The baseline study covers 7 days of 24 hours continues measurements.

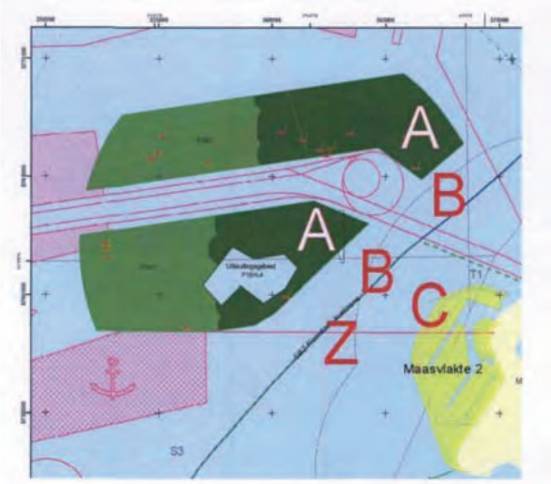

Figure 3.1 Area map with Maasvlakte 2 and the dredging areas (green). The big letters indicate the areas for source level measurements of A) the dredging; B) the transport and C) the dumping of sand. Z denotes the area for the noise background measurements [2].

Figure 13: Location Z background noise 2008

In September 2009 the actual source levels plus the continues measurements of the background noise (same location as 2008) will be measured. Measuring protocols and a “roadmaps” are being prepared and extensively discussed with all parties concerned view the safety aspects involved.
Once available, after validation and verification, these source sound levels will be used by others, outside the scope of MV2, to carry out scientific research with those sea mammals and fish that could be sensitive to underwater sound propagation.

4.7 ToTSM Pilot Study

Instead of complying with the permits requirement, i.e. providing every fortnight, vertical profiles in 3 “representative” sections, POR has opted for a different approach after - and in consultation with the authorities. In 2007 – 2008 a pilot project was sponsored by the POR in which it was demonstrated that data assimilation of remote sensing satellite images into numerical models for TSM could work and would resulting a more realistic result. During the EIA the numerical modelling had been extended beyond the state of the art at that time by implementing a water – seabed interaction module. This made it possible to simulate continues recording in which storm events were registered showing large increases of the silt concentration over the vertical. Continues CEFAS measurement at Noordwijk from 2001 and 2002 were used for calibration and partly for validation. The data of the Ports’ silt measurement program will be providing more validation data (time series for 2007 – 2015).

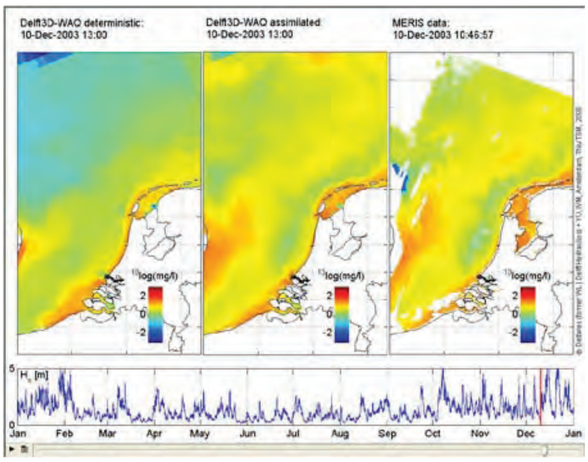

Figure 14 **:** Assimilated results ToTSM Pilot Project

Profiles measured in the field so far show that, depending on depth and point in the tide curve, values vary between 5 – 10 mg/l to 10 to 20 mg/l. During storm conditions these values go up as far as 1.000 mg/l (actual measured profile just after storm in May 2009)
The satellite images, interpreted by IVM, provide TSM for the top layer. In the MoS2 program (see further on) algorithms will be developed to translate the measured (actual) profiles and the amount s given by the remote sensing images. IVM not only gives a TSM amount per pixel but also provides a fault value. This combination of value and fault per pixel combined with the fled measurements will make assimilation technically feasible and provide realistic silt patterns as for instance: weekly or monthly averages.

5. MONITORING 2009 - 2015

5.1 Benthos: Re-colonisation

In the coming years the benthos studies (2006 & 2008) consisting of 300 points will be repeated.
In order to see and measure any changes the benthic communities need to be exposed to a long term exposure of "extra" silt relative to the variations in the natural background values in order to show up in the survey. Measuring each year is therefore no needed.

However in 2009 there will be a type of baseline study for the re-colonisation. The survey consists of 100 points located in and around the borrow area. From the 2006 & 2208 surveys a good impression exists in the benthic communities in the sand extraction surroundings. For the re-colonisation a more detailed picture is needed. Two approaches have been combined in the re-colonisation set up. In the borrow area 2 square are defined, each having a 100.0 x 100.0 m2 area. Like wise 2 areas of the same size are defined outside but in close proximity to the borrow area for comparison purposes. In each square 10 random box core and benthic sledge samples are taken. The 60 points remaining are spread over a larger area to allow the analysis of transects.
In June and July 2009 the field work was carried out by the consortium of IMARES-NIOO.
The laboratory analysis followed thereafter. Reporting is expected December 2009.

For 2010 an extensive benthic survey (300 point) might again be scheduled. Further analysis of the 2006, 2008 and the 2009 data set shall be evaluated against each other and compared to other survey along the coast. This analysis is scheduled for the last quarter of 2009.

5.2 Seabed composition: silt fraction of top layer.

All benthic survey carried out after January 2009 will result in new data set for further analysis.
Investigated will be the accumulation of sediment as a result of the construction of MV2 and whether or not the appearance of new benthic communities after re-colonisation can be attributed (correlated) to the measured changes in silt content. Most probably a more in-depth study will be needed into the water – bottom exchange for silt, as this is a critical parameter in the numerical modelling.

5.3 Mismatch algae bloom & cockle, growth rates

In the EIA many effect chains were investigated, as a result of the extra amount of fines brought in suspension along the Dutch coast by the sand extraction for MV2. One of the effect chain predicted, in a worst case scenario, is that there would be a negative impact through the hampered growth of cockles on ducks when the hatching and the bloom did not coincide, but lagged.

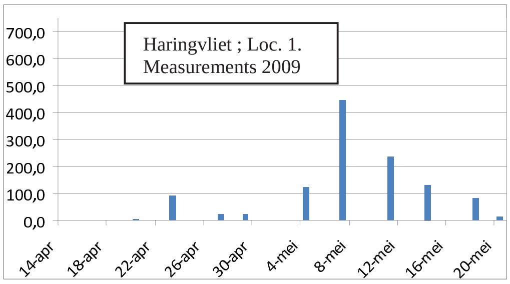

Figure 15 : Number of cockles per litre

Yvonne van Kruchten in her Master Thesis (TUD, 2008) investigated the probabilities of a mismatch between the chlorophyll bloom and the presence of the cockle larvae. This chance associated with this worst case scenario turned out to be rather small.

Never the less it was decided to set-up a special monitoring program to look into this effect chain in more detail. In April and May 2009 twice a week samples were taken from 3 locations in The Haringvliet. The samples were analysed for chlorophyll and the amount of cockle larvae. It could be demonstrated that enough eatable chlorophyll of the right size was present for the cockle larvae. The number of larvae developed quick and after reaching a peak on 8 May (~ 450 no. /liter). The figure below shows the amount of cockles during the sample period. From the graph it is learned that after this date larvae went to the bottom to settle. On 20 May nearly all cockled have settled, at least they were no longer present in the water column.

It also became clear that there was not a wealthy bloom of algae (Phaeocystis) in the North Sea. Phaeocystis are normally reported when an extreme bloom is visible (on satellite images) along the Dutch coast. It shall be noted that Phaeocystis are way too big for cockle larvae to eat.

A follow-up survey on 27 June and XX July on the beach in the Haringvliet between the high water and just below the low water line showed that a very limited number of juvenile cockle were found. Most probably the storm of 28 May has caused a great mortality. The next survey in October 2009 will have to shed some more light on this aspect when again cockles will be sampled (if present). The growth rate (size and weight) can only be established if indeed juvenile cockles are found in October 2009.

5.4 Silt Measurements

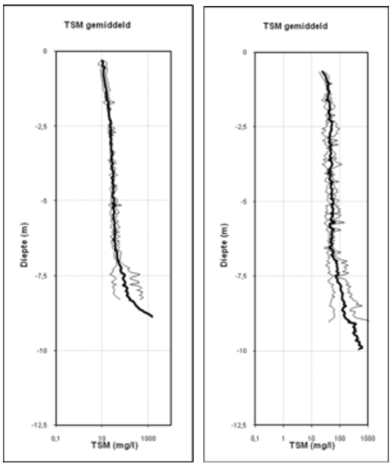

In 2009 again silt profiles will be measured. Instead of the 3 times 100 point, 6 times 50 of the 100 points will be sampled as the coincidence with the juvenile fish is no longer needed. In total 5 weeks are reserved for the measurements. Each week 50 different points, randomly spread out over the total area, are sampled. One extra week is available for additional measurements. In 2007 one (1) section consisting of 3 point was measured over a period of 13 hours near Noordwijk. In 2009 more than one section will be measured for 13 hours. A longer section, approx 50 km, will be continuously (intermittent sailing form one to the other) sampled. This needs to be done once at neap tide and the second time at springtide. The purpose is to establish the width of the “freshwater” river, the stratification, salinity gradients, and the various currents and up-welling phenomena (Ref. 5). This information is needed for the verification of the MoS2 modelling.

Figure 16 *:* Silt profile near Egmond just before & after the height of the summer storm on 28 & 29 May 2009 respectively

5.5 MoS2

The **Mo**del **S**upported **Mo**nitoring of **T**SM (MoS2) is the follow-up and continuation of the pilot project ToTSM : Integration of Remote Sensing and Modelling of Total Suspended Matter in the Dutch coastal zone, Delftwares & IVM (see Ref) which was carried out in 2007-08. A new model of the Southern part of the North Sea will be constructed in which the strip along the Dutch coast will on a fine mash/grid system.
All the lessons and experiences obtained during the pilot study will be incorporated in the new model.
The MoS2-model is based on Delft-3D package. The model is 3D and will have 13 layers in the vertical. The model will be calibrated hydraulically for water levels and currents (long term time series available), after calibration the fine sediment modelling will be run and calibrated on the field data collected in 2007 by POR (zee under baseline studies). The data collected after the start of the sand extraction earlier this year (2009 and onwards) will be used for validation and data assimilation. The remote sensing analysis of the 2007 and onwards collected satellite images provide for each pixel of the image a value for the TSM and the fault associated with the calculated value. This can be done for TSM and for transparency (Kd-values). All data obtained from the satellite images (however scarce it may seem) will be used in the Ensemble Kalmann filtering. In fact any time series: temperature, salinity, etc. collected by buoys will qualify for assimilation.
In 2010 the new model will be operational (Beta version) and will provide the silt atlas of the distribution of fines along the Dutch coast for 2007. The atlas for 2009 will follow thereafter. In the satellite images the actual sand mining is incorporated. By the constant assimilation and looking at the internal “book keeping of the program and the changes made in the parameters, at the end of a whole year, the program can be improved. The MoS2 will be fed with the daily amount of sand taken from the seabed including the concentrations of resulting fines. By running the assimilated model in hind cast mode for 2009, but without the input of the sand extraction volumes, the impact without the construction of MV2 is shown. The difference of the two model runs will give the contribution of MV2 in the ecological impact.

5.6 Underwater sound

The actual measuring of source levels for TSHD working their normal dredge routine is scheduled for September 2009. At present measurement protocols and “roadmaps” are defined. All aspects of working with a TSHD, placing of sand through bottom doors or valves, rain bowing and pumping ashore, will be present in that period. Leading when dealing with these protocols and the so-called roadmap will always be the safety aspects involved, this shall be guaranteed under all circumstances.
It is anticipated that one measurement campaign of 6 to 7 days might be sufficient. The background will again the monitored on a 7/24 format at a fixed location. The other measurement will be by small boat and only during day-time for safety reasons.

6. CLOSING WORDS

The above article is rather factual and does not contain any in depth analysis nor real evaluations.
The baseline studies show the situation as it was at the time of carrying out the surveys and studies. The progress monitoring has just started. However the main reason for not having any evaluations is that it is not the POR that will do the evaluation but the relevant authorities (PMR / RWS / LNV) i.e. 5 years after the start of the construction of MV2. POR just will hand over the collected and validated data. Intermediate analysis by POR may be needed if POR proposes changes in the permit conditions. Thus POR will do some (inhouse) analysis, if sufficient data is available, but will not publicise these (intermediate) results, unless the authorities agree on doing so.

During the presentation of the paper in November at the Conference more data will be available. If possible one or two topics of the monitoring will be presented and discussed in more detail.

REFERENCES

EIA studies for Maasvlakte2
Official Site of Maasvlakte 2 (Dutch and English language)
http://www.maasvlakte2.com

Municipality Rotterdam's website: (Partner in MPR, all dossiers MV2; in Dutch language only)
http://www.dsv.rotterdam.nl/smartsite2137288.dws

E**nvironmental Committee's website** (all EIA documents of MV2, in Dutch language only)
http://217.26.114.41/mv2/

Yvonne van Kruchten e.a. (2009)
A Probabilistic Analysis of the Ecological Effects of Sand Mining for Maasvlakte 2
Terra & Aqua (short version):
http://www.terra-et-aqua.com/dmdocuments/terra114_4.pdf
M.Sc report in full (2008), (in the English language)
Technical University of Delft
http://repository.tudelft.nl/view/ir/uuid:4556db23-1172-4e8f-b5fa-9af9676a0c79/

Pilot Project ToTSM
ToTSM: Integration of Remote Sensing and Modelling of Total Suspended Matter in the Dutch coastal zone, Deltares & IVM. 2008. Report could be obtained from POR on request

Measurement of underwater background noise Maasvlakte 2
TNO Report: TNO-DV 2009 C212
Baseline study: Report could be obtained from POR on request

Dr. Ir. Gerben de Boer, (2009) PhD thesis
On the interaction between tides and stratification in the Rhine Region of Freshwater influence.

Baseline reports : Benthos 2006 , Silt survey 2007,
Reports handed over to Dutch Authorities, as data delivery according to the relevant permits
Reports not yet available for public distribution.

Van Ledden, Bolle, Boon, Borst, van Prooijen & de Ronde.
Innovative highlights in the environmental impact assessment Maasvlakte 2
ICCE 2008, Hamburg, Aug. 31 Sept 5, 2008